EXTRACTING SIGNALS AND GRAPHICAL MODELS FROM COMPRESSED MEASUREMENTS

A Dissertation
Presented to
The Academic Faculty

By

Hang Zhang

In Partial Fulfillment
of the Requirements for the Degree
Doctor of Philosophy in the
School of Electrical and Computer Engineering
College of Engineering

Georgia Institute of Technology

December 2021

EXTRACTING SIGNALS AND GRAPHICAL MODELS FROM COMPRESSED MEASUREMENTS

Thesis committee:

Professor Faramarz Fekri, Advisor
School of Electrical and Computer Engineering
Georgia Institute of Technology

Professor Mark P. Styczynski
School of Chemical and Biomolecular Engineering
Georgia Institute of Technology

Professor Mark A. Davenport
School of Electrical and Computer Engineering
Georgia Institute of Technology

Professor Yao Xie
School of Industrial and Systems Engineering
Georgia Institute of Technology

Professor David V. Anderson
School of Electrical and Computer Engineering
Georgia Institute of Technology

Date approved: December, 2021

To my parents

for their enduring love and unconditional support.

ACKNOWLEDGMENTS

First and foremost I would like to thank my advisor Prof. Faramarz Fekri for his continuous support and advice during the course of my Ph.D. research. His kindness, forgiveness, enthusiasm, and working ethics have made a huge impact on my mindset beyond research. I would also like to thank my thesis committee members: Prof. Mark A. Davenport, Prof. David V. Anderson, Prof. Mark P. Styczynski, and Prof. Yao Xie, for their precious time in serving my thesis committee and their invaluable feedback. [1]

I would also want to thank all my fellow group members and collaborators, i.e., Dr. Jun Zou, Dr. Arash Einolghozati, Dr. Afshin Abdi, and Mr. Yashas Malur Saidutta for their helpful discussions. Furthermore, I would like to thank my other friends in Georgia Tech: Dr. Yun Long, Dr. Qiang Hu, Dr. Cen Lin, Dr. Yinjun Liu and Dr. Xuchen Zhang. Special thanks go to Dr. Yang Zhang, whose encouragement and support have helped me pass the most difficult time during my Ph.D. Moreover, I want to express my gratitude towards Dr. Taiyun Chi, Dr. Jongseok Park, Dr. Yunyi Gong, Dr. Sensen Li, Dr. Tso-wei Li, and Mr. Tzu-yuan Huang, with whom I spent countless evenings and weekends in school. Their academic achievements are perfect examples of how hard-working pays off. Besides, I want to thank Ms. Rui Zhang and her boyfriend Mr. Wenlong Mou.

In addition, I want to express my sincere gratitude to Dr. Ping Li for his hospitality and invaluable advice during my internship. I also want to Dr. Martin Slawski for introducing me to the world of statistics and his helpful suggestions. Moreover, I want to thank Mr. Xiangyi Chen, Dr. Yi Hao, Mr. Chen Li, Dr. Xiaoyun Li, Dr. Jun-kun Wang, Dr. Weijie Zhao, Dr. Fan Zhou, and Dr. Zhixin Zhou, with whom I had a pleasant time and from whom learned a lot during the internships.

Last but not the least, I want to thank my parents for their enduring love and unconditional support to pursue my academic dream.

[1] This material is based upon work supported by the National Science Foundation under Grant No. CCF-2007807 and ECCS-2027195.

TABLE OF CONTENTS

LIST OF TABLES

LIST OF FIGURES

SUMMARY

The thesis is to give an integrated approach to efficiently learn the interdependency relation among high dimensional signal components and reconstruct signals from observations collected in a linear sensing system. Broadly speaking, the topics can be divided into three parts: (i) interdependency relation learning; (ii) sensing system design; and (iii) signal reconstruction.

Interdependency relation learning. Previous works on learning graphical models usually assume direct observation of samples without measurement noise. However, this assumption may be impractical or too expensive in real-world applications. To handle such problems, one may turn to indirect observations. In this thesis, we study interdependency of random variables with both parametric and non-parametric methods. First, for a Gaussian distributed random vector $\mathbf{X}$, we reconstruct the corresponding graphical structure from noisy indirect measurements by modifying the covariance estimation in gLasso and CLIME. For the first time, we show that *the correct graphical structure can be recovered under the indefinite sensing system using low number of samples*. The results suggest that, with fewer samples than the length of signal, we can still recover the graph structure of a high dimensional signal from its low dimensional observations.

Second, we consider the non-parametric method. We assume random vector $\mathbf{X}$ follows the nonparanormal distribution. In particular, we assume the joint distribution of $\mathbf{g}(\mathbf{X})$ exhibits a Gaussian distribution $\mathcal{N}(\boldsymbol{\mu}, \boldsymbol{\Sigma})$, i.e., $\mathbf{X}$ behaves as multivariate Gaussian after some transformation $\mathbf{g}(\cdot)$. Under mild conditions, we show that our graph-structure estimator can obtain the correct structure, from which we can derive the minimum sample number and the projection dimension. Additionally, we obtain a non-asymptotic uniform bound on the estimation error of the *cumulative distribution function* (CDF) of $\mathbf{X}$ from indirect observations with inexact knowledge of the noise distribution. To the best of our knowledge, this bound is derived for the first time and may serve as an independent interest.

Sensing system design. We study the problem of sensor design from the viewpoint of inference in probabilistic graphical models. The most used algorithm for inference in graphical model is the so-called *belief propagation* (or message passing). Generally speaking, in factor graphs, it is used to compute the posterior probabilities. Provided the factor graph contain no loops, the belief propagation will generate the accurate posterior probabilities. In this thesis, for the first time, we leverage the analytical tool of the message passing algorithm and design a sensing matrix that can provide a preferential treatment for a specific part of the whole signal. In particular, the proposed sensing system will allow to reconstruct a specific part of the signal with higher accuracy than the rest of the signal in a linear compressed sensing setup. To illustrate the benefits of our method, we first revisit a regular sensing scenario, where all signal components are treated equally. For the sparse signal, our method can reproduce the classical results of the compressive sensing. Then we turn to the preferential sensing scenario. Numerical experiments suggest our method leads to not only a significant reduction of the error within the high-priority part but also a modest reduction of the total error.

Signal reconstruction with an indefinite linear sensing system. Here we consider reconstruction of a high dimensional signal with an indefinite linear sensing system. Assuming a sparse signal, we investigate this problem from the viewpoint of *compressive sensing* and considers three problems as following. First, we consider the problem of signal reconstruction with inexact knowledge of the sensing system. Generally speaking, uncertainties in the sensing system weakens the system performance and reduces the reliability of recovered signals. Here, we specifically focus on recovering the sign values of signals instead of their exact values. We show that as long as the uncertainty in the sensing matrix is sparse, a thresholding mechanism can be developed to recover the sign vector. In particular, provided that the true signal satisfies certain conditions, the exact sign vector can be recovered with high probability even under uncertain sensing matrices.

Second, we formulate a novel optimization problem to reconstruct the pseudo-sparse

signal, when corrupted by noise, via the ℓ_∞ norm. In previous works, a noise whitening method is often used which leads to the noise folding phenomenon, increasing the noise energy greatly. We introduce a different approach and design a new optimization model to recover $\mathbf{x}$ with ℓ_∞ norm. For the analysis, we assume the noise to have a uniform magnitude and show that a unique solution close to the true values of pseudo-sparse signals can be obtained in an indefinite measurement system. For the numerical experiments, we abandon the uniform-magnitude assumption and return to the setting of Gaussian noise. Compared to the noise-whitening method, our method can greatly reduce the noise with only a modest sacrifice of the support-set recovery rate.

Third, we study a general framework for compressive sensing assuming the existence of the prior knowledge that the signal $\mathbf{x}$ belongs to the union of multiple convex sets. This framework, in a way, is a more general formulation of compressive sensing problems. In fact, by proper choices of these convex sets, the problem can be transformed to well known CS problems such as the sparse phase retrieval, quantized compressive sensing, and model-based CS. To begin with, we analyze the impact of this prior knowledge on the minimum number of measurements M to guarantee the uniqueness of the solution. Then we formulate a universal objective function for signal recovery, which is both computationally inexpensive and flexible. Moreover, an algorithm based on *multiplicative weight update* and *proximal gradient descent* is proposed and analyzed for signal reconstruction. Finally, we investigate as to how we can improve the signal recovery by introducing regularizers into the objective function.

CHAPTER 1
INTRODUCTION AND LITERATURE SURVEY

The thesis proposes an integrated framework to recover high-dimensional signals and/or learn graphical models from compressed measurements. Broadly speaking, the workflow can be divided into three phases:

- **Phase I: interdependency relation learning**. Given a designed sensing system, we will collect samples and design learning algorithms to uncover the dependency relations among the entries of the signals. Once the relations are learned, we can utilize them to further optimize the sensing system.

- **Phase II: sensing system design**. Equipped with some prior knowledge of signals, we leverage the tools from coding theory, to put it more specifically, *density evolution* (DE), to design the sensing system. Notably, our sensing system can provide preferential treatment for a specific part of the signals with higher-priority.

- **Phase III: signal reconstruction with indefinite linear sensing system**. Here, we focused on the signal reconstruction with a given sensing system. Problems considered in this phase include (i) signal reconstruction with inexact knowledge of the sensing system; (ii) signal reconstruction with the signal being contaminated by undesired noise; and (iii) signal reconstruction with the signal belonging to a union of convex sets.

The proposed research is at the intersection of the compressive sensing and all its related techniques with the current machine learning research, in particular graphical models. To begin with, we briefly review the existing related work, which thereby consists of two parts: (i) research on graphical models and (ii) research on compressive sensing.

1.1 Interdependency Relation Learning

In recent years, we have witnessed a surge in the use of of graphical models, which provides a general framework of representing the dependency relations among random variables, in a variety of applications such as biology, natural language processing and computer vision [1, 2]. For an arbitrary random vector $\mathbf{X} \in \mathbb{R}^p$, we can construct a graphical model $G = (V, E)$, known as *Markov Random Fields* (RMF), by associating each entry X_i with a node $v_i \in V$ and adding an edge $e = (v_i, v_j)$ to the edge set E if X_i and X_j are conditionally dependent given other random variables, where X_i and X_j denote the ith and jth entry of $\mathbf{X}$, respectively.

There have been extensive works on learning *Gaussian Graphical Model* (GGM) when samples of data $\mathbf{X}$ are directly observed [3, 4, 5, 6]. However, in certain applications, direct observations of the desired signal is not possible. Instead, the signal has to be measured indirectly. One potential application is the biological sensing system designed to detect the concentration of certain molecules, e.g. miRNAs, which are small molecules regulating the cell growth, development, differentiation, and are linked to a wide variety of human diseases [7, 8]. Expression analysis suggests that perturbed miRNA expression can be linked to cancer and heart diseases. As a result, we can use miRNAs as indicators for the disease diagnosis and even the disease intervention. Notice that one would require an expensive bio-sensor which responds exclusively to individual miRNA among over 1000 different miRNAs if a direct observation is required. However, turning to indirect observations allows us to use sensors which may not be specialized to each miRNA types separately. The cost reduction can be achieved, even with the same number of sensors as the direct observations, i.e., $d = p$. This thesis assumes that the measurements are given by a linear sensing matrix, i.e., $\mathbf{Y} = \mathbf{A}\mathbf{X} + \mathbf{W}$ where $\mathbf{Y}$ denotes the measurement results, $\mathbf{A}$ is the sensing matrix, $\mathbf{X}$ is the signal of interests, and $\mathbf{W}$ represents the Gaussian noise. Our goal is to study how to recover the graph structure from indirect measurements.

1.1.1 Parametric Method of Graphical Model Learning

The most related work is the GGM [1, 9], where random vector $\mathbf{X} \in \mathbb{R}^p$ satisfies the Gaussian distribution, i.e., $\mathbf{X} \sim \mathcal{N}(\mathbf{0}, \mathbf{\Sigma}^\natural)$. Let $\mathbf{\Theta}^\natural$ be the precision matrix of the random vector $\mathbf{X}$, i.e., $\mathbf{\Theta}^\natural = (\mathbf{\Sigma}^\natural)^{-1}$. One important characteristics of the GGM is that $\mathbf{\Theta}^\natural_{i,j} = 0$ if X_i and X_j are independent given the rest of entries $X_{\backslash\{i,j\}}$. Therefore we can associate the structure E with the support set S of the precision matrix $\mathbf{\Theta}^\natural$, where $S \triangleq \Big\{(i,j) \mid \Theta^\natural_{i,j} \neq 0,\ \forall i \neq j\Big\}$. This property of the precision matrix forms a foundation for many algorithms that recover the structure of GGM.

Related Work

The two most famous methods are (i) *Graphical Lasso* (gLasso) [3] and (ii) *constrained ℓ_1 minimization for inverse matrix estimation* CLIME [4].

- **Graphical Lasso**: Compared with the discrete graphical model, one of the major difference is that its joint probability can be written in a closed form [9]. In [3], the authors proposed gLasso, which can be regarded as an M-estimator [10] (Ch. 9). The basic assumption is that the ground-truth signal (i.e., the support set of the precision matrix) lies within a certain low-dimensional space. By minimizing the negative log-likelihood plus some specific regularizers, one can reconstruct the signal from insufficient samples, which is the major bottleneck in the high-dimensional statistics.

- **CLIME**. While sharing the same assumptions as to the gLasso, i.e., a sparse precision matrix, CLIME estimator takes a different approach without explicitly exploiting the joint distribution. Instead of maximizing the likelihood, the authors first obtain an empirical covariance matrix $\widehat{\mathbf{\Sigma}}_n$ and then force the precision matrix $\widehat{\mathbf{\Theta}}_n$ to approximate its inverse. Noteworthy, it can be applied to other models as well provided their precision matrices are sparse. Hence, its impact goes beyond the GGM or even the continuous graphical model. One example is its application to the mixture model [11].

Under mild conditions, both of these two estimators can obtain the underlying graphical structure. Furthermore, whenever some prior information or constraints on the structure of graphical model are available, other variations of GGM-learning such as GGM with hidden variables [6, 12], and GGM with an unknown block structure [13] have been proposed. For a more thorough discussion on this topic, please refer to [5, 10].

Additionally, there are also some works trying to accelerate the learning process [14, 15, 16, 17]. Since the computational issue is not our focus, we only list the references and omit a detailed discussion. Apart from the research on continuous RVs, other directions of research include discrete models and mixture models as discussed in the following.

Discrete Model. The most crucial model lying in this category is the Markov random field [18]. For the discrete model, the major difficulties can roughly be divided into two categories:

- **Computation of the partition function**. One widely-used trick to handle such problem is replacing the joint distribution with the conditional distribution [19, 20, 18].
- **Insufficient samples**. This problem is usually fixed by placing priors on the graphical structure with the most popular one being the sparsity assumption. Typical examples include [20, 19, 18]. In [20], the authors considered the Ising model where each random variable can only take values in $\{\pm 1\}$. In [19], the binary setting is extended to m different values. In [18], a different setting with generalized linear regression is considered.

Mixture Model. These works can be seen as a combination of the previous two models. For the conciseness, we omit the corresponding discussion and only list some of the most typical literatures [21, 22, 23, 24].

Our Contributions

In chapter 2, we consider learning the graphical structure of a p-dimensional Gaussian random variable $\mathbf{x}$, i.e., $\mathbf{x} \in \mathbb{R}^p \sim \mathcal{N}(\mu, \mathbf{\Sigma})$, $\mu \in \mathbb{R}^p, \mathbf{\Sigma} \in \mathbb{R}^{p \times p}$. Unlike the previous works which observe $\mathbf{x}$ directly, we consider the indirect observation scenario where samples $\mathbf{y}$ are obtained via an under-determined sensing matrix $\mathbf{A} \in \mathbb{R}^{d \times p}$ $(d < p)$, and possibly corrupted with some additive noise, i.e, $\mathbf{y} = \mathbf{A}\mathbf{x} + \mathbf{w}$. Assuming an sparse precision matrix $\mathbf{\Theta}^\natural$, we modify the gLasso in [3] and CLIME in [4] and propose two estimators namely M-gLasso and M-CLIME, respectively, to reconstruct the graphical structure of GGM when observations are collected indirectly through a matrix $\mathbf{A}$. Sufficient conditions to obtain the correct graphical structure are derived, and numerical experiment are provided for the verification.

- We investigate the statistical properties of the proposed algorithms in terms of the minimum sample size n. Denote deg as the maximum Markov blanket in the graphical model. When $d \to \infty$, we require $n \geq c_0 \sqrt{\text{deg}^2 \cdot \log p}$ ($c_0 > 0$ is some positive constant) for the correct structure recovery, which is the same as the direct observation setting in [20] when $d \to \infty$. Under the indefinite sensing matrix setting where $d < p$, we need to increase n to $\Omega\left(\text{deg}^2 \cdot (\log p)^3\right)$ for the precise graph recovery, which suggests fewer samples can be drawn when compared with the length of signal p.

- Unlike the previous results with direct observations in [3] and [4] where the correct recovery of the graphical structure only depends on the sample number n and the dimension of the signal p, our result with indirect observations is also affected by the projection dimension d, which is never involved in the analysis before. When infinite samples are drawn, i.e., $n \to \infty$, we only require $d \geq c_0 \sqrt{\text{deg} \cdot p \log p}$ for the exact recovery of graphical structure, where $c_0 > 0$ is some positive constant. Provided insufficient samples are drawn, i.e., $n < p$, the minimum projection dimension d increases to $\sqrt{\text{deg}} \cdot p^{3/4} \cdot (\log p)^{1/3}$ for the correct graphical structure. Notice that both the above scenarios allow d to be far

less than p, suggesting the feasibility of the indefinite sensing matrix setting.

1.1.2 Nonparametric Method of Graphical Model Learning

The most related works on the nonparametric learning of graphical model are [25, 26, 27, 28, 29, 24], which focus on the nonparanormal distributed random vector $\mathbf{X}$, i.e., the joint distribution $\mathbf{g}(\mathbf{X})$ follows the Gaussian distribution $\mathcal{N}(\boldsymbol{\mu}, \boldsymbol{\Sigma})$ after the transform of certain function $\mathbf{g}(\mathbf{X}) = [g_i(X_i) \cdots g_p(X_p)]^\top$. Let $\boldsymbol{\Theta}$ be the inverse of the covariance matrix $\boldsymbol{\Sigma}$, the conditional independence relation of $\mathbf{X}$ is completely incorporated into matrix $\boldsymbol{\Theta}$. To put more specifically, we have $\Theta_{i,j} = 0$ iff X_i and X_j are independent given the rest of entries $X_{\backslash\{i,j\}}$. Similar as the GGM, the goal of learning the graphical structure reduces to detecting the support set S of $\boldsymbol{\Theta}$, where $S \triangleq \{(i,j) \mid \Theta_{i,j} \neq 0,\ \forall i \neq j\}$.

Related Work

The basic idea in the previous work is to first estimate the covariance matrix and then plugging into the gLasso [3], CLIME [4], etc. The differences across the above works lie in the estimation method of the covariance matrix. In [25], the covariance matrix is estimated via the CDF estimator; while in [30], it is estimated by the Spearman's rho estimator. In an independent work, [27] pointed out the covariance matrix can be estimated by Kendall's tau estimator as well. Moreover, [30] only studied the rank-based estimators, while [27] also compared the rank-based estimators with the normal-score based estimator. Later, [28] proposed a projection based algorithm to accelerate the estimator in [27].

Apart from the graphical models following the nonparanormal distribution, other types of graphs include the graph with forest structure [27], graph with the elliptical distribution [29], latent Gaussian copula model [24], etc. Since they are not directly related to our work, a detailed discussion is omitted.

In addition to the above work, we also require some background knowledge about the density deconvolution dating at least back to [31, 32, 33], where kernel-based estimators

are proposed for the noise with infinite support set. To improve the performance for the noise with finite support, a ridge-parameter method is proposed in [34]. Similar work includes [35, 36]. Work [37] generalized [33] and gave a data-driven method to select the optimal bandwidth. Apart from the kernel-based methods, [38] presented a projection-based method based on the Meyer-type wavelets, which adapts to the super-smooth noise automatically. Notice the above works all assume the perfect knowledge of the noise distribution. Later, [39, 40, 41] studied the setting with unknown noise but all required repeated measurements to estimate the distribution of the noise.

Our Contributions

In chapter 3, we consider the nonparametric learning of the graphical structure of a p-dimensional random vector $\mathbf{X} \in \mathbb{R}^p$ under noisy measurements, namely, $\mathbf{Y} = \mathbf{A}\mathbf{X} + \mathbf{W}$, where $\mathbf{A} \in \mathbb{R}^{d\times p}$ denotes sensing matrix and $\mathbf{W}$ represents the additive measurement noise. To suppress the noise $\mathbf{W}$, we assume extra measurements being conducted, namely, $d > p$. Provided that the random vector $\mathbf{X}$ follows a nonparanormal distribution and the majority of variables in $\mathbf{X}$ are conditionally independent (i.e., an sparse graphical model), we propose an estimator to obtain the correct graphical structure together with the theoretical analysis of its properties, for example, the minimum sample number n and dimension d. Denote $\beta > 0$ as some fixed positive constant to be defined.

- We propose an estimator for the graphical structure together with the sufficient conditions for the correct recovery. We show that the sample number n must be at least $n \gg (\deg)^4 \log^4 n$, where deg denotes the maximum Markov blanket in the graph. Further, we obtain a lower bound on the dimension as $d \gg p + (\deg)^{\beta/4} \log^{\beta/4}(d-p)$, where $\beta > 0$ is some fixed positive constant to be defined.

- Additionally, our work is the first to consider the deconvolution estimator for the CDF with limited knowledge of the noise distribution. Compared with the previous work [39,

40, 41], our work does not assume perfect knowledge of noise distribution, and our estimator requires no additional steps to estimate the noise distribution. Moreover, we give a non-asymptotic uniform bound on the estimation error, that is, $\sup_x \left|\widehat{F}(x) - F(x)\right| \leq \frac{c_0 \log^2(np)}{(d-p)^{\beta/2}} + \frac{c_1}{\sqrt{n}}$ (cf. Thm. Theorem 3), where $\widehat{F}(\cdot)$ and $F(\cdot)$ denote the estimated marginal CDF and ground-truth marginal CDF, respectively, and c_0 and c_1 are some positive constants. The analysis to obtain these results is a technical ground break and is likely useful in other areas of statistics.

1.2 Sensing System Design

At the core of our work is the *message passing* (MP) algorithm over factor graphs [42, 43, 1, 44]. Generally, it is used to compute the posterior probabilities within the factor graphs (a bipartite graph with variable nodes and factor nodes), whose computation steps can be divided into two categories:

- **Product**: this operation is for the variable node, whose role is simply to multiply all the coming information, i.e., probabilistic messages, and to send a resulting message to the adjacent factor node.

- **Sum**: this operation is done by the factor node, whose role is to calculate the weighted sum of all incoming messages and transmit the resulting message to the variable node.

The *message passing* algorithm is also referred to as belief propagation, or sum-product, or min-sum algorithm. These different names are due to its constant rediscovery in different fields. In physics, this algorithm existed no later than 1935, when Bethe used a free-energy functional to approximate the partition function (cf. [43]). In the probabilistic inference, Pearl developed it in 1988 for the acyclic Bayesian network and showed it gave the exact inference [44]. The most interesting thing is its discovery in the coding theory. In early 1960s, Gallager proposed it to decode *low-density parity-check* (LDPC) codes over graphs under the name sum-product [42]. However, Gallagher work was almost forgotten and was

rediscovered again in 90s [45, 46]. Later [47] equipped it with the analytical tool called *density evolution* (DE) and used it for the design of LDPC codes.

1.2.1 Related Work

When narrowing down to the compressed sensing, MP has been widely used for signal reconstruction [48, 49, 50, 51, 52, 53, 54, 55, 56, 57, 58, 59, 60] and analyzing the performance under some specific sensing matrices.

In the context of the sparse sensing matrix, the authors in [61] first proposed a so-called *sudocode* construction technique and later presented a decoding algorithm based on the MP in [62]. In [63], the non-negative sparse signal $\mathbf{x}$ is considered under the binary sensing matrix. The work in [64] linked the channel encoding with the CS and presented a deterministic way of constructing sensing matrix based on high-girth LDPC code. In [65, 49, 51], the authors considered the verification-based decoding and analyzed its performance with DE. In [50], the spatial coupling is first introduced into CS and is evaluated with the decoding scheme adapted from [65]. However, all the above mentioned works focused on the noiseless setting, namely, $\mathbf{w} = \mathbf{0}$. In [53, 55, 56], the noisy measurement is considered. A sparse sensing matrix based on spatial coupling is analyzed in the large system limit with replica method and DE. They proved its recovery performance to be optimal when m increases at the same rate of n, i.e., $m = O(n)$.

Note that the above mentioned related works are not exhaustive due to their large volume. For a better understanding of the MP algorithm, the DE, and their application to the compressive sensing, we refer the interested readers to [43, 66, 56]. In addition to the work based on MP, there are other works based on LDPC codes or graphical models [67, 68, 69, 70, 71, 72, 73, 74, 75, 76, 77, 78, 79, 80, 81].

1.2.2 Our Contributions

In chapter 4, we consider the linear measurement system $\mathbf{y} = \mathbf{A}\mathbf{x} + \mathbf{w}$, where $\mathbf{y} \in \mathbb{R}^n$, $\mathbf{x} \in \mathbb{R}^n$, and $\mathbf{w}$ denote the measurements, the signal with certain structures, and the measurement noise, respectively [82]. Compared to the previous work exploiting MP [65, 49, 51, 50, 53, 55, 56, 57, 58], our focus is on the sensing matrix design of $\mathbf{A}$ rather than the decoding scheme. By viewing the high dimensional signal reconstruction from the low dimensional measurements as a message passing algorithm over a graphical model, we leverage tools from coding theory in the design of LDPC, i.e., DE, and provide a framework for the design of matrix $\mathbf{A}$.

Two design schemes for the sensing matrix, namely, (i) a regular sensing and (ii) a preferential sensing, are proposed and are incorporated into one single framework. As an illustration, we consider the ℓ_1 regularizer, which corresponds to Lasso, for both of the designs.

- **Regular Sensing**. We consider the k-sparse signal $\mathbf{x} \in \mathbb{R}^n$ and associate it with a prior distribution such that each entry is zero with probability $1 - k/n$. First we approximate this distribution with Laplacian prior by letting the probability mass near the origin point to be $1 - k/n$. Afterwards, we use our framework and reproduce the classical results in CS, i.e., $m \geq c_0 k \log n$, which is a lower bound on the number of measurements required to recover the signal.
- **Preferential Sensing**. We design the sensing matrix that would result in more accurate (or exact) recovery of the high-priority sub-block of the signal relative to the low-priority sub-block. Numerical experiments suggest our framework can (i) reduce the error in the high-priority sub-block significantly; (ii) and yet be able to reduce the error with regard to the whole signal modestly as well. Additionally, we emphasize that although we focus on two levels of priority in signal components in this work, we can easily extend the framework to the scenario where multiple levels of preferential treatment on the signal components are needed, by simply incorporating associated equations into the DE.

1.3 Signal Reconstruction with Indefinite Linear Sensing System

This part of work is closely related with *compressive sensing* (CS) [83, 84, 85], which studies the problem of reconstructing a sparse high dimensional signal $\mathbf{x}$ from the under-determined linear system $\mathbf{y} = \mathbf{A}\mathbf{x} + \mathbf{w}$, where $\mathbf{y}$ denotes the low dimensional observation, $\mathbf{A}$ denotes the sensing matrix, and $\mathbf{w}$ denotes the sensing noise. We consider three problems in the CS. In the following, we separately list the contributions of these three works and their corresponding related works.

1.3.1 Sparse Recovery of Sign Vectors under Uncertain Sensing Matrices

First, we consider the problem of signal reconstruction when there are uncertainties about sensing matrix coefficients [86].

Related Work

Past works [87, 88, 89, 90] in the context can be summarized as following. In [87], signal $\mathbf{x}$ is recovered by pretending the values of the sensing matrix are exact. In [91], sparse Bayesian learning is extended to reconstruct an sparse signal $\mathbf{x}$. In [88, 89], optimization problems are formulated to recover $\mathbf{x}$ and the perturbation matrix $\mathbf{E}$ simultaneously. In [88], this is achieved by adding a Frobenius norm penalizing the perturbation matrix $\mathbf{E}$. In [89], special structures are assumed on the perturbation matrix $\mathbf{E}$ and then $\mathbf{E}$ is recovered via a constraint optimization. All the above works focused on recovering the exact value of the signal $\mathbf{x}$. However, in some applications [92, 93, 94, 86, 95, 96, 97, 60], the sign values in the vector $\mathbf{x}$ is desired instead of the exact values of $\mathbf{x}$.

Our Contributions

In chapter 5, we consider recovering the sign vector under an uncertain sensing matrix. Our contributions are listed as the following.

- We consider a sparse perturbation matrix $\mathbf{E}$ and analyze its impact on the system performance. In general, perturbation matrix $\mathbf{E}$ is random and has different distributions in different applications. Typical examples of distributions include Gaussian distribution and an arbitrary distribution with limited range [97]. We consider a case that is unique to miRNA sensing in biology. Note that the (i, j)th element, Ψ_{ij}, in sensing matrix $\mathbf{\Psi}$ models the reaction between sensor i and miRNA j. If Ψ_{ij} is zero, it means that sensor i does not react to miRNA j. However, due to the stochastic nature of molecular binding in biological receptors (i.e., sensors), certain miRNAs may still have unexpected footprints on some sensors, i.e., unexpectedly changing some entries in the sensing matrix from zero to non-zero values [98]. Since this happens only for a small subset of miRNA and sensor pairs, the perturbation matrix $\mathbf{E}$ is sparse. Adopting our model in [79], we analyze the perturbation matrix $\mathbf{E}$ and study how it affects the system performance.

- We propose a thresholding mechanism to recover the sign vector under uncertain sensing matrices although its correct value cannot be guaranteed due the sensing matrix uncertainties. We studied sign vector recovery under quadratic measurement setting in [76], in the present work we consider linear measurements but with some random perturbations in the sensing matrix. In [96], a thresholding mechanism based on Dantzig and Lasso is proposed to get the correct sign vector without considering the sensing matrix uncertainties. In [97], sensing matrix uncertainties are assumed to be limited-range and sign vector is obtained by thresholding the solution to one specifically designed problem. Inspired by the above works, we introduce a framework that is tailored toward applications with constraints described. We have proved that the recovered sign vector is correct provided that certain assumptions hold.

1.3.2 Recovering Noisy-Pseudo-Sparse Signals from Linear Measurements via ℓ_∞

Second, we formulate a novel optimization problem to reconstruct the pseudo-sparse high-dimensional signal, which is contaminated by noise, via the ℓ_∞ norm [99].

Related Work

Consider the sensing relation $\mathbf{y} = \mathbf{A}(\mathbf{x}+\mathbf{e})+\mathbf{w}$, where $\mathbf{y}$ denotes the low-dimensional observation, $\mathbf{A}$ is the known sensing matrix, $\mathbf{x}$ is the sparse high-dimensional signal awaiting to be reconstructed, $\mathbf{e}$ is some small deviations, causing the signal to deviate slightly from the sparsity model, i.e., a pseudo sparse signal, and $\mathbf{w}$ denotes the measurement noise. In [100], a general model is proposed to handle perturbation $\mathbf{Ae}$. However, they do not provide any method as to how we modify the cost function to account for $\mathbf{Ae}$. Besides, due to the indefinite nature of sensing matrix $\mathbf{A}$, their formulation cannot be modified to to incorporate $\mathbf{e}$ as in our setting. In [101], parsimony constraint $\|\mathbf{Ae}\|_1$ is introduced to handle $\mathbf{Ae}$. However, the method cannot be extended to Gaussian noise. In [102, 103], the support set T is assumed to be known and $\mathbf{e}$ only corrupts the value of zero elements in $\mathbf{x}$. To recover $\mathbf{x}$, [103] proposed a *cancel-and-recover* method, which projects $\mathbf{A}(\mathbf{x}+\mathbf{e})$ onto the orthogonal space spanned by columns of matrix $\mathbf{A}$. In [102], objective function $\|\mathbf{x}\|_1$ is modified to $\|\mathbf{x}_T\|_1$ and the robustness of the recovery algorithm is guaranteed under some conditions. In [104], the same model is considered. The authors treat $\mathbf{Ae}+\mathbf{w}$ as some non-white Gaussian noise and propose to first whiten the noise $\mathbf{Ae}+\mathbf{w}$ and then transform it into the traditional CS measurement model. But this method can lead to noise-folding phenomenon, seriously degrading the recovery performance.

Our Contributions

In chapter 6, we pursue a novel approach to tackle this problem directly instead of methods such as noise-whitening and with no assumption on the support set. The contributions of our work can be summarized as the following.

- We take into account the shape of Gaussian, i.e., non-drastically increasing $\|\mathbf{e}\|_\infty$, and propose a new optimization model. In traditional approaches, only the energy of $\mathbf{e}$ is constrained by $\|\mathbf{e}\|_2 \leq \sigma^2$. We add a new penalty term $\|\mathbf{e}\|_\infty$ to prevent individual components of $\mathbf{e}$ to grow too large. Further, different from [104], our method does not perform noise whitening and can recover the sparse signal $\mathbf{x}$ and its Gaussian deviation $\mathbf{e}$ simultaneously. The simulation results suggest that our method greatly improves the recovery accuracy compared with that of the noise whitening method [104].

- We consider a simplified case and give a theoretical analysis to facilitate model understanding. First we prove that recovering the exact solution is not possible but a unique solution $\widehat{\mathbf{x}}$ in its proximity can be obtained. Then we provide a lower bound on the number of measurements to guarantee the unique solution. Adopting the same model as in [79] for the measurement matrix, we show that a unique solution $(\widehat{\mathbf{x}}, \widehat{\mathbf{e}})$ can be obtained with high probability with an indefinite measurement matrix $\mathbf{A}$, i.e. $m < n$.

1.3.3 Sparse Signal Reconstruction with a Multiple Convex Sets Domain

Third, in chapter 7 we study a general framework for compressive sensing assuming the existence of the prior knowledge that the signal $\mathbf{x}$ belongs to the union of multiple convex sets, $\mathbf{x} \in \bigcup_i \mathcal{C}_i$ [105].

Related Work

We first discuss the work regarding the analysis of the statistical properties, from which we can obtain the minimum sensor number m. Broadly speaking, there are at least 3 types of methods to analyze the sensor number m. The most related work takes the viewpoint from stochastic geometry. In [106], the authors transform the problem into counting faces of randomly projected polytopes. Work [107] consider the Gaussian sensing matrix and

transform the correct recovery problem into the *mesh escaping problem*, which concerns with the condition where two subspaces fail to intersect with each other. With the tools invented by [108], [107] can easily reproduce the classical results regarding the sensor number m, namely, $m \geq c_0 k \log n$ for a k-sparse signal, where $c_0 > 0$ is some constant. Noteworthy, this method can be easily extended to other norms apart from ℓ_1. Later, [109] generalized the Gaussian setting to a broader class of matrices. In addition to the geometric method, other directions of work include RIP-based method [110] and AMP-based method [58, 111, 66]. Since they are not directly related to our work, we only mention their names without detailed discussions.

Another line of research regards the computational method. Accelerated proximal gradient descent [112], FISTA [112, 113] are the most widely used optimization algorithm. Besides, the problem-specific algorithms are proposed. In [114], the author studied the minimum number of measurements M under different models, i.e., shape of $\mathcal{L}_i$, and modified CoSaMP algorithms [83] to reconstruct signal. In [115], the authors expanded the signal onto different basis and transformed model-based CS to be block-sparse CS. In [116], the author studied model-based CS with incomplete sensing matrix information and reformulated it as a matrix completion problem.

Our Contributions

Our contribution can be divided into two parts in general: the statistical property and associated optimization method.

- We analyze the minimum number of measurements to ensure uniqueness of the solution. We first show that the conditions for the uniqueness can be represented as $\min_{u \in E} \|\mathbf{A}\mathbf{u}\|_2 > 0$, for an appropriate set E. Assuming the entries of the sensing matrix $\mathbf{A}$ are i.i.d. Gaussian, we relate the probability of uniqueness to the number of measurements, M. Our results show that depending on the structure of $\mathcal{C}_i$'s, the number of measurements can be reduced significantly.

- We propose a novel formulation and the associated optimization algorithm to reconstruct the signal $\mathbf{x}$. First, note that existing algorithms on e.g., model-based CS are not applicable to our problem as they rely heavily on the structure of constraint sets. For example, a key idea in model-based CS is to consider expansion of $\mathbf{x}$ onto the basis of each convex set $\mathcal{C}_i$ and then rephrase the constraint as the block sparsity on the representation of $\mathbf{x}$ on the union of bases. However, such an approach may add complicated constraints on the coefficients of $\mathbf{x}$ in the new basis, as the sets $\mathcal{C}_i$'s are not necessarily simple subspaces.

  Note that although $\mathcal{C}_i$'s are assumed to be convex, their union $\bigcup_i \mathcal{C}_i$ is not necessarily a convex set, which makes the optimization problem (Equation 7.2.2) hard to solve. By introducing an auxiliary variable, $\mathbf{p}$, we convert the non-convex optimization problem to a biconvex problem. Using *multiplicative weight update* [117] from online learning theory [118], we design an algorithm with convergence speed of $\mathcal{O}(T^{-1/2})$ to a local minimum. Further, we investigate improving the performance of the algorithm by incorporating appropriate regularization. Compared to the naive idea of solving L simultaneous optimization problems

$$\min_{\mathbf{x}} \ \|\mathbf{x}\|_1, \ \text{ s.t. } \mathbf{y} = \mathbf{A}\mathbf{x}, \quad \mathbf{x} \in \mathcal{C}_i,$$

  and choosing the best solution out of L results, our method is computationally less-expensive and more flexible.

1.4 Notations

We denote $c, c_0, c_i > 0$ as arbitrary fixed positive constants. Notice that the specific values may not be necessarily identical even if they share the same name. For arbitrary real numbers a and b, we denote $a \lesssim b$ if there exists some $c_0 > 0$ such that $a \leq c_0 b$. Similarly we define $a \gtrsim b$. We write $a \asymp b$ when $a \lesssim b$ and $a \gtrsim b$ hold simultaneously. The maximum of a and b is denoted as $a \vee b$; while the minimum is denoted as $a \wedge b$. We have $a \propto b$ when a is proportional to b. The imaginary number $\sqrt{-1}$ is denoted as $\mathbb{j}$.

For an arbitrary matrix $\mathbf{M} \in \mathbb{R}^{m_1 \times m_2}$, we denote $\mathbf{M}_i$ as its i-th column and M_{ij} as the (i,j)-th entry. Its Frobenious norm $\|\mathbf{M}\|_{\mathrm{F}}$ is defined as $\sqrt{\sum_{i,j} M_{i,j}^2}$. Furthermore, we define $\|\!|\mathbf{M}|\!\|_{a,b}$ as $\max_{\|\mathbf{z}\|_a=1} \|\mathbf{M}\mathbf{z}\|_b$. Two special cases are $\|\!|\mathbf{M}|\!\|_{1,1}$ and $\|\!|\mathbf{M}|\!\|_{\infty,\infty}$, which can be written as $\|\!|\mathbf{M}|\!\|_{1,1} \triangleq \max_j \sum_i |M_{i,j}|$, and $\|\!|\mathbf{M}|\!\|_{\infty,\infty} \triangleq \max_i \sum_j |M_{i,j}|$, respectively. The operator norm $\|\mathbf{M}\|_{\mathrm{OP}}$ can be viewed as a shorthand for $\|\!|\mathbf{M}|\!\|_{2,2}$. Additionally, we need the element-wise norm $\|\cdot\|_1$ and $\|\cdot\|_\infty$, which are defined as $\|\mathbf{M}\|_1 \triangleq \sum_{i,j} |M_{i,j}|$ and $\|\mathbf{M}\|_\infty \triangleq \max_{i,j} |M_{i,j}|$, respectively. Moreover, we define $\|\!|\mathbf{M}|\!\|_{\text{off,F}} \triangleq \sqrt{\sum_{i \neq j} M_{i,j}^2}$, $\|\!|\mathbf{M}|\!\|_{1,\text{off}} \triangleq \sum_{i \neq j} |M_{i,j}|$, and $\|\!|\mathbf{M}|\!\|_{\text{off},\infty} \triangleq \max_{i \neq j} |M_{i,j}|$. The inner product $\langle \mathbf{M}_1, \mathbf{M}_2 \rangle$ between matrices $\mathbf{M}_1$ and $\mathbf{M}_2$ is defined as $\sum_{i,j} (\mathbf{M}_1)_{i,j} (\mathbf{M}_2)_{i,j}$.

CHAPTER 2

PARAMETRIC LEARNING OF GRAPHICAL MODELS

2.1 Introduction

Graphical models provide a general framework of representing the dependency relations among random variables. They have a broad spectrum of applications in biology, natural language processing and computer vision [1, 2], etc. For an arbitrary random vector $\mathbf{X} \in \mathbb{R}^p$, we can construct a graphical model $G = (V, E)$ by associating each entry X_i with a node $v_i \in V$ and adding an edge $e = (v_i, v_j)$ to the edge set E if X_i and X_j are conditionally dependent given other random variables, where X_i and X_j denote the ith and jth entry of $\mathbf{X}$, respectively.

Discovery of the graph structure from a collection of direct observations of $\mathbf{X}$ has been widely studied in the past [3, 4, 25, 27, 28, 29, 24]. However, in some applications, direct observations of the desired signal is not possible. Instead, the signal has to be measured indirectly. Further, one commonly encountered problem is that the observations are contaminated with measurement noise, which leads to inaccurate estimation of the graphical structure. Inspired by these challenges, we consider the graph structure recovery under an indirect linear measurement scenario from the desired signal as

$$\mathbf{Y}^{(s)} = \mathbf{A}\mathbf{X}^{(s)} + \mathbf{W}^{(s)}, \;\; 1 \leq s \leq n, \tag{2.1.1}$$

where $\mathbf{Y}^{(s)}$ denotes the sth measurement, $\mathbf{A} \in \mathbb{R}^{d \times p}$ denotes the sensing matrix, and $\mathbf{W} \in \mathbb{R}^d$ denotes the sensing noise. Assuming the random vector $\mathbf{X}$ to be Gaussian distributed, the goal of this chapter is to learn the pair-wise independence relation (structure) of an undirected graphical model, i.e., Markov random fields, from the observations $\{\mathbf{Y}^{(s)}\}_{1 \leq s \leq n}$ with a parametric method.

Notations Let $\mathbf{X} \in \mathbb{R}^p$ follow the Gaussian distribution with zero mean and covariance $\mathbf{\Sigma}^\natural$, i.e., $\mathbf{X} \sim \mathcal{N}(\mathbf{0}, \mathbf{\Sigma}^\natural)$. We assume that most entries of X are pair-wise conditionally independent, i.e., the precision matrix $\mathbf{\Theta}^\natural = (\mathbf{\Sigma}^\natural)^{-1}$ is sparse. Let S be the support set of $\mathbf{\Theta}^\natural$, namely, $S = \left\{(i,j) : \ \mathbf{\Theta}^\natural_{ij} \neq 0\right\}$, and define $\deg \triangleq \max_i \|\mathbf{\Theta}^\natural_i\|_0$ and $\kappa_{\mathbf{\Sigma}} \triangleq \left\|\left|\mathbf{\Sigma}^\natural\right|\right\|_{\infty,\infty}$. Note that the deg, i.e., **the maximum of the number of non-zero elements** in a column, is the maximum Markov blanket in the graphical model. Furthermore, we define $\mathbf{\Gamma}$ as $\mathbf{\Sigma}^\natural \otimes \mathbf{\Sigma}^\natural$, such that $\mathbf{\Gamma}_{(i_1,j_1),(i_2,j_2)} = \mathrm{Cov}(X_{i_1}X_{j_1}, X_{i_2}X_{j_2})$, where $\otimes$ is the kronecker product [119], and $\kappa_{\mathbf{\Gamma}}$ as $\left\|(\mathbf{\Gamma}_{SS})^{-1}\right\|_{\infty,\infty}$.

2.2 Problem Formulation

With n indirect observations $\left\{\mathbf{Y}^{(i)}\right\}_{i=1}^n$, our goal is to recover the graphical structure of $\mathbf{X}$, i.e., the support set $S \triangleq \left\{(i,j) \mid \Theta^\natural_{i,j} \neq 0, \ \forall\, i \neq j\right\}$ of the precision matrix of $\mathbf{X}$. The relation between $\mathbf{Y}$ and $\mathbf{X}$ is given as

$$\mathbf{Y} = \mathbf{A}\mathbf{X} + \mathbf{W},$$

where $\mathbf{A} \in \mathbb{R}^{d\times p}$ is an under-determined matrix with $d < p$, and $\mathbf{W}$ denotes the measurement noise with each entry $\mathbf{W}_{ij}$ being a Gaussian RV with zero mean and variance σ^2, i.e., $\mathbf{W}_{ij} \sim \mathcal{N}(0, \sigma^2)$. Note that with an arbitrary measurement matrix $\mathbf{A}$ and without imposing any constraint, it would be impossible to recover S. A simple example is $\mathbf{A} = [\mathbf{I}_{d\times d}\ \mathbf{0}_{d\times(p-d)}]$. It can be easily verified that the structure of the last $(p-d)$ entries of $\mathbf{X}$ cannot be recovered as no information about those entries are captured by the measurements. In our analysis, as in most compressive sensing literature, we assume that $\mathbf{A}$ is drawn randomly from a Gaussian distribution, i.e., entries of $\mathbf{A}$ follow i.i.d. Gaussian distribution. Without loss of generality, we assume that each column of $\mathbf{A}$ is both centered and normalized, i.e., A_{ij} is iid distributed $\mathcal{N}(0,1)$ for all i and j. Moreover, to avoid measurements being dominated by one or a small group of X_i's, we assume that $\mathrm{Var}(X_i) = 1$,

$1 \leq i \leq p$.

The goal is recovering the graphical structure of $\mathbf{X}$, i.e., the support set of $\mathbf{\Theta}^\natural$, from the measurements $\left\{\mathbf{Y}^{(i)}\right\}_{i=1}^n$. As such, we propose two estimators, M-CLIME and M-gLasso, whose details are given in Algorithm 1 and Algorithm 2.

Comparisons with MLE. The major drawback of ML estimation is that it is **non-convex** under our setting: the covariance matrix of $\mathbf{Y}$ is $\mathbf{A}^\top \mathbf{\Sigma}_X \mathbf{A}$ while the sparsity constraint is placed on the precision matrix $\mathbf{\Theta}_X = (\mathbf{\Sigma}_X)^{-1}$. Compared with the ML estimator, our estimator has an amenable analytical structure and is computational-friendly.

Algorithm 1 M-gLasso Estimator.

Input: Samples $\left\{\mathbf{Y}^{(i)}\right\}_{i=1}^n \in \mathbb{R}^p$ and sensing matrix $\mathbf{A} \in \mathbb{R}^{d\times p}$.
Stage I: Estimate the covariance matrix $\widehat{\mathbf{\Sigma}}_n^{\text{param}}$ as

$$\widehat{\mathbf{\Sigma}}_n^{\text{param}} = \mathbf{I} + \frac{1}{d+1}\left[\mathbf{A}^\top\left(\frac{1}{n}\sum_{i=1}^n \mathbf{Y}^{(i)}\mathbf{Y}^{(i)\top}\right)\mathbf{A}\right]_{\text{off}}, \tag{2.2.1}$$

where $[\cdot]_{\text{off}}$ denotes the operation of picking non-diagonal entries,
Stage II: Obtain $\widehat{\mathbf{\Theta}}_G^{\text{param}}$ as

$$\widehat{\mathbf{\Theta}}_G^{\text{param}} = \underset{\mathbf{\Theta}\succ\mathbf{0}}{\text{argmin}} - \log\det(\mathbf{\Theta}) + \text{Tr}(\widehat{\mathbf{\Sigma}}_n^{\text{param}}\mathbf{\Theta}) + \lambda_G^{\text{param}}\|\mathbf{\Theta}\|_{1,\text{off}}, \tag{2.2.2}$$

where $\lambda_G^{\text{param}} > 0$ is some positive constants.
Output: Estimated precision matrix $\widehat{\mathbf{\Theta}}_G^{\text{param}}$.

2.3 Theoretical Properties of Covariance Matrix Estimator

Here we describe the properties of our proposed GGM structure learning algorithms, namely, M-gLasso (Algorithm 1) and M-CLIME (Algorithm 2). We will show that a correct graphical structure can be obtained when the penalty coefficient λ_G^{param} in (Equation 2.2.2) is properly chosen. The core of the analysis lies in bounding the error of the covariance estimation, i.e., $\left\|\widehat{\mathbf{\Sigma}}_n - \mathbf{\Sigma}^\natural\right\|_\infty \lesssim \tau_\infty$, where $\widehat{\mathbf{\Sigma}}_n^{\text{param}}$ is defined in (Equation 2.3.2), and the

Algorithm 2 M-CLIME Estimator.

Input: Samples $\left\{\mathbf{Y}^{(i)}\right\}_{i=1}^{n} \in \mathbb{R}^p$ and sensing matrix $\mathbf{A} \in \mathbb{R}^{d\times p}$.
Stage I: Estimate the covariance matrix $\widehat{\mathbf{\Sigma}}_n^{\text{param}}$ as in Stage I in Algorithm 1.
Stage II: Obtain $\widetilde{\mathbf{\Theta}}_C^{\text{param}}$ as

$$\widetilde{\mathbf{\Theta}}_C^{\text{param}} = \text{argmin}_{\mathbf{\Theta}} \|\mathbf{\Theta}\|_1, \ \text{ s.t. } \left\|\widehat{\mathbf{\Sigma}}_n^{\text{param}}\mathbf{\Theta} - \mathbf{I}\right\|_\infty \leq \lambda_C^{\text{param}}, \tag{2.2.3}$$

where λ_C^{param} is some positive constant.
Stage III: Obtain the symmetric matrix $\widehat{\mathbf{\Theta}}_C^{\text{param}}$ from $\widetilde{\mathbf{\Theta}}_C^{\text{param}}$ as

$$(\widehat{\mathbf{\Theta}}_C^{\text{param}})_{ij} = \begin{cases} (\widetilde{\mathbf{\Theta}}_C^{\text{param}})_{ij}, & \text{if } \left|(\widetilde{\mathbf{\Theta}}_C^{\text{param}})_{ij}\right| < \left|(\widetilde{\mathbf{\Theta}}_C^{\text{param}})_{ji}\right|; \\ (\widetilde{\mathbf{\Theta}}_C^{\text{param}})_{ji}, & \text{otherwise.} \end{cases}$$

Output: Estimated precision matrix $\widehat{\mathbf{\Theta}}_C^{\text{param}}$.

threshold parameter τ_∞ is written as

$$\begin{aligned} \tau_\infty \triangleq & \ \frac{c_0\sqrt{d\log p}}{d+1}\max_i \left\|\mathbf{\Sigma}_i^\natural\right\|_2 + \frac{c_1\log p}{d+1}\left(1+\frac{c_2 p}{d}\right)\left\|\!\left|\mathbf{\Sigma}^\natural\right|\!\right\|_{\text{off,F}} \\ & + \frac{c_3\log p\sqrt{dp}}{\sqrt{n}(d+1)} + \frac{c_4 p(\log p)^{3/2}}{\sqrt{n}(d+1)}\left(1+\frac{c_2 p}{d}\right) + \frac{c_5 p\sqrt{\log p}}{\sqrt{d}(d+1)} \\ & + \frac{c_6\sigma^2\log p}{d}\left[1+c_7\left(\sqrt{\frac{d}{n}}\vee\frac{d}{n}\right)\right]. \end{aligned} \tag{2.3.1}$$

Then we have the following lemma.

Lemma 1. *Consider the covariance estimator* $\widehat{\mathbf{\Sigma}}_n^{\text{param}}$ *which reads*

$$\widehat{\mathbf{\Sigma}}_n^{\text{param}} = \mathbf{I} + \frac{1}{d+1}\left[\mathbf{A}^\top\left(\frac{1}{n}\sum_{i=1}^n \mathbf{Y}^{(i)}\mathbf{Y}^{(i)\top}\right)\mathbf{A}\right]_{\text{off}}, \tag{2.3.2}$$

where $(\cdot)_{\text{off}}$ *denotes the operation of picking non-diagonal entries. We then have* $\|\widehat{\mathbf{\Sigma}}_n^{\text{param}} - \mathbf{\Sigma}^\natural\|_\infty \lesssim \tau_\infty$ *holding with probability at least* $1 - c_0 p^{-1} - c_1 p^2 e^{-c_2 d} - c_3 p^2 e^{-c_4 p}$.

Provided all non-zero elements in the ground-truth precision matrix $\mathbf{\Theta}^\natural$ are greater than $c\tau_\infty$, where c is some positive constant, we will show that a correct graphical structure can be obtained when the penalty coefficients are properly chosen. The formal statement comes

as follows in Theorem 1 and Theorem 2.

2.3.1 Proof Outline

By the definition of our estimator, $\left\|\widehat{\mathbf{\Sigma}}_n^{\text{param}} - \mathbf{\Sigma}^{\natural}\right\|_{\infty} = \max_{i\neq j}\left|\left(\widehat{\mathbf{\Sigma}}_n^{\text{param}}\right)_{i,j} - \mathbf{\Sigma}^{\natural}_{i,j}\right|$, we only consider the off-diagonal entries

$$\left\|\widehat{\mathbf{\Sigma}}_n^{\text{param}} - \mathbf{\Sigma}\right\|_{\text{off},\infty} \leq \frac{1}{d+1}\underbrace{\left\|\mathbf{A}^\top\mathbf{A}\mathbf{\Sigma}_n^{\text{param}}\mathbf{A}^\top\mathbf{A} - (d+1)\mathbf{\Sigma}_n^{\text{param}}\right\|_{\text{off},\infty}}_{\vartheta_1} + \underbrace{\left\|\mathbf{\Sigma}_n^{\text{param}} - \mathbf{\Sigma}^{\natural}\right\|_{\text{off},\infty}}_{\vartheta_2},$$

where $\mathbf{\Sigma}_n^{\text{param}}$ is defined as $n^{-1}(\sum_{i=1}^n \mathbf{X}^{(i)}\mathbf{X}^{(i)\top})$. Then we separately bound ϑ_1 and ϑ_2. To bound ϑ_1, we first define $\mathbf{Z} = \mathbf{A}^\top\mathbf{A}\mathbf{\Sigma}_n^{\text{param}}\mathbf{A}^\top\mathbf{A}$, which gives

$$\mathbb{P}\left(\vartheta_1 \geq \delta\right) = \mathbb{P}\left(\max_{i\neq j}|Z_{i,j} - \mathbb{E}Z_{i,j}| \geq \delta\right) \leq \sum_{i\neq j}\mathbb{P}\left(|Z_{i,j} - \mathbb{E}Z_{i,j}| \geq \delta,\ i\neq j\right). \quad (2.3.3)$$

W.l.o.g. we assume $i = 1$ and $j = 2$. Define T_i, $1 \leq i \leq 6$ as

$$\begin{aligned}
T_1 &\triangleq \left(\mathbf{\Sigma}_n^{\text{param}}\right)_{1,2}\|\mathbf{A}_1\|_2^2\|\mathbf{A}_2\|_2^2;\\
T_2 &\triangleq \left(\mathbf{\Sigma}_n^{\text{param}}\right)_{2,1}\left(\langle\mathbf{A}_1,\mathbf{A}_2\rangle\right)^2;\\
T_3 &\triangleq \sum_{\ell\neq 1}\left(\mathbf{\Sigma}_n^{\text{param}}\right)_{2,\ell}\|\mathbf{A}_2\|_2^2\langle\mathbf{A}_1,\mathbf{A}_\ell\rangle + \sum_{\ell\neq 2}\left(\mathbf{\Sigma}_n^{\text{param}}\right)_{\ell,1}\|\mathbf{A}_1\|_2^2\langle\mathbf{A}_2,\mathbf{A}_\ell\rangle;\\
T_4 &\triangleq \sum_{\ell\neq 1,2}\left(\mathbf{\Sigma}_n^{\text{param}}\right)_{\ell,\ell}\langle\mathbf{A}_1,\mathbf{A}_\ell\rangle\langle\mathbf{A}_2,\mathbf{A}_\ell\rangle;\\
T_5 &\triangleq \sum_{\substack{\ell_1,\ell_2\neq 1,2\\ \ell_1\neq\ell_2}}\left(\mathbf{\Sigma}_n^{\text{param}}\right)_{\ell_1,\ell_2}\langle\mathbf{A}_1,\mathbf{A}_{\ell_1}\rangle\langle\mathbf{A}_2,\mathbf{A}_{\ell_2}\rangle;\\
T_6 &\triangleq n^{-1}\mathbf{A}_1^\top\left(\sum_{\ell=1}^n\mathbf{W}^{(\ell)}\mathbf{W}^{(\ell)\top}\right)\mathbf{A}_2.
\end{aligned}$$

To study the concentration behavior of $|Z_{i,j} - \mathbb{E}Z_{i,j}|$, $i \neq j$, we decompose Z_{12} into $\sum_{k=1}^6 T_k$ resulting $|Z_{1,2} - \mathbb{E}Z_{1,2}| \lesssim \sum_{k=1}^6|T_k - \mathbb{E}T_k|$. Then we will prove the following

equation holds with probability exceeding $1 - c_0 p^{-3} - c_1 e^{-c_2 p} - c_3 e^{-c_4 d}$,

$$
\begin{aligned}
|T_1 - \mathbb{E}T_1| &\lesssim \sqrt{\frac{\log p}{d}} \left(\left| \Sigma^{\natural}_{1,2} \right| + \sqrt{\frac{\log p}{n}} \right); \\
|T_2 - \mathbb{E}T_2| &\lesssim \frac{\log p}{d} \left(\left| \Sigma^{\natural}_{2,1} \right| + \sqrt{\frac{\log p}{n}} \right); \\
|T_3 - \mathbb{E}T_3| &\lesssim \sqrt{\frac{\log p}{d}} \left(\left\| \mathbf{\Sigma}^{\natural}_1 \right\|_2 + \left\| \mathbf{\Sigma}^{\natural}_2 \right\|_2 + \sqrt{\frac{p \log p}{n}} \right); \\
|T_4 - \mathbb{E}T_4| &\lesssim \frac{p\sqrt{\log p}}{d^{3/2}} \left(1 + c_0 \sqrt{\frac{\log p}{n}} \right) + \frac{\sqrt{p \log p}}{d} \left(1 + c_0 \sqrt{\frac{\log p}{n}} \right); \\
|T_5 - \mathbb{E}T_5| &\lesssim \frac{\log p}{d} \left(1 + \frac{c_1 p}{d} \right) \left(\left\| \left\| \mathbf{\Sigma}^{\natural} \right\| \right\|_{\text{off,F}} + p \sqrt{\frac{\log p}{n}} \right); \\
|T_6 - \mathbb{E}T_6| &\lesssim c_0 \sigma^2 \left(1 + c_1 \sqrt{\frac{\log p}{d}} \right) \sqrt{\frac{\log p}{d}} \left(1 + c_2 \left(\sqrt{\frac{d}{n}} \vee \frac{d}{n} \right) \right). \qquad (2.3.4)
\end{aligned}
$$

Combining (Equation 2.3.3) and (Equation 2.3.4) will yield the upper-bound for ϑ_1. Meanwhile for ϑ_2, we can invoke the standard result in [4], which gives $\vartheta_2 \lesssim \sqrt{\log p / n}$, and complete the proof.

2.4 Theoretical Properties of M-gLasso

We assume that the **irrepresentable condition**, which is stated as in Assumption 1 and previously used in [3].

Assumption 1. *There exists a positive constant $\alpha \in (0, 1]$ such that $\left\| \left\| \mathbf{\Gamma}_{S^c S} (\mathbf{\Gamma}_{SS})^{-1} \right\| \right\|_{1,1} \leq 1 - \alpha$.*

Under the above assumptions, the proposed M-gLasso estimator (Equation 2.2.2) has the following properties.

Theorem 1. *Let $\tau_\infty \lesssim \frac{\alpha}{6(\alpha+8)(\deg) \cdot \kappa^3_{\mathbf{\Sigma}} \kappa_{\mathbf{\Gamma}}}$, and set $\lambda_G^{\text{param}} = 8\tau_\infty / \alpha$. Then, with probability at least $1 - c_0 p^{-1} - c_1 p^2 e^{-c_2 d} - c_3 p^2 e^{-c_4 p}$, the matrix $\widehat{\mathbf{\Theta}}_G^{\text{param}}$ has the following properties*

- $(\widehat{\mathbf{\Theta}}_G^{\text{param}})_{i,j} = 0$ *for all* (i,j) *outside the support set* S, $(i,j) \in S^c$,
- *if* $\min_{(i,j)\in S} |\mathbf{\Theta}^{\natural}_{i,j}| \geq 2\kappa_{\mathbf{\Gamma}}(1+8\alpha^{-1})\tau_{\infty}$, *then* $\text{sign}(\widehat{\mathbf{\Theta}}_G^{\text{param}}) = \text{sign}(\mathbf{\Theta}^{\natural})$,

where c_i, $0 \leq i \leq 4$, *are some fixed positive constants independent of* n, d *and* p.

This theorem proves that M-gLasso can detect all conditionally independent pairs (the graph edges), provided that the non-zero elements $\mathbf{\Theta}^{\natural}_{i,j}$, $(i,j) \in S$, are strong enough, i.e., the absolute value of non-zero elements in $\mathbf{\Theta}^{\natural}$ are above some fixed threshold.

2.4.1 Discussions

In the following, we provide more insights regarding: (i) the minimum sample size and (ii) the minimum projection dimension d. An illustration of the infeasible region of n and d is plotted in Figure 2.1.

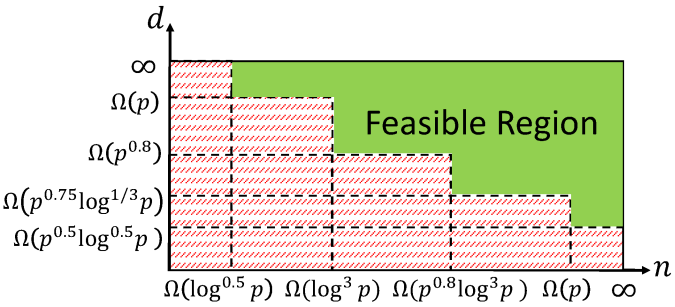

Figure 2.1: Infeasible region w.r.t number n and dimension d.

Minimum Sample Size n**.** In the high-dimensional setting, it is desirable to reduce the sample number n to less than the dimension of signal p, i.e., $n < p$. This subsection discusses the minimum sample size n under indirect observations.

Intuitively, large sample size n and dimension d, which corresponds to number of sensors in the real world applications, contribute to a more accurate recovery of the graphical structure. First we compute the minimum sample size n by letting $d \to \infty$. Treating α, $\kappa_{\mathbf{\Sigma}}$, and $\kappa_{\mathbf{\Gamma}}$ as some positive constants, Theorem 1 requires that $\deg \cdot \tau_{\infty}$ to be some positive constant, from which we can obtain the minimum sample size $n \gtrsim \sqrt{\deg^2 \cdot \log p}$. This

result coincides with the traditional setting where samples $\mathbf{X}^{(i)}$, $1 \leq i \leq n$ are observed directly (cf. Sec. $9.3.4$ in [5]).

For the case of indefinite sensing matrix $\mathbf{A} \in \mathbb{R}^{d\times p}$ ($d < p$), we need to increase the sample number n to the order of $\Omega\left(\deg^2 \cdot (\log p)^3\right)$, which is obtained by setting $d = cp$, where $0 < c < 1$ is some positive constant. When d reduces to $\Omega(p^{0.8})$, we need to further inflate the sample number n to be at least $\deg^2(\log p)^3 p^{0.8}$, which is still less than order p.

Minimum Projection Dimension d. This part investigates the minimum projection dimension d and proves the possibility of exact recovery of graph with an indefinite sensing matrix $\mathbf{A} \in \mathbb{R}^{d\times p}$ such that $d < p$. First we consider the special case where infinite samples are available, i.e., $n \to \infty$. Intuitively, more samples will lead to a more accurate estimation, which is captured by (Equation 2.3.1). As $n \to \infty$, the parameter τ approaches

$$\begin{aligned}\tau_\infty \simeq\ & \frac{c_0\sqrt{d\log p}}{d+1}\max_i \left\|\mathbf{\Sigma}_i^\natural\right\|_2 + \frac{c_6\sqrt{p\log p}}{d+1} + \frac{c_7 p\sqrt{\log p}}{\sqrt{d}(d+1)} \\ & + \frac{c_1\log p}{d+1}\left(1+\frac{c_2 p}{d}\right)\left|\!\left|\!\left|\mathbf{\Sigma}^\natural\right|\!\right|\!\right|_{\text{off,F}}.\end{aligned}$$

However, unlike covariance estimation from directly observed data, in indirect measurements, there is still a gap τ_∞ between the true and estimated covariance even with infinite number of measurements. This is caused by the under-determined sensing matrix $\mathbf{A}$. According to the assumption in Theorem 1, we require $\deg \cdot \tau_\infty$ to be less than some positive constant, which yields

$$d \gtrsim \deg^2 \cdot \log p \left(\max_i \left\|\mathbf{\Sigma}_i^\natural\right\|_2^2\right) \vee \sqrt{\deg \cdot p\log p \left|\!\left|\!\left|\mathbf{\Sigma}^\natural\right|\!\right|\!\right|_{\text{off,F}}} \vee \sqrt{\deg \cdot p\log p}. \tag{2.4.1}$$

Denote $0 < c^{'}, c^{''} < 1$ as some fixed constants. Provided that $\left|\!\left|\!\left|\mathbf{\Sigma}^\natural\right|\!\right|\!\right|_{\text{off,F}} = o\left(p\right)$ and $\max_i \left\|\mathbf{\Sigma}_i^\natural\right\|_2 = o(\sqrt{p})$, we can reduce (Equation 2.4.1) to

$$d \gtrsim \deg^2 \cdot \log p \cdot p^{1-c^{'}} \vee \sqrt{\deg \cdot \log p} \cdot p^{1-c^{''}},$$

which suggests the feasibility of the indefinite sensing matrix $\mathbf{A}$. If $\left\|\left\|\mathbf{\Sigma}^{\natural}\right\|\right\|_{\text{off,F}}$ reduces to some positive constant, the above requirement for d further reduces to $O(\sqrt{\text{deg} \cdot p \log p})$, which is approximately of order $\sqrt{\text{deg} \cdot p} \ll p$.

Under the high-dimensional setting where we require $n \leq p$, we need d to be at least

$$\begin{aligned} d \gtrsim & \sqrt{\text{deg} \cdot p \log p \cdot \left\|\left\|\mathbf{\Sigma}^{\natural}\right\|\right\|_{\text{off,F}}} \vee \sigma^2 \text{deg} \cdot \log p \\ & \vee p^{3/4} \left(\log p\right)^{1/3} \sqrt{\text{deg}} \vee \text{deg}^2 \cdot \log p \cdot \left(\max_i \left\|\mathbf{\Sigma}_i^{\natural}\right\|_2^2\right), \end{aligned}$$

which is less than p given that $\left\|\left\|\mathbf{\Sigma}^{\natural}\right\|\right\|_{\text{off,F}} = o\left(p\right)$ and $\max_i \left\|\mathbf{\Sigma}_i^{\natural}\right\|_2 = o(\sqrt{p})$. If $\left\|\left\|\mathbf{\Sigma}^{\natural}\right\|\right\|_{\text{off,F}}$ is some fixed positive constant, we can reduce the dimension d to $\sqrt{\text{deg}} \cdot p^{3/4}(\log p)^{1/3}$, approximately of the order $(\text{deg})^{1/2}\, p^{3/4}$.

2.4.2 Proof Outline

The analysis is based on **primal-dual method**, which is adapted from [3]. First we write the optimality condition for (Equation 2.2.2) as

$$\widehat{\mathbf{\Sigma}}_n^{\text{param}} - \left(\widehat{\mathbf{\Theta}}_G^{\text{param}}\right)^{-1} + \lambda_G^{\text{param}} \mathbf{G} = \mathbf{0}, \tag{2.4.2}$$

where $\mathbf{G}$ is the sub-gradient [120] of $\left\|\left\|\widehat{\mathbf{\Theta}}_G^{\text{param}}\right\|\right\|_{1,\text{off}}$ and is defined as

$$G_{ij} \triangleq \begin{cases} \text{sgn}(\widehat{\mathbf{\Theta}}_G^{\text{param}})_{i,j}, & \text{if } (\widehat{\mathbf{\Theta}}_G^{\text{param}})_{i,j} \neq 0; \\ \in [-1, 1], & \text{otherwise.} \end{cases}$$

for $i \neq j$. However, because of the complexity of (Equation 2.4.2), directly bounding the deviation $\|\widehat{\mathbf{\Theta}}_G^{\text{param}} - \mathbf{\Theta}^{\natural}\|_{\infty}$ can be difficult. Instead, we construct a pair $\left(\widetilde{\mathbf{\Theta}}_G^{\text{param}}, \widetilde{\mathbf{G}}\right)$ which satisfies: (i) $\widetilde{\mathbf{G}}$ is the sub-differential of $\left\|\left\|\widetilde{\mathbf{\Theta}}_G^{\text{param}}\right\|\right\|_{1,\text{off}}$; and (ii) the pair $(\widetilde{\mathbf{\Theta}}_G^{\text{param}}, \widetilde{\mathbf{G}})$ satisfies the condition in (Equation 2.4.2). Then we show it coincides with the solution of (Equation 2.2.2). The basic rational is as follows. First we verify that $\widehat{\mathbf{\Theta}}_G^{\text{param}}$ is the unique solution of (Equation 2.4.2). Since our constructed pairs $(\widetilde{\mathbf{\Theta}}_G^{\text{param}}, \widetilde{\mathbf{G}})$ satisfies the condition

in (Equation 2.4.2), which corresponds to the solution (Equation 2.2.2) exclusively, we can hence show the constructed pair $(\widetilde{\mathbf{\Theta}}_G^{\text{param}}, \widetilde{\mathbf{G}})$ is the identical solution of (Equation 2.2.2), namely, $(\widehat{\mathbf{\Theta}}_G^{\text{param}}, \mathbf{G})$. Afterwards, we can upper bound $\|\widehat{\mathbf{\Theta}}_G^{\text{param}} - \mathbf{\Theta}^\natural\|_\infty$ by investigating $\|\widetilde{\mathbf{\Theta}}_G^{\text{param}} - \mathbf{\Theta}^\natural\|_\infty$, which is more amenable for the analysis as following.

Stage I: construct $\widetilde{\mathbf{\Theta}}_G^{\text{param}}$. Given the oracle information of the support set S, we obtain $(\widetilde{\mathbf{\Theta}}_G^{\text{param}})_S$ as

$$(\widetilde{\mathbf{\Theta}}_G^{\text{param}})_S = \text{argmin}_{\substack{\mathbf{\Theta}\succ\mathbf{0} \\ \mathbf{\Theta}=\mathbf{\Theta}^\top, \mathbf{\Theta}_{S^c}=\mathbf{0}}} - \log\det\mathbf{\Theta} + \left\langle \widehat{\mathbf{\Sigma}}_n^{\text{param}}, \mathbf{\Theta} \right\rangle + \lambda_G^{\text{param}} \|\!|\mathbf{\Theta}|\!\|_{1,\text{off}}.$$

The rest of entries in $\widetilde{\mathbf{\Theta}}_G^{\text{param}}$, namely $(\widetilde{\mathbf{\Theta}}_G^{\text{param}})_{S^c}$, is set to zero.

Stage II: construct $\widetilde{\mathbf{G}}$. For the entry $(i,j) \in S$, we set $\widetilde{G}_{i,j} = \text{sign}(\widetilde{\mathbf{\Theta}}_G^{\text{param}})_{i,j}$. For the entry (i,j) that is outside of the support set S, we set $\widetilde{G}_{i,j}$ as

$$\widetilde{G}_{i,j} = \lambda_{n,G}^{-1} \left[\left(\widetilde{\mathbf{\Theta}}_G^{\text{param}} \right)^{-1}_{i,j} - (\widehat{\mathbf{\Sigma}}_n^{\text{param}})_{i,j} \right].$$

The goal of this step is to ensure that $\left(\widetilde{\mathbf{\Theta}}_G^{\text{param}}, \widetilde{\mathbf{G}}\right)$ satisfies (Equation 2.4.2).

Stage III: verify $\widetilde{\mathbf{G}}$ to be the sub-differential of $\left\|\!\left| \widetilde{\mathbf{\Theta}}_G^{\text{param}} \right|\!\right\|_{1,\text{off}}$. For the index $(i,j) \in S$, we can verify that they are the sub-differential of $\left| \left(\widetilde{\mathbf{\Theta}}_G^{\text{param}} \right)_{i,j} \right|$. The major focus is to show $|\widetilde{G}_{i,j}| < 1$ hold with high probability for the entry $(i,j) \in S^c$ given the condition in Theorem 1.

In the following analysis, we verify that $|\widetilde{G}_{i,j}| < 1$, which yields the upper-bound on $\|\widetilde{\mathbf{\Theta}}_G^{\text{param}} - \mathbf{\Theta}^\natural\|_\infty$ as a byproduct. We first need the necessary lemmas from [3].

Lemma 2 (Lemma 6 in [3]). *Suppose that* $r \triangleq 2\kappa_{\mathbf{\Gamma}} \left(\left\| \widehat{\mathbf{\Sigma}}_n^{\text{param}} - \mathbf{\Sigma}^\natural \right\|_\infty + \lambda_G^{\text{param}} \right) \leq \frac{1 \wedge \left(\kappa_{\mathbf{\Sigma}}^2 \kappa_{\mathbf{\Gamma}} \right)^{-1}}{3\kappa_{\mathbf{\Sigma}} \text{deg}}$, *then* $\left\| \widetilde{\mathbf{\Theta}}_G^{\text{param}} - \mathbf{\Theta}^\natural \right\|_\infty \leq r$.

Lemma 3 (Lemma 5 in [3]). *Provided that we have* $\left\|\widetilde{\mathbf{\Theta}}_G^{\text{param}} - \mathbf{\Theta}^\natural\right\|_\infty \leq (3\kappa_{\mathbf{\Sigma}}\text{deg})^{-1}$, *then*

$$\left\|\left(\widetilde{\mathbf{\Theta}}_G^{\text{param}}\right)^{-1} - \mathbf{\Theta}^{\natural-1} + \mathbf{\Theta}^{\natural-1}\left(\widetilde{\mathbf{\Theta}}_G^{\text{param}} - \mathbf{\Theta}^\natural\right)\mathbf{\Theta}^{\natural-1}\right\|_\infty \leq \frac{3}{2}\text{deg}\cdot\ \kappa_{\mathbf{\Sigma}}^3\left\|\widetilde{\mathbf{\Theta}}_G^{\text{param}} - \mathbf{\Theta}^\natural\right\|_\infty^2.$$

Lemma 4 (Lemma 4 in [3]). *If we have*

$$\left\|\widehat{\mathbf{\Sigma}}_n^{\text{param}} - \mathbf{\Sigma}^\natural\right\|_\infty \vee \left\|\left(\widetilde{\mathbf{\Theta}}_G^{\text{param}}\right)^{-1} - \mathbf{\Theta}^{\natural-1} + \mathbf{\Theta}^{\natural-1}\left(\widetilde{\mathbf{\Theta}}_G^{\text{param}} - \mathbf{\Theta}^\natural\right)\mathbf{\Theta}^{\natural-1}\right\|_\infty \leq \alpha\lambda_G^{\text{param}}/8,$$

we conclude that $|\widetilde{G}_{i,j}| < 1$.

Now, setting $\lambda_G^{\text{param}} = 8\tau_\infty/\alpha$, first we verify the conditions in Lemma 2. We have

$$r \overset{①}{\leq} 2\left(1 + 8\alpha^{-1}\right)\kappa_{\mathbf{\Gamma}}\tau_\infty \overset{②}{\leq} (3\kappa_{\mathbf{\Sigma}}\text{deg})^{-1}\left(1 \wedge \left(\kappa_{\mathbf{\Sigma}}^2\kappa_{\mathbf{\Gamma}}\right)^{-1}\right),$$

where in ① we use $\left\|\widehat{\mathbf{\Sigma}}_n^{\text{param}} - \mathbf{\Sigma}^\natural\right\|_\infty \leq \tau_\infty$ from Lemma 1, and in ② we use the assumptions of τ_∞ in Theorem 1. Then we conclude that

$$\left\|\widetilde{\mathbf{\Theta}}_G^{\text{param}} - \mathbf{\Theta}^\natural\right\|_\infty \leq 2\kappa_{\mathbf{\Gamma}}\ \left(\left\|\widehat{\mathbf{\Theta}}_n - \mathbf{\Theta}^\natural\right\|_\infty + \frac{8\tau_\infty}{\alpha}\right) \leq (3\kappa_{\mathbf{\Sigma}}\text{deg})^{-1}.$$

Invoking Lemma 3, we have

$$\left\|\left(\widetilde{\mathbf{\Theta}}_G^{\text{param}}\right)^{-1} - \mathbf{\Theta}^{\natural-1} + \mathbf{\Theta}^{\natural-1}\left(\widetilde{\mathbf{\Theta}}_G^{\text{param}} - \mathbf{\Theta}^\natural\right)\mathbf{\Theta}^{\natural-1}\right\|_\infty \leq \frac{3}{2}\text{deg}\times\ \kappa_{\mathbf{\Sigma}}^3\tau_\infty^2 \overset{③}{\leq} \tau_\infty,$$

where ③ is due to the requirement of τ_∞ in Theorem 1. In the end, we verify the condition in Lemma 4,

$$\alpha\lambda_G^{\text{param}}/8 = \tau_\infty \geq \left\|\widehat{\mathbf{\Sigma}}_n^{\text{param}} - \mathbf{\Sigma}^\natural\right\|_\infty \vee \left\|\left(\widetilde{\mathbf{\Theta}}_G^{\text{param}}\right)^{-1} - \mathbf{\Theta}^{\natural-1} + \mathbf{\Theta}^{\natural-1}\left(\widetilde{\mathbf{\Theta}}_G^{\text{param}} - \mathbf{\Theta}^\natural\right)\mathbf{\Theta}^{\natural-1}\right\|_\infty,$$

which concludes the proof.

2.5 Theoretical Properties of M-CLIME

We now modify the CLIME estimator in [4] and propose the *modified*-CLIME estimator, denoted by M-CLIME for indirect measurement scenario. The analysis of the proposed M-gLasso estimator required limiting the number of non-zero elements in columns without bounding their magnitude. For the analysis of M-CLIME estimator, we assume that $\mathbf{\Theta}^\natural$ lies within the region

$$\mathcal{U} = \left\{ \mathbf{\Theta} \mid \mathbf{\Theta} \succ \mathbf{0}, \quad \|\mathbf{\Theta}\|_{1,1} \leq M \right\},$$

where M is a fixed constant. This imposes an extra conditions on the magnitude of $\mathbf{\Theta}^\natural$. Define the element-wise hard-thresholding estimator $\mathcal{T}(\mathbf{\Theta}; \tau)$ as $\text{sign}(\mathbf{\Theta})\mathbb{1}(|\mathbf{\Theta}| \geq \tau)$. Then we have the following results.

Theorem 2. *Let* $\mathbf{\Theta}^\natural \in \mathcal{U}$ *and* $\min_{(i,j)\in S} |\mathbf{\Theta}^\natural_{i,j}| \geq 8M^2\tau_\infty$. *Then*

$$\text{sign}\left(\mathcal{T}\left(\widehat{\mathbf{\Theta}}_C^{\text{param}}; 4M^2\tau_\infty\right)\right) = \text{sign}(\mathbf{\Theta}^\natural) \tag{2.5.1}$$

holds with probability at least $1 - c_0 p^{-1} - c_1 p^2 e^{-c_2 d} - c_3 p^2 e^{-c4p}$, *where* c_i, $0 \leq i \leq 4$, *are some positive constants when setting the coefficient* $\lambda_C^{\text{param}} = c_4 M \tau_\infty$.

Compared with the M-gLasso estimator, M-CLIME is computationally more demanding. However, it can tolerate a larger threshold τ_∞ on values of $\|\widehat{\mathbf{\Theta}}_C^{\text{param}} - \mathbf{\Theta}^\natural\|_\infty$ when the dependencies among $\mathbf{X}$, i.e., $\min_{(i,j)\in S} |\mathbf{\Theta}^\natural_{i,j}|$, are strong enough. Apart from these two differences, its statistical properties are similar to M-gLasso in terms of the minimum sample complexity n, the minimum projection dimension d, and the differential privacy. Hence the corresponding discussions are omitted for a concise presentation.

2.5.1 Proof Outline

The key part is to bound $\left\|\widehat{\mathbf{\Theta}}_C^{\text{param}} - \mathbf{\Theta}^\natural\right\|_\infty$, which is adapted from [4] and conditioned on the event $\left\|\widehat{\mathbf{\Sigma}}_n^{\text{param}} - \mathbf{\Sigma}^\natural\right\|_\infty \leq \tau_\infty$ as in Lemma 1.

Stage I: We verify that $\mathbf{\Theta}^\natural$ lies within the region $\left\|\widehat{\mathbf{\Sigma}}_n^{\text{param}}\mathbf{\Theta}^\natural - \mathbf{I}\right\|_\infty \leq \lambda_C^{\text{param}}$ when setting $\lambda_C^{\text{param}} = M\tau_\infty$.

Stage II: We bound the element-wise ℓ_∞ norm on $\widehat{\mathbf{\Theta}}_C^{\text{param}} - \mathbf{\Theta}^\natural$, which reads

$$\begin{aligned}\left\|\widehat{\mathbf{\Theta}}_C^{\text{param}} - \mathbf{\Theta}^\natural\right\|_\infty &= \left\|\mathbf{\Theta}^\natural\mathbf{\Sigma}^\natural\left(\widehat{\mathbf{\Theta}}_C^{\text{param}} - \mathbf{\Theta}^\natural\right)\right\|_\infty \\ &\leq M\left[2\lambda_C^{\text{param}} + \left(\left\|\widehat{\mathbf{\Theta}}_C^{\text{param}}\right\|_{1,1} + \left\|\widehat{\mathbf{\Theta}}^\natural\right\|_{1,1}\right)\left\|\mathbf{\Sigma}^\natural - \widehat{\mathbf{\Sigma}}_n^{\text{param}}\right\|_\infty\right].\end{aligned}$$

After showing $\left\|\widehat{\mathbf{\Theta}}_C^{\text{param}}\right\|_{1,1} \leq \left\|\mathbf{\Theta}^\natural\right\|_{1,1}$, we conclude $\left\|\widehat{\mathbf{\Theta}}_C^{\text{param}} - \mathbf{\Theta}^\natural\right\|_\infty \leq 4M\lambda_C^{\text{param}}$.

Stage III: We prove (Equation 2.5.1) given the conditions in Theorem 2. First we show that $(\widehat{\mathbf{\Theta}}_C^{\text{param}})_{i,j} = 0$ if $\mathbf{\Theta}_{i,j}^\natural = 0$. This is because

$$\left|(\widehat{\mathbf{\Theta}}_C^{\text{param}})_{i,j}\right| \leq \left\|\widehat{\mathbf{\Theta}}_C^{\text{param}} - \mathbf{\Theta}^\natural\right\|_\infty \leq 4M^2\tau_\infty.$$

Due to the definition of hard-thresholding estimator $\mathcal{T}\left(\mathbf{\Theta}; 4M^2\tau_\infty\right)$, this entry will shrink to zero. Then we show that $\text{sign}((\widehat{\mathbf{\Theta}}_C^{\text{param}})_{i,j}) = \text{sign}(\mathbf{\Theta}_{i,j}^\natural)$ for $(i,j) \in S$. We assume that $(\widehat{\mathbf{\Theta}}_C^{\text{param}})_{i,j} > 0$ w.l.o.g. Then we have

$$\left|(\widehat{\mathbf{\Theta}}_C^{\text{param}})_{i,j}\right| \geq \left|\mathbf{\Theta}_{i,j}^\natural\right| - \left\|\widehat{\mathbf{\Theta}}_C^{\text{param}} - \mathbf{\Theta}^\natural\right\|_\infty \overset{④}{\geq} 4M\tau_\infty^2,$$

where ④ is due to the assumption in Theorem 2. Hence, we conclude that the sign is preserved by $\mathcal{T}\left(\mathbf{\Theta}; 4M^2\tau_\infty\right)$.

2.6 Numerical Experiments with Synthetic Data

The following context presents the numerical experiments. We only apply the M-gLasso estimator in Algorithm 1 because (i) M-CLIME has prohibitively high computational burden; and (ii) M-CLIME shares similar statistical properties with M-gLasso.

2.6.1 Impact of Sample Number n

We adopt the classical setting as [5] (9.5, P 252), where the ground-truth precision matrix $\mathbf{\Theta}^\natural$ is set to be

$$\left(\mathbf{\Theta}^\natural\right)_{ij} = \begin{cases} \rho_1, & \text{if } i = j; \\ \rho_2, & \text{if } |i-j| = 1; \\ 0, & \text{otherwise.} \end{cases}$$

Same as [5], we set $\rho_1 = 1$ and $\rho_2 = 0.4$. For other possible values of ρ_i, $i \in \{1, 2\}$, we should observe similar behaviors. [1] First we create samples $\mathbf{X}^{(i)}$ and then mask it by the sensing relation $\mathbf{Y}^{(i)} = \mathbf{A}\mathbf{X}^{(i)} + \mathbf{W}^{(i)}$, where $A_{ij} \overset{\text{i.i.d}}{\sim} \mathcal{N}(0, 1)$ and $\mathbf{W}^{(i)} \sim \mathcal{N}(\mathbf{0}, \sigma^2 \mathbf{I}_{n\times n})$. With our estimator M-gLasso, we reconstruct $\widehat{\mathbf{\Theta}}_G^{\text{param}}$ and evaluate it with the recall rate and precision rate. The results are shown in Figure 2.2 and Figure 2.3, respectively.

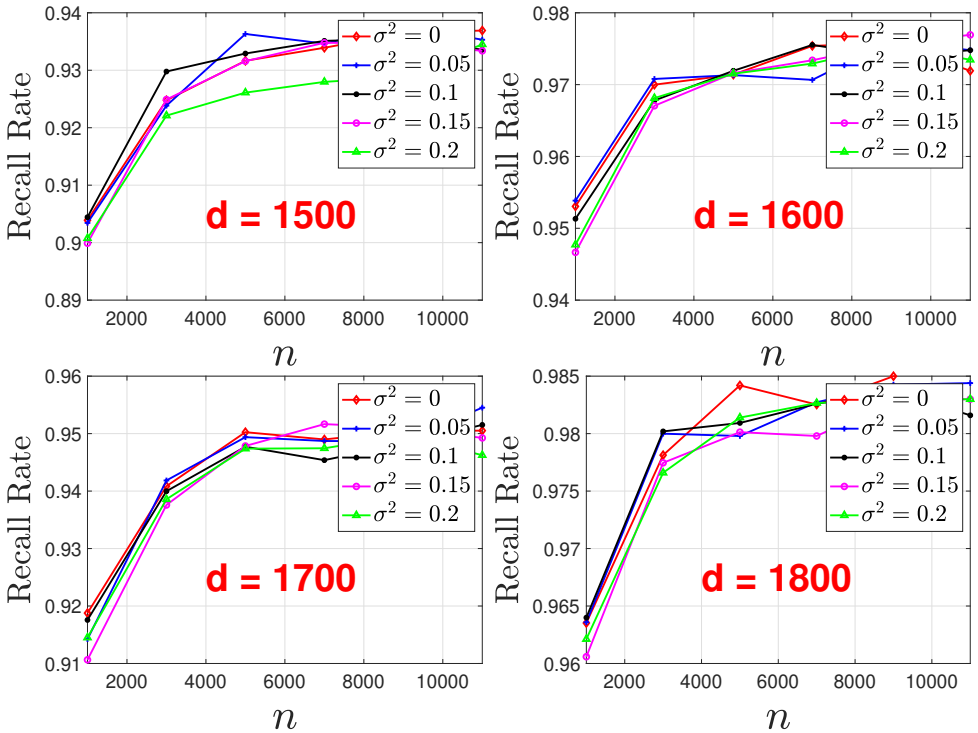

Figure 2.2. We study the impact of sample size n on the recall rate. The signal dimension p is fixed as 2000.

[1] Notice that $\Sigma^\natural_{ii} \neq 1$ in this setting. Hence we need to adapt the estimation of the diagonal elements of $\widehat{\Sigma}$.

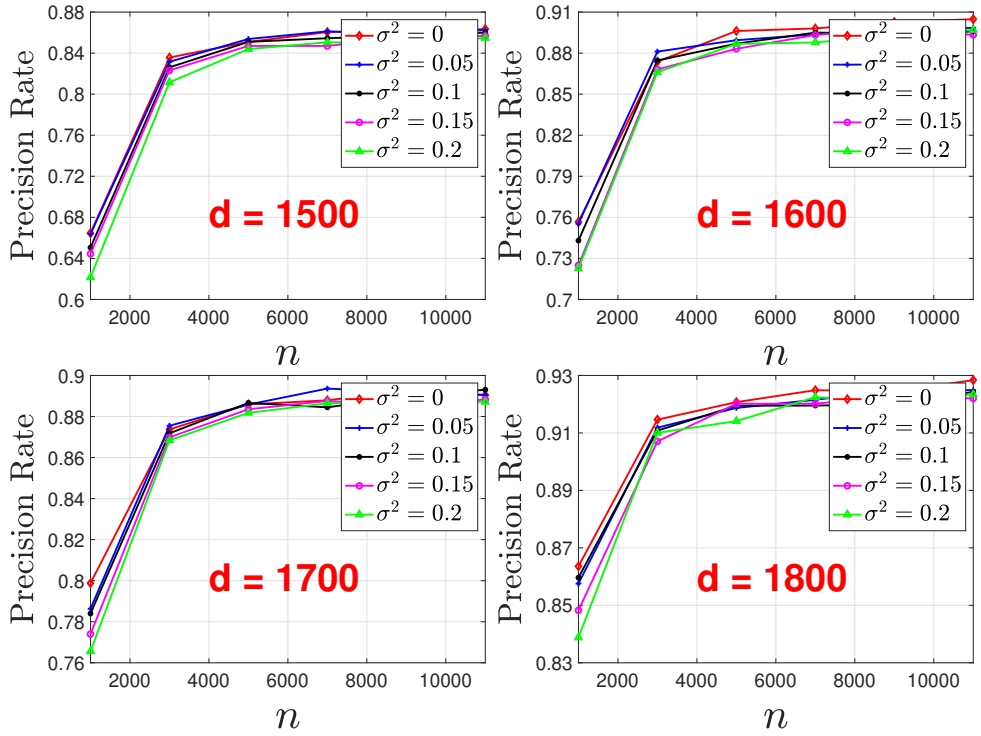

Figure 2.3. We study the impact of sample size n on the precision rate. The signal dimension p is fixed as 2000.

2.6.2 Discussions

From Figures 2.2 and 2.3, we confirm that the edge of graphical model can be selected correctly with high probability even when the dimension of the projection space is much lower than the dimension of the signal. In addition, we notice a threshold effect on n when $\sigma^2 = 1$ in Figure 2.3. This can be explained by the parameter τ_∞ in (Equation 2.3.1), which contains the term $\frac{c_8\sigma^2 \log p}{d}(1 + c_9(\sqrt{\frac{d}{n}} \vee \frac{d}{n}))$. If d is not high enough, this term is still lower-bounded by $c_8\sigma^2 \log p/d$ even as $n \to \infty$, which means a large τ_∞ and further the violation of the assumption in Theorem 1.

Generally speaking, we find larger sample size n, higher dimension d, and lower noise variance σ^2 contribute to the more accurate edge selection, which is consistent with our intuition and verifies Theorem 1.

2.7 Numerical Experiments with Real-world Database

We now consider the real-world databases, which consists of 5 databases: Carolina Breast Cancer (GSE148426) with 2497 samples (patients) [121], Lung Cancer (GSE137140) with 3924 samples [8], Ovarian Cancer (GSE106817) with 4046 samples [122], Colorectal Cancer (GSE115513) with 1513 samples [123], and Esophageal Squamous Cell Carcinoma (GSE122497) with 5531 samples [124]. For each patient in the database, the measurements are given as the concentration of miRNAs. The miRNAs are known to have dependency among each other, i.e., a non-diagonal precision matrix, and hence there is an underlying graphical model describing these dependency structure based on the associated precision matrix. In our experiments we will use the recovered/ estimated precision matrix inside a classification task. The accuracy of the classification algorithm under two precision matrices, one estimated from direct observation referred to as the *Baseline* method in Table 2.1 and another from indirect observation using our method, will be presented for performance comparison.

Table 2.1. Classification Accuracy (CA) on real-world databases, namely, GSE148426 [121], GSE137140 [8], GSE106817 [122], GSE115513 [123], and GSE122497 [124]. The baseline corresponds to the precision matrix $\mathbf{\Theta}_i$, $i \in \{1, 2\}$, trained by direct observations.

d/p	GSE 148426	GSE 137140	GSE 106817	GSE 115513	GSE 122497
0.1	0.49	0.37	0.46	0.49	0.38
0.2	0.49	0.49	0.50	0.49	0.70
0.5	0.49	0.63	0.50	0.50	0.74
1.0	0.51	0.64	0.50	0.50	0.77
2.0	0.51	0.64	0.50	0.50	0.77
5.0	0.51	0.64	0.50	0.50	0.77
10.0	0.51	0.64	0.50	0.50	0.77
Baseline	0.51	0.63	0.5	0.48	0.75

2.7.1 Preprocess

For each database, there are multiple types of data, namely, healthy vs non-healthy, benign cancer vs non-benign cancer, etc. Based on the labels, we first divide the whole dataset into

two types of data and separately preprocess them. For each type, we split the data into the training and testing sets $\{\mathcal{D}^i_{\text{train}}, \mathcal{D}^i_{\text{test}}\}$, $i \in \{1, 2\}$. The sensing matrix $\mathbf{A}$ is assumed to be $A_{ij} \overset{\text{i.i.d}}{\sim} \mathcal{N}(0, 1)$ and the measurement noise $\mathbf{w}$ is set to be zero.

2.7.2 Training

Using the training set $\mathcal{D}^i_{\text{train}}$, which are directly observed from the desired signal (miRNAs), we first select the penalty coefficients in graphical lasso via cross-validation. Then estimate the precision matrix via the graphical Lasso and use it as the baseline $\mathbf{\Theta}_i$, $i \in \{1, 2\}$ as they are obtained through direct observation. We denote $\mathbf{\Theta}_1$ for $\mathcal{D}^1$ while $\mathbf{\Theta}_2$ for $\mathcal{D}^2$. Then we mask the training set with the synthetic sensing matrix $\mathbf{A}$ and create indirect observation of data. Last we estimate the precision matrix $\widehat{\mathbf{\Theta}}_i$, from the indirect observations, i.e., $\mathbf{A}\mathcal{D}^i_{\text{train}}$ using M-gLasso, $i \in \{1, 2\}$.

2.7.3 Testing

Notice that the ground-truth precision matrix $\mathbf{\Theta}^\natural_i$, $i \in \{1, 2\}$ cannot be obtained in the real-world applications, even with the direct observations. Hence a direct comparison between $\mathbf{\Theta}^\natural_i$ and $\widehat{\mathbf{\Theta}}_i$ cannot be performed. To evaluate the performance of the algorithm, we take an indirect way by using *quadratic discriminant analysis* [125] to perform classification in the testing set $\{\mathcal{D}^1_{\text{test}} \bigcup \mathcal{D}^2_{\text{test}}\}$, with the estimated matrix $\widehat{\mathbf{\Theta}}_i$, $i \in \{1, 2\}$. Then we compare with the classification accuracy when using $\mathbf{\Theta}_i$, $i \in \{1, 2\}$. The summary of the classification rates are shown in Table 2.1.

2.7.4 Discussion

From the tables we conclude that our estimated precision matrix $\widehat{\mathbf{\Theta}}_i$ achieves almost the same classification accuracy with the baseline $\mathbf{\Theta}_i$ when $d = p$, and is only a slightly worse when $d = 0.5p$, i.e., the dimension of the projection space under the indirect observation is half of the dimension of the signal space. In some special cases, we even see some

improvements with indirect observations. One possible reason is that the features are mixed by sensing matrix $\mathbf{A}$, which lead to better quantities for the classification.

2.8 Conclusions

We studied the problem of learning the graphical structure of Gaussian graphical model by using only indirect observations, i.e., the observations obtained via compressive sensing of the desired signal. Assuming the sensing matrix to be indefinite Gaussian matrix, we proposed two estimators, M-CLIME and M-gLasso, and showed that the correct reconstruction can be guaranteed under mild conditions, from which the relation between the sample number n, dimension of signal p, and projection dimension d are obtained. In addition, we provided numerical experiments, from both synthetic and real world miRNA data, to corroborate the correctness of our theorems.

CHAPTER 3

NON-PARAMETRIC LEARNING OF GRAPHICAL MODELS

3.1 Introduction

In this chapter, we extend the parametric method of learning the pair-wise independence relation (structure) of graphical models under indirect observations in chapter 2 to the non-parametric method. Same as the previous chapter, we assume the indirect sensing relation reading as

$$\mathbf{Y}^{(s)} = \mathbf{A}\mathbf{X}^{(s)} + \mathbf{W}^{(s)}, \;\; 1 \leq s \leq n,$$

where $\mathbf{Y}^{(s)}$ denotes the sth measurement, $\mathbf{A} \in \mathbb{R}^{d \times p}$ denotes the sensing matrix, and $\mathbf{W} \in \mathbb{R}^{d}$ denotes the sensing noise. Our goal is to learn the graphical structure from the indirect measurements $\{\mathbf{Y}^{(s)}\}_{1 \leq s \leq n}$ with a non-parametric method.

Different from the previous chapter which focuses only on the Gaussian distributed random vector $\mathbf{X}$, this chapter considers a much broader family of distributions, i.e., the nonparanormal distribution, which means the joint distribution $\mathbf{g}(\mathbf{X})$ exhibits a Gaussian distribution of $\mathcal{N}(\boldsymbol{\mu}, \boldsymbol{\Sigma})$ after the transform of certain function $\mathbf{g}(\mathbf{X}) = \; [g_i(X_i) \; \cdots \; g_p(X_p)]^\top$. A rigorous definition of nonparanormal distribution is deferred to Defition 1 later in this chapter.

Compared with the previous work on non-parametric learning method which assumes direct measurements under the noiseless setting, our work considers the noisy indirect measurements. How to obtain a reliable estimation of the transform function $\mathbf{g}(\cdot)$ in the presence of the measurement noise $\mathbf{W}$ constitutes the technical bottleneck. To handle such an issue, we relax the constraint that sensing matrix $\mathbf{A}$ is under-determined. In fact, whether a compressive sensing system, i.e., $d < p$, can be used to estimate the transform function

$\mathrm{g}(\cdot)$ still remains an open-problem.

3.2 Background

We begin the discussion with some background knowledge on the nonparanormal distribution.

Definition 1 (Nonparanormal)**.** *We call a set of random variables* $\mathbf{X} = [X_i \ \cdots \ X_p]^\top$ *follow the* nonparanomral distribution*, namely,* $\mathbf{X} \sim \text{NPN}(\mathrm{g}, \boldsymbol{\mu}, \boldsymbol{\Sigma})$*, if there exists a set of functions* $\{g_j\}_{1 \le j \le p}$ *such that* $\mathbf{Z} = [g_1(X_1) \ \cdots \ g_p(X_p)]^\top$ *follows the Gaussian distribution, i.e.,* $\mathbf{Z} \sim \mathcal{N}(\boldsymbol{\mu}, \boldsymbol{\Sigma})$.

Assume that $\mathbf{X}$ satisfies the nonparanormal assumption, i.e., $\mathbf{X} \sim \text{NPN}(\mathrm{g}, \boldsymbol{\mu}, \boldsymbol{\Sigma})$. Let $\boldsymbol{\Theta}$ be the inverse matrix of the covariance matrix $\boldsymbol{\Sigma}$.

Lemma 5 (Lemma 3 in [25])**.** *Random variables* X_i *and* X_j *are pairwise conditionally independent, i.e.,* $X_i \perp X_j \left| X_{\setminus i,j} \right.$*, iff* $\boldsymbol{\Theta}_{ij} = 0$.

Thus, the pair-wise independence relation across the entries of $\mathbf{X}$ is fully incorporated into the matrix $\boldsymbol{\Theta}$. Denote the marginal distribution function of the ith entry X_i as $F_i(\cdot)$ and define the function $h_i(x) = \Phi^{-1}(F_i(x))$, where $\Phi(\cdot)$ is the CDF of the standard normal RV, namely, $\Phi(\cdot) = \frac{1}{\sqrt{2\pi}} \int_{-\infty}^{(\cdot)} e^{-t^2/2} dt$. According to [25], we can estimate function $g_i(\cdot)$ by estimating function $h_i(\cdot)$, from which we can conclude the bottleneck in estimating the graphical structure lies in the estimation of the CDF functions, i.e., $F_i(\cdot), 1 \le i \le p$. Different from the previous work [25], our sensing relation assumes noisy indirect measurements instead of noiseless direct measurements, which bring extra difficulties.

Notations The imaginary number $\sqrt{-1}$ is denoted as $\mathbb{j}$. The support set S is defined as $S = \{(i,j) \mid \boldsymbol{\Theta}_{i,j} \neq 0, \ \forall\, i,j\}$, where $\boldsymbol{\Theta}$ is the inverse of the covariance matrix $\boldsymbol{\Sigma}$. Moreover, we define the maximum Markov blanket in the graphical model as deg, or equivalently the maximum of the non-zero entries in an arbitrary column of $\boldsymbol{\Theta}$, i.e., $\text{deg} \triangleq \max_i \|\boldsymbol{\Theta}_i\|_0$. The parameter $\kappa_{\boldsymbol{\Sigma}}$ is defined as $\left\|\boldsymbol{\Sigma}\right\|_{\infty,\infty}$. Furthermore, we define the Fisher information

matrix of $\mathbf{\Sigma}$ be $\mathbf{\Gamma} \triangleq \mathbf{\Sigma} \otimes \mathbf{\Sigma}$, where $\otimes$ is the kronecker product [126]. The parameter $\kappa_{\mathbf{\Gamma}}$ is defined as $\left\|\left(\mathbf{\Gamma}_{SS}\right)^{-1}\right\|_{\infty,\infty}$.

3.3 Problem Formulation

We start this section with a formal restatement of the sensing relation reading as

$$\mathbf{Y}^{(s)} = \mathbf{A}\mathbf{X}^{(s)} + \mathbf{W}^{(s)}, \;\; 1 \leq s \leq n, \tag{3.3.1}$$

where $\mathbf{Y}^{(s)} \in \mathbb{R}^d$ denotes the sth reading, $\mathbf{A} \in \mathbb{R}^{d \times p}$ $(d > p)$ is the sensing matrix with each entry A_{ij} being a standard normal RV, i.e., $A_{ij} \sim \mathcal{N}(0,1)$, $\mathbf{X}^{(s)} \in [0,1]^p$ denotes the sth sample, and $\mathbf{W}^{(s)} \in \mathbb{R}^d$ denotes the measurement noise with each entry $\mathbf{W}_{ij}$ being a Gaussian RV with zero mean and variance σ^2, i.e., $\mathbf{W}_{ij} \sim \mathcal{N}(0, \sigma^2)$.

Our goal is to uncover the graphical structure (or pair-wise independence) of $\mathbf{X}$, or equivalently, to detect the support set of the matrix $\mathbf{\Theta}$ from the indirect observations $\left\{\mathbf{Y}^{(s)}\right\}_{1 \leq s \leq n}$. Before proceed, we first list the assumptions.

- We assume extra measurements being conducted, i.e., $d > p$, which is to suppress the sensing noise and improve the performance of graphical structure recovery.
- We assume that random vector $\mathbf{X}$ follows a nonparanormal distribution and most entries are pair-wise independent, i.e., the matrix $\mathbf{\Theta}$ is sparse, a widely-used assumption in previous works [25, 27, 30].

3.4 Graphical Structure Estimator

This section presents the estimator for the graphical structure. According to Lemma 5, we conclude the bottleneck in estimating the graphical structure lies in the estimation of the CDF functions, i.e., $F_i(\cdot)$, $1 \leq i \leq p$. Different from the previous work [25], our sensing relation assumes noisy indirect measurement instead of noiseless direct measurement,

which brings extra difficulties.

Algorithm 3 Graphical Structure Estimator.

Input: Samples $\{\mathbf{Y}^{(i)}\}_{i=1}^n \in \mathbb{R}^p$ and sensing matrix $\mathbf{A} \in \mathbb{R}^{d\times p}$.
Stage I. We reconstruct the values $\widehat{\mathbf{X}}^{(s)}$ via the *least-square* (LS) estimator reading as

$$\widehat{\mathbf{X}}^{(s)} = \text{argmin}_{\mathbf{X}} \left\| \mathbf{Y}^{(s)} - \mathbf{A}\mathbf{X} \right\|_2. \tag{3.4.1}$$

Stage II. We estimate the marginal distribution function $\widehat{F}_i(\cdot)$ for the ith entry from the samples $\{\widehat{X}_i^{(s)}\}_{1\le s\le n}$ reading as

$$\widehat{F}_i(x) = \frac{1}{2} - \frac{1}{n\pi}\sum_{s=1}^n \int_0^\infty \frac{\sin\left[t(\widehat{X}_i^{(s)} - x)\right]}{t} \times \frac{\exp\left(-\frac{\sigma^2 t^2}{2(d-p)}\right)}{\exp\left(-\frac{\sigma^2 t^2}{d-p}\right) \vee \gamma t^a} dt, \tag{3.4.2}$$

where $\gamma > 0$ and $a > 1$ are some fixed positive constants. Then we truncate the estimated CDF function as

$$\widehat{F}_i^{\text{tr}}(x) = \begin{cases} \delta_{n,d,p}, & \widehat{F}_i(x) \le \delta_{n,d,p}; \\ \widehat{F}_i(x), & \delta_{n,d,p} \le \widehat{F}_i(x) \le 1-\delta_{n,d,p}; \\ 1-\delta_{n,d,p}, & \widehat{F}_i(x) \ge 1-\delta_{n,d,p}, \end{cases} \tag{3.4.3}$$

where $\delta_{n,d,p} > 0$ is some pre-determined parameter.
Stage III. First, we estimate the mean $\widehat{m}_i$ and the variance $\widehat{v}_i$ as

$$\widehat{m}_i = \frac{1}{n}\sum_{s=1}^n \widehat{X}_i^{(s)}; \quad \widehat{v}_i = \sqrt{\frac{1}{n-1}\sum_{s=1}^n \left(\widehat{X}_i^{(s)} - \widehat{m}_i\right)^2 - \frac{n}{n-1}\frac{\sigma^2}{d-p}}.$$

Then we estimate the covariance matrix $\widehat{\mathbf{\Sigma}}_n^{\text{non-param}}$ as

$$\widehat{\mathbf{\Sigma}}_n^{\text{non-param}} = \frac{1}{n}\sum_{s=1}^n \left[\widehat{\mathbf{h}}\left(\widehat{X}^{(s)}\right) - \widehat{\boldsymbol{\mu}}\right]\left[\widehat{\mathbf{h}}\left(\widehat{X}^{(s)}\right) - \widehat{\boldsymbol{\mu}}\right]^\top, \tag{3.4.4}$$

where the ith entry of $\widehat{\mathbf{h}}$ is defined as $\widehat{h}_i(x) = \widehat{m}_i + \widehat{v}_i\Phi^{-1}(\widehat{F}_i^{\text{tr}}(x))$, and $\widehat{\boldsymbol{\mu}}$ is the estimated mean of $\widehat{\mathbf{h}}(\cdot)$, namely, $n^{-1}\sum_{s=1}^n \widehat{\mathbf{h}}(\mathbf{X}^{(s)})$.
Stage IV. We reconstruct the matrix $\widehat{\mathbf{\Theta}}_G^{\text{non-param}}$ as

$$\widehat{\mathbf{\Theta}}_G^{\text{non-param}} = \text{argmin}_{\mathbf{\Theta}} \log\det(\mathbf{\Theta}) - \text{Tr}\left(\mathbf{\Theta}\widehat{\mathbf{\Sigma}}_n^{\text{non-param}}\right) + \lambda_G^{\text{non-param}}\|\mathbf{\Theta}\|_1, \tag{3.4.5}$$

where $\lambda > 0$ is some positive constant for the regularizer $\|\mathbf{\Theta}\|_1$.
Output: Estimated matrix $\widehat{\mathbf{\Theta}}_G^{\text{non-param}}$.

The basic idea of our estimator is to first transform the sensing relation in (Equation 3.3.1) to the additive model such that $\widehat{\mathbf{X}}^{(s)} = \mathbf{X}^{(s)} + \widehat{\mathbf{W}}^{(s)}$, where $\widehat{\mathbf{W}}^{(s)}$ is defined as $\left(\mathbf{A}^\top\mathbf{A}\right)^{-1}\mathbf{A}\mathbf{W}^{(s)}$. Then our task reduces to estimating the marginal CDF from the samples $\widehat{\mathbf{X}}^{(s)}$, which is contaminated by the noise $\widehat{\mathbf{W}}^{(s)}$. This problem can be broadly categorized as the *density deconvolution* problem in statistics. When comparing with the previous work, we can ac-

cess some inexact knowledge of the distribution of $\widehat{\mathbf{W}}^{(s)}$. To put more specifically, we can only compute its mean and the approximated value of its variance as

$$\mathbb{E}(\widehat{w}_i) = 0, \;\; \text{Var}(\widehat{w}_i) \approx \frac{\sigma^2}{d-p}, \tag{3.4.6}$$

where $\widehat{w}_i$ denotes the ith entry of the noise $\widehat{\mathbf{W}}$. Whereas the previous work such as [31, 32, 33, 34] assumes perfect knowledge of the distribution, and the work [39, 40, 41] assumes total ignorance of the distribution and requires extra steps to estimate the variance of noise $\{\widehat{\mathbf{W}}^{(s)}\}_{1\leq s\leq n}$. The computation procedure of (Equation 3.4.6) is deferred to Lemma 32 and the details of the estimator is summarized in Algorithm 3.

3.5 Properties of CDF Estimator

This section investigates the properties of the marginal CDF estimator in (Equation 3.4.2) where each entry X_i is within the region $[0, 1]$. We begin the discussion by presenting the assumptions.

Definition 2 (Density family $\mathcal{F}_{\alpha,L}$)**.** *The density family $\mathcal{F}_{\alpha,L}$ is defined as the set of all distributions whose density functions $f(\cdot)$ and characteristic functions $\phi(\cdot)$ possess the following properties:*

- *The density functions $f(\cdot)$ satisfy $\int_{-\infty}^{\infty} x^2 f(x)dx < \infty$;*
- *The characteristic functions $\phi(\cdot)$ satisfy $\int_{-\infty}^{\infty} |\phi(t)|^2 (1+t^2)^{\alpha} dt \leq L$.*

We also need the following two assumptions.

Assumption 2. *For an arbitrary entry X_i, we assume its distribution belongs to the density family $\mathcal{F}_{\alpha,L}$ such that $\alpha > -\frac{1}{2}$.*

Assumption 3. *For an arbitrary entry X_i, we assume its density function $f_i(\cdot)$ is bounded by some constant L_f, i.e., $|f_i(\cdot)| \leq L_f$.*

Setting the parameter a as some fixed positive constant and using $\gamma \asymp \log(np)\left(\frac{\sigma^2}{d-p}\right)^{a/4}$, we can prove that the estimation error of the CDF estimator converges to zero with high probability, which is formally stated in the following theorem.

Theorem 3. *Under the Assumptions 2 and 3,*

$$\sup_{x\in[0,1]}\left|F_i(x)-\widehat{F}_i(x)\right| \leq (\log n)\varepsilon_x + \ c_1\sqrt{\varepsilon_x} + \frac{c_2}{\sqrt{n}}, \tag{3.5.1}$$

for $1 \leq i \leq p$*, holds with probability exceeding* $1-o(1)$ *when setting* $\gamma \asymp \log(np)\left(\frac{\sigma^2}{d-p}\right)^{\frac{a}{4}}$. *The parameter* ε_x *is defined as*

$$\varepsilon_x \triangleq \frac{\log^{2/a}(np)\sigma}{\sqrt{d-p}} + \frac{\log^2(np)}{(d-p)^{\frac{a}{4}}} + \left(\frac{\sigma^2}{d-p}\right)^{\frac{2\alpha+1}{4}} + \frac{1}{n}, \tag{3.5.2}$$

where $a > 1$ *is some pre-determined positive constant.*

To the best of our knowledge, this is the first non-asymptotic uniform bound on the estimation error of a CDF deconvolution estimator with inexact knowledge of the noise variance. Details of the proof is deferred to section B.1.

Remark 1. *A more readable form of* ε_x *defined in* (Equation 3.5.2) *is given as*

$$\varepsilon_x \asymp \frac{\log^2(np)}{(d-p)^{\beta}} + \frac{1}{n},$$

where β *is defined as* $\frac{1}{2} \wedge \frac{a}{4} \wedge \frac{2\alpha+1}{4}$. *Thus, we can simplify the bound in* (Equation 3.5.1) *as*

$$\sup_{x\in[0,1]}\left|F_i(x)-\widehat{F}_i(x)\right| \lesssim \frac{\log(np)}{(d-p)^{\beta/2}} + \frac{1}{\sqrt{n}}.$$

3.5.1 Proof Outline

At the core of the proof is the Talagrand inequality (cf. 2.6 in [127]), which is stated as

$$\mathbb{P}\left[\left|\left\|\widehat{F}-F\right\|_\infty-\mathbb{E}\left\|\widehat{F}-F\right\|_\infty\right|\geq t\right]\lesssim\exp\left(-\frac{nt}{KC_U}\log\left(1+\frac{ntC_U}{V}\right)\right),$$

where C_U is the uniform bound for $\left\|\widehat{F}-F\right\|_\infty$, i.e., $\left\|\widehat{F}-F\right\|_\infty\leq C_U$ for all x and s, and the variance V satisfies

$$V\geq n\sup_{x\in[0,1]}\mathbb{E}\left|F_i(x)-\widehat{F}_i(x)\right|^2+16C_U\cdot\left(\mathbb{E}\left|F_i(x)-\widehat{F}_i(x)\right|\right).$$

Step I. We first verify that

$$\left|F_i(x)-\widehat{F}_i(x)\right|\leq C_U$$

holds universally for all possible x.

Step II. We first prove

$$\mathbb{E}\left|F_i(x)-\widehat{F}_i(x)\right|^2\lesssim\frac{\log^{2/a}(np)\sigma}{\sqrt{d-p}}+\frac{(\log(np))^2}{(d-p)^{\frac{a}{4}}}+\left(\frac{\sigma^2}{d-p}\right)^{\frac{2\alpha+1}{4}}+\frac{1}{n}.$$

Define the function $\widetilde{F}(\cdot)$ as

$$\widetilde{F}(x)=\frac{1}{2}-\frac{1}{\pi}\int_0^\infty\frac{1}{t}\Im\left[\frac{\phi_{\widehat{w}}(-t)\widehat{\phi}_{\widehat{X}}(t)}{|\phi_{\widehat{w}}(t)|^2\vee\gamma t^a}e^{-\mathbb{j}tx}\right]dt,$$

we perform the decomposition

$$\mathbb{E}\left|F_i(x)-\widehat{F}_i(x)\right|^2\leq2\mathbb{E}\left|\widehat{F}(x)-\widetilde{F}(x)\right|^2+2\mathbb{E}\left|\widetilde{F}(x)-F(x)\right|^2.$$

Afterwards, we complete the proof by separately proving

$$\mathbb{E}\left|\widehat{F}(x)-\widetilde{F}(x)\right|^2\lesssim\frac{\log^{2/a}(np)\sigma}{\sqrt{d-p}}$$

and

$$\mathbb{E}\left|\widetilde{F}(x)-F(x)\right|^2 \lesssim \frac{(\log(np))^2}{(d-p)^{\frac{a}{4}}}+\left(\frac{\sigma^2}{d-p}\right)^{\frac{2\alpha+1}{4}}+\frac{1}{n}.$$

Step III. We bound the expectation $\mathbb{E}\left\|F_i-\widehat{F}_i\right\|_\infty$ as

$$\mathbb{E}\left\|F_i-\widehat{F}_i\right\|_\infty \leq \mathbb{E}\left|F_i(x)-\widehat{F}_i(x)\right|+\frac{c_0}{\sqrt{n}}.$$

Setting t as $V\log n/n$, we conclude

$$\sup_x \Delta_x \leq \mathbb{E}\sup_x \Delta_x + \frac{cV\log n}{n}$$

holds with probability exceeding $1-O(n^{-c})$.

3.6 Theoretical Properties of Graphical Structure Estimator

The technical challenges in this part can be divided as two parts: (i) choosing the appropriate truncation parameter $\delta_{n,d,p}$ in (Equation 3.4.3); and (ii) estimating the covariance matrix with the noisy samples $\left\{\mathbf{Y}^{(s)}\right\}_{1\leq s\leq n}$.

Denote the oracle empirical covariance matrix $\mathbf{\Sigma}_n^{\text{non-param}}$ as

$$\mathbf{\Sigma}_n^{\text{non-param}} \triangleq \frac{1}{n}\sum_{s=1}^n \mathbf{h}(\mathbf{X}^{(s)})\mathbf{h}(\mathbf{X}^{(s)})^\top - \left(\frac{1}{n}\sum_{s=1}^n \mathbf{h}(\mathbf{X}^{(s)})\right)\left(\frac{1}{n}\sum_{s=1}^n \mathbf{h}(\mathbf{X}^{(s)})\right)^\top, \quad (3.6.1)$$

where $h(\cdot)$ denotes the oracle estimator of the transform functions in Def. 1. The core of the analysis lies on bounding the estimation error of the covariance matrix in terms of the ℓ_∞. In comparison with the previous work [25], we cannot directly access the samples $\left\{\mathbf{X}^{(s)}\right\}_{1\leq s\leq n}$. Instead, we have to use the perturbed samples $\{\widehat{\mathbf{X}}^{(s)}\}_{1\leq s\leq n}$, which will lead to additional errors in estimating the covariance matrix. How to bound these errors constitutes the technical bottleneck.

Define β as $\frac{1}{2} \wedge \frac{a}{4} \wedge \frac{2\alpha+1}{4}$ and set $\delta_{n,d,p}$ in (Equation 3.4.3) as

$$\delta_{n,d,p} = \frac{c_0}{(\log n)n^{1/4}} + \frac{c_1 \log^2(np)}{\sqrt{\log(d-p)}(d-p)^{\beta/4}}. \tag{3.6.2}$$

We conclude

Theorem 4. *Under the Assumption 2 and Assumption 3, we have*

$$\left\| \mathbf{\Sigma}_n^{\text{non-param}} - \widehat{\mathbf{\Sigma}}_n^{\text{non-param}} \right\|_\infty \lesssim \sqrt{\log n \vee \log(d-p)} \left(\frac{\sqrt{\log n}}{n^{1/4}} \vee \frac{\sqrt{\log(d-p)}}{(d-p)^{\beta/4}} \right),$$

with probability exceeding $1 - o(1)$*, where* $\delta_{n,d,p}$ *is set as* (Equation 3.6.2)*,* β *is defined as* $\frac{1}{2} \wedge \frac{a}{4} \wedge \frac{2\alpha+1}{4}$*, and* $\mathbf{\Sigma}_n^{\text{non-param}}$ *and* $\widehat{\mathbf{\Sigma}}_n^{\text{non-param}}$ *are defined in* (Equation 3.6.1) *and* (Equation 3.4.4)*, respectively.*

Having obtained the covariance matrix $\widehat{\mathbf{\Sigma}}_n^{\text{non-param}}$, we estimate the graphical structure of $\mathbf{X}$ by plugging $\widehat{\mathbf{\Sigma}}_n^{\text{non-param}}$ into the graphical lasso estimator [5], which is put in (Equation 3.4.5). Same as the parametric method, we assume the **irrepresentable condition** to analyze the properties of the graphical structure estimator,

Assumption 4. *There exists a positive constant* $\theta \in (0, 1]$ *such that* $\left\| \mathbf{\Gamma}_{S^c S} (\mathbf{\Gamma}_{SS})^{-1} \right\|_{1,1} \leq 1 - \theta$*.*

Then, we adopt the same strategy as in Theorem 1 and obtain the conditions for the correct recovery of graphical structure under Assumptions 2, 3, and 4, which is stated as

Theorem 5. *Set* $\lambda_G^{\text{non-param}} \asymp \frac{\sqrt{\log n \vee \log(d-p)}}{\theta} \left(\frac{\sqrt{\log n}}{n^{1/4}} \vee \frac{\sqrt{\log(d-p)}}{(d-p)^{\beta/4}} \right)$ *and define* $\beta = \frac{1}{2} \wedge \frac{a}{4} \wedge \frac{2\alpha+1}{4}$*. Provided that*

$$\sqrt{\log n \vee \log(d-p)} \left(\frac{\sqrt{\log n}}{n^{1/4}} \vee \frac{\sqrt{\log(d-p)}}{(d-p)^{\beta/4}} \right) \lesssim \frac{\theta}{(\theta+8)(\text{deg}) \cdot \kappa_{\mathbf{\Sigma}}^3 \kappa_{\mathbf{\Gamma}}}, \tag{3.6.3}$$

we have $(\widehat{\mathbf{\Theta}}_G^{\text{non-param}})_{i,j} = 0$ *for all* (i, j) *outside the support set* S*, i.e.,* $(i, j) \in S^c$*, with*

probability $1 - o(1)$*, where* c_i*,* $0 \le i \le 4$*, are some fixed positive constants independent of* n, d *and* p*, Furthermore, if*

$$\min_{(i,j)\in S} |\mathbf{\Theta}_{i,j}| \ge 2\kappa_\Gamma(1 + 8\theta^{-1})\sqrt{\log n \vee \log(d-p)} \left(\frac{\sqrt{\log n}}{n^{1/4}} \vee \frac{\sqrt{\log(d-p)}}{(d-p)^{\beta/4}} \right),$$

we have $\text{sign}(\widehat{\mathbf{\Theta}}_G^{\text{non-param}}) = \text{sign}(\mathbf{\Theta}^\natural)$ *with probability* $1 - o(1)$.

3.6.1 Discussions

Following the same logic as in the discussion of the parametric method, we can obtain the minimum sample number n in terms of dimension d, and length p from (Equation 3.6.3). Treating parameters θ, deg, $\kappa_{\mathbf{\Sigma}}$, and $\kappa_{\mathbf{\Gamma}}$ as some constants, the condition (Equation 3.6.3) requires the left-hand side to be constant.

Minimum Sample Size n**.** We can show that

$$n \gtrsim (\text{deg})^4 \log^2 n \left(\log^2 n \vee \log^2(d-p) \right).$$

In contrast, the previous work [25] only requires the sample number n to satisfy $n \gtrsim (\text{deg})^4 \log^4(n)$. Hence our result experience a loss of up to $\frac{\log^2(d-p)}{\log^2(n)} \vee 1$. Since this inflation is closely related to the dimension d, we conclude the loss is due to the indirect measurement scheme.

Minimum Projection Dimension d**.** For the dimension d, we require

$$d \ge p + (\text{deg})^{\beta/4} \log^{\beta/8}(d-p) \left(\log^{\beta/8} n \vee \log^{\beta/8}(d-p) \right),$$

which is a slightly larger than the dimension p. To the best of our knowledge, this is the first condition involving the dimension d for the nonparametric learning of the graphical

structure. Whether we can use a compressive sensing system, namely, $d < p$, for the nonparametric method still remains an open-problem.

3.6.2 Proof Outline

The core of the proof is Theorem 4. Define $\widehat{\varphi}_i^{(s)}$, $\widetilde{\varphi}_i^{(s)}$, and $\varphi_i^{(s)}$ as

$$\begin{aligned}
\widehat{\varphi}_i^{(s)} &= \widehat{h}_i(\widehat{X}_i^{(s)}); \\
\widetilde{\varphi}_i^{(s)} &= \widehat{h}_i(X_i^{(s)}); \\
\varphi_i^{(s)} &= h_i(X_i^{(s)}).
\end{aligned}$$

The (i,j)th entries of the corresponding covariance matrices $\widehat{\mathbf{\Sigma}}_n^{\text{non-param}}$, $\widetilde{\mathbf{\Sigma}}_n^{\text{non-param}}$, and $\mathbf{\Sigma}_n^{\text{non-param}}$ are written as

$$\begin{aligned}
\left(\widehat{\mathbf{\Sigma}}_n^{\text{non-param}}\right)_{i,j} &= \frac{1}{n}\sum_{s=1}^{n} \widehat{\varphi}_i^{(s)}\widehat{\varphi}_j^{(s)} - \widehat{\mu}_i\widehat{\mu}_j; \\
\left(\widetilde{\mathbf{\Sigma}}_n^{\text{non-param}}\right)_{i,j} &= \frac{1}{n}\sum_{s=1}^{n} \widetilde{\varphi}_i^{(s)}\widetilde{\varphi}_j^{(s)} - \widetilde{\mu}_i\widetilde{\mu}_j; \\
(\mathbf{\Sigma}_n^{\text{non-param}})_{i,j} &= \frac{1}{n}\sum_{s=1}^{n} \varphi_i^{(s)}\varphi_j^{(s)} - \mu_i\mu_j.
\end{aligned}$$

We bound the deviation between $\mathbf{\Sigma}_n^{\text{non-param}}$ and $\widehat{\mathbf{\Sigma}}_n^{\text{non-param}}$ as

$$\left\|\mathbf{\Sigma}_n^{\text{non-param}} - \widehat{\mathbf{\Sigma}}_n^{\text{non-param}}\right\|_\infty \leq \left\|\mathbf{\Sigma}_n^{\text{non-param}} - \widetilde{\mathbf{\Sigma}}_n^{\text{non-param}}\right\|_\infty + \left\|\widetilde{\mathbf{\Sigma}}_n^{\text{non-param}} - \widehat{\mathbf{\Sigma}}_n^{\text{non-param}}\right\|_\infty.$$

The proof is complete by showing

$$\left\|\boldsymbol{\Sigma}_n^{\text{non-param}} - \widetilde{\boldsymbol{\Sigma}}_n^{\text{non-param}}\right\|_\infty \lesssim \frac{\sqrt{\log n}}{n^{1/4}} \vee \frac{\sqrt{\log(d-p)}}{(d-p)^{\beta/4}};$$

$$\left\|\widehat{\boldsymbol{\Sigma}}_n^{\text{non-param}} - \widetilde{\boldsymbol{\Sigma}}_n^{\text{non-param}}\right\|_\infty \lesssim \sqrt{\log n \vee \log(d-p)} \left(\frac{\sqrt{\log n}}{n^{1/4}} \vee \frac{\sqrt{\log(d-p)}}{(d-p)^{\beta/4}}\right) + \frac{L\sigma\left(\log n \vee \log(d-p)\right)}{c_0 \log^2(np)(d-p)^{1/4}},$$

hold with high probability.

Having showed that the correct graphical structure can be obtained under mild conditions, next we will present some numerical experiments to validate our theoretical analysis.

3.7 Simulation Results

This section presents the numerical results consisting of both the synthetic data and the real-world database.

3.7.1 Synthetic Data Case

We construct the sparse precision matrix $\boldsymbol{\Theta}$ as

$$\Theta_{i,j} = \begin{cases} \rho_1, & \text{if } i = j; \\ \rho_2, & \text{if } |i-j| = 1; \\ 0. & \text{otherwise,} \end{cases}$$

which is previously adopted in [3]. The corresponding edge set of is denoted as E. We fix the signal length p as 100 and evaluate the performance with the following three types of marginal distribution for the random vector $\mathbf{X}$:

- uniform distribution within the region $[0, 1]$;
- exponential distribution, i.e., e^{-z} for $z \geq 0$;
- Gaussian mixture, i.e., $0.25 \sum_{i=1}^{4} \mathcal{N}(\mu_i, 10^{-2})$, where $\mu_i \in \{\pm 0.25, \pm 0.5\}$.

We set ρ_1 and ρ_2 as 1 and 0.4, respectively. For the baseline in Table 3.1, we assume the underlying distribution of $\mathbf{X}$ to be jointly Gaussian. With direct observations, we learn the graphical structure with graphical lasso. The recall rate and precision rate is shown in Table 3.1. For the uniform and exponential distribution, our algorithm has a significant improvement in terms of both the recall rate and precision rate. While for mixture Gaussian, the improvement is modest. This phenomenon may justify the approximation of mixture Gaussian with Gaussian distribution, which is widely used in the field of coding theory, machine learning, etc.

Table 3.1. Recall rate and precision rate. The signal length p is fixed as 100 and σ^2 is fixed as 1.0. The sample number corresponding to the baseline is set as 175, the maximum sample number.

	Uniform		**Exponential**		**Gauss Mixture**	
n	Recall Rate	Precision Rate	Recall Rate	Precision Rate	Recall Rate	Precision Rate
$d = 200$						
100	0.9315	0.9257	0.9839	0.9029	0.9732	0.9114
115	0.9342	0.9527	0.9866	0.9043	0.9758	0.9331
130	0.9369	0.9555	0.9906	0.9323	0.9826	0.9363
145	0.9450	0.9655	0.9946	0.9375	0.9866	0.9534
160	0.9490	0.9756	0.9946	0.9527	0.9866	0.9638
175	0.9490	0.9793	0.9946	0.9504	0.9879	0.9712
$d = 300$						
100	0.9584	0.9347	0.9852	0.9074	0.9852	0.9176
115	0.9651	0.9400	0.9799	0.9070	0.9906	0.9191
130	0.9812	0.9545	0.9919	0.9276	0.9933	0.9290
145	0.9812	0.9549	0.9933	0.9333	0.9933	0.9298
160	0.9852	0.9597	0.9973	0.9411	0.9946	0.9376
175	0.9839	0.9656	0.9973	0.9458	0.9960	0.9513
$d = 500$						
100	0.9745	0.9455	0.9812	0.9097	0.9879	0.9126
115	0.9758	0.9758	0.9866	0.9320	0.9893	0.9320
130	0.9758	0.9813	0.9919	0.9467	0.9906	0.9343
145	0.9826	0.9826	0.9946	0.9470	0.9933	0.9477
160	0.9879	0.9879	0.9946	0.9502	0.9946	0.9537
175	0.9893	0.9893	0.9973	0.9619	0.9960	0.9604
Baseline	0.3356	0.1834	0.3765	0.0497	0.8188	0.8538

3.7.2 Real-World Data

We now consider the real-world databases, which consists of 5 databases: Carolina Breast Cancer (GSE148426) with 2497 samples (patients) [121], Lung Cancer (GSE137140) with 3924 samples [8], Ovarian Cancer (GSE106817) with 4046 samples [122], Colorectal Cancer (GSE115513) with 1513 samples [123], and Esophageal Squamous Cell Carcinoma (GSE122497) with 5531 samples [124]. Each database is divided into two categories, i.e., **Healthy group** and **Patients**, where the measurements are given as the concentration of miRNAs. The miRNAs are known to have dependency among each other, i.e., a non-diagonal precision matrix, and hence there is an underlying graphical model describing these dependency structure based on the associated precision matrix.

The sensing matrix $\mathbf{A} \in \mathbb{R}^{d\times p}$ is assumed to be $A_{ij} \overset{\text{i.i.d}}{\sim} \mathcal{N}(0,1)$ and the variance of the measurement noise is set to one, $W_i \overset{\text{i.i.d}}{\sim} \mathcal{N}(0,1)$. The goal is to reconstruct the underlying dependency graph among miRNAs.

Evaluation. We adopt the nonparametric method for the evaluation due to its wider applications. The precision matrix $\mathbf{\Theta}$ learned with noiseless direct measurements using the method in [25] is assumed to be the ground-truth. We evaluate the performance of our estimator via the recall rate and the precision rate of the edge selection, which are shown in Table 3.2 and Table 3.3, respectively. These experiments confirm that our estimator can obtain the correct dependency relation with high-probability.

3.8 Conclusions

This is the first work on the nonparametric learning of the graphical structure with noisy indirect measurements. Assuming the random vector follows the nonparanormal distribution and the graphical structure is sparse, we proposed a practical estimator based on the deconvolution estimator of the CDF and graphical lasso. Considering the setting with inexact knowledge of the noise distribution, we established a non-asymptotic uniform

Table 3.2. Recall rate of edge selection on real-world databases, namely, GSE148426 [121], GSE137140 [8], GSE106817 [122], GSE115513 [123], and GSE122497 [124]. The precision matrix $\mathbf{\Theta}$ learned by direct observations is assumed to be the ground-truth.

	Healthy group					Unhealthy group				
d/p	GSE 148426	GSE 137140	GSE 106817	GSE 115513	GSE 122497	GSE 148426	GSE 137140	GSE 106817	GSE 115513	GSE 122497
2	0.9494	0.8892	0.9	0.9856	0.7659	0.9424	0.9692	1	0.9856	0.8379
5	1	0.9950	1	1	0.9220	1	0.9692	1	1	0.9632
10	1	1	1	1	0.9707	1	1	1	1	0.9963
12	1	1	1	1	0.9805	1	1	1	1	1
15	1	1	1	1	0.9902	1	1	1	1	1
20	1	1	1	1	1	1	1	1	1	1

Table 3.3. Precision rate of edge selection on real-world databases, namely, GSE148426 [121], GSE137140 [8], GSE106817 [122], GSE115513 [123], and GSE122497 [124]. The precision matrix $\mathbf{\Theta}$ learned by direct observations is assumed to be the ground-truth.

	Healthy group					Unhealthy group				
d/p	GSE 148426	GSE 137140	GSE 106817	GSE 115513	GSE 122497	GSE 148426	GSE 137140	GSE 106817	GSE 115513	GSE 122497
2	1	1	1	0.9548	1	0.9704	0.9692	1	0.9581	1
5	0.9080	0.9900	1	0.9176	1	0.9205	0.9692	1	0.9207	0.9924
10	0.9080	0.9341	0.9091	0.9207	0.9900	0.9205	0.9420	1	0.9268	0.9854
12	0.9080	0.9475	0.9259	0.9237	0.9901	0.9329	0.9420	1	0.9268	0.9645
15	0.9080	0.9566	0.9434	0.9299	0.9621	0.9456	0.9420	1	0.9299	0.9645
20	0.9518	0.9613	0.9615	0.9393	0.9535	0.9586	0.9420	1	0.9457	0.9784

bound on the errors of the CDF estimation for the first time, which constitutes one of the major technical contribution. Moreover, we showed our estimator can generate the correct graphical structure under mild conditions, from which the sufficient condition for the sample number n and dimension d can be obtained, namely, $n \gg (\deg)^4 \log^4 n$ and $d \gg p + (\deg)^{\beta/4} \log^{\beta/4}(d-p)$. Simulations with both synthetic data and real-world data are provided to confirm the correctness of our theorems.

CHAPTER 4
DESIGN OF COMPRESSIVE SENSING SYSTEMS USING DENSITY EVOLUTION

4.1 Introduction

In this chapter, we focus on the compressive sensing problem in a linear sensing system $\mathbf{y} = \mathbf{A}\mathbf{x}^\natural + \mathbf{w}$, where $\mathbf{y} \in \mathbb{R}^m$, $\mathbf{x}^\natural \in \mathbb{R}^n$, and $\mathbf{w}$ denote the measurements, the signal with certain structures, and the measurement noise, respectively. To ensure reliable recovery of $\mathbf{x}^\natural$ from $\mathbf{y}$, sensing matrix $\mathbf{A}$ needs to satisfy certain conditions. Typical conditions include incoherence in [85], RIP in [110, 128], *neighborhood stability* in [129], *irrespresentable condition* in [130], etc. While all the above works treat each entry of $\mathbf{x}^\natural$ equally, in certain applications entries of $\mathbf{x}^\natural$ may have unequal importance from the recovery perspective. One practical application in image processing is JPEG compression, where coefficients corresponding to the high-frequency part are more critical than the rest of coefficients. [1]

In this chapter, we propose a heuristic but general design framework of $\mathbf{A}$ to meet the requirements of the signal reconstruction such as placing more importance on the accuracy of a certain components of the signal. First, we transform the signal reconstruction to the inference problem in graphical models adopting the Bayesian viewpoint. This idea is widely used and has been adopted to derive *approximate message passing* (AMP). Then, we transform the problem of sensing matrix design to the problem of designing the graphical model. Leveraging the tools from coding theory, namely, *density evolution* (DE), we relate the performance of the signal reconstruction with the connectivity of the graphical model. Ultimately, we formulate bi-convex optimization problems to design the sensing matrix, which can be efficiently solved. Two design schemes for the sensing matrix, namely, (i)

[1] An introduction can be found in https://jpeg.org/jpeg/documentation.html.

a regular sensing and (ii) a preferential sensing, are proposed and are incorporated into a single framework.

Notations We have $a \propto b$ when a is proportional to b. For two distributions d_1 and d_2, we denote $d_1 \cong d_2$ if they are the equal up to some normalization.

4.2 Problem Description

We begin this section with a formal statement of our problem. Consider the linear measurement system

$$\mathbf{y} = \mathbf{A}\mathbf{x}^\natural + \mathbf{w}, \tag{4.2.1}$$

where $\mathbf{y} \in \mathbb{R}^m$, $\mathbf{A} \in \mathbb{R}^{m\times n}$, $\mathbf{x}^\natural \in \mathbb{R}^n$, and $\mathbf{w} \in \mathbb{R}^m$, respectively, denote the observations, the sensing matrix, the signal, and the additive sensing noise with its ith entry $w_i \overset{\text{i.i.d}}{\sim} \mathcal{N}(0, \sigma^2)$. We would like to recover $\mathbf{x}^\natural$ with the regularized M-estimator, which is written as

$$\widehat{\mathbf{x}} = \text{argmin}_{\mathbf{x}} \frac{1}{2\sigma^2}\|\mathbf{y} - \mathbf{A}\mathbf{x}\|_2^2 + f(\mathbf{x}), \tag{4.2.2}$$

where $f(\cdot)$ is the regularizer used to enforce certain underlying structure for signal $\widehat{\mathbf{x}}$. Our goal is to design a sparse sensing matrix $\mathbf{A}$ which provides preferential treatment for a sub-block of the signal $\mathbf{x}^\natural$. In other words, the objective is to have a sub-block of the signal to be recovered with lower probability of error when comparing with the rest of $\mathbf{x}^\natural$. Before we proceed, we list our two assumptions:

- Measurement system $\mathbf{A}$ is assumed to be sparse. Further, $\mathbf{A}$ is assumed to have entries with with $\mathbb{E}A_{ij} = 0$, and $A_{ij} \in \{0, \pm A^{-1/2}\}$, where an entry $A_{ij} = A^{-1/2}$ (or $-A^{1/2}$) implies a positive (negative) relation between the i^{th} sensor and the j^{th} signal component. Having zero as entry implies no relation.

- The regularizer $f(\mathbf{x})$ is assumed to be separable such that $f(\mathbf{x}) = \sum_{i=1}^{n} f_i(x_i)$. If it is not mentioned specifically, we assume all functions $f_i(\cdot)$ are the same.

First we transform (Equation 4.2.1) to a factor graph [131]. Adopting the viewpoint of Bayesian reasoning, we can reinterpret M-estimator in (Equation 4.2.2) as the *maximum a posteriori* (MAP) estimator and rewrite it as

$$\widehat{x} = \text{argmax}_x \exp\left(-\frac{\|\mathbf{y} - \mathbf{A}\mathbf{x}\|_2^2}{2\sigma^2}\right) \times \exp\left(-f(\mathbf{x})\right).$$

The first term $\exp\left(-\frac{\|\mathbf{y}-\mathbf{A}\mathbf{x}\|_2^2}{2\sigma^2}\right)$ is viewed as the probability $\mathbb{P}(\mathbf{y}|\mathbf{x})$ while the second term $\exp(-f(\mathbf{x}))$ is regarded as the prior imposed on $\mathbf{x}$. Notice the term $e^{-f(\cdot)}$ may not necessarily be the true prior on $\mathbf{x}^\natural$.

As in [66], we associate (Equation 4.2.2) with a factor graph $\mathcal{G} = (\mathcal{V}, \mathcal{E})$, where $\mathcal{V}$ denotes the node set and $\mathcal{E}$ is the edge set. First we discuss set $\mathcal{V}$, which consists of two types of nodes: variable nodes and check nodes. We represent each entry x_i as a variable node v_i and each entry y_a as a check node c_a. Additionally, we construct a check node corresponds to each prior $e^{-f(x_i)}$. Then we construct the edge set $\mathcal{E}$ by: (i) placing an edge between the check node of the prior $e^{-f(x_i)}$ and the variable node v_i, and (ii) introducing an edge between the variable node v_i and c_j iff A_{ij} is non-zero. Thus, the design of $\mathbf{A}$ is transformed to the problem of graph connectivity in $\mathcal{E}$.

4.3 Sensing Matrix for Regular Sensing (RS)

With the aforementioned graphical model, we can view recovering $\mathbf{x}^\natural$ as an inference problem, which can be solved via the message-passing algorithm [131]. Adopting the same notations as in [66] as shown in Figure 4.1, we denote $m_{i\to a}^{(t)}$ as the message from the variable node v_i to check node c_a at the t^{th} round of iteration. Likewise, we denote $\widehat{m}_{a\to i}^{(t)}$ as the message from the check node c_a to variable node v_i. Then message-passing algorithm

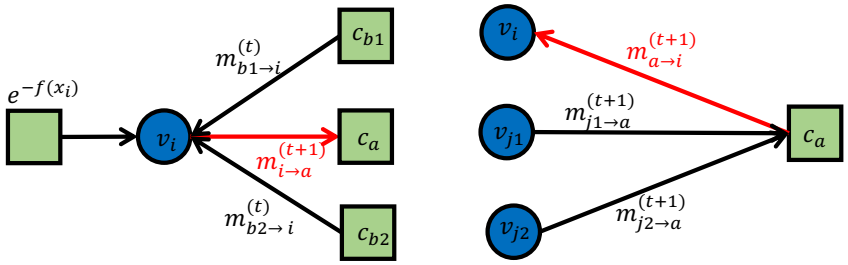

Figure 4.1. Illustration of the message-passing algorithm, where the square icons represent the check nodes while the circle icons represent the variable nodes.

is written as

$$m_{i\to a}^{(t+1)}(x_i) \cong e^{-f(x_i)} \prod_{b\in\partial i\backslash a} \widehat{m}_{b\to i}^{(t)}(x_i); \tag{4.3.1}$$

$$\widehat{m}_{a\to i}^{(t+1)}(x_i) \cong \int \prod_{j\in\partial a\backslash i} m_{j\to a}^{(t+1)}(x_i) \cdot e^{-\frac{\left(y_a-\sum_{j=1}^{n} A_{aj}x_j\right)^2}{2\sigma^2}} dx_j, \tag{4.3.2}$$

where ∂i and ∂a denote the neighbors connecting with v_i and c_a, respectively, and the symbol $\cong$ refers to the equality up to the normalization. At the tth iteration, we recover x_i by maximizing the posterior probability

$$\widehat{x}_i = \text{argmax}_{x_i}\mathbb{P}(x_i|\mathbf{y}) \approx \text{argmax}_{x_i} e^{-f(x_i)} \prod_{a\in\partial i} \widehat{m}_{a\to i}^{(t)}(x_i). \tag{4.3.3}$$

In the design of matrix $\mathbf{A}$, there are some general desirable properties that we wish to hold (specific requirements will be discussed later): (i) a correct signal reconstruction under the noiseless setting; and (ii) minimum number of measurements, or equivalently minimum m. Before proceeding, we first introduce the generating polynomials $\lambda(\alpha) = \sum_i \lambda_i \alpha^{i-1}$ and $\rho(\alpha) = \sum_i \rho_i \alpha^{i-1}$, which correspond to the degree distributions for variable nodes and check nodes, respectively. We denote the coefficient λ_i as the fraction of variable nodes with degree i, and similarly we define ρ_i for the check nodes. An illustration of the generating polynomials $\lambda(\alpha)$ and $\rho(\alpha)$ is shown in Figure 4.2.

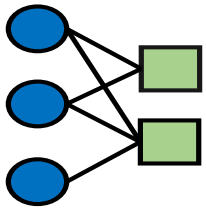

Figure 4.2. Illustration of the generating polynomials: $\lambda(\alpha) = \frac{1}{3} + \frac{2\alpha}{3}$ and $\rho(\alpha) = \frac{\alpha}{2} + \frac{\alpha^2}{2}$. The square icons represent the check nodes while the circle icons represent the variable nodes.

4.3.1 Density evolution for RS

To design the matrix $\mathbf{A}$, we study the reconstruction of $\mathbf{x}^\natural$ from $\mathbf{y}$ via the convergence analysis of the message-passing over the factor graph. Due to the parsimonious setting of $\mathbf{A}$, we have $\mathcal{E}$ to be sparse and propose to borrow a tool known as *density evolution* (DE) [132, 131, 133] that is already proven to be very powerful in analyzing the convergence in sparse graphs resulting from LDPC.

Basically, DE views $m_{i\to a}^{(t)}$ and $\widehat{m}_{a\to i}^{(t)}$ as RVs and tracks the changes of their probability distribution. When the message-passing algorithm converges, we would expect their distributions to become more concentrated. However, different from discrete RVs, continuous RVs $m_{i\to a}^{(t)}$ and $\widehat{m}_{a\to i}^{(t)}$ in our case require infinite bits for their precise representation in general, leading to complex formulas for DE. To handle such an issue, we approximate $m_{i\to a}^{(t)}$ and $\widehat{m}_{a\to i}^{(t)}$ as Gaussian RVs, i.e., $m_{i\to a} \sim \mathcal{N}(\mu_{i\to a}, v_{i\to a})$ and $\widehat{m}_{a\to i} \sim \mathcal{N}(\widehat{\mu}_{a\to i}, \widehat{v}_{a\to i})$, respectively. Since the Gaussian distribution is uniquely determined by its mean and variance, we will be able to reduce the DE to finite dimensions as in [133, 53, 55].

In our work, the DE tracks two quantities $E^{(t)}$ and $V^{(t)}$, which denote the deviation from the mean and average of the variance, respectively, and are defined as

$$E^{(t)} = \frac{1}{m \cdot n} \sum_{i=1}^{n} \sum_{a=1}^{m} \left(\mu_{i\to a}^{(t)} - x_i^\natural \right)^2;$$
$$V^{(t)} = \frac{1}{m \cdot n} \sum_{i=1}^{n} \sum_{a=1}^{m} v_{i\to a}^{(t)}.$$

Then we can show that the DE analysis yields

$$E^{(t+1)} = \mathbb{E}_{\text{prior}(s)}\mathbb{E}_z\left[h_{\text{mean}}\left(s + \sum_{i,j}\rho_i\lambda_j z\sqrt{\frac{i}{j}E^{(t)} + \frac{A\sigma^2}{j}}; \sum_{i,j}\rho_i\lambda_j\frac{A\sigma^2 + iV^{(t)}}{j}\right) - s\right]^2; \tag{4.3.4}$$

$$V^{(t+1)} = \mathbb{E}_{\text{prior}(s)}\mathbb{E}_z h_{\text{var}}\left(s + \sum_{i,j}\rho_i\lambda_j z\sqrt{\frac{i}{j}E^{(t)} + \frac{A\sigma^2}{j}}; \sum_{i,j}\rho_i\lambda_j\frac{A\sigma^2 + iV^{(t)}}{j}\right), \tag{4.3.5}$$

where prior$(\cdot)$ denotes the true prior on the entries of $\mathbf{x}^\natural$, z is a standard normal RV $\mathcal{N}(0,1)$. The functions $h_{\text{mean}}(\cdot)$ and $h_{\text{var}}(\cdot)$ are to approximate the mean $\mu_{i\to a}$ and variance $v_{i\to a}$, which are given by

$$\begin{aligned} h_{\text{mean}}(\mu; v) &= \lim_{\gamma\to\infty}\frac{\int x_i e^{-\gamma f(x_i)} e^{-\frac{\gamma(x_i-\mu)^2}{2v}} dx_i}{\int e^{-\gamma f(x_i)} e^{-\frac{\gamma(x_i-\mu)^2}{2v}} dx_i}; \\ h_{\text{var}}(\mu; v) &= \lim_{\gamma\to\infty}\frac{\gamma\int x_i^2 e^{-\gamma f(x_i)} e^{-\frac{\gamma(x_i-\mu)^2}{2v}} dx_i}{\int e^{-\gamma f(x_i)} e^{-\frac{\gamma(x_i-\mu)^2}{2v}} dx_i} - \left(h_{\text{mean}}(\mu; v)\right)^2. \end{aligned} \tag{4.3.6}$$

For detailed explanations and the proof, we refer interested readers to the Appendix.

4.3.2 Sensing matrix design for RS

Once the values of polynomial coefficients $\{\lambda_i\}_i$ and $\{\rho_i\}_i$ are determined, we can construct a random graph $\mathcal{G} = (\mathcal{V}, \mathcal{E})$, or equivalently the sensing matrix $\mathbf{A}$, by setting A_{ij} as $\mathbb{P}(A_{ij} = A^{-1/2}) = \mathbb{P}(A_{ij} = -A^{-1/2}) = \frac{1}{2}$, if there is an edge $(v_i, c_j) \in \mathcal{E}$; otherwise we set A_{ij} to zero. Hence the sensing matrix construction reduces to obtaining the feasible values of $\{\lambda_i\}_i$ and $\{\rho_i\}_i$ while satisfying certain properties for the signal reconstruction as discussed in the following.

Our first requirement is to have a perfect signal reconstruction under the noiseless scenario ($\sigma^2 = 0$). This implies that

- the algorithm must converge, i.e., $\lim_{t\to\infty} V^{(t)} = 0$;

- the average error should shrink to zero, i.e., $\lim_{t\to\infty} E^{(t)} = 0$.

Second, we wish to minimize the number of measurements. Using the fact that $n\left(\sum_i i\lambda_i\right) = m\left(\sum_i i\rho_i\right) = \sum_{i,j} \mathbb{1}((v_i, c_j) \in \mathcal{E})$, we formulate the above two design criteria as the following optimization problem

$$\min_{\substack{\boldsymbol{\lambda}\in\Delta_{\mathsf{dv}_{\mathsf{max}}-1};\\ \boldsymbol{\rho}\in\Delta_{\mathsf{dc}_{\mathsf{max}}-1}}} \quad \frac{m}{n} = \frac{\sum_{i\geq 2} i\lambda_i}{\sum_{i\geq 2} i\rho_i}, \tag{4.3.7}$$

$$\text{s.t.} \quad \lim_{t\to\infty} \left(E^{(t)}, V^{(t)}\right) = (0,0); \tag{4.3.8}$$

$$\lambda_1 = \rho_1 = 0, \tag{4.3.9}$$

where Δ_{d-1} denotes the d-dimensional simplex, namely, $\Delta_{d-1} = \left\{\mathbf{z} \in \mathbb{R}^d \mid \sum_i z_i = 1, z_i \geq 0\right\}$. Note that the spaces of $\boldsymbol{\lambda}$ and $\boldsymbol{\rho}$ are discrete RVs and $\Delta_{(\cdot)-1}$ are the corresponding convex hulls. The constraint in (Equation 4.3.9) is to avoid one-way message passing as in [133, 47].

Generally speaking, we need to run DE numerically to check the requirement (Equation 4.3.8) for every possible values of $\{\lambda_i\}_i$ and $\{\rho_i\}_i$. However, for certain choices of regularizers $f(\cdot)$, we can reduce the requirement (Equation 4.3.8) to a closed-form equation. As an example, we set the prior in (Equation 4.3.1) to be a Laplacian distribution, i.e., $e^{-\beta|x|}$. In this case, the regularizer $f(\cdot)$ in (Equation 4.2.2) becomes $\beta\|\cdot\|_1$ and the M-estimator in (Equation 4.2.2) transforms to Lasso [134].

4.3.3 Example of regular sensing with a Laplacian prior

Assuming the signal $\mathbf{x}^\natural$ is k-sparse, i.e., $\left\|\mathbf{x}^\natural\right\|_0 \leq k$, we would like to recover $\mathbf{x}^\natural$ with the regularizers $\beta\|\cdot\|_1$. Following the approaches in [57] in the noiseless case, we can show that

$$\begin{aligned} E^{(t+1)} &= \mathbb{E}_{\text{prior}(s)}\mathbb{E}_{z\sim\mathcal{N}(0,1)}\left[\mathsf{prox}\left(s + a_1 z\sqrt{E^{(t)}}; \beta a_2 V^{(t)}\right) - s\right]^2; \\ V^{(t+1)} &= \mathbb{E}_{\text{prior}(s)}\mathbb{E}_{z\sim\mathcal{N}(0,1)}\left[\beta a_2 V^{(t)} \mathsf{prox}'\left(s + a_1 z\sqrt{E^{(t)}}; \beta a_2 V^{(t)}\right)\right], \end{aligned} \tag{4.3.10}$$

where a_1 is defined as $\sum_{i,j} \rho_i \lambda_j \sqrt{i/j}$, and a_2 is defined as $\sum_{i,j} \rho_i \lambda_j (i/j)$. Further, operator $\mathsf{prox}(a; b)$ is the soft-thresholding estimator defined as $\text{sign}(a) \max(|a| - b, 0)$, and operator $\mathsf{prox}'(a; b)$ is the derivative w.r.t. the first argument.

Remark 2. *Unlike SE that only tracks $E^{(t)}$ [57], our DE takes into account both the average variance $V^{(t)}$ and the deviation from mean $E^{(t)}$. Assuming $V^{(t)} \propto \sqrt{E^{(t)}}$, our DE equation w.r.t. $E^{(t)}$ in* (Equation 4.3.10) *reduces to a similar form as SE.*

Having discussed its relation with SE, we now show that our DE can reproduce the classical results in compressive sensing, namely, $m \geq c_0 k \log(n/k) = O(k \log n)$ (cf. [135]) under the regular sensing matrix design, i.e., when all variable nodes have the same degree dv and the check nodes have the same degree dc. Before we proceed, we first approximate the ground-truth distribution with the Laplacian prior. Assuming that the entries of $\mathbf{x}^\natural$ are iid and $\mathbf{x}^\natural \in \mathbb{R}^n$ is k-sparse, each entry becomes zero with probability $(1 - k/n)$. Hence we set β such that the probability mass within the region $[-c_0, c_0]$ (where c_0 is some small positive constant) with the Laplacian prior is equal to $1 - k/n$. That is

$$\frac{\beta}{2} \int_{|\alpha| \leq c_0} e^{-\beta|\alpha|} d\alpha = 1 - \frac{k}{n}.$$

This results in $\beta = n/(c_0 n \log(n/k))$. Then we conclude the following

Theorem 6. *Let $\mathbf{x}^\natural$ be a k-sparse signal and assume that β is set to $n/(c_0 \log(n/k))$. Then, the necessary conditions for $\lim_{t\to\infty} \left(E^{(t)}, V^{(t)}\right) = (0, 0)$ in* (Equation 4.3.10) *results in $a_1^2 \leq n/k$ and $a_2 \leq n/(c_0 k \log(n/k))$, where a_1 and a_2 are defined as $\sum_{i,j} \rho_i \lambda_j \sqrt{i/j}$ and $\sum_{i,j} \rho_i \lambda_j (i/j)$, respectively.*

When turning to the regular design, namely, all variable nodes are with the degree dv and likewise all check nodes are with degree dc, we can write a_1 and a_2 as $\sqrt{n/m}$ and n/m, respectively. Invoking Theorem 6 will then yield the classical result of the lower bound on the number of measurements $m \geq c_0 k \log(n/k)$. The technical details are deferred to section C.1.

In addition to the Laplacian prior, we also considered the Gaussian prior, i.e., $e^{-\beta\|\mathbf{x}\|_2^2}$, which makes the M-estimator in (Equation 4.2.2) the ridge regression [136]. Corresponding discussion is left to section C.2 for interested readers.

4.4 Sensing Matrix for Preferential Sensing (PS)

Having discussed the regular sensing scheme, this section explains as to how we apply our DE framework to design the sensing matrix $\mathbf{A}$ such that we can provide preferential treatment for different entries of $\mathbf{x}^\natural$. For example, the high priority components will be recovered more accurately than the low priority parts of $\mathbf{x}^\natural$.

4.4.1 Density evolution for PS

Dividing the entire $\mathbf{x}^\natural$ into the high-priority part $\mathbf{x}_H^\natural \in \mathbb{R}^{n_H}$ and low-priority part $\mathbf{x}_L^\natural \in \mathbb{R}^{n_L}$, we separately introduce the generating polynomials $\lambda_H(\alpha) = \sum \lambda_{H,i}\alpha^{i-1}$ and $\lambda_L(\alpha) = \sum \lambda_{L,i}\alpha^{i-1}$ for the high-priority part $\mathbf{x}_H^\natural$ and the low-priority part $\mathbf{x}_L^\natural$, respectively. Note that $\lambda_{H,i}$ and likewise $\lambda_{L,i}$ denote the fraction of variable nodes corresponding to high-priority part and low-priority part with degree i. Similarly, we introduce the generating polynomials $\rho_H(\alpha) = \sum_i \rho_{H,i}\alpha^{i-1}$ and $\rho_L(\alpha) = \sum_i \rho_{L,i}\alpha^{i-1}$ for the check nodes connecting the high-priority part $\mathbf{x}_H^\natural$ and the low-priority part $\mathbf{x}_L^\natural$, respectively.

Generalizing the analysis of the regular sensing, we separately track the average error and variance for $\mathbf{x}_H^\natural$ and $\mathbf{x}_L^\natural$. For the high-priority part $\mathbf{x}_H^\natural$, we define E_H as $\sum_m \sum_{i\in H} \left(\mu_{i\to a} - x_i^\natural\right)^2 /(m\cdot n_H)$ and V_H as $\sum_m \sum_{i\in H} v_{i\to a}/(m\cdot n_H)$, where n_H denotes the length of the high-priority $\mathbf{x}_H^\natural$. Analogously we define E_L and V_L for the low-priority part $\mathbf{x}_L^\natural$. We then write the corresponding DE as

$$\begin{aligned} E_H^{(t+1)} &= \mathbb{E}_{\text{prior}(s)}\mathbb{E}_{z\sim\mathcal{N}(0,1)}\left[h_{\text{mean}}\left(s + z\cdot b_{H,1}^{(t)}; b_{H,2}^{(t)}\right) - s\right]^2; \\ V_H^{(t+1)} &= \mathbb{E}_{\text{prior}(s)}\mathbb{E}_{z\sim\mathcal{N}(0,1)}\left[h_{\text{var}}\left(s + z\cdot b_{H,1}^{(t)}; b_{H,2}^{(t)}\right)\right], \end{aligned} \tag{4.4.1}$$

where $b_{H,1}^{(t)}$ and $b_{H,2}^{(t)}$ are defined as

$$b_{H,1}^{(t)} = \sum_{\ell,i,j} \lambda_{H,\ell}\rho_{L,i}\rho_{H,j}\sqrt{\frac{A\sigma^2 + iE_L^{(t)} + jE_H^{(t)}}{\ell}};$$
$$b_{H,2}^{(t)} = \sum_{\ell,i,j} \lambda_{H,\ell}\rho_{L,i}\rho_{H,j}\frac{A\sigma^2 + iV_L^{(t)} + jV_H^{(t)}}{\ell}.$$

The definitions of h_{mean} and h_{var} are as in (Equation 4.3.6). Switching the index H with L yields the DE w.r.t. the pair $\left(E_L^{(t+1)}, V_L^{(t+1)}\right)$. Notice we can also put different regularizers $f_H(\cdot)$ and $f_L(\cdot)$ for $\mathbf{x}_H^\natural$ and $\mathbf{x}_L^\natural$. In this case, we need to modify the regularizers $f(\cdot)$ in (Equation 4.3.6) to $f_H(\cdot)$ and $f_L(\cdot)$, respectively.

4.4.2 Sensing matrix design for PS

In addition to the constraints used in (Equation 4.3.7), the sensing matrix for preferential sensing must satisfy the following constraint:

Consistency requirement w.r.t. edge number. Consider the total number of edges incident with the high-priority part $\mathbf{x}_H^\natural$, $\sum_{i\in H} \mathbb{1}\left((v_i, c_a) \in \mathcal{E}\right)$. From the viewpoint of the variable nodes, we can compute this number as $n_H\left(\sum_i i\lambda_{H,i}\right)$. Likewise, from the viewpoint of the check nodes, the total number of edges is obtained as $\sum_{i\in H} \mathbb{1}\left((v_i, c_a) \in \mathcal{E}\right) = m\left(\sum_i i\rho_{H,i}\right)$. Since the edge number should be the same with either of the above two counting methods, we obtain

$$\sum_{i\in H} \mathbb{1}\left[(v_i, c_a) \in \mathcal{E}\right] = n_H\left(\sum_i i\lambda_{H,i}\right) = m\left(\sum_i i\rho_{H,i}\right).$$

Similarly, the consistency requirement for the edges connecting to the low-priority part $\mathbf{x}_L^\natural$ would give $\sum_{i\in L} \mathbb{1}\left((v_i, c_a) \in \mathcal{E}\right) = m(\sum_i i\rho_{L,i}) = n_L(\sum_i i\lambda_{L,i})$.

Moreover, we may have additional constraints depending on the measurement noise:

- **Preferential sensing for the noiseless measurement.** In the noiseless setting ($\sigma =$

0), we require V_H and V_L diminish to zero to ensure the convergence of the MP algorithm. Besides, we require the average error $E_H^{(t)}$ in the high-priority part $\mathbf{x}_H^\natural$ to be zero. Therefore, the requirements can be summarized as

Requirement 5. *Under the noiseless setting, i.e., $\sigma = 0$, we require the quantities $E_H^{(t)}, V_H^{(t)}$, and $V_L^{(t)}$ in* (Equation 4.4.1) *converge to zero*

$$\lim_{t\to\infty} \left(E_H^{(t)}, V_H^{(t)}, V_L^{(t)}\right) = (0, 0, 0)\,, \tag{4.4.2}$$

which implies the MP converges and the high-priority part $\mathbf{x}_H^\natural$ can be perfectly reconstructed.

Notice that no constraint is placed on the average error $E_L^{(t)}$ for the low-priority part $\mathbf{x}_L^\natural$, since it is given a lower priority in reconstruction.

- **Preferential sensing for the noisy measurement.** Different from the noiseless setting, the high-priority part $\mathbf{x}_H^\natural$ cannot be perfectly reconstructed in the presence of measurement noise, i.e., $\lim_{t\to\infty} E_H^{(t)} > 0$. Instead we consider the difference across iterations, namely, $\delta_{E,H}^{(t)} = E_H^{(t+1)} - E_H^{(t)}$ and $\delta_{E,L}^{(t)} = E_L^{(t+1)} - E_L^{(t)}$, which corresponds to the convergence rate. To provide an extra protection for the high-priority part $\mathbf{x}_H^\natural$, we would like $\delta_H^{(t)}$ to decrease at a faster rate. Hence, the following requirement:

  Requirement 6. *There exits a positive constant T_0 such that the average error $E_H^{(t)}$ converges faster than $E_L^{(t)}$ whenever $t \geq T_0$, i.e., $\left|\delta_{E,H}^{(t)}\right| \leq \left|\delta_{E,L}^{(t)}\right|$.*

Apart from the above constraints, we also require $\lambda_{L,1} = \lambda_{H,1} = \rho_{L,1} = \rho_{H,1} = 0$ to avoid one-way message passing [47, 131, 133]. Summarizing the above discussion, the design of the sensing matrix $\mathbf{A}$ for minimum number of measurements m reduces to the following

optimization problem

$$\min_{\substack{\boldsymbol{\lambda}_L \in \Delta_{\mathsf{dv_L}-1}, \\ \boldsymbol{\lambda}_H \in \Delta_{\mathsf{dv_H}-1}, \\ \boldsymbol{\rho}_L \in \Delta_{\mathsf{dc_H}-1}, \\ \boldsymbol{\rho}_H \in \Delta_{\mathsf{dc_L}-1}}} \frac{m}{n} = \frac{n_L \left(\sum_i i\lambda_{L,i}\right) + n_H \left(\sum_i i\lambda_{H,i}\right)}{\sum_i i \left(\rho_{L,i} + \rho_{H,i}\right)}; \tag{4.4.3}$$

$$\text{s.t.} \quad \frac{\sum_i i\lambda_{L,i}}{\sum_i i\lambda_{H,i}} \times \frac{\sum_i i\rho_{H,i}}{\sum_i i\rho_{L,i}} = \frac{n_H}{n_L}; \tag{4.4.4}$$

$$\text{Requirement (5) and (6)}; \tag{4.4.5}$$

$$\lambda_{L,1} = \lambda_{H,1} = \rho_{L,1} = \rho_{H,1} = 0, \tag{4.4.6}$$

where Δ_{d-1} denotes the d-dimensional simplex, and the parameters $\mathsf{dv_H}$ and $\mathsf{dc_L}$ denote the maximum degree w.r.t. the variable nodes corresponding to the high-priority part $\mathbf{x}_H^\natural$ and low-priority part $\mathbf{x}_L^\natural$, respectively. Similarly we define the maximum degree $\mathsf{dc_H}$ and $\mathsf{dc_L}$ w.r.t. the check nodes.

The difficulties of the optimization problem in (Equation 4.4.3) come from two-fold: (i) requirements from DE; and (ii) non-convex nature of (Equation 4.4.3). In the following scenario, we will revisit the example of ℓ_1 regularizer and show how to simplify the optimization problem in (Equation 4.4.3).

4.4.3 Example of preferential sensing with a Laplacian prior

Consider a sparse signal $\mathbf{x}^\natural$ whose high-priority part $\mathbf{x}_H^\natural \in \mathbb{R}^{n_H}$ and the low-priority part $\mathbf{x}_L^\natural \in \mathbb{R}^{n_L}$ are k_H-sparse and k_L-sparse, respectively. In addition, we assume $\frac{k_H}{n_H} \gg \frac{k_L}{n_L}$, implying that the high-priority part $\mathbf{x}_H^\natural$ contains more data.

Ideally, we need to numerically run the DE update equation in (Equation 4.4.1) to check whether the requirement in (Equation 4.4.5) holds or not, which can be computationally prohibitive. In practice, we would relax these conditions to arrive at some closed forms. The following outlines our relaxation strategy with all technical details being deferred to the Appendix.

Relaxation of Requirement 5. First we require the variance converge to zero, i.e., $\lim_{t\to\infty}\left(V_H^{(t)}, V_L^{(t)}\right) = (0,0)$. The derivation of its necessary condition consists of two parts: (i) we require the point $(0,0)$ to be a fixed point of the DE equation w.r.t. $V_H^{(t)}$ and $V_L^{(t)}$; and (ii) we require that the average variance $\left(V_H^{(t)}, V_L^{(t)}\right)$ to converge in the region where the magnitudes of $V_H^{(t)}$ and $V_L^{(t)}$ are sufficiently small.

The main technical challenge lies in investigating the convergence of $\left(V_H^{(t)}, V_L^{(t)}\right)$. Define the difference $\delta_{V,H}^{(t)}$ and $\delta_{V,L}^{(t)}$ across iterations as $\delta_{V,H}^{(t)} \triangleq V_H^{(t+1)} - V_H^{(t)}$ and $\delta_{V,L}^{(t)} \triangleq V_L^{(t+1)} - V_L^{(t)}$, respectively. Then, we obtain a linear equation

$$\begin{bmatrix} \delta_V^{(H)}(t+1) \\ \delta_V^{(L)}(t+1) \end{bmatrix} = \mathbf{L}_V^{(t)} \begin{bmatrix} \delta_V^{(H)}(t) \\ \delta_V^{(L)}(t) \end{bmatrix}$$

via the Taylor-expansion. Imposing the convergence constraints on $V_H^{(t)}$ and $V_L^{(t)}$, i.e., $\lim_{t\to\infty}\left(\delta_{V,H}^{(t)}, \delta_{V,L}^{(t)}\right) = (0,0)$, yields the condition $\inf_t \left\|\mathbf{L}_V^{(t)}\right\|_{\text{OP}} \leq 1$. That is

$$\begin{aligned} &\left[\left(\frac{\beta_H k_H}{n_H}\sum_\ell \frac{\lambda_{H,\ell}}{\ell}\right)^2 + \left(\frac{\beta_L k_L}{n_L}\sum_\ell \frac{\lambda_{L,\ell}}{\ell}\right)^2\right] \\ \times &\left[\left(\sum_i i\rho_{H,i}\right)^2 + \left(\sum_i i\rho_{L,i}\right)^2\right] \leq 1. \end{aligned} \tag{4.4.7}$$

Then we turn to the behavior of $E_H^{(t)}$. Assuming $E_L^{(t)}$ converges to a fixed non-negative constant $E_L^{(\infty)}$, we would like $E_H^{(t)}$ to converge to zero. Following the same strategy as above, we obtain the following condition

$$\frac{k_H}{n_H}\left(\sum_\ell \frac{\lambda_{H,\ell}}{\sqrt{\ell}}\right)^2 \left[\left(\sum_i \sqrt{i}\rho_{H,i}\right)^2 + \left(\sum_i \sqrt{i}\rho_{L,i}\right)^2\right] \leq 1. \tag{4.4.8}$$

The technical details are deferred to section C.4.

Relaxation of Requirement 6. First we define the difference across iterations as $\delta_{E,H}^{(t)} = E_H^{(t+1)} - E_H^{(t)}$ and $\delta_{E,L}^{(t)} = E_L^{(t+1)} - E_L^{(t)}$. Using the Requirement 6, we perform the Taylor

expansion w.r.t. the difference $\delta_{E,H}^{(t)}$ and $\delta_{E,L}^{(t)}$, and obtain the linear equation

$$\begin{bmatrix} \delta_{E,H}^{(t+1)} \\ \delta_{E,L}^{(t+1)} \end{bmatrix} = \begin{bmatrix} L_{E,11} & L_{E,12} \\ L_{E,21} & L_{E,22} \end{bmatrix} \begin{bmatrix} \delta_{E,H}^{(t)} \\ \delta_{E,L}^{(t)} \end{bmatrix}.$$

To ensure the reduction of $\delta_{E,H}^{(t)}$ at a faster rate than $\delta_{E,L}^{(t)}$, we would require $L_{E,11} \leq L_{E,21}$ and $L_{E,12} \leq L_{E,22}$. This results in

$$\frac{k_H}{n_H}\left(\sum_{\ell}\frac{\lambda_{H,\ell}}{\sqrt{\ell}}\right)^2 \leq \frac{k_L}{n_L}\left(\sum_{\ell}\frac{\lambda_{L,\ell}}{\sqrt{\ell}}\right)^2. \tag{4.4.9}$$

Summarizing the above discussion, we transform the constraint in (Equation 4.4.5) to the closed-form and find the local optimum of (Equation 4.4.3), which is bi-convex, via an alternating minimization method.

4.5 Potential Generalizations

This section discusses two possible generalizations, i.e., non-exponential family priors and reconstruction via a MMSE decoder. The design principles of the sensing matrix are exactly the same as (Equation 4.3.7) and (Equation 4.4.3) except that the DE equations need to be modified.

4.5.1 Non-exponential priors

Previous sections assume the prior to be $e^{-f(\mathbf{x})}$, which belongs to the exponential family distributions. In this subsection, we generalize it to arbitrary distributions $\widehat{\text{prior}}(\mathbf{x})$. One example of the non-exponential distribution is sparse Gaussian, i.e., $\frac{k}{n}e^{-(x-\mu)^2/2\sigma^2} + \left(1-\frac{k}{n}\right)\delta(x)$, which is used to model k-sparse signals. With the generalized prior, the MP

in (Equation 4.3.1) is modified to

$$
\begin{aligned}
m_{i\to a}^{(t+1)}(x_i) &\cong \widehat{\text{prior}}(x_i) \prod_{b\in\partial i\backslash a} \widehat{m}_{b\to i}^{(t)}(x_i); \\
\widehat{m}_{a\to i}^{(t+1)}(x_i) &\cong \int \prod_{j\in\partial a\backslash i} m_{j\to a}^{(t+1)}(x_i) \times e^{-\frac{\left(y_a-\sum_{j=1}^{n} A_{aj}x_j\right)^2}{2\sigma^2}} dx_j,
\end{aligned} \tag{4.5.1}
$$

and the decoding step at each iteration becomes

$$
\widehat{x}_i = \text{argmax}_{x_i}\mathbb{P}(x_i|\mathbf{y}) \approx \text{argmax}_{x_i}\widehat{\text{prior}}(x_i) \cdot \prod_{a\in\partial i} \widehat{m}_{a\to i}^{(t)}(x_i). \tag{4.5.2}
$$

Moreover, the functions $h_{\text{mean}}(\cdot;\cdot)$ and $h_{\text{var}}(\cdot;\cdot)$ in (Equation 4.3.4) are modified to $\widehat{h}_{\text{mean}}(\cdot;\cdot)$ and $\widehat{h}_{\text{var}}(\cdot;\cdot)$ as

$$
\begin{aligned}
\widehat{h}_{\text{mean}}(\mu;v) &= \lim_{\gamma\to\infty} \frac{\int x_i \cdot e^{\gamma \log \widehat{\text{prior}}(x_i)} \cdot e^{-\frac{\gamma(x_i-\mu)^2}{2v}} dx_i}{\int e^{\gamma \log \widehat{\text{prior}}(x_i)} \cdot e^{-\frac{\gamma(x_i-\mu)^2}{2v}} dx_i}; \\
\widehat{h}_{\text{var}}(\mu;v) &= \lim_{\gamma\to\infty} \frac{\gamma \int x_i^2 \cdot e^{\gamma \log \widehat{\text{prior}}(x_i)} \cdot e^{-\frac{\gamma(x_i-\mu)^2}{2v}} dx_i}{\int e^{\gamma \log \widehat{\text{prior}}(x_i)} \cdot e^{-\frac{\gamma(x_i-\mu)^2}{2v}} dx_i} - \left(\widehat{h}_{\text{mean}}(\mu;v)\right)^2.
\end{aligned}
$$

Afterwards, we can design the sensing matrix with the same procedure as in (Equation 4.3.7) and (Equation 4.4.3).

4.5.2 MMSE decoder

Notice that both (Equation 4.3.3) and (Equation 4.5.2) reconstruct the signal by minimizing the error probability $\mathbb{P}\left(\widehat{\mathbf{x}} \neq \mathbf{x}^\natural\right)$, which can be regarded as a MAP decoder. This subsection considers MMSE decoder, which is to minimize the ℓ_2 error, i.e., $\left\|\widehat{\mathbf{x}} - \mathbf{x}^\natural\right\|_2$. The message-passing procedure stays the same as (Equation 4.5.1) while the decoding procedure needs to be modified to

$$\widehat{x}_i = \int x_i \mathbb{P}(x_i|\mathbf{y}) dx_i \approx \int \left(x_i \cdot \widehat{\text{prior}}(x_i) \cdot \prod_{a \in \partial i} \widehat{m}_{a \to i}^{(t)}(x_i) \right) dx_i.$$

Moreover, the functions $h_{\text{mean}}(\cdot;\cdot)$ and $h_{\text{var}}(\cdot;\cdot)$ in the DE in (Equation 4.3.4) are modified to $\widetilde{h}_{mean}(\cdot;\cdot)$ and $\widetilde{h}_{\text{var}}(\cdot;\cdot)$ as

$$\widetilde{h}_{\text{mean}}(\mu; v) = \frac{\int x_i \cdot \widehat{\text{prior}}(x_i) \cdot e^{-\frac{(x_i-\mu)^2}{2v}} dx_i}{\int \widehat{\text{prior}}(x_i) \cdot e^{-\frac{(x_i-\mu)^2}{2v}} dx_i};$$

$$\widetilde{h}_{\text{var}}(\mu; v) = \frac{\int x_i^2 \cdot \widehat{\text{prior}}(x_i) \cdot e^{-\frac{(x_i-\mu)^2}{2v}} dx_i}{\int \widehat{\text{prior}}(x_i) \cdot e^{-\frac{(x_i-\mu)^2}{2v}} dx_i} - \left(\widetilde{h}_{\text{mean}}(\mu; v) \right)^2.$$

Having discussed two potential directions of generalization, next we will present the numerical experiments.

4.6 Numerical Experiments

This section presents the numerical experiments using both synthetic data and real-world data. We consider the sparse signal and compare the design of preferential sensing with that of the regular sensing. For the simplicity of the code design and the construction of the corresponding sensing matrix, we fix the degrees $\{\rho_{H,i}\}$ and $\{\rho_{L,i}\}$ of the check nodes to $\rho_{H,\mathsf{dc_H}} = 1$ and $\rho_{L,\mathsf{dc_L}} = 1$, respectively. Therefore, each check node has $\mathsf{dc_H}$ edges connecting to the high-priority part $\mathbf{x}_H^\natural$ and has $\mathsf{dc_L}$ edges connecting to the low-priority part $\mathbf{x}_L^\natural$. Then we construct the sensing matrix with the algorithm being illustrated in Algorithm 4.

We evaluate two types of sensing matrices for the preferential sensing, namely, $\mathbf{A}_{\text{preferential}}^{(\text{init})}$ and $\mathbf{A}_{\text{preferential}}^{(\text{final})}$, which correspond to the distributions $\{\boldsymbol{\lambda}_H\}$ and $\{\boldsymbol{\lambda}_L\}$ in the initialization phase and at the final outcome of Algorithm 4. As the baseline, we design the sensing matrix $\mathbf{A}_{\text{regular}}$ via (Equation 4.3.7) which provides regular sensing with an additional constraint which enforces equal edge number with $\mathbf{A}_{\text{preferential}}^{(\text{final})}$ for a fair comparison.

Algorithm 4 Design of Sensing Matrix for Preferential Sensing.

- **Input**: maximum variable node degree $\mathsf{dv_{max}}$, check node degree $\mathsf{dc_H}$ and $\mathsf{dc_L}$, signal lengths n_H and n_L, sparsity numbers k_H and k_L, and iteration number T.
- **Initialization**: set $\beta_H \asymp \log\left(\frac{n_H}{k_L}\right), \beta_L \asymp \log\left(\frac{n_L}{k_L}\right)$. Then we initialize $\{\lambda_{H,i}\}$ and $\{\lambda_{L,i}\}$ as

$$\begin{aligned}
&\min_{\substack{\boldsymbol{\lambda}_H \in \Delta_{\mathsf{dv_{max}}-1}, \\ \boldsymbol{\lambda}_L \in \Delta_{\mathsf{dv_{max}}-1}}} \sum_i i\lambda_{H,i}, \\
\text{s.t. } & n_H \mathsf{dc_L}\left(\sum_i i\lambda_{H,i}\right) = n_L \mathsf{dc_H}\left(\sum_i i\lambda_{L,i}\right); \\
& \left(\frac{\beta_H k_H}{n_H}\sum_\ell \frac{\lambda_{H,\ell}}{\ell}\right)^2 + \left(\frac{\beta_L k_L}{n_L}\sum_\ell \frac{\lambda_{L,\ell}}{\ell}\right)^2 \le \frac{1}{(\mathsf{dc_H})^2 + (\mathsf{dc_L})^2}; \\
& \sum_\ell \frac{\lambda_{H,\ell}}{\sqrt{\ell}} \le \frac{\sqrt{n_H}}{\sqrt{k_H}\sqrt{\mathsf{dc_H} + \mathsf{dc_L}}}; \\
& \lambda_{L,1} = \lambda_{H,1} = 0,
\end{aligned}$$

  which is equivalent to (Equation 4.4.3) without the Requirement 6.
- **Iterative Update:** denote $\boldsymbol{\lambda}_H^{(t)}$ (or $\boldsymbol{\lambda}_L^{(t)}$) as the updated version of $\boldsymbol{\lambda}_{(H)}$ (or $\boldsymbol{\lambda}_{(L)}$) in the tth iteration.
  - **For time** $t = 1$ **to** T**:** update $\boldsymbol{\lambda}_H^{(t)}$ and $\boldsymbol{\lambda}_L^{(t)}$ by alternating minimization of (Equation 4.4.3) with Requirement 5 and Requirement 6 being replaced by (Equation 4.4.7), (Equation 4.4.8), and (Equation 4.4.9).
    1. **Update** $\boldsymbol{\lambda}_H^{(t)}$ with $\boldsymbol{\lambda}_L$ being fixed to be $\boldsymbol{\lambda}_L^{(t-1)}$;
    2. **Update** $\boldsymbol{\lambda}_L^{(t)}$ with $\boldsymbol{\lambda}_H$ being fixed to be $\boldsymbol{\lambda}_H^{(t)}$.
- **Output**: degree distribution $\boldsymbol{\lambda}_H^{(T)}$ and $\boldsymbol{\lambda}_L^{(T)}$.

4.6.1 Experiments with synthetic data

Experiment set-up. We fix the check node degrees $\mathsf{dc_H}$ and $\mathsf{dc_L}$ as 5 and let the maximum variable node degree $\mathsf{dv_{max}}$ as 50. The magnitude of the non-zero entries is set to 1. Then we

study the recovery performance with varying $\mathsf{SNR} = \left\|\mathbf{x}^\natural\right\|_2^2/\sigma^2$. The following numerical experiments separately study the impact of the signal length n_H and n_L and the impact of the sparsity number k_H and k_L.

Impact of sparsity number

We fix the length n_H of the high-priority part $\mathbf{x}_H^\natural$ as 100 and the length n_L of the low-priority part $\mathbf{x}_L^\natural$ as 400. The simulation results are plotted in Figure 4.3.

We first investigate the recovery performance w.r.t. the high priority part $\mathbf{x}_H^\natural$. Using the sensing matrix $\mathbf{A}_{\text{regular}}$ (regular sensing) as the baseline, we conclude that our sensing matrix $\mathbf{A}_{\text{preferential}}^{(\text{final})}$ (preferential sensing) achieves better performance when the signal is more sparse. Consider the case when $\mathsf{SNR} = 100$. When $k_H = k_L = 10$, the ratio $\|\widehat{\mathbf{x}}_H - \mathbf{x}_H^\natural\|_2/\|\mathbf{x}_H^\natural\|_2$ for $\mathbf{A}_{\text{preferential}}^{(\text{final})}$ is approximately 0.35 while that of the $\mathbf{A}_{\text{regular}}$ is 0.86. When the sparsity number k_H and k_L increase to 15, the improvement is approximately $(0.85 - 0.4)/0.85 \approx 53\%$. When the sparsity number k_H and k_L increase to 20, the corresponding improvement further decreases to $(0.95 - 0.55)/0.95 \approx 42\%$.

When turning to the reconstruction error $\left\|\widehat{\mathbf{x}} - \mathbf{x}^\natural\right\|_2/\left\|\mathbf{x}^\natural\right\|_2$ w.r.t. the whole signal, we notice a similar phenomenon, i.e., a sparser signal contributes to better performance. Additionally, we notice the sensing matrix $\mathbf{A}_{\text{preferential}}^{(\text{final})}$ achieves significant improvements in comparison to its initialized version $\mathbf{A}_{\text{preferential}}^{(\text{init})}$.

Impact of signal length

We also studied various settings in which the length n_H of the high-priority part $\mathbf{x}_H^\natural$ is set to $\{150, 200, 250, 300\}$ and the corresponding length n_L of the low-priority part $\mathbf{x}_L^\natural$ is set to $\{600, 800, 1000, 1200\}$. The simulation results are plotted in Figure 4.4.

Compared to regular sensing, our sensing matrix $\mathbf{A}_{\text{preferential}}^{(\text{final})}$ can reduce the error in the high-priority part $\mathbf{x}_H^\natural$ significantly. For example, when $\mathsf{SNR} = 100$, the ratio $\|\widehat{\mathbf{x}}_H - \mathbf{x}_H^\natural\|_2/\|\mathbf{x}_H^\natural\|_2$ reduces between $40\% \sim 60\%$ with the sensing matrix $\mathbf{A}_{\text{preferential}}^{(\text{final})}$. Meanwhile,

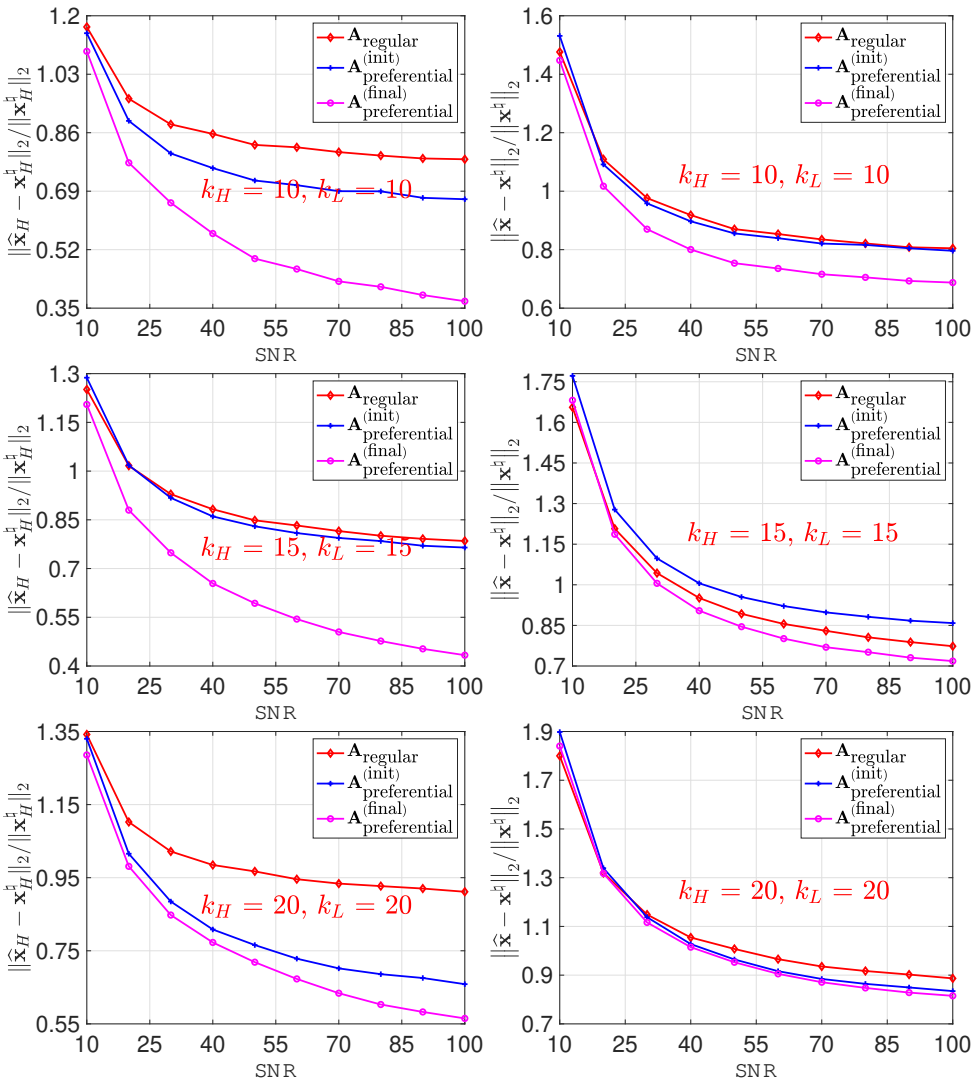

Figure 4.3. Comparison of preferential sensing vs regular sensing. The length n_H of the high-priority part $\mathbf{x}_H^\natural$ is set as 100; while the length n_L of the low-priority part $\mathbf{x}_L^\natural$ is set as 400. (**Left panel**) We evaluate the reconstruction performance w.r.t. the high-priority part $\|\widehat{\mathbf{x}}_H - \mathbf{x}_H^\natural\|_2/\|\mathbf{x}_H^\natural\|_2$. (**Right panel**) We evaluate the reconstruction performance w.r.t. the whole signal $\|\widehat{\mathbf{x}} - \mathbf{x}^\natural\|_2/\|\mathbf{x}^\natural\|_2$.

w.r.t. the whole signal $\mathbf{x}^\natural$, the ratio $\left\|\widehat{\mathbf{x}} - \mathbf{x}^\natural\right\|_2/\left\|\mathbf{x}^\natural\right\|_2$ decreases with a smaller magnitude.

4.6.2 Experiments with real-world data

We compare the performance of sensing matrices for images using (i) MNIST dataset [137], which consists of 10000 images in the testing set and 60000 images in the training set; and (ii) Lena image.

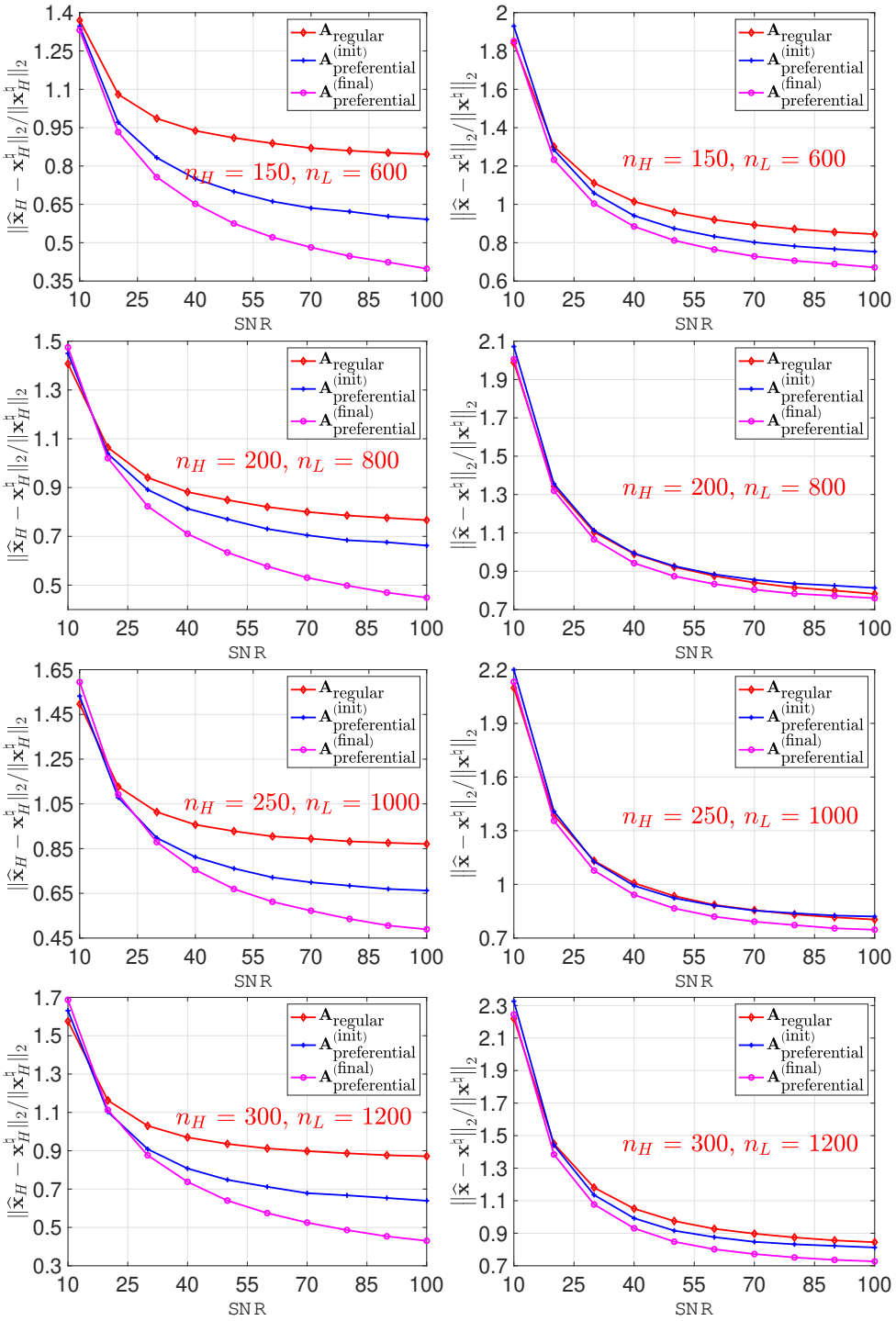

Figure 4.4. Comparison of preferential sensing vs regular sensing. Both the sparsity number k_H and k_L are set as 15. (**Left panel**) We evaluate the reconstruction performance w.r.t. the high-priority part $\|\widehat{\mathbf{x}}_H - \mathbf{x}_H^\natural\|_2/\|\mathbf{x}_H^\natural\|_2$. (**Right panel**) We evaluate the reconstruction performance w.r.t. the whole signal $\|\widehat{\mathbf{x}} - \mathbf{x}^\natural\|_2/\|\mathbf{x}^\natural\|_2$.

To obtain a sparse representation for each image, we perform a 2D Haar transform $\mathcal{H}(\cdot)$, which generates four sub-matrices being called as the approximation coefficients (at the coarsest level), horizontal detail coefficients, vertical detail coefficients, and diagonal detail coefficients. The approximation coefficients are at the coarsest level and are treated as the high-priority part $\mathbf{x}_H^\natural$; while the horizontal detail coefficients, vertical detail coefficients, and diagonal detail coefficients are regarded as the low-priority part $\mathbf{x}_L^\natural$. Hence we can write the sensing relation in (Equation 4.2.1) as

$$\mathbf{y} = \mathbf{A}\mathcal{H}(\text{Image}) + \mathbf{w}, \tag{4.6.1}$$

where Image denotes the input image, $\mathcal{H}(\cdot)$ denotes the vectorized version of the coefficients and is viewed as the sparse ground-truth signal, and $\mathbf{w}$ denotes the sensing noise. The sensing matrix $\mathbf{A}$ is designed such that the approximation coefficients of $\mathcal{H}(\text{Image})$ can be better reconstructed.

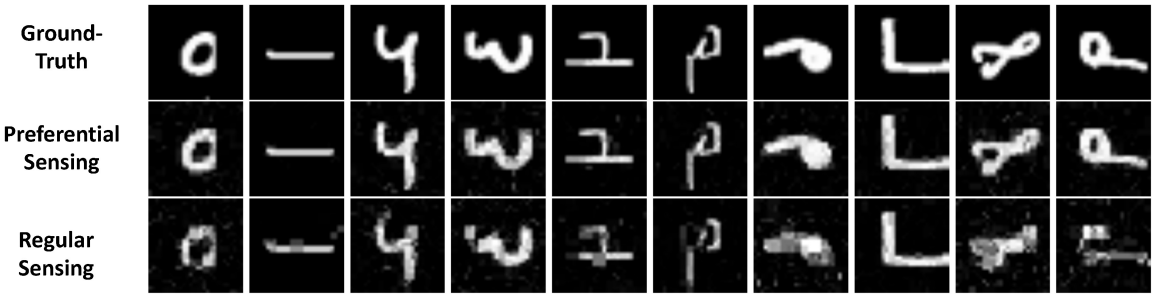

Figure 4.5. The performance comparison between the sensing matrix for preferential sensing $\mathbf{A}_{\text{preferential}}^{(\text{final})}$ and sensing matrix for regular sensing $\mathbf{A}_{\text{regular}}$. (**Top**) The ground-truth images. (**Middle**) The reconstructed images with the sensing matrix $\mathbf{A}_{\text{preferential}}^{(\text{final})}$. (**Bottom**) The reconstructed images with the sensing matrix $\mathbf{A}_{\text{regular}}$.

4.6.3 Experiments with MNIST

Experiment set-up. We set the images from MNIST as the input images, which consists of 10000 images in the testing set and 60000 images in the training set with each image being of dimension 28×28.

The whole datasets can be divided into 10 categories with each category representing a

digit from zero to nine. For each digit, we design one unique sensing matrix. The lengths n_H and n_L are set to $(28/2)^2 = 196$ and $3 \times (28/2)^2 = 588$, respectively. The sparsity coefficients k_H and k_L varied among different digits.

Discussion. To evaluate the performance, we define ratios $r_{H,(\cdot)}$ and $r_{W,(\cdot)}$ as

$$r_{H,(\cdot)} \triangleq \frac{\|\widehat{\mathbf{x}}_H - \mathbf{x}_H^\natural\|_2}{\|\mathbf{x}_H^\natural\|_2};$$
$$r_{W,(\cdot)} \triangleq \frac{\|\widehat{\mathbf{x}} - \mathbf{x}^\natural\|_2}{\|\mathbf{x}^\natural\|_2},$$

which correspond to the ℓ_2 error in the high-priority part $\mathbf{x}_H^\natural$ and the entire signal $\mathbf{x}^\natural$, respectively. We use the sensing matrix $\mathbf{A}_{\text{regular}}$ as the benchmark. In addition, we omit the results of $\mathbf{A}^{(\text{init})}_{\text{preferential}}$, since the sensing matrix $\mathbf{A}^{(\text{final})}_{\text{preferential}}$ has better performance.

The results are listed in Table 4.1. A subset of the reconstructed images are shown in Figure 4.5. From the Table 4.1 and Figure 4.5, we conclude that our sensing matrix $\mathbf{A}^{(\text{final})}_{\text{preferential}}$ for the preferential sensing can better preserve the images when comparing with the sensing matrix $\mathbf{A}_{\text{regular}}$ for the regular sensing.

Figure 4.6. (**Left**) Ground-truth image. (**Middle**) Reconstructed image via sensing matrix $\mathbf{A}^{(\text{final})}_{\text{preferential}}$ for preferential sensing. (**Right**) Reconstructed image via sensing matrix $\mathbf{A}_{\text{regular}}$ for regular sensing.

4.6.4 Experiments with Lena Image

Experiment set-up. We evaluate the benefits of using $\mathbf{A}^{(\text{final})}_{\text{preferential}}$ for the Lena image with dimension 512×512. Notice that the sensing matrix would have been prohibitively large

Table 4.1. The index $i = p$ corresponds to the sensing matrix $\mathbf{A}^{\text{(final)}}_{\text{preferential}}$ for the preferential sensing; while the index $i = r$ corresponds to the sensing matrix $\mathbf{A}_{\text{regular}}$ for the regular sensing. We define the ratio $r_{H,(i)}$ ($i = \{p, r\}$) as the error w.r.t. the high priority part, namely, $\|\widehat{\mathbf{x}}_H - \mathbf{x}_H^\natural\|_2 / \|\mathbf{x}_H^\natural\|_2$. Similarly we define the ratio $r_{W,(i)}$ ($i = \{p, r\}$) as the ratio w.r.t. the whole signal, namely, $\|\widehat{\mathbf{x}} - \mathbf{x}^\natural\|_2 / \|\mathbf{x}^\natural\|_2$. Moreover, we put the results corresponding to the sensing matrix $\mathbf{A}^{\text{(final)}}_{\text{preferential}}$ in the bold font.

	Training Set				Testing Set			
Digit	$r_{H,(p)}$	$r_{H,(r)}$	$r_{W,(p)}$	$r_{W,(r)}$	$r_{H,(p)}$	$r_{H,(r)}$	$r_{W,(p)}$	$r_{W,(r)}$
0	**0.28315**	0.5154	**0.44818**	0.60131	**0.30292**	0.45749	**0.46283**	0.56486
1	**0.16746**	0.33751	**0.29332**	0.41599	**0.1511**	0.45264	**0.2659**	0.51864
2	**0.26303**	0.50365	**0.42984**	0.59959	**0.24896**	0.4233	**0.42216**	0.52556
3	**0.24613**	0.43677	**0.42514**	0.53163	**0.26446**	0.46766	**0.43534**	0.56189
4	**0.28331**	0.44377	**0.44623**	0.53791	**0.30092**	0.4445	**0.45804**	0.53749
5	**0.28405**	0.53511	**0.45727**	0.6198	**0.27258**	0.47044	**0.44382**	0.56622
6	**0.28801**	0.39436	**0.45053**	0.51701	**0.27084**	0.5086	**0.44134**	0.59534
7	**0.25503**	0.41621	**0.41809**	0.52896	**0.27266**	0.51329	**0.41693**	0.5783
8	**0.31263**	0.51918	**0.47618**	0.61492	**0.32731**	0.48163	**0.48699**	0.5837
9	**0.30171**	0.54394	**0.45241**	0.61799	**0.27385**	0.55313	**0.43116**	0.62785

if we used the whole image as the input. To put more specifically, we would need a matrix with the width $512^2 = 262144$. To handle such issue, we divide the whole images into a set of sub-blocks with dimensions 32×32 and design one sensing matrix with the width $32^2 = 1024$. For each sub-block, we first obtain a sparse representation with the 2D Haar transform and then reconstruct the signal in (Equation 4.6.1).

Discussion. The comparison of results is plotted in Figure 4.6, from which we conclude that the sensing matrix $\mathbf{A}^{\text{(final)}}_{\text{preferential}}$ has much better performance in image reconstruction in comparison with the sensing matrix $\mathbf{A}_{\text{regular}}$. The ratios $r_{H,(p)}$ and $r_{H,(r)}$ are computed as 0.0446 and 0.3029, respectively; while the ratio $r_{W,(p)}$ and $r_{W,(r)}$ are computed as 0.0709 and 0.3144, respectively.

Remark 3. *The degree distributions $\lambda_H(\cdot)$ and $\lambda_L(\cdot)$ of the variable nodes for the sensing matrix $\mathbf{A}^{\text{(final)}}_{\text{preferential}}$ are obtained as*

$$
\begin{aligned}
&\lambda_H(\alpha) \\
&= 0.0057856\alpha + 0.025915\alpha^2 + 0.36394\alpha^3 + 0.35183\alpha^4 \\
&+ 0.10333\alpha^5 + 0.04134\alpha^6 + 0.021619\alpha^7 + 0.013508\alpha^8 \\
&+ 0.0094374\alpha^9 + 0.0070906\alpha^{10} + 0.0056\alpha^{11} \\
&+ 0.0045851\alpha^{12} + 0.0038574\alpha^{13} + 0.0033145\alpha^{14} \\
&+ 0.0028963\alpha^{15} + .0025659\alpha^{16} + 0.0022992\alpha^{17} \\
&+ 0.0020801\alpha^{18} + 0.0018973\alpha^{19} + 0.0017428\alpha^{20} \\
&+ 0.0016109\alpha^{21} + 0.001497\alpha^{22} + 0.001398\alpha^{23} \\
&+ 0.0013111\alpha^{24} + 0.0012344\alpha^{25} + 0.0011662\alpha^{26} \\
&+ 0.0011053\alpha^{27} + 0.0010506\alpha^{28} + 0.0010013\alpha^{29} \\
&+ 0.0009565\alpha^{30} + 0.00091576\alpha^{31} + 0.00087852\alpha^{32} \\
&+ 0.00084436\alpha^{33} + 0.00081292\alpha^{34} + 0.00078388\alpha^{35} \\
&+ 0.00075697\alpha^{36} + 0.00073197\alpha^{37} + 0.00070867\alpha^{38} \\
&+ 0.00068691\alpha^{39} + 0.00066652\alpha^{40} + 0.00064738\alpha^{41} \\
&+ 0.00062937\alpha^{42} + 0.00061238\alpha^{43} + 0.00059633\alpha^{44} \\
&+ 0.00058114\alpha^{45} + 0.00056673\alpha^{46} + 0.00055304\alpha^{47} \\
&+ 0.00054001\alpha^{48} + 0.0005276\alpha^{49}; \\
&\lambda_L(\alpha) = \alpha.
\end{aligned}
$$

The check node degrees $\mathsf{dc_H}$ *and* $\mathsf{dc_L}$ *are both set as* 4*. Meanwhile the sensing matrix* $\mathbf{A}_{\text{regular}}$ *designed in* (Equation 4.3.7) *is a regular sensing matrix whose variable node and check node degree distributions are given by* $\lambda(\alpha) = \alpha^2$ *and* $\rho(\alpha) = \alpha^7$*, respectively.*

4.7 Conclusions

We presented a general framework of the sensing matrix design for a linear measurement system. Focusing on a sparse sensing matrix $\mathbf{A}$, we associated it with a graphical model $\mathcal{G} = (\mathcal{V}, \mathcal{E})$ and transformed the design of $\mathbf{A}$ to the connectivity problem in $\mathcal{G}$. With the density evolution technique, we proposed two design strategies, i.e., regular sensing and preferential sensing. In the regular sensing scenario, all entries of the signal are recovered with equal accuracy; while in the preferential sensing scenario, the entries in the high-priority sub-block are recovered more accurately (or exactly) relative to the entries in the low-priority sub-block. We then analyzed the impact of the connectivity of the graph on the recovery performance. For the regular sensing, our framework can reproduce the classical result of Lasso, i.e., the number of measurements m should be at least in the order $O(k \log n)$, where n is the length of the signal and k is the sparsity number. For the preferential sensing, our framework can lead to a significant reduction of the reconstruction error in the high-priority part and a modest reduction of the error in the whole signal. Numerical experiments with both the synthetic data and real-world data are presented to corroborate our claims.

CHAPTER 5
SPARSE RECOVERY OF SIGN VECTORS UNDER UNCERTAIN SENSING MATRICES

5.1 Introduction

Generally speaking, uncertainties in the sensing matrix weakens the system performance and reduces the reliability of recovered signals. Meanwhile in some applications [86, 97, 96], the sign values of signals instead of their exact values may be needed. One such an application is detecting irregular concentration patterns of biomarker miRNAs, a small non-coding RNA molecules for monitoring certain diseases [86]. Let entries of vector $\mathbf{z}$ be the concentration of miRNAs. Let signal vector $\Delta\mathbf{z}$ be concentration changes in all miRNAs between two consecutive measurements, $\Delta\mathbf{z} = \mathbf{z}_1 - \mathbf{z}_2$. Since the number of biomarker miRNAs is small compared to the total number of miRNA types, $\mathbf{x} \triangleq \Delta\mathbf{z}$ can be assumed to be an sparse vector as the concentrations of non-biomarker miRNAs have subtle changes between two consecutive measurements. For disease diagnosis, only directions of changes in entries of $\mathbf{x}$ over multiple measurements $\mathbf{z}_1$, $\mathbf{z}_2$, rather than the exact values, are desirable. In other words, sign$(\Delta\mathbf{z})$, $\Delta\mathbf{z} = \mathbf{z}_1 - \mathbf{z}_2$, is the parameter of interest. Note that since the measurements are linear, we will drop Δ from the abstraction of the problem for simplicity of presentation.

This chapter will show that as long as the uncertainty in the sensing matrix is sparse, a thresholding mechanism can be developed to recover the sign vector. In particular, provided that the true signal satisfies certain conditions, the exact sign vector can be recovered with high probability even under uncertain sensing matrices.

5.2 Problem Formulation

Consider the sensing system

$$\mathbf{y} = \mathbf{\Psi}\mathbf{x} + \mathbf{w},$$

$$\mathbf{\Psi} = \mathbf{A} + \mathbf{E},$$

where $\mathbf{y} \in \mathbb{R}^m$ denotes the reading, $\mathbf{x} \in \mathbb{R}^n$ is the k-sparse signal, and $\mathbf{w} \in \mathbb{R}^m$ denotes the sensing noise. Further, $\mathbf{A} \in \mathbb{R}^{m\times n}$ $(m < n)$ represents the ideal desirable sensing matrix, but $\mathbf{\Psi} \in \mathbb{R}^{m\times n}$ denotes the actual resulting sensing matrix because of the perturbation matrix $\mathbf{E} \in \mathbb{R}^{m\times n}$. To recover signal $\mathbf{x}$, ideally we would adopt the optimization

$$\min_{\mathbf{x}} \ \|\mathbf{x}\|_1, \ \text{s.t.} \ \ \|\mathbf{y} - \mathbf{\Psi}\boldsymbol{x}\|_2 \leq \sigma^2,$$

where σ^2 denotes the maximum norm of noise. However, due to the inaccessibility of true matrix $\mathbf{\Psi}$, we modify the constraint to be $\|\mathbf{y} - \mathbf{A}\mathbf{x}\|_2 \leq \sigma'^2$. Hence, our optimization problem is modified to

$$\widehat{\mathbf{x}} = \text{argmin}_{\mathbf{x}} \ \|\mathbf{x}\|_1, \ \ \text{s.t.} \ \ \|\mathbf{y} - \mathbf{A}\mathbf{x}\|_2 \leq \sigma'^2, \tag{5.2.1}$$

where σ'^2 denotes the modified noise norm that should be set to allow the true $\mathbf{x}$ satisfy the constraint. Denote $\widehat{\mathbf{x}}$ as the solution to (Equation 5.2.1). In the following, we will analyze the solution $\widehat{\mathbf{x}}$ and propose a thresholding method to get the correct sign vector $\text{sign}(\mathbf{x})$ with $\widehat{\mathbf{x}}$ under the existence of perturbation matrix $\mathbf{E}$.

Before proceeding, we denote the support set of $\mathbf{x}$ as T, i.e., the index set of non-zero entries $\{i : \ x_i \neq 0\}$. Then, we construct $[\mathbf{x}_T \ \mathbf{x}_{T^c}]$, such that $\mathbf{x}_T$ represents the entries x_i with its indices to be within the support set T while $\mathbf{x}_{T^c}$ denotes the rest of entries in $\mathbf{x}$. Besides, we define the difference between solution $\widehat{\mathbf{x}}$ and true signal $\mathbf{x}$ as $\mathbf{h} = \widehat{\mathbf{x}} - \mathbf{x}$. Similarly, we form $\mathbf{h}_T$ and $\mathbf{h}_{T^c}$ from $\mathbf{h}$. Further, we assume $\|\mathbf{x}\|_2$ is upper bounded by some constant C.

5.3 Theoretical Foundation

Structure of this section can be divided into three components. First, we will analyze the perturbation matrix $\mathbf{E}$. Then we will set σ'^2 and bound $\|\mathbf{Ah}\|_2^2$. Finally, we will investigate the infinity norm of $\mathbf{h}$. Notice that to recover sparse signal $\mathbf{x}$, sensing matrix $\mathbf{A}$ should be designed to facilitate the recovery, whose property can be characterized by the following two concepts: coherence ρ and RIP-constant δ_k [83].

Definition 3 (Coherence)**.** *For sensing matrix $\mathbf{A} \in \mathbb{R}^{m\times n}$, the coherence ρ is defined as*

$$\rho = \max_{i\neq j} \frac{|\langle \mathbf{A}_i, \mathbf{A}_j \rangle|}{\|\mathbf{A}_i\|_2 \|\mathbf{A}_j\|_2},$$

where $\mathbf{A}_i$ and $\mathbf{A}_j$ denote the ith and jth columns of matrix $\mathbf{A}$, respectively.

Definition 4 (RIP-constant)**.** *For sensing matrix $\mathbf{A}$, its RIP constant δ_k is defined as the minimum value that satisfies*

$$(1-\delta_k)\|\mathbf{x}\|_2^2 \leq \|\mathbf{Ax}\|_2^2 \leq (1+\delta_k)\|\mathbf{x}\|_2^2$$

for all k-sparse $\mathbf{x}$.

5.3.1 Analysis of Perturbation Matrix

We now analyze the perturbation matrix $\mathbf{E}$. Different distributions of matrix $\mathbf{E}$ results in different types of errors in the sensing matrix $\mathbf{\Psi}$ [87, 138, 97]. Motivated by the biological application, we consider a unique case as following. Note that the (i,j)th entry of $\mathbf{\Psi}$ models the reaction between ith sensor and jth miRNA. If Ψ_{ij} is zero, it means that sensor i does not react to miRNA j. However, due to the stochastic nature of molecular binding, certain miRNAs may still bound to a binding site in a sensor (to which they are not expected to) and create undesirable footprints. Hence, some entries of Ψ that are expected (by design) to be zero could turn out to be non-zero. Since this happens occasionally, the

perturbation matrix $\mathbf{E}$ can be assumed sparse.

As our model in [79], we may assume

$$p_E(e_{ij}) = \frac{p_E}{\sqrt{2\pi}\sigma_E} \exp\left(-e_{ij}^2/2\sigma_E^2\right) + (1-p_E)\delta(e_{ij}=0),$$

where $\delta(e_{ij}=0)$ is the delta function and σ_E^2 denotes the variance. Here, p_E controls the sparsity in matrix $\mathbf{E}$.

Note that $\|\mathbf{E}\mathbf{x}\|_2 = \|\mathbf{E}_T\mathbf{x}_T\|_2$, which implies only those columns with indices are in the support set $\boldsymbol{T}$ can contribute to the norm $\|\mathbf{E}\mathbf{x}\|_2$. Therefore, we only need to consider the sub-matrix $\mathbb{R}^{m\times k}$ of $\mathbf{E}$. We have the following lemma.

Lemma 6. *For an arbitrary sub-matrix $\mathbf{E}^{(k)} \in \mathbb{R}^{m\times k}$, the expectation of its maximal singular value $\sigma_{\max}(\mathbf{E}^{(k)})$ is bounded by*

$$\mathbb{E}\sigma_{\max}(\mathbf{E}^{(k)}) \le C\sqrt{p_E}\sigma_E(\sqrt{m}+\sqrt{k}),$$

where $C>0$ is some constant.

Proof. Define process $X_{\boldsymbol{u},\boldsymbol{v}}$ and Gaussian process $Y_{\boldsymbol{u},\boldsymbol{v}}$ with $\boldsymbol{v}\in\mathbb{R}^k$, $\boldsymbol{u}\in\mathbb{R}^m$, and $\|\boldsymbol{v}\|_2 = \|\boldsymbol{u}\|_2 = 1$ as,

$$X_{\boldsymbol{u},\boldsymbol{v}} = \left\langle \boldsymbol{u}, \mathbf{E}^{(k)}\boldsymbol{v}\right\rangle, \quad Y_{\boldsymbol{u},\boldsymbol{v}} = \sqrt{p_E}\sigma_E\left\langle \mathbf{G}, \boldsymbol{u}\right\rangle + \sqrt{p_E}\sigma_E\left\langle \mathbf{h}, \boldsymbol{v}\right\rangle,$$

where $\mathbf{G}$ and $\mathbf{h}$ are random variables with the distributions $\mathbf{G}\sim\mathcal{N}(0,\boldsymbol{I}_m)$, and $\mathbf{h}\sim\mathcal{N}(0,\boldsymbol{I}_k)$, respectively.

First, we calculate the distance $\mathbb{E}\|X_{\boldsymbol{u},\boldsymbol{v}} - X_{\boldsymbol{w},\boldsymbol{z}}\|_2^2$ as

$$\begin{aligned}
&\mathbb{E}\|X_{\boldsymbol{u},\boldsymbol{v}} - X_{\boldsymbol{w},\boldsymbol{z}}\|_2^2 = p_E\sigma_E^2\sum_{ij}(u_iv_j - w_iz_j)^2 \\
&= p_E\sigma_E^2\|\boldsymbol{u}-\boldsymbol{w}\|_2^2 + p_E\sigma_E^2\|\boldsymbol{v}-\boldsymbol{z}\|_2^2 + 2p_E\sigma_E^2\left(\langle\boldsymbol{u},\boldsymbol{w}\rangle - \|\boldsymbol{w}\|_2^2\right)\left(\|\boldsymbol{v}\|_2^2 - \langle\boldsymbol{v},\boldsymbol{z}\rangle\right) \\
&\le p_E\sigma_E^2\|\boldsymbol{u}-\boldsymbol{w}\|_2^2 + p_E\sigma_E^2\|\boldsymbol{v}-\boldsymbol{z}\|_2^2.
\end{aligned}$$

Then we calculate the distance $\mathbb{E}\|Y_{\boldsymbol{u},\boldsymbol{v}} - Y_{\boldsymbol{w},\boldsymbol{z}}\|_2^2$ as

$$\mathbb{E}\|Y_{\boldsymbol{u},\boldsymbol{v}} - Y_{\boldsymbol{w},\boldsymbol{z}}\|_2^2 = \ p_E\sigma_E^2\|\boldsymbol{u} - \boldsymbol{w}\|_2^2 + \ p_E\sigma_E^2\|\boldsymbol{v} - \boldsymbol{z}\|_2^2.$$

Since $\mathbb{E}\|X_{\boldsymbol{u},\boldsymbol{v}} - X_{\boldsymbol{w},\boldsymbol{z}}\|_2^2 \leq \ \mathbb{E}\|Y_{\boldsymbol{u},\boldsymbol{v}} - Y_{\boldsymbol{w},\boldsymbol{z}}\|_2^2$, by Talagrand's comparison equality [139], we should have

$$\mathbb{E}_{\mathbf{E}^{(k)}} \sup_{\boldsymbol{u},\boldsymbol{v}} X_{\boldsymbol{u},\boldsymbol{v}} = \ \mathbb{E}_{\mathbf{E}^{(k)}}\sigma_{max}(\mathbf{E}^{(k)}) \leq \ C\mathbb{E}_{\mathbf{G},\mathbf{h}} \sup_{\boldsymbol{u},\boldsymbol{v}} Y_{\boldsymbol{u},\boldsymbol{v}} = C\sqrt{p_E}\sigma_E(\sqrt{n} + \sqrt{k}),$$

where $C > 0$ is some constant and completes the proof. □

Having obtained an upper bound for $\mathbb{E}\sigma_{\max}(\mathbf{E}^{(k)})$, we will then show that the maximal singular value $\sigma_{\max}(\mathbf{E}^{(k)})$ is not sufficiently larger than this bound in most cases.

Lemma 7. *For all sub-matrices $\mathbf{E}^{(k)} \in \mathbb{R}^{m\times k}$, the maximal singular value $\sigma_{\max}(\mathbf{E}^{(k)})$ satisfies*

$$\sigma_{\max}(\mathbf{E}^{(k)}) \leq \ C\sqrt{p_E}\sigma_E(\sqrt{m} + \sqrt{k}) + t, \ \ t > 0,$$

with probability at least $1 - \binom{n}{k}\exp(-t^2/2)$.

Proof. Take an arbitrary sub-matrix $\mathbf{E}^{(k)} \in \mathbb{R}^{m\times k}$ from $\mathbf{E}$. Define binary matrix $\mathbf{M}^{(k)}$ as

$$M_{ij}^{(k)} = \begin{cases} 0, & E_{ij}^{(k)} = 0; \\ 1, & \text{otherwise}, \end{cases}$$

where $M_{ij}^{(k)}$ and $E_{ij}^{(k)}$ denote the (i,j)th entry in matrices $\mathbf{M}^{(k)}$ and $\mathbf{E}^{(k)}$, respectively. Then we can couple $\mathbf{E}^{(k)}$ with a Gaussian matrix $\mathbf{G}^{(k)}$ and $\mathbf{M}^{(k)}$ such that $\mathbf{E}^{(k)} = \mathbf{M}^{(k)} \circ \mathbf{G}^{(k)}$,

where $\circ$ denotes the Hadamard product [119], i.e., $E_{ij}^{(k)} = M_{ij}^{(k)} G_{ij}^{(k)}$. Then we have

$$
\begin{aligned}
&\mathbb{P}\left\{\sigma_{\max}(\mathbf{E}^{(k)}) \geq\ C\sqrt{p_E}\sigma_E(\sqrt{m}+\sqrt{k}) + t\right\} \\
&\leq \mathbb{P}\left\{\sigma_{\max}(\mathbf{E}^{(k)}) \geq\ \mathbb{E}\sigma_{\max}(\mathbf{E}^{(k)}) + t\right\} \\
&= \mathbb{E}\mathbb{1}\left\{\sigma_{\max}(\mathbf{E}^{(k)}) - \mathbb{E}\ \sigma_{\max}(\mathbf{E}^{(k)}) \geq t\right\} \\
&= \mathbb{E}_{\mathbf{M}^{(k)}}\mathbb{E}_{\mathbf{E}^{(k)}|\mathbf{M}^{(k)}}\mathbb{1}\left\{\sigma_{\max}(\mathbf{E}^{(k)}) - \mathbb{E}\ \sigma_{\max}(\mathbf{E}^{(k)}) \geq t\right\} \\
&=\ \mathbb{E}_{\mathbf{M}^{(k)}}\mathbb{P}\left\{\sigma_{\max}(\mathbf{E}^{(k)}) - \mathbb{E}\ \sigma_{\max}(\mathbf{E}^{(k)}) \geq t \mid \mathbf{M}^{(k)}\right\} \\
&\overset{①}{\leq} e^{-t^2/2},\ \ t > 0,
\end{aligned}
\tag{5.3.1}
$$

where ① is because entries in $\mathbf{G}^{(k)}$ is gaussian and the mapping is a 1-Lipschitz function, so we can use Theorem 5.6 in [140]. Note that there are $\binom{n}{k}$ different types of sub-matrices $\mathbf{E}^{(k)}$ in total. Hence, the event that all sub-matrices $\mathbf{E}^{(k)}$ satisfy (Equation 5.3.1) holds with probability at least $1 - \binom{n}{k}\exp(-t^2/2)$. □

5.3.2 Bound on $\sigma^{'2}$ and $\|\mathbf{Ah}\|_2$

We now determine $\sigma^{'2}$ and obtain bound for $\|\mathbf{Ah}\|_2$. Since the true signal $\mathbf{x}$ should satisfy the constraint $\|\mathbf{y} - \mathbf{Ax}\|_2 \leq \sigma^{'2}$, we have

$$
\begin{aligned}
\|\mathbf{y} - \mathbf{Ax}\|_2 =\ \ \|\boldsymbol{\Psi x} + \mathbf{w} - \mathbf{Ax}\|_2 =\ \|\mathbf{Ex} + \mathbf{w}\|_2 \\
\leq\ \|\mathbf{w}\|_2 + \|\mathbf{Ex}\|_2 \leq\ \sigma^2 + \sigma_{\max}(\mathbf{E}^{(k)})C.
\end{aligned}
$$

Therefore, to ensure the constraint in (Equation 5.2.1), $\sigma^{'2}$ should be at least $\sigma^2 + \sigma_{\max}(\mathbf{E}^{(k)})C$. On the other hand, setting $\sigma^{'2}$ to a large value may lead to a trivial solution $\mathbf{0}$. In the sequel, we set $\sigma^{'2}$ as $\sigma^2 + \sigma_{\max}(\mathbf{E}^{(k)})C$ and obtain the following lemma.

Lemma 8. *The relation* $\|\mathbf{Ah}\|_2 \leq\ 2(\sigma_E\sqrt{p_E m} + \sigma_E\sqrt{p_E k} + t)C + 2\sigma^2$ *holds with probability at least* $1 - \binom{n}{k}\exp(-t^2/2),\ t > 0$.

Proof. We have

$$\|\mathbf{Ah}\|_2 = \|\mathbf{Ax} - \mathbf{A}\widehat{\mathbf{x}}\|_2 = \|\mathbf{Ax} - \mathbf{y} + \mathbf{y} - \mathbf{A}\widehat{\mathbf{x}}\|_2$$
$$\leq \|\mathbf{Ax} - \mathbf{y}\|_2 + \|\mathbf{y} - \mathbf{A}\widehat{\mathbf{x}}\|_2 \leq 2\sigma^{'2} = 2\sigma^2 + 2\sigma_{\max}(\mathbf{E}^{(k)})C.$$

Since the relation $\sigma_{\max}(\mathbf{E}^{(k)}) \leq \sqrt{p_E}\sigma_E(\sqrt{m} + \sqrt{k}) + t,\ t > 0$ holds with probability at least $1 - \binom{n}{k}\exp(-t^2/2)$, by Lemma 7, the proof is completed. □

5.3.3 Bound on $\|\mathbf{h}\|_\infty$

We now obtain an upper bound on $\|\mathbf{h}\|_\infty$ using $\|\mathbf{Ah}\|_2$.

Remark 4. *The deviation* $\mathbf{h}$ *satisfies [83, 141]* $\|\mathbf{h}_{T^c}\|_1 \leq \|\mathbf{h}_T\|_1$.

Since this remark can be driven easily from widely known results in compressive sensing [83, 141], we omit the proof.

Lemma 9. *The infinity norm of* $\mathbf{h}$ *satisfies*

$$\|\mathbf{h}\|_\infty \leq \frac{\|\mathbf{Ah}\|_2}{\min_{1\leq i\leq n}\|\mathbf{A}_i\|_2} + 2\rho\sqrt{k}\|\mathbf{h}_T\|_2.$$

Proof. Inspired by the proof in [97], we first define the covariance matrix $\Sigma \in \mathbb{R}^{n\times n}$ with its (i, j) entry written as

$$\Sigma_{ij} = \frac{\langle \mathbf{A}_i, \mathbf{A}_j\rangle}{\|\mathbf{A}_i\|_2\|\mathbf{A}_j\|_2}.$$

Easily we can verify that the matrix $\mathbf{\Sigma}$ satisfies

$$\mathbf{\Sigma}_{ii} = 1,\ \ 1 \leq i \leq n,$$
$$|\mathbf{\Sigma}_{ij}| \leq \rho,\ \ 1 \leq i \neq j \leq n.$$

For the simplicity of following analysis, let $\mathbf{B}$ be a matrix whose ith column is $\mathbf{B}_i \triangleq \mathbf{A}_i/\|\mathbf{A}_i\|_2$. Easily we can verify that $\mathbf{B}^{\mathrm{T}}\mathbf{B} = \mathbf{\Sigma}$.

Consider the inner product $\langle \mathbf{c}_i, \mathbf{\Sigma h}\rangle$, where $\mathbf{c}_i \in \boldsymbol{R}^m$ denotes the vector with all entries to be zero except the ith entry. Then, we have

$$\langle \mathbf{c}_i, \mathbf{\Sigma h} \rangle = \left\langle \mathbf{\Sigma}^{\mathrm{T}} \mathbf{c}_i, \mathbf{h} \right\rangle = h_i + \sum_{j \neq i} \Sigma_{ji} h_j.$$

Moving terms around, we obtain $h_i = \langle \mathbf{c}_i, \mathbf{\Sigma h} \rangle - \sum_{j \neq i} \Sigma_{ji} h_j$. Then, we can bound $\|\mathbf{h}\|_\infty$ as

$$\begin{aligned} \|\mathbf{h}\|_\infty = \max_i |h_i| &\leq \|\mathbf{\Sigma h}\|_\infty + \left\| \sum_{i \neq j} \Sigma_{ji} h_i \right\|_\infty \\ &\leq \|\mathbf{\Sigma h}\|_\infty + \rho \left| \sum_{i \neq j} h_i \right| \leq \|\mathbf{\Sigma h}\|_\infty + \rho \|\mathbf{h}\|_1. \end{aligned}$$

We then obtain bounds for both $\|\mathbf{\Sigma h}\|_\infty$ and $\|\mathbf{h}\|_1$. First, we bound the term $\|\mathbf{\Sigma h}\|_\infty$ as

$$\begin{aligned} \|\mathbf{\Sigma h}\|_\infty = \left\|\mathbf{B}^{\mathrm{T}} \mathbf{B h}\right\|_\infty &= \max_{1 \leq i \leq n} \left|\mathbf{B}_i^{\mathrm{T}} \mathbf{B h}\right| \leq \max_{1 \leq i \leq n} \|\mathbf{B}_i\|_2 \|\mathbf{B h}\|_2 \\ &\leq \|\mathbf{B h}\|_2 \max_{1 \leq i \leq n} \|\mathbf{B}_i\|_2 = \|\mathbf{B h}\|_2 \leq \frac{\|\mathbf{A h}\|_2}{\min_{1 \leq i \leq n} \|\mathbf{A}_i\|_2}. \end{aligned}$$

Then, we bound the term $\|\mathbf{h}\|_1$ as

$$\|\mathbf{h}\|_1 = \|\mathbf{h}_T\|_1 + \|\mathbf{h}_{T^c}\|_1 \overset{(a)}{\leq} 2\|\mathbf{h}_T\|_1 \leq 2\sqrt{k} \|\mathbf{h}_T\|_2,$$

where (a) is due to Remark 4. Combining the above two bounds, we complete the proof.

□

In the above analysis, we have shown that $\|\mathbf{h}\|_\infty$ is closely related to $\|\mathbf{A h}\|_2$ and $\|\mathbf{h}_T\|_1$. Since $\|\mathbf{A h}\|_2$ has already been bounded, our next goal is to find a bound for $\|\mathbf{h}_T\|_1$. Our analysis will obtain the bound via two concepts: the coherence ρ and the RIP-constant δ_{2k}. First, we use ρ.

Lemma 10. *Given that $\rho < (3\alpha k)^{-1}, \alpha > 1$, then we have*

$$\|\mathbf{h}_T\|_2 \leq \sqrt{\frac{\alpha}{\alpha - 1}} \frac{\|\mathbf{A h}\|_2}{\min_{1 \leq i \leq n} \|\mathbf{A}_i\|_2}.$$

Proof. First, we verify that the lemma holds for the trivial case of $\|\mathbf{h}\|_2 = 0$. For the

non-trivial case $\|\mathbf{h}\|_2 \neq 0$, we have the following inequality [96, 97],

$$\min_{\mathbf{h}\neq 0,\ \|\mathbf{h}_{T^C}\|_1 \leq \|\mathbf{h}_T\|_1} \frac{\|\mathbf{Bh}\|_2}{\|\mathbf{h}_T\|_2} \geq \sqrt{1-\frac{1}{\alpha}},$$

for all support $|T| \leq k$. Moving the terms, we have the inequality

$$\|\mathbf{h}_T\|_2 \leq \sqrt{\frac{\alpha}{\alpha-1}}\,\|\mathbf{Bh}\|_2 \leq \sqrt{\frac{\alpha}{\alpha-1}}\,\frac{\|\mathbf{Ah}\|_2}{\min_{1\leq i\leq n}\|\mathbf{A}_i\|_2},$$

which completes the proof. □

Note that the above lemma requires $\rho < (3\alpha k)^{-1},\ \alpha > 1$. For large k, this lemma requires small coherence ρ; often leading to the undesirable requirement of large number of sensors m. In the following, we will bound $\|\mathbf{h}_T\|_1$ with the RIP-constant δ_{2k}. Compared with coherence, δ_{2k} is hard to compute, which may limit its application. However, it usually results in a tighter upper bound.

Lemma 11. *Provided that RIP-constant associated with matrix* $\mathbf{A}$ *satisfy* $\delta_{2k} < \sqrt{2}-1$ *, we have [141, 83]*

$$\|\mathbf{h}_T\|_2 \leq \frac{\sqrt{1+\delta_{2k}}}{1-(1+\sqrt{2})\delta_{2k}}\|\mathbf{Ah}\|_2.$$

The proof is provided in [141, 83]. Note that the existence of $\mathbf{E}$ does not affect the proof. Combining Lemma 8, Lemma 10, and Lemma 11, we obtain the upper bound for $\|\mathbf{h}\|_\infty$ in Lemma 9.

5.4 Thresholding Mechanism

In the previous section, we have obtained an upper bound for $\|\mathbf{h}\|_\infty$. In this section, we will propose a thresholding mechanism based on this bound to get the sign vector and prove the recovered sign vector to be correct given certain conditions hold. Inspired by [96], we adapt

thresholding to our setting to get the correct sign vector. Define thresholding parameter τ_1 and τ_2 as

$$\tau_1 \triangleq \left(1+2\rho\frac{\sqrt{k(1+\delta_{2k})}}{1-(1+\sqrt{2})\delta_{2k}}\right)\left[2\sigma^2+\frac{(C\sqrt{p_E}\sigma_E(\sqrt{m}+\sqrt{k})+t)}{\min_{1\le i\le n}\|\mathbf{A}_i\|_2}\right],$$
$$\tau_2 \triangleq \left(1+2\rho\sqrt{\frac{k\alpha}{\alpha-1}}\right)\frac{2\sigma^2+(C\sqrt{p_E}\sigma_E(\sqrt{m}+\sqrt{k})+t)}{\min_{1\le i\le n}\|\mathbf{A}_i\|_2}.$$

Define τ as

$$\tau=\begin{cases}\tau_1, & \text{if } \rho\ge\dfrac{1}{3k};\\ \min(\tau_1,\tau_2), & \text{otherwise,}\end{cases}$$

which corresponds to the upper bound for $\|\mathbf{h}\|_\infty$. Then we perform thresholding to the recovered value $\widehat{\mathbf{x}}$ and get $\widetilde{\mathbf{x}}$ via

$$\tilde{x}_i=\left\{(|\widehat{x}_i|-\tau)_+\right\}\text{sign}(\widehat{x}_i),$$

where $\tilde{x}_i$ and $\widehat{x}_i$ denote the ith component of $\widetilde{\mathbf{x}}$ and $\widehat{\mathbf{x}}$, respectively. Further, $(\cdot)_+ = \max(0,\cdot)$. Then we have the following theorem.

Theorem 7. *Provided that* $\min_{x_i\neq 0}|x_i|>2\tau$*, the thresholded result* $\widetilde{\mathbf{x}}$ *would give the correct sign vector, i.e.,* $\text{sign}(\tilde{x}_i)=\text{sign}(x_i)$*, with probability at least* $1-\binom{n}{k}\exp(-t^2/2)$*,* $t>0$.

Proof. Our proof is inspired by [96]. According to Lemma 6, we have shown that $\sigma_{max}(\mathbf{E}^{(k)})$ is less than $C\sqrt{p_E}\sigma_E(\sqrt{m}+\sqrt{k})+t$ with probability $1-\binom{n}{k}e^{-t^2/2}$. Hence τ is the upper bound for $\|\mathbf{h}\|_\infty$ with probability at least $1-\binom{n}{k}e^{-t^2/2}$, i.e.,

$$\|\mathbf{h}\|_\infty\le\tau.$$

To study the sign vector recovery, our proof in below analyzes the support set T and its

complement T^c.

- Consider $i \in T^c$, i.e., x_i is zero. Then we have $\tilde{x}_i = 0$. Otherwise, we have

$$\|\mathbf{h}\|_\infty = \max_j \|x_j - \widehat{x}_j\|_1 \geq \|x_i - \widehat{x}_i\|_1 > \tau,$$

  which is contradictory to the fact that $\|\mathbf{h}\|_\infty \leq \tau$.

- Consider $i \in T$, i.e., $x_i \neq 0$. Without loss of generality, we assume x_i to be positive. Based on the relation $\|\mathbf{h}\|_\infty \leq \tau$, we have

$$\|\widehat{x}_i - x_i\| \leq \tau \Longrightarrow x_i - \tau \leq \widehat{x}_i \leq x_i + \tau.$$

  According to the assumption that $\min_{x_i \neq 0} |x_i| > 2\tau$, we have $\widehat{x}_i > \tau$. Thus, sign$(\tilde{x}_i) > 0$.

Combining the above two cases, we complete the proof. □

Therefore, we have proved that the sign vector of $\boldsymbol{x}$ can be correctly recovered even under the existence of the perturbation matrix $\mathbf{E}$ provided that $\min_{x_i \neq 0} |x_i| > 2\tau$.

Remark 5. *If the assumption* $\min_{x_i \neq 0} |x_i| > 2\tau$ *does not hold, we can still prove that if* $x_i = 0$*, then we will have* $\tilde{x}_i = 0$*. However, certain non-zero entries in* $\boldsymbol{x}$ *with small magnitude may not be detected due the the sensing matrix uncertainties.*

5.5 Simulation Results

In Figure 5.1, we plot *cumulative distribution function* (CDF) of maximum singular value of matrix $\mathbf{E}$ under different sparsity parameters p_E. Here we set $m = 500$, $k = 4$, and $\sigma_E = 1.0$. The plots show that $\sigma_{\max}(\mathbf{E}^{(k)})$ often concentrates around the value $\sqrt{p_E}\sigma_E(\sqrt{m} + \sqrt{k})$, which suggests the constant $C \approx 1$ and is adopted in the following simulations. Further, larger p_E (i.e., denser matrix $\mathbf{E}^{(k)}$) increases $\mathbb{E}\sigma_{\max}(\mathbf{E}^{(k)})$ which is consistent with our theoretical analysis and intuition.

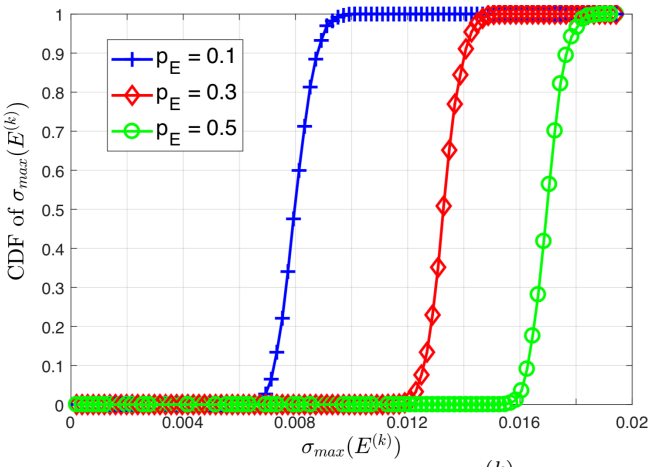

Figure 5.1. CDF of maximum singular value of matrix $\mathbf{E}^{(k)}$ when $m = 500$, $k = 4$, and $\sigma_E^2 = 0.001$.

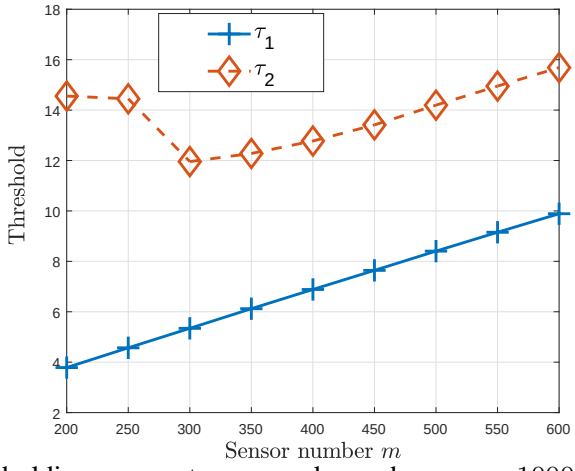

Figure 5.2. Thresholding parameters τ_1 and τ_2 when $n = 1000$, $k = 1$, $p_E = 0.5$, $\sigma_E^2 = 0.001$, and $C = 10.0$.

Figure 5.2 shows the relation between the thresholding parameters τ_1 and τ_2 and the number of sensors m. The entries in the sensing matrix $\mathbf{A}$ are i.i.d distributed following $\mathcal{N}(0, \frac{1}{m})$. Since the RIP constant δ_{2k} is hard to compute, we adopt its expectation $\sqrt{2k/m}$ as an approximation. Note that δ_{2k} concentrates around its expectation and the approximation is quite close to the exact value. Comparing the two plots, we confirm that τ_1 serves as a better bound than τ_2.

In Figure 5.3, we study the relation between the error rate and the variance σ_E^2. Here we treat the recovery as wrong even if there is one mismatch between the recovered sign vector $\text{sign}(\widetilde{\mathbf{x}})$ and the true sign vector $\text{sign}(\mathbf{x})$. In Region I, the true value $\mathbf{x}$ satisfies the

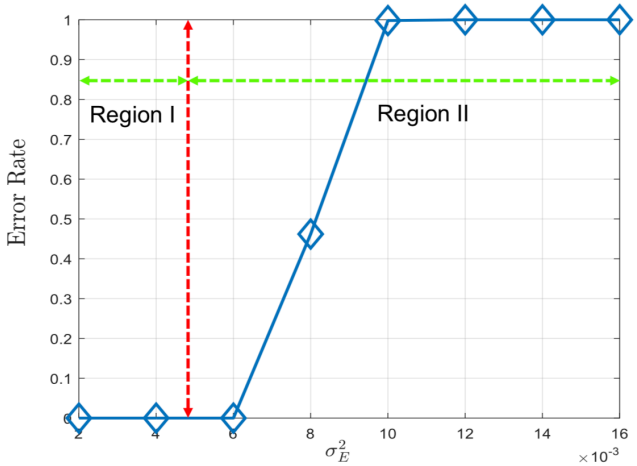

Figure 5.3. Recovery error rate when $n = 500$, $m = 100$, $k = 1$, $p_E = 0.05$, $\sigma^2 = 0$, and $C = 10.0$.

assumption in Theorem (Theorem 7) whereas in Region II it does not. We can see that there is almost no wrong recovery in Region I, which is consistent with our theorem. However in Region II, the recovery results become unreliable, even though we may still get a correct recovery in certain cases as shown in Figure 5.3.

5.6 Conclusions

We proposed a thresholding strategy to recover the sign values under an uncertain sensing matrix. We provided a sufficient condition under which with high probability the reconstructed sign value will be correct. Using simulation results, we confirmed that the maximal eigenvalue corresponding to the matrix $\mathbf{E}^{(k)}$ concentrates around its expectation, as our analysis suggested. Further, we compared two thresholding parameters τ_1 and τ_2. The simulation shows that τ_1 serves as a better bound than τ_2, although τ_2 is easier to compute. Further, the simulation results confirmed our analysis that the recovered sign values via thresholding are correct as long as the assumption of the theorem is satisfied. For the cases that the assumption does not hold, the simulation implied that the recovered results are unreliable.

CHAPTER 6

RECOVERING NOISY-PSEUDO-SPARSE SIGNALS FROM LINEAR MEASUREMENTS VIA INFINITY NORM

6.1 Introduction

Compressive Sensing (CS) [142, 83, 85] considers the problem of recovering a sparse signal $\mathbf{x} \in \mathbb{R}^n$ from m (linear) measurements. However, in many practical situations [99, 100, 101, 102, 143], the signal is not exactly sparse. Instead the signal may be best modeled as $\mathbf{x} + \mathbf{e}$ where $\mathbf{x}$ is the dominant sparse component and $\mathbf{e}$ is some small deviations, causing the signal to deviate slightly from the sparsity model, i.e., a pseudo sparse signal.

Numerical experiments suggest a straightforward application of CS algorithms to recover sparse signal $\mathbf{x}$ in the above settings may fail due to the non-sparsity of $\mathbf{x} + \mathbf{e}$. In the previous work [104], such issue is handled by a noise-whitening method. However, their method can severely inflate the R.I.P. constant [83] associated with the sensing matrix and damage the system performance. A detailed explanation is deferred to the next section.

In this chapter, we exploit the statistical properties of the noise distribution and propose a novel objective function for the signal reconstruction. Numerical results suggest our new objective function can lead to a significant error reduction in terms of ℓ_2 norm with almost negligible loss in the detection rate of the support set of signal $\mathbf{x}$.

6.2 Sensing Model

The sensing model we consider here is given by

$$\mathbf{y} = \mathbf{A}\mathbf{x}^\natural + \mathbf{A}\mathbf{e}^\natural = \mathbf{A}\mathbf{x}^\natural + \widetilde{\mathbf{w}},$$

where $\mathbf{y} \in \mathbb{R}^m$ denotes the observation, and $\mathbf{A} \in \mathbb{R}^{m \times n}$ denotes the sensing matrix. We use $(\cdot)^\natural$ to represent the ground-truth, i.e., we represent sparse signal as $\mathbf{x}^\natural \in \mathbb{R}^n$ and model the noise-like behavior of non-significant components of the signal by $\mathbf{e}^\natural$. Further, we assume that $\mathbf{e}^\natural$ follows the distribution $\mathcal{N}(0, \sigma^2\mathbf{I})$. It can be easily verified that $\widetilde{\mathbf{w}} = \mathbf{A}\mathbf{e}^\natural$ is a Gaussian $\mathcal{N}(0, \mathbf{A}\mathbf{A}^{\mathrm{T}}\sigma^2)$ noise. Before we proceed, we first briefly discuss the noise-whitening method proposed in [104].

First, the authors propose to whiten the noise $\widetilde{\mathbf{w}}$ by multiplying the measurements by the matrix $\boldsymbol{Q} = (\mathbf{A}\mathbf{A}^{\mathrm{T}})^{-1/2}$. Then, the sensing model was transformed to the conventional CS measurement

$$\mathbf{Q}\mathbf{y} = \mathbf{Q}\mathbf{A}\mathbf{x}^\natural + \mathbf{Q}\mathbf{A}\mathbf{e}^\natural,$$

where the noise $\mathbf{Q}\mathbf{A}\mathbf{e}^\natural$ is now distributed as $\mathcal{N}(0, \sigma^2\mathbf{I})$. Hence, one can solve the following optimization problem to recover the sparse signal $\mathbf{x}^\natural$;

$$\min_{\mathbf{x}} \ \|\mathbf{x}\|_1, \ \text{ s.t. } \ \|\mathbf{Q}\mathbf{y} - \mathbf{Q}\mathbf{A}\mathbf{x}\|_2^2 \leq C, \tag{6.2.1}$$

where C is the upper bound on the new noise energy. However, this method ignores the statistical properties of the Gaussian distribution and may inflate the R.I.P. constant significantly, which usually corresponds to a performance degradation.

In our work, we notice that for Gaussian distributed $\mathbf{e}^\natural$, we have $\|\mathbf{e}^\natural\|_\infty = \max_i |e_i^\natural|$ be bounded as

$$\frac{1}{\sqrt{2}}\sqrt{\sigma^2 \log n} \leq \mathbb{E}\|\mathbf{e}^\natural\|_\infty \leq \sqrt{\sigma^2 \log n},$$

(see e.g., [140] Sec. 2.5 and Thm. 13.4). We introduce the penalty term $\|\cdot\|_\infty$ to the objective function and formulate our proposed optimization problem, without performing

any noise whitening, as

$$\begin{aligned} &\min_{\mathbf{x},\mathbf{e}} \ \|\mathbf{x}\|_1 + \lambda\|\mathbf{e}\|_\infty, \\ &\text{s.t. } \mathbf{y} = \mathbf{A}\mathbf{x} + \mathbf{A}\mathbf{e}, \quad \|\mathbf{e}\|_2^2 \leq C, \end{aligned} \tag{6.2.2}$$

where λ is a non-negative constant, controlling the trade-off between the sparse component $\mathbf{x}$ and deviation $\mathbf{e}$. Note that for $\lambda = 0$, our formulation in (Equation 6.2.2) is reduced to similar form as (Equation 6.2.1).

Remark 6. *Moreover, minimizing the ℓ_∞ usually leads to a more uniformly distributed results [144]. In many applications, we may assume that the deviation $\mathbf{e}$ is bounded. Adding the penalty term $\|\mathbf{e}\|_\infty$ can contribute to a more accurate estimation of $\mathbf{e}$.*

Notation We denote the solution of (Equation 6.2.2) by $(\widehat{\mathbf{x}}, \widehat{\mathbf{e}})$. T is the support set of the sparse signal $\mathbf{x}^\natural$, i.e., $\{i : \ x_i^\natural \neq 0\}$. In addition, in our analysis, we set $C = \|\mathbf{e}^\natural\|_2^2$ in (Equation 6.2.2).

6.3 Main Results

To facilitate the understanding of (Equation 6.2.2), in this section we provide a theoretical analysis of our proposed algorithm in the sense of the performance error and number of measurements required to achieve this performance. Before we proceed, we need the following assumptions.

First we assume that the non-zero values of the sparse signal have a relatively large magnitude compared to the deviation counterpart $\mathbf{e}$, i.e., $\min_{x_i^\natural \neq 0} |x_i^\natural| > 2\|\mathbf{e}^\natural\|_\infty$. Otherwise, the support set of $\mathbf{x}$ cannot be reliably determined even with the exact knowledge of $\mathbf{x}^\natural + \mathbf{e}^\natural$. Moreover, due to the difficulties of analyzing the infinity norm $\|\cdot\|_\infty$ of Gaussian distributed $\mathbf{e}^\natural$, we consider a simplified case, where the magnitudes of the components of $\mathbf{e}^\natural$ are uniform, in this section. This setting is purely for the mathematical convenience and we will restore to Gaussian distributed $\mathbf{e}^\natural$ in the simulations.

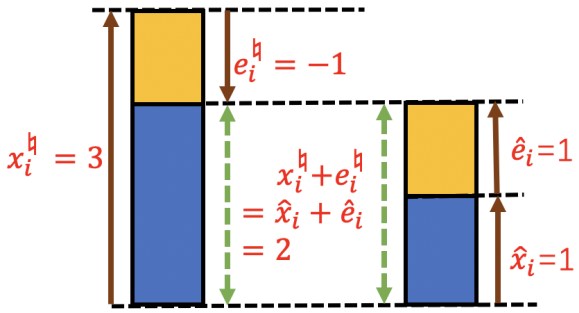

Figure 6.1. Impossibility of achieving exact solution: $|\widehat{x}_i| = 1$, $|\widehat{e}_i| = 1$ while $|x_i^\natural| = 3$, $|e_i^\natural| = 1$.

6.3.1 Exact Solution Analysis

First we observe that recovering exact $(\mathbf{x}^\natural, \mathbf{e}^\natural)$ would be impossible due to the ambiguity in $\mathbf{e}^\natural$ (see Figure 6.1 for an illustrative example). However, we will show that a unique solution $(\widehat{\mathbf{x}}, \widehat{\mathbf{e}})$ can be guaranteed within the proximity of $(\mathbf{x}^\natural, \mathbf{e}^\natural)$.

We first consider the oracle case, where $\mathbf{x}^\natural + \mathbf{e}^\natural$ and $\|\mathbf{e}^\natural\|_\infty$ are perfectly known, to gain insights of (Equation 6.2.2). Note that if we cannot recover $(\mathbf{x}^\natural, \mathbf{e}^\natural)$ under the oracle case, it is hopeless to recover them in the practical case where the above information are missing. For both the noise-whitening method and our proposed method, the following can be proven.

Lemma 12. *Suppose that* $\min_{i\in T} |x_i^\natural| > 2\|\mathbf{e}^\natural\|_\infty$. *Then,*

$$\operatorname{sign}(\widehat{x}_i) = \operatorname{sign}(\widehat{e}_i), \quad \forall\, \widehat{x}_i \neq 0,$$

holds for the recovered signal $(\widehat{\mathbf{x}}, \widehat{\mathbf{e}})$.

The proof is given in Appendix. Due to Lemma 12, the closest we can get to the true values $(\mathbf{x}^\natural, \mathbf{e}^\natural)$ via solving (Equation 6.2.2) is given by

$$\begin{cases} (\widetilde{x}_i, \widetilde{e}_i) = \operatorname{sign}(x_i^\natural + e_i^\natural)\left(|x_i^\natural + e_i^\natural| - |e_i^\natural|, |e_i^\natural|\right), & i \in T; \\ (\widetilde{x}_i, \widetilde{e}_i) = (x_i^\natural, e_i^\natural), & i \in T^c. \end{cases} \tag{6.3.1}$$

Property 1. *For* $(\widetilde{\mathbf{x}}, \widetilde{\mathbf{e}})$ *as in* (Equation 6.3.1)*, it can be easily verified that* $\widetilde{e}_i = \text{sign}(\widetilde{e}_i)\|\widetilde{\mathbf{e}}\|_\infty$ *and* $\text{sign}(\widetilde{x}_i) = \text{sign}(\widetilde{e}_i) = \text{sign}(x_i^\natural + e_i^\natural)$.

This property is easy to verify and we omit its proof. In the sequel, we show that $(\widetilde{\mathbf{x}}, \widetilde{\mathbf{e}})$ can be obtained uniquely. Fortunately, the maximum deviation $\|\widetilde{\mathbf{x}} - \mathbf{x}^\natural\|_2$ between $\widetilde{\mathbf{x}}$ and $\mathbf{x}^\natural$ is at most $2\sqrt{k}\|\mathbf{e}^\natural\|_\infty = 2\sqrt{k/n}\|\mathbf{e}^\natural\|_2$, which is often negligible as $k \ll n$.

6.3.2 Analysis of the Solution Uniqueness

We now prove the uniqueness of solution $(\widehat{\mathbf{x}}, \widehat{\mathbf{e}})$. Define the joint tangent cone $\mathcal{T}^\lambda_{\widetilde{\boldsymbol{x}},\widetilde{\boldsymbol{e}}}$ as

$$\mathcal{T}^\lambda_{\widetilde{\boldsymbol{x}},\widetilde{\boldsymbol{e}}} \triangleq \left\{ (\mathbf{a}, \mathbf{b}) : \|\widetilde{\boldsymbol{x}} + t\mathbf{a}\|_1 + \lambda\|\widetilde{\boldsymbol{e}} + t\mathbf{b}\|_\infty \leq \|\widetilde{\boldsymbol{x}}\|_1 + \lambda\|\widetilde{\boldsymbol{e}}\|_\infty, \ \exists\, t \geq 0 \right\},$$

which contains all descending directions from point $(\widetilde{\boldsymbol{x}}, \widetilde{\boldsymbol{e}})$. Further, define set $\Omega_{\widetilde{\boldsymbol{x}},\widetilde{\boldsymbol{e}}}$ as

$$\Omega_{\widetilde{\boldsymbol{x}},\widetilde{\boldsymbol{e}}} = \left\{ \mathbf{a} + \mathbf{b} : \ (\mathbf{a}, \mathbf{b}) \in \mathcal{T}^\lambda_{\widetilde{\boldsymbol{x}},\widetilde{\boldsymbol{e}}} \setminus (\mathbf{0}, \mathbf{0}), \ \langle \mathbf{b}, \widetilde{\boldsymbol{e}} \rangle < 0 \right\}. \tag{6.3.2}$$

We can form the following lemma for the uniqueness.

Lemma 13. *Provided that* $k < \lambda < n - k$*, the solution* $(\widehat{\mathbf{x}}, \ \widehat{\mathbf{e}})$ *is unique and is equal to* $(\widetilde{\mathbf{x}}, \widetilde{\mathbf{e}})$ *if*

$$\Omega_{\widetilde{\mathbf{x}},\widetilde{\mathbf{e}}} \bigcap \mathbb{S}^{n-1} \bigcap \text{null}(\mathbf{A}) = \emptyset, \tag{6.3.3}$$

where $\mathbb{S}^{n-1}$ *denotes the* n*-dimensional unit-sphere.*

Despite of the similar forms as in [79, 107], we cannot directly apply their proof technique to Lemma 13, which is due to the replacement of tangent cone $\mathcal{T}^\lambda_{\widetilde{\boldsymbol{x}},\widetilde{\boldsymbol{e}}}$ with set $\Omega_{\widetilde{\boldsymbol{x}},\widetilde{\boldsymbol{e}}}$. Detailed explanation is given as the following. When dealing with tangent cone $\mathcal{T}^\lambda_{\widetilde{\boldsymbol{x}},\widetilde{\boldsymbol{e}}}$ as in [79, 107], zero element $\mathbf{0}$ can be safely ignored in the analysis since it corresponds to the case where $\mathbf{a} = \mathbf{b} = \mathbf{0}$, i.e., desired solution $(\widetilde{\mathbf{x}}, \widetilde{\mathbf{e}})$ is obtained. While in our case, zero elements $\mathbf{0} \in \Omega_{\widetilde{\boldsymbol{x}},\widetilde{\boldsymbol{e}}}$ suggests $\mathbf{a} + \mathbf{b} = \mathbf{0}$ in (Equation 6.3.2) rather than $\mathbf{a} = \mathbf{b} = \mathbf{0}$, which still contains solution ambiguity. Hence, a more delicate analysis is required and we put it in

Appendix.

To avoid the prohibitive computational cost of directly verifying (Equation 6.3.3), we instead investigate the equivalent condition

$$\min_{\mathbf{u}\in\Omega_{\widetilde{\mathbf{x}},\widetilde{\mathbf{e}}}\bigcap\mathbb{S}^{n-1}} \|\mathbf{A}\mathbf{u}\|_2 \ > 0. \tag{6.3.4}$$

For the simplicity of notations, in the rest of the paper, we will use Ω to refer to $\Omega_{\widetilde{\mathbf{x}},\widetilde{\mathbf{e}}}$.

6.3.3 Lower Bound for the Number of Measurements

In this subsection, we assume as in [79], each measurement has footprint from only a limited number of signal components, i.e., entries in $\mathbf{x}$. As in [79], we also assume the entries of $\mathbf{a}$ are i.i.d. according to the distribution

$$\mathbb{P}(A_{ij} = a) = (1-p)\delta(a) + \frac{p}{\sqrt{2\pi}}\ \exp\left(-\frac{a^2}{2}\right). \tag{6.3.5}$$

Here $\delta(\cdot)$ is the delta function and a is a Gaussian r.v.. An entry is zero with the large probability $1-p$. Hence, each measurement can read a linear combination of only a few signals.

We study the conditions satisfying (Equation 6.3.4). As such, we first relate it to Gaussian width [108, 107] of space Ω. Then we study the relation between the number of measurement and the Gaussian width. Similar to [79], we can show the following result.

Theorem 8. *Provided that $m \geq \omega^2(\Omega)+1$, the optimization problem (Equation 6.2.2) has a unique solution $(\widetilde{\mathbf{x}},\ \widetilde{\mathbf{e}})$ with the probability at least $1-\exp\left(-\frac{p}{2}[a_m-\omega(\Omega)]^2\right)$, where $a_m = \sqrt{2}\Gamma\left(\frac{m+1}{2}\right)/\Gamma\left(\frac{m}{2}\right)$ and $\omega(\Omega)$ is the Gaussian width of Ω, defined by*

$$\omega(\Omega) = \mathbb{E}_{\mathbf{g}} \sup_{\mathbf{u}\in\Omega\bigcap\mathbb{S}^{n-1}} \langle \mathbf{g}, \mathbf{u}\rangle\,,\ \ \mathbf{g}\sim\mathcal{N}(\mathbf{0},\mathbf{I}). \tag{6.3.6}$$

In the following, our goal becomes finding an upper bound for $\sup[\omega^2(\Omega)]$. Setting m to be $\sup[\omega^2(\Omega)]+1$ would guarantee the uniqueness of the solution with high probability as stated in Theorem 8.

Theorem 9. *To satisfy the constraint in Theorem Theorem 8, it is sufficient that*

$$m \geq \left(\sqrt{n}-(1-2^{-n})\sqrt{\frac{\log n}{2}}-\frac{2^{\frac{1}{2}-n}}{\sqrt{\pi}}\right)^2+1. \tag{6.3.7}$$

Due to the complicated structure of Ω, its Gaussian width $\omega(\Omega)$ cannot be directly upper-bounded with the existing methods as in [139, 107, 105]. Instead, we need a delicate analysis, which consists of the following two steps: (i) construct a complementary set Θ for Ω; (ii) lower-bound its Gaussian width $\omega(\Theta)$. The detailed calculation is in the Appendix.

Remark 7. *This theorem suggests that we can obtain a unique solution* $(\widetilde{\mathbf{x}},\widetilde{\mathbf{e}})$ *with an indefinite measurement matrix* $\mathbf{a}$ *at the rate of* $m \sim \mathcal{O}\left(n-\sqrt{n\log n}\right)$. *Although this bound seems to be a marginal improvement compared with the bound* $m \sim \mathcal{O}(k\log n)$ *associated with the traditional CS [142, 83], our signal setting is different from them in that our signal* $\mathbf{x}^\natural+\mathbf{e}^\natural$ *is not sparse. Meanwhile the number of measurements* m *can be further reduced with more accurate bounds for* $\omega(\Omega)$ *and our simulations also suggest our proposed method greatly outperforms the existing work as in* (Equation 6.2.1)*.*

Remark 8. *Although the* $\mathbf{x}^\natural$*'s non-zero number* k *is missing in the above bound* (Equation 6.3.7)*, it is involved in our previous analysis such that* (i) *we require* $k<\lambda<n-k$ *and* (ii) *the maximum deviation between* $\left\|\widetilde{\mathbf{x}}-\mathbf{x}^\natural\right\|_2$ *is bounded by* $2\sqrt{k/n}\left\|\mathbf{e}^\natural\right\|_2$.

6.4 Simulation

In the previous sections, we considered the ideal case that $\mathbf{e}$ has uniformly distributed magnitude for the analytical convenience and we restore to the Gaussian setting in this

section. For the simulations, we set $n = 300$, $m = 70$, and $k = 2$. To evaluate the performance of the proposed algorithm, we consider two different metrics: the error norm $\|\widehat{\mathbf{x}} - \mathbf{x}^\natural\|_2^2$ and the correct recovery rate of the support set $\mathbb{P}\{\text{supp}(\widehat{\mathbf{x}}) = \text{supp}(\mathbf{x}^\natural)\}$.

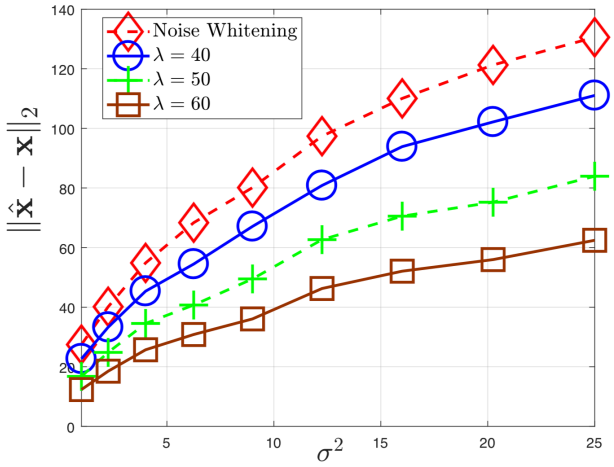

Figure 6.2: $\|\widehat{\mathbf{x}} - \mathbf{x}\|_2$ versus variance of $\mathbf{e}$.

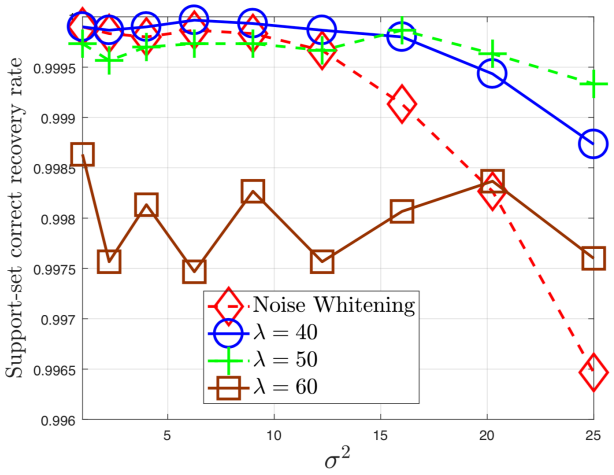

Figure 6.3: Prob. of correct support set recovery vs variance of $\mathbf{e}$.

Figure 6.2 shows the error $\|\widehat{\mathbf{x}} - \mathbf{x}^\natural\|_2^2$ versus the variance σ^2 of $\mathbf{e}^\natural$ for various λ's in both the proposed scheme and the noise-whitening method [104]. Generally, larger λ usually leads to better performance in our scheme. For example, at $\sigma = 5$, our proposed algorithm for $\lambda = 60$ can reduce the error norm by more than 50% relative to the noise whitening method [104]. However, by increasing λ further, there is a subtle performance gain (or even loss) in our algorithm.

We have plotted the probability of correct recovery of support set in Figure 6.3 for different noise variances. It is observed that our algorithm can beat the noise-whitening method in the beginning. When $\lambda = 40$, our results can improve the correct rate from 99.75% to 99.95%. However, our algorithm sometimes falls behind the noise-whitening method as we increase λ. But the gap between our method and the noise whitening method is rather subtle, i.e., less than 0.3%. Overall, taking into account the large improvement in $\|\widehat{\mathbf{x}} - \mathbf{x}^\natural\|_2^2$, the small sacrifice in the support set recovery rate is most likely acceptable.

6.5 Conclusions

In this chapter, we proposed a new method to recover a noisy-pseudo-sparse signal from linear measurements. To facilitate its understanding, we studied the ideal case where the entries of the signal deviation are uniformly distributed and showed that, even with this constraint, finding the exact solution is impossible. However, we proved that a unique solution in the proximity of true value could be obtained. We analyzed the probability of obtaining a unique solution when the measurement matrix is sparse-Gaussian and bounded the required number of measurements to obtain such a solution. In the end, we went back to the Gaussian setting of signal deviation and our simulations suggested relative to the noise whitening method, our algorithm can reduce error by 50% at the expense of less than 0.3% loss in support-set recovery rate.

CHAPTER 7
SPARSE SIGNAL RECONSTRUCTION WITH A MULTIPLE CONVEX SETS DOMAIN

7.1 Introduction

This chapter considers reconstructing the sparse signal from an ill-posed inverse problem. Different from the setting of traditional *compressive sensing* (CS) [142, 110, 83], we assume the existence of extra prior knowledge that $\mathbf{x}$ lies in the union of some convex sets, $\mathbf{x} \in \bigcup_{i=1}^{L} \mathcal{C}_i$, where L denotes the number of constraint sets and $\mathcal{C}_i$ is the i-th convex constraint set. This problem (i.e., given measurement $\mathbf{y}$, solving for $\mathbf{x}$) turns out to be a rather general form of CS. For example, setting $\bigcup \mathcal{C}_i = \mathbb{R}^n$ simplifies our problem to the traditional CS problem. In the following, we will further show that by appropriate choices of these convex sets, our setting can include *sparse phase retrieval* [145, 146, 147], *quantized compressive sensing* [148], and *model-based CS* [114] problems. A detailed discussion is given as follows.

- **Sparse Phase retrieval.** Consider the noiseless phase retrieval problem in which the measurements are given by

$$y_i = |\langle \mathbf{a}_i,\ \mathbf{x} \rangle|^2,\ \ 1 \leq i \leq l,$$

  where y_i is the i-th measurement and $\mathbf{a}_i$ denotes the corresponding coefficients. Considering the first measurement, the constraint $\sqrt{y_1} = |\langle \mathbf{a}_1,\ \mathbf{x} \rangle|$ can be represented via $\mathbf{x} \in \mathcal{B}_+^{(1)} \bigcup \mathcal{B}_-^{(1)}$ where $\mathcal{B}_+^{(1)} = \{\mathbf{x} :\ \langle \mathbf{a}_1, \mathbf{x} \rangle = \sqrt{y_1}\}$ and $\mathcal{B}_-^{(1)} = \{\mathbf{x} :\ \langle \mathbf{a}_1, \mathbf{x} \rangle = -\sqrt{y_1}\}$. Following these steps, the constraints $\{y_i = \langle \mathbf{a}_i, \mathbf{x} \rangle^2\}_{i=1}^{l}$ can be transformed to $\mathbf{x} \in \bigcap_i \left(\mathcal{B}_+^{(i)} \bigcup \mathcal{B}_-^{(i)}\right) = \bigcup_{j=1}^{2^l} \mathcal{C}_j$, for some appropriately defined C_j's given by the intersection of different $\mathcal{B}_{\pm}^{(i)}$. Setting sensing matrix $\mathbf{A} = \mathbf{0}$ will restore the phase retrieval to

our setting.

- **Quantized compressive sensing.** In this scenario, the measurements are quantized, i.e.,

$$y_i = Q(\langle \mathbf{a}_i,\ \mathbf{x} \rangle),\ 1 \leq i \leq L,$$

where $Q(\cdot)$ is the quantizer. Since $Q^{-1}(\cdot)$ is an interval on real line, $\mathcal{C}_i$ would be a convex set and the quantized CS can be easily transformed to our setting.

- **Model-based compressive sensing.** These lines of works [114, 115, 116] are the most similar work to our model, where they consider

$$\mathbf{y} = \mathbf{A}\mathbf{x}^\natural,\ \ \mathbf{x}^\natural \in \bigcup_i \mathcal{L}_i.$$

Here, $\mathcal{L}_i$ is assumed to be a linear space whereas the only assumption we make on the models is being a convex set. Hence, their model can be regarded as a special case of our problem.

7.2 System Model

We start the discussion with a formal restatement of our problem. Let $\mathbf{A} \in \mathbb{R}^{M \times N}$ be the measurement matrix, and consider the setup

$$\mathbf{y} = \mathbf{A}\mathbf{x}^\natural, \quad \text{and} \quad \mathbf{x}^\natural \in \bigcup_{i=1}^{L} \mathcal{C}_i, \tag{7.2.1}$$

where $\mathbf{x}^\natural$ is a K-sparse high-dimensional signal, $\mathbf{y} \in \mathbb{R}^M$ is the measurement vector, and $\mathcal{C}_i \subset \mathbb{R}^N$, $i = 1, 2, \ldots, L$, is a convex set.

Due to the sparsity of $\mathbf{x}^\natural$, we propose to reconstruct $\mathbf{x}^\natural$ via

$$\widehat{\mathbf{x}} = \text{argmin}_{\mathbf{x}}\ \|\mathbf{x}\|_1, \quad \text{s.t. } \mathbf{y} = \mathbf{A}\mathbf{x}, \quad \mathbf{x} \in \bigcup_{i=1}^{L} \mathcal{C}_i, \tag{7.2.2}$$

where $\widehat{\mathbf{x}}$ denotes the reconstructed signal. In the following, we will study the inverse problem in (Equation 7.2.2) from two perspectives; the statistical and the computational aspects.

7.3 Statistical Property

In this section, we will find the minimum number of measurements M to $\widehat{\mathbf{x}} = \mathbf{x}^\natural$, i.e., $\mathbf{d} = \mathbf{0}$. For the simplicity of analysis, we assume that the entries $A_{i,j}$ of $\mathbf{A}$ are i.i.d. normal $\mathcal{N}(0, 1)$.

Definition 5. *The tangent cone $\mathcal{T}_\mathbf{x}$ for $\|\mathbf{x}\|_1$ is defined as [107]*

$$\mathcal{T}_\mathbf{x} \triangleq \{\mathbf{e} : \ \|\mathbf{x} + t\mathbf{e}\|_1 \leq \|\mathbf{x}\|_1, \ \exists\, t \geq 0\}.$$

Geometric interpretation of $\mathcal{T}_\mathbf{x}$ is that it contains all directions that lead to smaller $\|\cdot\|_1$ originating from $\mathbf{x}$. In the following analysis, we use $\mathcal{T}$ as a compact notation for $\mathcal{T}_{\mathbf{x}^\natural}$. Easily we can prove that $\mathbf{d} \in \mathcal{T}$.

Definition 6. *The Gaussian width $\omega(\cdot)$ associated with set U is defined as $\omega(U) \triangleq \mathbb{E} \sup_{\mathbf{x}\in U} \langle \mathbf{g}, \ \mathbf{x}\rangle$, $\mathbf{g} \sim \mathcal{N}(\mathbf{0}, \mathbf{I})$, [108].*

Define cone $\widetilde{\mathcal{C}}_{i,j}$ as

$$\widetilde{\mathcal{C}}_{i,j} \triangleq \ \left\{\mathbf{z} \ \middle| \ \mathbf{z} = t(\mathbf{x}_1 - \mathbf{x}_2), \ \exists\, t > 0, \ \mathbf{x}_1 \in \mathcal{C}_i, \mathbf{x}_2 \in \ \mathcal{C}_j\right\},$$

which denotes the cone consisting of all vectors $\mathbf{z}$ that are parallel with $\mathbf{x}_1 - \mathbf{x}_2$, $\mathbf{x}_1 \in \mathcal{C}_i$, and $\mathbf{x}_2 \in \mathcal{C}_j$. Then we define event $\mathcal{E}$ as

$$\mathcal{E} \triangleq \ \left\{\bigcup_{i,j} \left(\text{null}(\mathbf{A}) \bigcap \mathcal{T} \bigcap \widetilde{\mathcal{C}}_{i,j}\right) = \{\mathbf{0}\}\right\}.$$

Lemma 14. *We can guarantee the correct recovery of* $\mathbf{x}$*, i.e.,* $\widehat{\mathbf{x}} = \mathbf{x}^\natural$*, iff we have event* $\mathcal{E}$ *to be satisfied.*

Proof. This proof is fundamentally the same as [79, 107]. Let $\mathbf{d} \triangleq \widehat{\mathbf{x}} - \mathbf{x}^\natural$ be the deviation of the reconstructed signal $\widehat{\mathbf{x}}$ from the true signal $\mathbf{x}^\natural$. First we prove that $\mathcal{E}$ leads to $\widehat{\mathbf{x}} \neq \mathbf{x}^\natural$. Provided $\mathbf{d} \triangleq \widehat{\mathbf{x}} - \mathbf{x}^\natural \neq \mathbf{0}$, we then have a $\widehat{\mathbf{x}} \neq \mathbf{x}^\natural$ such that $\|\widehat{\mathbf{x}}\|_1 \leq \|\mathbf{x}^\natural\|_1$. Setting $\mathbf{e} \parallel \mathbf{d}$, we hav a non-zero $\mathbf{e} \in \text{null}(\mathbf{A}) \bigcap \mathcal{T} \bigcap (\bigcup_{i,j} \widetilde{\mathcal{C}}_{i,j})$, which violates $\mathcal{E}$.

Then we prove that $\widehat{\mathbf{x}} \neq \mathbf{x}^\natural$ implies $\mathcal{E}$. Assume that there exists non-zero $\mathbf{e}$ such that

$$\mathbf{e} \in \text{null}(\mathbf{A}) \bigcap \mathcal{T} \bigcap \left(\bigcup_{i,j} \widetilde{\mathcal{C}}_{i,j} \right).$$

We can show that signal $\mathbf{x}^\natural + t\mathbf{e}$, where t is some positive constant such that $\|\mathbf{x}^\natural + t\mathbf{e}\|_1 \leq \|\mathbf{x}^\natural\|_1$, satisfying constraints described by (Equation 7.2.1). This implies that $\mathbf{d} = t\mathbf{e} \neq \mathbf{0}$ and the wrong recovery of $\mathbf{x}^\natural$. □

Since a direct computation of the probability of event $\mathcal{E}$ can be difficult, we analyze the following equivalent event,

$$\min_{\mathbf{x} \in \mathcal{T} \bigcap (\bigcup_{i,j} \widetilde{\mathcal{C}}_{ij})} \|\mathbf{A}\mathbf{x}\|_2 > 0.$$

Using Gordon's escape from mesh theorem [108], we obtain the following result that relates $\mathbb{P}(\mathcal{E})$ with the number of measurements M.

Theorem 10. *Let* $a_M = \mathbb{E}\|\mathbf{g}\|_2$*, where* $\mathbf{g} \in \mathcal{N}(\mathbf{0}, \mathbf{I}_{M \times M})$*, and* $\omega(\cdot)$ *denotes the Gaussian width. Provided that* $a_M \geq \omega(\mathcal{T})$ *and* $(1 - 2\epsilon)a_M \geq \omega(\widetilde{\mathcal{C}}_{ij})$ *for* $1 \leq i, j \leq L$ *and* $\epsilon > 0$*, we have*

$$\mathbb{P}(\mathcal{E}) \geq 1 - \Bigg(\underbrace{\mathbb{P}\left(\min_{\mathbf{u} \in \mathcal{T}^c \backslash \{\mathbf{0}\}} \|\mathbf{A}\mathbf{u}\|_2 > 0 \right)}_{\mathcal{P}_1} \wedge \underbrace{\mathbb{P}\left(\min_{\boldsymbol{u} \in \bigcap \widetilde{\mathcal{C}}_i^c \backslash \{\mathbf{0}\}} \|\mathbf{A}\mathbf{u}\|_2 > 0 \right)}_{\mathcal{P}_2} \Bigg),$$

where $a \wedge b$ denotes the minimum of a and b, and $\mathcal{P}_1$ and $\mathcal{P}_2$ can be bounded as

$$\mathcal{P}_1 \leq 1 \wedge \exp\left(-\frac{\left(a_M - \omega(\mathcal{T})\right)^2}{2}\right)$$

$$\mathcal{P}_2 \leq 1 \wedge \frac{3}{2}\exp\left(-\frac{\epsilon^2 a_M^2}{2}\right) + \sum_{i \leq j} \exp\left(-\frac{\left((1-2\epsilon)a_M - \ \omega(\widetilde{\mathcal{C}}_{ij})\right)^2}{2}\right).$$

Theorem 10 links the probability of correct recovery of (Equation 7.2.2) with the number of measurements M, and the "size" of constraint set. Detailed explanation is given as the following. To ensure high-probability of $\mathcal{E}$, we would like to $\mathcal{P}_1 \wedge \mathcal{P}_2$ to approach zero, which requires large value of a_M. Meanwhile, a_M is a monotonically increasing function of the sensor number M. Hence, we can obtain the minimum sensor number M requirement by unique recovery via investigating a_M.

Remark 9. *Notice that $\mathcal{P}_1$ is associated with the descent cone $\mathcal{T}$ of the optimization function, namely, $\|\mathbf{x}\|_1$, while $\mathcal{P}_2$ is associated with the prior knowledge $\mathbf{x} \in \bigcup_i \mathcal{C}_i$. Theorem 10 implies that event $\mathcal{E}$ (uniqueness) holds with higher probability than the traditional CS due to the extra constraint $\mathbf{x} \in \bigcup_i \mathcal{C}_i$. If we fix $\mathbb{P}(\mathcal{E})$, we can separately calculate the corresponding M with and without the constraint $\mathbf{x} \in \bigcup_i \mathcal{C}_i$. The difference ΔM would indicate the savings in the number of measurements due to the additional structure $\mathbf{x} \in \bigcup_i \mathcal{C}_i$ over the traditional CS.*

One simple example is attached below to illustrate the improvement brought by Theorem 10.

Example 1. *Consider the constraint set*

$$\mathcal{C}_i = \{(0, \cdots, 0, x_i, \cdots, x_{K+i},\ 0, \cdots, 0)\},$$

where $1 \leq i \leq N - K$. We study the asymptotic behavior of Theorem 10 when N is of order $\mathcal{O}(K^c)$, where $c > 1$ is constant. In the sequel we will show that Theorem 10 gives us

the order $M = \mathcal{O}(K)$ to ensure solution uniqueness as K approaches infinity, which gives us the same bound as shown in [114] and suggests the tightness of our result.

Setting $\epsilon = 1/4$, we can bound $\mathcal{P}_2$ as

$$\mathcal{P}_2 \leq \frac{3}{2}\exp\left(-\frac{a_M^2}{32}\right) + \frac{N^2}{2}\exp\left(-\frac{(a_M - 2a_{2K})^2}{8}\right),$$

provided $a_M \geq 2a_K$. With the relation $\frac{M}{\sqrt{M+1}} \leq a_M \leq \sqrt{M}$ [108, 107] and setting $M = 3K$, we have

$$\mathcal{P}_2 \leq c_1\exp(-c_2 K) + c_3 N^2\exp(-c_4 K),$$

where $c_1, c_2, c_3, c_4 > 0$ are some positive constants. Since $N = \mathcal{O}(K^c)$, we can see $\mathcal{P}_2$ shrinks to zero as K approaches infinity, which implies the solution uniqueness.

Comparing with the traditional CS theory without prior knowledge $x \in \bigcup_i \mathcal{C}_i$, our bound reduces the number of measurements from $M = \mathcal{O}(K\log N/K) = \mathcal{O}(K\log K)$ to $M = \mathcal{O}(K)$.

7.4 Computational Algorithm

Apart from the statistical property, another important aspect of (Equation 7.2.2) is to design an efficient algorithm. One naive idea is to consider and solve L separate optimization problems

$$\widehat{\mathbf{x}}^{(i)} = \text{argmin}_{\mathbf{x}}\ \|\mathbf{x}\|_1, \ \text{ s.t. } \ \mathbf{y} = \mathbf{A}\mathbf{x}, \ \ \mathbf{x} \in \mathcal{C}_i,$$

and then selecting the best one, i.e., the sparsest reconstructed signal among all $\widehat{\mathbf{x}}^{(i)}$'s. However, this method has two drawbacks:

- It requires solving L separate optimization problems, which in many applications might be prohibitively large and difficult to handle, but the proposed method is based on one single optimization procedure.

- It is inflexible. For example, some prior knowledge of which $\mathcal{C}_i$ the true signal $\mathbf{x}^\natural$ is more likely to reside might be available. The above method cannot incorporate such priors.

To overcome the above drawbacks, we (i) reformulate (Equation 7.2.2) to a more tractable objective function, and (ii) propose a computationally efficient algorithm to solve it. In the following, we assume that $\mathbf{x}$ is bounded in the sense that for a constant R, $\|\mathbf{x}\|_2 \leq R$.

7.4.1 Reformulation of the Objective Function

We introduce an auxiliary variable $\mathbf{p}$ and rewrite the Lagrangian form in (Equation 7.2.2) as

$$\min_{\mathbf{x}} \min_{\mathbf{p}\in\Delta_L} \sum_i p_i \left(\|\mathbf{x}\|_1 + \widetilde{\mathbb{I}}(\mathbf{x} \in \mathcal{C}_i) + \frac{\lambda_1}{2}\|\mathbf{y} - \mathbf{A}\mathbf{x}\|_2^2 + \frac{\lambda_2 \|\mathbf{x}\|_2^2}{2} \right), \tag{7.4.1}$$

where Δ_L is the simplex $\{p_i \geq 0,\ \sum_i p_i = 1\}$, $\widetilde{\mathbb{I}}(\cdot)$ is the truncated indicator function, which is 0 when its argument is true and is some large finite number C otherwise, and $\lambda_1, \lambda_2 > 0$ are the Lagrange multipliers. The term $\|\mathbf{y} - \mathbf{A}\mathbf{x}\|_2^2$ is used to penalize for the constraint $\mathbf{y} = \mathbf{A}\mathbf{x}$ while $\|\mathbf{x}\|_2^2$ corresponds to the energy constraint $\|\mathbf{x}\|_2 \leq R$. It can be easily shown that solving (Equation 7.4.1) for large enough C ensures $\mathbf{x} \in \bigcup_i^L \mathcal{C}_i$.

Algorithm 5 Non-convex Proximal Multiplicative Weighting Algorithm.

- **Initialization**: Initialize all variables with uniform weight $p_i^{(0)} = L^{-1}$ and $\mathbf{x}^{(0)} = \mathbf{0}$.
- **For time** $t = 1$ **to** T**:** We update $p_i^{(t+1)}$ and $\mathbf{x}^{(t)}$ as

$$p_i^{(t+1)} \cong p_i^{(t)} e^{-\eta_p^{(t)} f_i(\mathbf{x}^{(t)})} \tag{7.4.2}$$

$$\mathbf{x}^{(t+1)} = \mathsf{prox}_{\eta_w^{(t)}\|\cdot\|_1} \left[\mathbf{x}^{(t)} - \eta_x^{(t)} \sum_i p_i^{(t)} \left(\nabla_x h_i(\mathbf{x}^{(t)}) + \lambda_1 \mathbf{A}^\top(\mathbf{A}\mathbf{x}^{(t)} - \mathbf{y}) + \lambda_2 \mathbf{x}^{(t)} \right) \right], \tag{7.4.3}$$

  where $p_i^{(t)}$ denotes the ith element of $\mathbf{p}^{(t)}$, and the proximal operator $\mathsf{prox}_{\|\cdot\|_1}(\mathbf{x})$ is defined as $\mathrm{argmin}_{\mathbf{z}} \left(\|\mathbf{z}\|_1 + \frac{1}{2}\|\mathbf{z} - \mathbf{x}\|_2^2 \right)$ [113].
- **Output**: Calculate the average value $\bar{\mathbf{p}} = \frac{\sum_t \mathbf{p}^{(t)}}{T}$ and value $\bar{\mathbf{x}} = \frac{\sum_t \mathbf{x}^{(t)}}{T}$. Then output $\widehat{\mathbf{x}}$ by projecting $\bar{\mathbf{x}}$ onto the set of $\bigcup_i \mathcal{C}_i$.

Apart from the universality, our formulation has the following benefits:

- It is memory efficient. Compared with the naive idea that needs to store L different $\widehat{\mathbf{x}}^{(i)}$, our method only needs to track one $\widehat{\mathbf{x}}$ and one redundant variable $\mathbf{p}$. This reduces the storing memory from $\mathcal{O}(NL)$ to $\mathcal{O}(N+L)$.

- It is very flexible. We can easily adjust to the case that $\mathbf{x}$ belongs to the intersection, i.e., $\mathbf{x} \in \bigcap_i \mathcal{C}_i$ via modifying $\min_{\mathbf{p}\in\Delta_L}$ in (Equation 7.4.1) to $\max_{\mathbf{p}\in\Delta_L}$.

Besides, to the best of our knowledge, this is the first time that such a formulation (Equation 7.4.1) is proposed. In the following, we will focus on the computational methods. Note that the difficulties in solving (Equation 7.4.1) are due to two aspects:

- Optimization over $\mathbf{p}$: Although classical methods to minimize over $\mathbf{p}$ with fixed $\mathbf{x}$, e.g., *alternating minimization* and ADMM [149], can calculate local minimum efficiently (due to the bi-convexity of (Equation 7.4.1), they can be easily trapped in the local-minima. This is because some entries in $\mathbf{p}$ can be set to zero and hence $\mathbf{x}$ will be kept away from the corresponding set $\mathcal{C}_i$ thereafter. To handle this problem, we propose to use *multiplicative weight update* [117] and update $\mathbf{p}$ with the relation $\mathbf{p}^{(t+1)} \propto \mathbf{p}^{(t)} e^{-\eta_p^{(t)} f_i(\mathbf{x})}$, where $\mathbf{p}^{(t)}$ denotes $\mathbf{p}$'s value in the tth iteration. This update relation avoids the sudden change of $\mathbf{p}^{(t)}$'s entries from non-zero to zero, which could have forced $\mathbf{x}^{(t)}$ being trapped in a local minimum.

- Optimization over $\mathbf{x}$: Due to the non-smoothness of $\widetilde{\mathbb{1}}(\mathbf{x} \in \mathcal{C}_i)$ and $\|\mathbf{x}\|_1$ in (Equation 7.4.1) and the difficulties in calculating their sub-gradients, directly minimizing (Equation 7.4.1) would be computationally prohibitive. We propose to first approximate $\widetilde{\mathbb{1}}(\mathbf{x} \in \mathcal{C}_i)$ with a smooth function $h_i(\mathbf{x})$ and update $\mathbf{x}^{(t)}$ with the relation (Equation 7.4.3) used in *proximal gradient descent* [112].

Definition 7 (L_g-strongly smooth [112]). *Function $g(\cdot) : \mathcal{X} \mapsto \mathbb{R}$ is L_g-strongly smooth iff*

$$g(\mathbf{y}) \leq g(\mathbf{x}) + \langle \nabla g(\mathbf{x}),\ \mathbf{y} - \mathbf{x} \rangle + \frac{L_g}{2}\|\mathbf{x} - \mathbf{y}\|_2^2,$$

for all $\mathbf{x},\ \mathbf{y}$ in the domain $\mathcal{X}$.

7.4.2 Non-convex Proximal Multiplicative Weighting Algorithm

Here we directly approximate the truncated indicator function $\widetilde{\mathbb{1}}(\mathbf{x} \in \mathcal{C}_i)$ by $L_{h,i}$ strongly-smooth convex penalty functions $h_i(\mathbf{x})$, which may be different for different shapes of convex sets. For example, consider the convex set $\mathcal{C}_i$ in Example 1. We may define $h_i(\mathbf{x}) = \sum_{j \notin [i,i+K]}^{N} x_j^2$, where $[a, b]$ denotes the region from a to b. While for the set $\{\mathbf{x} : \langle \mathbf{a}, \mathbf{x} \rangle \leq b\}$, we may instead adopt the modified log-barrier function with a finite value. Then (Equation 7.4.1) can be rewritten as

$$\min_{\mathbf{p}} \min_{\mathbf{x}} \quad \mathcal{L}(\mathbf{p}, \mathbf{x}) \triangleq \sum_{i=1}^{L} p_i f_i(\mathbf{x}), \tag{7.4.4}$$

where $f_i(\mathbf{x})$ is defined as

$$f_i(\mathbf{x}) \triangleq \|\mathbf{x}\|_1 + h_i(\mathbf{x}) + \frac{\lambda_1}{2}\|\mathbf{y} - \mathbf{A}\mathbf{x}\|_2^2 + \frac{\lambda_2}{2}\|\mathbf{x}\|_2^2.$$

Hence, the optimization problem in (Equation 7.4.4) can be solved via Algorithm 5.

Lemma 15. *$h(\mathbf{x}) \triangleq \sum_i p_i h_i(\mathbf{x}) + \frac{\lambda_1\|\mathbf{y}-\mathbf{A}\mathbf{x}\|_2^2}{2} + \frac{\lambda_2\|\mathbf{x}\|_2^2}{2}$ is strongly-smooth with some positive constant denoted as L_h.*

Proof. First, we can check that $\frac{\lambda_1\|\mathbf{y}-\mathbf{A}\mathbf{x}\|_2^2}{2} + \frac{\lambda_2\|\mathbf{x}\|_2^2}{2}$ is strongly-smooth. Denote the corresponding parameter as $L_{h,0}$. Meanwhile, due to the construction of $h_i(\mathbf{x})$, it is strongly-smooth for every i. Since p_i is non-negative for every i, we can easily prove the following inequality

$$h(\mathbf{x}_1) \geq h(\mathbf{x}_2) + \langle \nabla h(\mathbf{x}_2), \mathbf{x}_1 - \mathbf{x}_2 \rangle + \frac{L_h}{2}\|\mathbf{x}_1 - \mathbf{x}_2\|_2^2,$$

where L_h is defined as $\min(L_{h,i})$, $0 \leq i \leq L$. □

Then we have the following theorem.

Theorem 11. *Let* $\eta_x^{(t)} = \eta_x \leq L_h^{-1}$*, and* $\eta_p^{(t)} = R_f^{-1}\sqrt{2\log L/T}$*, where* $|f_i(\cdot)| \leq R_f$*,* $\|\mathbf{x}\|_2 \leq R$*. Then we have*

$$\left|\frac{\min_{\mathbf{p}} \sum_t \mathcal{L}(\mathbf{p}, \mathbf{x}^{(t)})}{T} - \frac{\sum_t \mathcal{L}(\mathbf{p}^{(t)}, \mathbf{x}^{(t)})}{T}\right| + \left|\frac{\sum_t \mathcal{L}(\mathbf{p}^{(t)}, \mathbf{x}^{(t)})}{T} - \frac{\min_{\mathbf{x}} \sum_t \mathcal{L}(\mathbf{p}^{(t)}, \mathbf{x})}{T}\right|$$
$$\leq \frac{2R^2}{\eta_x T} + R_f\sqrt{\frac{\log L}{T}},$$

where T *denotes the number of iterations.*

Due to the difficulties in analyzing the global optimum, in Theorem 11 we focus on analyzing the closeness between the average value $\frac{\sum_t \mathcal{L}(\mathbf{p}^{(t)}, \mathbf{x}^{(t)})}{T}$ to its local minimum. The first term denotes the gap between average value $\frac{\sum_t \mathcal{L}(\mathbf{p}^{(t)}, \mathbf{x}^{(t)})}{T}$ and the optimal value of $\mathcal{L}(\mathbf{p}, \mathbf{x})$ with $\mathbf{x}^{(t)}$ being fixed. Similarly, the second term represents the gap with $\mathbf{p}^{(t)}$ being fixed. As $T \to \infty$, the sum of these two bounds approaches to zero at the rate of $\mathcal{O}(T^{-1/2})$.

Moreover note that setting $\eta_p^{(t)}$ requires the oracle knowledge of T, which is impractical. This artifacts can easily be fixed by the doubling trick (cf. Sec. 2.3.1 in [118]). In addition, we have proved the following theorem.

Theorem 12. *Let* $\eta_w^{(t)} \leq L_h^{-1}$*, where* $|f_i(\cdot)| \leq R_f$*. Then we have*

$$\frac{1}{T}\sum_t \|\mathbf{x}^{(t+1)} - \mathbf{x}^{(t)}\|_2^2 \leq \frac{2\mathcal{L}(\mathbf{p}^{(0)}, \mathbf{x}^{(0)})}{L_h T} + \frac{4R_f^2 \sum_t \eta_p^{(t)}}{L_h T}.$$

This theorem discusses the convergence speed with respect to the $\mathbf{x}^{(t)}$ update. Due to the $\mathcal{O}(T^{-1})$ of the first term on the right side of the above inequality, the best convergence rate we can obtain is $\mathcal{O}(T^{-1})$, which is achievable by $\eta_p^{(t)} \propto t^{-2}$. However, using fixed learning rate η_p as in Theorem 11 would result in the convergence rate of $\mathcal{O}(T^{-1/2})$.

7.4.3 Regularization for $\mathbf{p}$

Another drawback of the naive method is that they cannot exploit the prior knowledge. For example, if we know that the true $\mathbf{x}^\natural$ is most likely to reside in set $\mathcal{C}_1$. With the naive

method, we cannot use this information but separately solve (Equation 7.2.2) for all L sets. In the sequel, we will show that our formulation (Equation 7.4.1) can incorporate such prior knowledge by adding regularizers for $\mathbf{p}$, and bring certain performance improvement.

Note that we can interpret p_i, the i-th element of $\mathbf{p}$ in (Equation 7.4.4) as the likelihood of $\mathbf{x}^\natural \in \mathcal{C}_i$. Without any prior knowledge about which set $\mathcal{C}_i$ the true signal $\mathbf{x}^\natural$ resides, variable $\mathbf{p}$ is uniformly distributed among all possible distributions Δ_L. When certain prior information is available, its distribution is skewed towards certain distributions, namely $\mathbf{q}$.

Here we adopt $\|\cdot\|_2^2$ to regularize $\mathbf{p}$ towards $\mathbf{q}$ and write the modified function $\mathcal{LR}(\mathbf{p}, \mathbf{x})$ as

$$\mathcal{LR}(\mathbf{p}, \mathbf{x}) = \mathcal{L}(\mathbf{p}, \mathbf{x}) + \frac{\lambda_3}{2}\|\mathbf{p} - \mathbf{q}\|_2^2,$$

where $\lambda_3 > 0$ is a constant used to balance $\mathcal{L}(\mathbf{p}, \mathbf{x})$ and $\frac{1}{2}\|\mathbf{p} - \mathbf{q}\|_2^2$. Based on different applications, other norms such as KL-divergence or l_1 norm can be used as the regularizer. Then we substitute the update equation (Equation 7.4.2) as

$$\mathbf{p}^{(t+1)} = \mathbb{P}_\Delta\left(\mathbf{p}^{(t)} - \eta_p^{(t)}\mathbf{g}^{(t)}\right),$$

where $\mathbf{g}^{(t)} = \nabla_{\mathbf{p}^{(t)}}\mathcal{LR}(\mathbf{p}, \mathbf{x}^{(t)}) = \mathbf{f}(\mathbf{x}^{(t)}) + \lambda_3(\mathbf{p}^{(t)} - \mathbf{q})$, and $\mathbf{f}(\mathbf{x}^{(t)})$ denotes the vector whose ith element is $f_i(\mathbf{x}^{(t)})$. Similar as above, we obtain the following theorems.

Theorem 13. *Provided that* $\|\mathbf{g}^{(t)}\|_2 \leq R_g$*, by setting* $\eta_x^{(t)} = \eta_x \leq L_h^{-1}$ *and* $\eta_p^{(t)} = (\lambda t)^{-1}$ *we conclude that*

$$\left|\frac{\min_{\mathbf{p}}\sum_t \mathcal{LR}(\mathbf{p}, \mathbf{x}^{(t)})}{T} - \frac{\sum_t \mathcal{LR}(\mathbf{p}^{(t)}, \mathbf{x}^{(t)})}{T}\right| + \left|\frac{\sum_t \mathcal{LR}(\mathbf{p}^{(t)}, \mathbf{x}^{(t)})}{T} - \frac{\min_{\mathbf{x}}\sum_t \mathcal{LR}(\mathbf{p}^{(t)}, \mathbf{x})}{T}\right|$$
$$\leq \frac{R_g^2 \log T}{2\lambda_3 T} + \frac{R^2}{2\eta_x T},$$

Comparing with Theorem 11, Theorem 13 implies that the regularizers improve the optimal rate from $\mathcal{O}(T^{-1/2})$ to $\mathcal{O}(\log T/T)$. Therefore, our framework can exploit the prior information to improve the recovery performance whereas the naive method of iterative

computation fails to achieve as such.

Theorem 14. *Provided that* $\|\mathbf{g}^{(t)}\|_2 \leq R_g$*, by setting* $\eta_w^{(t)} = \eta_x \leq L_h^{-1}$ *we conclude that*

$$\frac{1}{T}\sum_t \|\mathbf{x}^{(t+1)} - \mathbf{x}^{(t)}\|_2^2 \leq \frac{2\mathcal{L}\mathcal{R}(\mathbf{p}^{(0)}, \mathbf{x}^{(0)})}{L_h T} + \frac{2R_g^2}{L_h T}\sum_t \left(\eta_p^{(t)} + \frac{\lambda_3\left(\eta_p^{(t)}\right)^2}{2}\right).$$

In this case, if we set $\eta_p^{(t)}$ as t^{-2}, then $\frac{1}{T}\sum_t \|\mathbf{x}^{(t+1)} - \mathbf{x}^{(t)}\|_2^2$ would decrease at the rate of $\mathcal{O}(T^{-1})$, which is the same as Theorem 12.

7.5 Conclusions

We studied the compressive sensing with a multiple convex-set domain. First we analyzed the impact of prior knowledge $\mathbf{x} \in \bigcup_i \mathcal{C}_i$ on the minimum number of measurements M to guarantee uniqueness of the solution. We gave an illustrative example and showed that significant savings in M can be achieved. Then we formulated a universal objective function and developed an algorithm for the signal reconstruction. We showed that in terms of the speed of convergence to local minimum, our proposed algorithm based on *multiplicative weight update* and *proximal gradient descent* can achieve the optimal rate of $\mathcal{O}(T^{-1/2})$. Further, in terms of $T^{-1}\|\mathbf{x}^{(t+1)} - \mathbf{x}^{(t)}\|_2^2$, the optimal speed increases to $\mathcal{O}(T^{-1})$. Moreover, provided that we have a prior knowledge about $\mathbf{p}$, we showed that we can improve the optimal recovery performance by $\|\cdot\|_2^2$ regularizers, and hence increasing the above convergence rate from $\mathcal{O}(T^{-1/2})$ to $\mathcal{O}\left(\frac{\log T}{T}\right)$.

CHAPTER 8
CONCLUSIONS AND FUTURE DIRECTIONS

This chapter summarizes the thesis research and presents the future directions.

8.1 Summary of Present Work

This thesis presents an integrated framework of learning dependency relation and signal reconstruction, which consists of three parts.

Interdependency relation learning. First, we presented the parametric method of learning the graphical structure with indirect observations. Assuming the random vector is Gaussian distributed and the majority of entries are conditionally independent, we proposed two novel estimators, namely, M-CLIME and M-gLasso, and analyzed their properties. For the first time, we showed that the correct graphical structure can be correctly obtained under the indefinite sensing system ($d < p$) with insufficient samples ($n < p$). One feasible parameter setting is when dimension d is at the order of $\Omega\left(p^{0.8}\right)$ and sample number n is at the order of $\Omega\left(p^{0.8}\log^3 p\right)$. Numerical experiments suggest a threshold phenomenon may appear if the projection dimension d is not large enough, which is consistent with our theorem.

Second, we extended the parametric method to the non-parametric method of learning graphical models. Relaxing distribution assumption of the random vector $\mathbf{X}$, namely, from Gaussian distribution to nonparanormal distribution, we proposed a practical estimator based on the deconvolution estimator of the CDF and graphical Lasso. Under mild conditions, we showed our graphical structure estimators can obtain the correct structure, from which the minimum sample number n and dimension d can be obtained, that is, $n \gtrsim (\text{deg})^4 \log^4 n$ and $d \gtrsim p + (\log(d-p))^c$, where $c > 0$ is some positive constant. As a byproduct, we obtained a non-asymptotic uniform bound on the estimation error of the

CDF with inexact knowledge of the noise distribution. To the best of our knowledge, this bound never exists before and may serve as independent interests. Additionally, we compared the parametric method and non-parametric method when the underlying distributions are uniform, exponential, and Gaussian mixture, respectively. Numerical experiments suggest the non-parametric method can result in a significant performance improvement under the uniform and exponential setting and a modest improvement under the Gaussian mixture setting. Furthermore, we applied our algorithm to multiple real-world miRNA datasets and verified its effectiveness.

Sensing system design. We presented a general framework to design a sparse sensing matrix $\mathbf{A} \in \mathbb{R}^{m\times n}$, for a linear measurement system $\mathbf{y} = \mathbf{A}\mathbf{x}^\natural + \mathbf{w}$, where $\mathbf{y} \in \mathbb{R}^n$, $\mathbf{x}^\natural \in \mathbb{R}^n$, and $\mathbf{w}$ denote the measurements, the signal with certain structures, and the measurement noise, respectively. By viewing the signal reconstruction from the measurements as a message passing algorithm over a graphical model, we leveraged the density evolution technique and incorporated two design schemes, namely, (i) a regular sensing and (ii) a preferential sensing, into a single framework. To the best of our knowledge, this is the first work that uses density evolution to design the sensing system in CS. In the regular sensing scenario, we considered the ℓ_1 regularizer, which corresponds to Lasso estimator, as an illustration. Noteworthy, our framework can reproduce the classical result of Lasso, i.e., $m \geq c_0 k \log(n/k)$ after a proper distribution approximation, where $c_0 > 0$ is some fixed constant. In the preferential sensing scenario, we formulated the sensing system design as a bi-convex optimization problem, which can be efficiently solved via an alternating method. In the end, we evaluated our design method with both the synthetic and real-world data. For the synthetic data, we showed our sensing system can give a significant reduction of the ℓ_2 error in the high-priority part and a modest reduction of the ℓ_2 error in the whole signal when compared with the matrix designed with the previous method. For the real-world data, we evaluated our sensing matrix with both the MNIST dataset and the Lenka image. Numerical experiments suggest our sensing system can reconstruct the original

images with better qualities and confirm the superiority of our method.

Signal reconstruction with indefinite linear sensing system. First, we considered recovering the sign value of the signal with uncertain sensing matrix. Assuming the perturbation matrix to be sparse Gaussian, we proposed a thresholding strategy and gave a sufficient condition, under which with high probability the reconstructed sign value will be correct. Numerical experiments verify the correctness of our theorem and suggest the recovery performance is unstable once the sufficient condition is violated.

Second, we proposed a new objective function to recover a noisy-pseudo-sparse signal from linear measurements. We gave a theoretical analysis of the reconstructed signal's properties. For the convenience of analysis, we studied the ideal case where the entries of the signal deviation are uniformly distributed and proved that a unique solution in the proximity of ground-truth could be obtained with an indefinite sensing matrix. Moreover, we provided simulation results with the Gaussian noise and showed a significant reduction (approximately 50%) in the ℓ_2 error of the signal reconstruction with our method.

Third, we studied the compressive sensing with a multiple convex-set domain, where the sparse signal is assumed to reside within the union of several convex sets. Notice that multiple CS problems can be recasted as this problem with certain algebraic manipulations. From the statistical perspective, we analyzed the impact of prior knowledge $\mathbf{x} \in \bigcup_i \mathcal{C}_i$ on the minimum number of measurements M to guarantee uniqueness of the solution. To illustrate the significant savings resulted from the prior knowledge, we present an illustrative example in which the number M reduces from $\mathcal{O}(K \log K)$ to $\mathcal{O}(K)$ (K is the sparsity number of the signal). From the computational perspective, we formulated a universal objective function and designed an optimization algorithm based on *multiplicative weight update* and *proximal gradient descent*. Compared with the previous method that iteratively reconstructs the sparse signal for each convex set $\mathcal{C}_i$, our method enjoys the following benefits.

- **Reduce the storage size**. Our algorithm reduces the storage size from $\mathcal{O}(NL)$ to

$\mathcal{O}(N + L)$, where N is the length of signal and L is the number of convex sets.

- **Capable of exploiting prior knowledge for acceleration of algorithm**. Without the prior knowledge of the distributions on the union $\bigcup_i \mathcal{C}_i$, our algorithm can converge to the local minimum at the speed of $\mathcal{O}(T^{-1/2})$, where T is the number of iterations. Given the prior knowledge, the convergence rate will increase to $\mathcal{O}(\log T/T)$.

8.2 Summary of Future Directions

This section lists the possible directions of the future research.

Interdependency relation learning. In the parametric method of graphical structure learning, our current work assumes the random vector to be Gaussian distributed. In the future research, we can extend the analysis to other types of graphs, e.g., graphs for discrete random variables. Further, we only considered undirected graphs. One may extend the work to Bayesian graphs.

For the nonparametric method of the graphical structure learning, we can turn to the setting of compressive sensing system, i.e., with an indefinite sensing matrix $\mathbf{A} \in \mathbb{R}^{d\times p}$. To the best of our knowledge, whether we can use insufficient sensors to detect the correct graphical structure with non-parametric method is still an open problem.

Furthermore, one can focus on other methods of covariance matrix estimation. Possible directions include Spearman's rho estimator, Kendall's tau estimator, etc. Moreover, other types of graphical models such as graphs with forest structure, graph with the elliptical distribution, and latent Gaussian models can be investigated.

Additionally, we can revisit our current work on graphical structure recovery from the viewpoint of the privacy. Consider the setting where the direct inquiry about $\mathbf{X}$ cannot be returned due to the privacy concern, for example when $\mathbf{X}$ denotes some health or financial information. Our goal then becomes learning the structure of graphical models without leaking the exact information about one particular sample. How to balance the performance of the graphical structure recovery and the data privacy constitutes as another promising

future research direction.

Sensing system design. For the design of compressive sensing system with density evolution, our current work only specifies the degree distributions of the variable nodes and check nodes. Meanwhile, the previous work [55, 53] suggest that the spatial coupling technique can lead to significant performance improvement of the signal reconstruction. Hence, one potential direction of future research will be incorporating the structural information into the design framework. Additionally, one can extend the work to design the compressive sensing system $\{\mathbf{a}_i\}_{1\leq i\leq p}$, for the non-linear sensing relation, i.e., $y_i = f_i\left(\langle \mathbf{a}_i, \mathbf{x}\rangle\right) + \text{noise}$.

Moreover, one can revisit the problem of sensing system design from the perspective of robustness. Notice that the practical sensing system can deviate from the designed sensing matrix, which may lead to serious performance degradation. In such case, how to design a sensing sensing that is robust to the undesirable deviations constitute another future research direction.

Signal reconstruction with indefinite linear sensing system. In our current analysis, we assume the linear sensing relation, namely, $\mathbf{y} = \mathbf{A}\mathbf{x} + \mathbf{w}$, which can be impractical in real-world applications. In our future research, we can revisit our previous problems by considering a general form of sensing relation, i.e.,

$$y_i = f_i\left(\langle \mathbf{a}_i, \mathbf{x}\rangle\right) + \text{noise},$$

where $f_i(\cdot)$ denotes some non-linear function, y_i denotes the ith reading, and $\mathbf{a}_i$ is the corresponding coefficient vector. Obtaining the minimum number of measurements for the signal recovery and the design of efficient reconstruction algorithms are two interesting questions awaiting to be answered.

Appendices

APPENDIX A

APPENDIX OF PARAMETRIC LEARNING OF GRAPHICAL MODELS

A.1 Proof of Lemma 1

For the convenience of analysis, we rescale the sensing matrix $\widetilde{\mathbf{A}}$ such that $\widetilde{A}_{ij} \sim \mathcal{N}(0, d^{-1})$.

Lemma 16. *Consider the covariance estimator* $\widehat{\mathbf{\Sigma}}_n^{\text{param}}$ *which reads*

$$\widehat{\mathbf{\Sigma}}_n^{\text{param}} = \mathbf{I} + \frac{d}{d+1}\left[\widetilde{\mathbf{A}}^\top\left(\frac{1}{n}\sum_{i=1}^{n}\mathbf{Y}^{(i)}\mathbf{Y}^{(i)\top}\right)\widetilde{\mathbf{A}}\right]_{\text{off}}, \tag{A.1.1}$$

where $(\cdot)_{\text{off}}$ *denotes the operation of picking non-diagonal entries. We then have* $\|\widehat{\mathbf{\Sigma}}_n^{\text{param}} - \mathbf{\Sigma}^\natural\|_\infty \lesssim \tau_\infty$ *holding with probability at least* $1 - c_0 p^{-1} - c_1 p^2 e^{-c_2 d} - c_3 p^2 e^{-c_4 p}$.

We begin the analysis by redefining the following events,

$$\begin{aligned}
\mathcal{E}_1 &\triangleq \left\{1 - c_0\sqrt{\frac{\log p}{d}} \le \left\|\widetilde{\mathbf{A}}_i\right\|_2 \le 1 + c_0\sqrt{\frac{\log p}{d}},\ \ \forall\, i\right\};\\
\mathcal{E}_2 &\triangleq \left\{|\left\langle\widetilde{\mathbf{A}}_i, \widetilde{\mathbf{A}}_j\right\rangle| \lesssim \sqrt{\frac{\log p}{d}} \vee \frac{\log p}{d},\ \ \forall\, i \neq j\right\};\\
\mathcal{E}_3 &\triangleq \left\{\left\|\widehat{\mathbf{\Sigma}}_n^{\text{param}} - \mathbf{\Sigma}^\natural\right\|_\infty \lesssim \sqrt{\frac{\log p}{n}}\right\};\\
\mathcal{E}_4(\mathbf{B}) &\triangleq \left\{\left\|\sum_{\ell\neq 1} B_\ell \widetilde{\mathbf{A}}_\ell\right\|_2 \lesssim \sqrt{\sum_{\ell\neq 1} B_\ell^2}\right\},\ \ \text{where } \mathbf{B} \in \mathbb{R}^p \text{ is a fixed vector.}
\end{aligned}$$

Additionally, we define $\Psi(\mathcal{E})$ as $\mathbb{E}\mathbb{1}(\mathcal{E})$. Moreover, our analysis focuses on the region when $d \gg \log p$.

A.1.1 Main Structure

Having collected all the lemmas, we turn to the proof of Lemma 1. Notice that by the definition of our estimator, $\left\|\widehat{\mathbf{\Sigma}}_n^{\text{param}} - \mathbf{\Sigma}^\natural\right\|_\infty = \max_{i\neq j}\left|\left(\widehat{\mathbf{\Sigma}}_n^{\text{param}}\right)_{i,j} - \mathbf{\Sigma}^\natural_{i,j}\right|$. Hence, we only consider the off-diagonal entries, which gives

$$
\begin{aligned}
&\left\|\widehat{\mathbf{\Sigma}}_n^{\text{param}} - \mathbf{\Sigma}^\natural\right\|_{\text{off},\infty} = \left\|\frac{d}{d+1}\widetilde{\mathbf{A}}^\top\left(\sum_{\ell=1}^n \mathbf{Y}^{(\ell)}\mathbf{Y}^{(\ell)\top}\right)\widetilde{\mathbf{A}} - \mathbf{\Sigma}^\natural\right\|_{\text{off},\infty} \\
\leq\ & 2\left\|\frac{d}{d+1}\widetilde{\mathbf{A}}^\top\widetilde{\mathbf{A}}\mathbf{\Sigma}_n^{\text{param}}\widetilde{\mathbf{A}}^\top\widetilde{\mathbf{A}} - \mathbf{\Sigma}^\natural\right\|_{\text{off},\infty} + \frac{2d}{n(d+1)}\left\|\widetilde{\mathbf{A}}^\top\left(\sum_{\ell=1}^n \mathbf{W}^{(\ell)}\mathbf{W}^{(\ell)\top}\right)\widetilde{\mathbf{A}}\right\|_{\text{off},\infty} \\
\overset{①}{=}\ & \frac{2d}{d+1}\underbrace{\left\|\widetilde{\mathbf{A}}^\top\widetilde{\mathbf{A}}\mathbf{\Sigma}_n^{\text{param}}\widetilde{\mathbf{A}}^\top\widetilde{\mathbf{A}} - \mathbb{E}_{\widetilde{\mathbf{A}}}\left(\widetilde{\mathbf{A}}^\top\widetilde{\mathbf{A}}\mathbf{\Sigma}_n^{\text{param}}\widetilde{\mathbf{A}}^\top\widetilde{\mathbf{A}}\right)\right\|_{\text{off},\infty}}_{\vartheta_1} \\
&+ \frac{2d}{d+1}\underbrace{\left\|\mathbb{E}_{\widetilde{\mathbf{A}}}\left(\widetilde{\mathbf{A}}^\top\widetilde{\mathbf{A}}\mathbf{\Sigma}_n^{\text{param}}\widetilde{\mathbf{A}}^\top\widetilde{\mathbf{A}}\right) - \mathbb{E}_{\widetilde{\mathbf{A}},\mathbf{X}}\left(\widetilde{\mathbf{A}}^\top\widetilde{\mathbf{A}}\mathbf{\Sigma}_n^{\text{param}}\widetilde{\mathbf{A}}^\top\widetilde{\mathbf{A}}\right)\right\|_{\text{off},\infty}}_{\vartheta_2} \\
&+ \frac{2d}{n(d+1)}\underbrace{\left\|\widetilde{\mathbf{A}}^\top\left(\sum_{\ell=1}^n \mathbf{W}^{(\ell)}\mathbf{W}^{(\ell)\top}\right)\widetilde{\mathbf{A}}\right\|_{\text{off},\infty}}_{\vartheta_3},
\end{aligned}
$$

where $\mathbf{\Sigma}_n^{\text{param}}$ is defined as $n^{-1}\left(\sum_{\ell=1}^n \mathbf{X}^{(\ell)}\mathbf{X}^{(\ell)\top}\right)$, and in ① we use

$$
\frac{d}{d+1}\mathbb{E}_{\widetilde{\mathbf{A}},\mathbf{X}}\left(\widetilde{\mathbf{A}}^\top\widetilde{\mathbf{A}}\mathbf{\Sigma}_n^{\text{param}}\widetilde{\mathbf{A}}^\top\widetilde{\mathbf{A}}\right) = \mathbf{\Sigma}^\natural.
$$

Then we separately upper-bound $\vartheta_1,\ \vartheta_2$, and ϑ_3 conditional on the event $\bigcap_{i=1}^3 \mathcal{E}_i$. For the conciseness in notations, define $\mathbf{Z} = \widetilde{\mathbf{A}}^\top\widetilde{\mathbf{A}}\mathbf{\Sigma}_n^{\text{param}}\widetilde{\mathbf{A}}^\top\widetilde{\mathbf{A}}$. Therefore $\vartheta_1 = \|\mathbf{Z} - \mathbb{E}\mathbf{Z}\|_{\text{off},\infty}$. For an arbitrary entry $Z_{i,j}$, we can expand it as

$$
Z_{i,j} = \sum_{\ell_1,\ell_2}(\mathbf{\Sigma}_n^{\text{param}})_{\ell_1,\ell_2}\left\langle\widetilde{\mathbf{A}}_i, \widetilde{\mathbf{A}}_{\ell_1}\right\rangle\left\langle\widetilde{\mathbf{A}}_j, \widetilde{\mathbf{A}}_{\ell_2}\right\rangle, \quad i\neq j.
$$

Compared to the existing work [3], our analysis of Z_{ij} involves fourth-order Gaussian chaos [150], which exhibits heavy tails, and constructs the major obstacle.

Stage I: Bounding ϑ_1. To obtain upper bound on ϑ_1, we first adopt the union bound and obtain

$$\mathbb{P}\left(\vartheta_1 \geq \delta\right) = \mathbb{P}\left(\max_{i\neq j} |Z_{i,j} - \mathbb{E}Z_{i,j}| \geq \delta\right) \leq \sum_{i\neq j} \mathbb{P}\left(|Z_{i,j} - \mathbb{E}Z_{i,j}| \geq \delta,\ i \neq j\right). \quad \text{(A.1.2)}$$

Then our focus is to bound the probability $\mathbb{P}\left(|Z_{i,j} - \mathbb{E}Z_{i,j}| \geq \delta,\ i \neq j\right)$. Without loss of generality, assume that $i = 1$ and $j = 2$ and expand $Z_{1,2}$ as $\sum_{i=1}^{5} T_i$, which reads

$$\begin{aligned}
T_1 &\triangleq \left(\boldsymbol{\Sigma}_n^{\text{param}}\right)_{1,2} \left\|\widetilde{\mathbf{A}}_1\right\|_2^2 \left\|\widetilde{\mathbf{A}}_2\right\|_2^2; \\
T_2 &\triangleq \left(\boldsymbol{\Sigma}_n^{\text{param}}\right)_{2,1} \left(\left\langle \widetilde{\mathbf{A}}_1, \widetilde{\mathbf{A}}_2 \right\rangle\right)^2; \\
T_3 &\triangleq \sum_{\ell\neq 1} \left(\boldsymbol{\Sigma}_n^{\text{param}}\right)_{2,\ell} \left\|\widetilde{\mathbf{A}}_2\right\|_2^2 \left\langle \widetilde{\mathbf{A}}_1, \widetilde{\mathbf{A}}_\ell \right\rangle + \sum_{\ell\neq 2} \left(\boldsymbol{\Sigma}_n^{\text{param}}\right)_{\ell,1} \left\|\widetilde{\mathbf{A}}_1\right\|_2^2 \left\langle \widetilde{\mathbf{A}}_2, \widetilde{\mathbf{A}}_\ell \right\rangle; \\
T_4 &\triangleq \sum_{\ell\neq 1,2} \left(\boldsymbol{\Sigma}_n^{\text{param}}\right)_{\ell,\ell} \left\langle \widetilde{\mathbf{A}}_1, \widetilde{\mathbf{A}}_\ell \right\rangle \left\langle \widetilde{\mathbf{A}}_2, \widetilde{\mathbf{A}}_\ell \right\rangle; \\
T_5 &\triangleq \sum_{\substack{\ell_1,\ell_2\neq 1,2 \\ \ell_1\neq\ell_2}} \left(\boldsymbol{\Sigma}_n^{\text{param}}\right)_{\ell_1,\ell_2} \left\langle \widetilde{\mathbf{A}}_1, \widetilde{\mathbf{A}}_{\ell_1} \right\rangle \left\langle \widetilde{\mathbf{A}}_2, \widetilde{\mathbf{A}}_{\ell_2} \right\rangle.
\end{aligned}$$

Now, we separately bound the deviations $|T_i - \mathbb{E}T_i|$, $1 \leq i \leq 5$. First, we have

$$\begin{aligned}
&|T_1 - \mathbb{E}T_1| = \left|\left(\boldsymbol{\Sigma}_n^{\text{param}}\right)_{1,2}\right| \times \left|\left\|\widetilde{\mathbf{A}}_1\right\|_2^2 \left\|\widetilde{\mathbf{A}}_2\right\|_2^2 - 1\right| \\
&= \left|\left(\boldsymbol{\Sigma}_n^{\text{param}}\right)_{1,2}\right| \times \left|\left\|\widetilde{\mathbf{A}}_1\right\|_2 \left\|\widetilde{\mathbf{A}}_2\right\|_2 - 1\right| \times \left(\left\|\widetilde{\mathbf{A}}_1\right\|_2 \left\|\widetilde{\mathbf{A}}_2\right\|_2 + 1\right) \\
&\overset{②}{\leq} \left|\left(\boldsymbol{\Sigma}_n^{\text{param}}\right)_{1,2}\right| \times \left(\left|\left\|\widetilde{\mathbf{A}}_1\right\|_2 - 1\right| \left\|\widetilde{\mathbf{A}}_2\right\|_2 + \left|\left\|\widetilde{\mathbf{A}}_2\right\|_2 - 1\right|\right) \times \left(\left(1 + c_0\sqrt{\log p/d}\right)^2 + 1\right) \\
&\overset{③}{\leq} \left|\left(\boldsymbol{\Sigma}_n^{\text{param}}\right)_{1,2}\right| \times c_0\sqrt{\log p/d}(2 + c_0\sqrt{\log p/d}) \times \left(\left(1 + c_0\sqrt{\log p/d}\right)^2 + 1\right) \\
&\overset{④}{\lesssim} \left|\left(\boldsymbol{\Sigma}_n^{\text{param}}\right)_{1,2}\right| \sqrt{\log p/d} \overset{⑤}{\lesssim} \sqrt{\frac{\log p}{d}} \left(\left|\Sigma_{1,2}^{\natural}\right| + \sqrt{\frac{\log p}{n}}\right),
\end{aligned} \quad \text{(A.1.3)}$$

where in ② and ③ we condition on event $\mathcal{E}_1$, ④ is due to $d \gg \log p$, and ⑤ is by the definition of event $\mathcal{E}_3$.

For $|T_2 - \mathbb{E}T_2|$, by invoking Lemma 21,

$$|T_2 - \mathbb{E}T_2| \lesssim |\,(\mathbf{\Sigma}_n^{\text{param}})_{2,1}\,| \times \left(\frac{\log p}{d} + \frac{\sqrt{\log p}}{d^{3/2}}\right) \overset{⑥}{\lesssim} \left|(\mathbf{\Sigma}_n^{\text{param}})_{2,1}\right| \frac{\log p}{d}$$
$$\overset{⑦}{\lesssim} \frac{\log p}{d}\left(\left|\Sigma_{2,1}^{\natural}\right| + \sqrt{\frac{\log p}{n}}\right), \tag{A.1.4}$$

holds with probability exceeding $1 - 2p^{-3}$, where ⑥ is because $d \gg \log p$, and ⑦ is due to event $\mathcal{E}_3$.

We continue to bound $|T_3 - \mathbb{E}T_3|$ by

$$\begin{aligned}
&|T_3 - \mathbb{E}T_3| \\
\leq\ & \left\|\widetilde{\mathbf{A}}_1\right\|_2^2 \times \left|\sum_{\ell\neq 2} (\mathbf{\Sigma}_n^{\text{param}})_{1,\ell} \left\langle \widetilde{\mathbf{A}}_2, \widetilde{\mathbf{A}}_\ell \right\rangle\right| + \left\|\widetilde{\mathbf{A}}_2\right\|_2^2 \times \left|\sum_{\ell\neq 1} (\mathbf{\Sigma}_n^{\text{param}})_{\ell,2} \left\langle \widetilde{\mathbf{A}}_1, \widetilde{\mathbf{A}}_\ell \right\rangle\right| \\
\leq\ & \left(1 + c_0\sqrt{\frac{\log p}{d}}\right)^2 \left|\sum_{\ell\neq 2} (\mathbf{\Sigma}_n^{\text{param}})_{1,\ell} \left\langle \widetilde{\mathbf{A}}_2, \widetilde{\mathbf{A}}_\ell \right\rangle\right| + \left(1 + c_0\sqrt{\frac{\log p}{d}}\right)^2 \left|\sum_{\ell\neq 1} (\mathbf{\Sigma}_n^{\text{param}})_{\ell,2} \left\langle \widetilde{\mathbf{A}}_1, \widetilde{\mathbf{A}}_\ell \right\rangle\right| \\
\overset{⑧}{\lesssim}\ & \left(1 + c_0\sqrt{\frac{\log p}{d}}\right)^2 \times \sqrt{\frac{\log p}{d}} \left(\sqrt{\sum_{\ell\neq 2} (\mathbf{\Sigma}_n^{\text{param}})_{1,\ell}^2} + \sqrt{\sum_{\ell\neq 1} (\mathbf{\Sigma}_n^{\text{param}})_{\ell,2}^2}\right) \\
\overset{⑨}{\lesssim}\ & \sqrt{\frac{\log p}{d}} \left(\sqrt{\sum_{\ell\neq 2} (\mathbf{\Sigma}_n^{\text{param}})_{1,\ell}^2} + \sqrt{\sum_{\ell\neq 1} (\mathbf{\Sigma}_n^{\text{param}})_{\ell,2}^2}\right) \\
\overset{Ⓐ}{\lesssim}\ & \sqrt{\frac{\log p}{d}} \left(\left\|\mathbf{\Sigma}_1^{\natural}\right\|_2 + \left\|\mathbf{\Sigma}_2^{\natural}\right\|_2 + \sqrt{\frac{p\log p}{n}}\right)
\end{aligned} \tag{A.1.5}$$

which holds for probability exceeding $1 - c_0 p^{-3} - c_1 e^{-c_2 d}$, where in ⑧ we invoke Lemma 22, in ⑨ we use that $\mathbf{\Sigma}_n^{\text{param}}$ is symmetric and $d \gg \log p$, and Ⓐ is due to event $\mathcal{E}_3$.

To bound $|T_4 - \mathbb{E}T_4|$, we invoke Lemma 23,

$$
\begin{aligned}
& |T_4 - \mathbb{E}T_4| \\
\lesssim\ & \frac{\left|\sum_{\ell>2} (\mathbf{\Sigma}_n^{\text{param}})_{\ell,\ell}\right|}{d}\sqrt{\frac{\log p}{d}} \\
& + \frac{\sqrt{\log p}}{d}\left[\sqrt{\sum_{\ell>2} (\mathbf{\Sigma}_n^{\text{param}})_{\ell,\ell}^2} \vee \left(\sqrt{\log p}(\max_{\ell} |\, (\mathbf{\Sigma}_n^{\text{param}})_{\ell,\ell}\,|)\right)\right] \\
\overset{\text{Ⓑ}}{\lesssim}\ & \frac{p\sqrt{\log p}}{d^{3/2}}\left(1 + c_0\sqrt{\frac{\log p}{n}}\right) \\
& + \frac{\sqrt{p\log p}}{d}\underbrace{\left[\left(1 + c_0\sqrt{\frac{\log p}{n}}\right) \vee \sqrt{\frac{\log p}{p}}\left(1 + c_0\sqrt{\frac{\log p}{n}}\right)\right]}_{1+c_0\sqrt{\frac{\log p}{n}}},
\end{aligned}
\tag{A.1.6}
$$

holds with probability exceeding $1 - 2p^{-3}$, where Ⓑ is by definition of event $\mathcal{E}_3$.

The deviation $|T_5 - \mathbb{E}T_5|$ is bounded via Lemma 24, which gives

$$
|T_5 - \mathbb{E}T_5| \lesssim \frac{\log p}{d}\left(1 + c_0\sqrt{\frac{p}{d}}\right)^2 \left|\!\left|\!\left|\mathbf{\Sigma}^{\natural}\right|\!\right|\!\right|_{\text{off,F}} \tag{A.1.7}
$$

$$
\overset{\text{Ⓒ}}{\lesssim} \frac{\log p}{d}\left(1 + \frac{c_1 p}{d}\right)\left(\left|\!\left|\!\left|\mathbf{\Sigma}^{\natural}\right|\!\right|\!\right|_{\text{off,F}} + p\sqrt{\frac{\log p}{n}}\right), \tag{A.1.8}
$$

with probability exceeding $1 - 4p^{-3} - e^{-c_0 p}$, where in Ⓒ we condition on event $\mathcal{E}_3$.

Combining (Equation A.1.3), (Equation A.1.4), (Equation A.1.5), (Equation A.1.6), and (Equation A.1.7), we conclude that

$$
\begin{aligned}
|Z_{i,j} - \mathbb{E}Z_{i,j}| \lesssim\ & \sqrt{\frac{\log p}{d}}\left(\left\|\mathbf{\Sigma}_i^{\natural}\right\|_2 + \left\|\mathbf{\Sigma}_j^{\natural}\right\|_2\right) + \frac{\log p}{d}\left(1 + \frac{c_1 p}{d}\right)\left|\!\left|\!\left|\mathbf{\Sigma}^{\natural}\right|\!\right|\!\right|_{\text{off,F}} \\
& + \frac{\log p\sqrt{p}}{\sqrt{nd}} + \frac{c_0 p(\log p)^{3/2}}{n^{1/2}d}\left(1 + \frac{c_1 p}{d}\right) + \frac{\sqrt{p\log p}}{d} + \frac{p\sqrt{\log p}}{d^{3/2}},
\end{aligned}
$$

with probability $1 - c_0 p^{-3} - c_1 e^{-c_2 d} - c_3 e^{-c_4 p}$. We conclude the proof by plugging into (Equation A.1.2) and $\left|\!\left|\!\left|\mathbf{\Sigma}_n^{\text{param}} - \mathbf{\Sigma}^{\natural}\right|\!\right|\!\right|_{\text{off},\infty} \leq \left\|\mathbf{\Sigma}_n^{\text{param}} - \mathbf{\Sigma}^{\natural}\right\|_{\infty} \lesssim \sqrt{\log p/n}$ according to event $\mathcal{E}_3$.

Stage II: Bounding ϑ_2. We rewrite ϑ_2 as $\left\|\mathbf{\Sigma}_n^{\text{param}} - \mathbf{\Sigma}^{\natural}\right\|_{\text{off},\infty}$ and invoke event $\mathcal{E}_3$.

Stage III: Bounding ϑ_3. This stage is completed by invoking Lemma 25. Combing the above three stages will then yield the proof.

A.1.2 Supporting Lemmas

We first compute the values of $\Psi(\mathcal{E}_i)$, $1 \leq i \leq 3$.

Lemma 17. $\Psi(\mathcal{E}_1) \geq 1 - 2p^{-1}$.

Proof. We conclude that

$$\mathbb{P}\left(\left|\left\|\widetilde{\mathbf{A}}_i\right\|_2 - 1\right| \geq c_0\sqrt{\frac{\log p}{d}},\ \exists 1 \leq i \leq p\right) \leq\ p\mathbb{P}\left(\left|\left\|\widetilde{\mathbf{A}}_i\right\|_2 - 1\right| \geq c_0\sqrt{\frac{\log p}{d}}\right)$$
$$\overset{①}{\leq}\ 4p\exp\left(-2d \times \frac{\log p}{d}\right) = 2p^{-1},$$

where ① is due to the properties of χ^2 distribution.

□

Lemma 18. *Conditional on $\mathcal{E}_1$, we have $\Psi(\mathcal{E}_2) \geq 1 - 2p^{-1}$.*

Proof. Due to the independence between $\widetilde{\mathbf{A}}_i$ and $\widetilde{\mathbf{A}}_j$, where $i \neq j$. We can condition on $\widetilde{\mathbf{A}}_i$ and view $\left\langle \widetilde{\mathbf{A}}_i, \widetilde{\mathbf{A}}_j \right\rangle$ as a Gaussian RV with mean zero and variance $d^{-1}\left\|\widetilde{\mathbf{A}}_i\right\|_2^2$, namely, $\mathcal{N}\left(0, d^{-1}\left\|\widetilde{\mathbf{A}}_i\right\|_2^2\right)$. Then we conclude that

$$\Psi\left(\overline{\mathcal{E}}_2 \mid \mathcal{E}_1\right) \overset{①}{\leq}\ p^2\Psi\left(\left|\left\langle \widetilde{\mathbf{A}}_i, \widetilde{\mathbf{A}}_j \right\rangle\right| \geq \delta \mid \mathcal{E}_1\right) \overset{②}{\leq} 2p^2\left(\Phi\left(-\frac{\sqrt{d}\delta}{\left\|\widetilde{\mathbf{A}}_i\right\|_2}\right) \times \Psi(\mathcal{E}_1)\right)$$
$$\overset{③}{\leq}\ 2p^2\left(\exp\left(-\frac{d\delta^2}{2\left\|\widetilde{\mathbf{A}}_i\right\|_2^2}\right) \times \Psi(\mathcal{E}_1)\right) \overset{④}{\leq} 2p^2\exp\left(-\frac{d\delta^2}{2\left(1 + c_0\sqrt{\log p/d}\right)^2}\right),$$

where ① is due to the union bound, in ② we denote $\Phi(t) = 1/\sqrt{2\pi}\int_{-\infty}^{t} e^{-x^2/2}dx$, the CDF of the normal distribution, ③ is because $\Phi(x) \leq e^{-x^2/2}$, and ④ is according to event $\mathcal{E}_1$.

In the end, we complete the proof by setting δ as $c_1\left(\sqrt{\frac{\log p}{d}}\vee\frac{\log p}{d}\right)$, which yields $\Psi(\overline{\mathcal{E}}_2\mid\mathcal{E}_1)\leq 2p^{-1}$. □

Lemma 19. $\Psi(\mathcal{E}_3)\geq 1-4p^{-1}$.

Proof. The proof can be found in the proof of Thm. 1 and Thm. 4 in [4]. □

Lemma 20. *For an arbitrary fixed vector* $\mathbf{B}\in\mathbb{R}^p$*, we have* $\Psi(\mathcal{E}_4(\mathbf{B}))\geq 1-e^{-0.8d}$.

Proof. Notice that $\sum_{\ell\neq 1}B_\ell\widetilde{\mathbf{A}}_\ell$ is a vector satisfying $\mathcal{N}\left(\mathbf{0},d^{-1}\left(\sum_{\ell\neq 1}B_\ell^2\right)\mathbf{I}\right)$. Hence, $\frac{d}{\sum_{\ell\neq 1}B_\ell^2}\|\sum_{\ell\neq 1}B_\ell\widetilde{\mathbf{A}}_\ell\|_2^2$ is a χ^2 RV with freedom d, which suggests

$$\begin{aligned}\mathbb{P}\left(\left\|\sum_{\ell\neq 1}B_\ell\widetilde{\mathbf{A}}_\ell\right\|_2^2\geq 4\left(\sum_{\ell\neq 1}B_\ell^2\right)\right)&=\mathbb{P}\left(\frac{d}{\sum_{\ell\neq 1}B_\ell^2}\left\|\sum_{\ell\neq 1}B_\ell\widetilde{\mathbf{A}}_\ell\right\|_2^2\geq 4d\right)\\&\overset{①}{\leq}\exp\left(\frac{d}{2}\left(\log 4-3\right)\right)\leq e^{-0.8d},\end{aligned}$$

where ① is due to the properties of χ^2 distribution. □

Lemma 21. *Conditional on event* $\mathcal{E}_1$*,*

$$\begin{aligned}\left|\sum_{\ell\neq 1}B_\ell\left\langle\widetilde{\mathbf{A}}_1,\widetilde{\mathbf{A}}_\ell\right\rangle^2-d^{-1}\left(\sum_{\ell\neq 1}B_\ell\right)\right|\lesssim\ &\frac{1}{d}\left(\sqrt{\log p}\sqrt{\sum_{\ell\neq 1}B_\ell^2}\vee(\log p)\left(\max_{\ell\neq 1}|B_\ell|\right)\right)\\&+\ \frac{\sum_{\ell\neq 1}B_\ell}{d}\sqrt{\frac{\log p}{d}}\end{aligned}$$

holds with probability exceeding $1-2p^{-3}$*, for an arbitrary fixed vector* $\mathbf{B}\in\mathbb{R}^p$.

Proof. First, we decompose the above term as

$$
\begin{aligned}
& \left| \sum_{\ell \neq 1} B_\ell \left\langle \widetilde{\mathbf{A}}_1, \widetilde{\mathbf{A}}_\ell \right\rangle^2 - d^{-1} \left(\sum_{\ell \neq 1} B_\ell \right) \right| \\
\leq \; & \frac{\left\| \widetilde{\mathbf{A}}_1 \right\|_2^2}{d} \left| \sum_{\ell \neq 1} B_\ell \left(\frac{\sqrt{d} \left\langle \widetilde{\mathbf{A}}_1, \widetilde{\mathbf{A}}_\ell \right\rangle}{\left\| \widetilde{\mathbf{A}}_1 \right\|_2} \right)^2 - \sum_{\ell \neq 1} B_\ell \right| + d^{-1} \left| \sum_{\ell \neq 1} B_\ell \right| \left| \left\| \widetilde{\mathbf{A}}_1 \right\|_2^2 - 1 \right| \\
\overset{①}{\leq} \; & \frac{1}{d} \left(1 + c_0 \sqrt{\frac{\log p}{d}} \right) \underbrace{\left| \sum_{\ell \neq 1} B_\ell \left(\frac{\sqrt{d} \left\langle \widetilde{\mathbf{A}}_1, \widetilde{\mathbf{A}}_\ell \right\rangle}{\left\| \widetilde{\mathbf{A}}_1 \right\|_2} \right)^2 - \sum_{\ell \neq 1} B_\ell \right|}_{T} + \frac{\left| \sum_{\ell \neq 1} B_\ell \right|}{d} \sqrt{\frac{\log p}{d}} \\
\overset{②}{\lesssim} \; & \frac{T}{d} + \frac{\left| \sum_{\ell \neq 1} B_\ell \right|}{d} \sqrt{\frac{\log p}{d}}
\end{aligned}
$$

where ① is due to the definition of event $\mathcal{E}_1$, and ② is because $d \gg \log p$. Our following analysis focuses on upper-bounding T. First we define $\mathbf{\Lambda}$ as $\mathbf{\Lambda} = [\Lambda_2 \; \cdots \; \Lambda_d]^\top$, where $\Lambda_i = \sqrt{d} \left\langle \widetilde{\mathbf{A}}_1, \widetilde{\mathbf{A}}_\ell \right\rangle / \left\| \widetilde{\mathbf{A}}_1 \right\|_2$. Then we can rewrite T as

$$
T = \sum_{\ell \neq 1} B_\ell \Lambda_i^2 = \mathbf{\Lambda}^\top \text{diag}(B_\ell)_{\ell \neq 2} \mathbf{\Lambda}.
$$

Due to the independence between $\widetilde{\mathbf{A}}_1$ and $\widetilde{\mathbf{A}}_\ell$, $\ell \neq 1$, we can condition $\widetilde{\mathbf{A}}_1$ and can view Λ_i as a Gaussian RV satisfying $\mathcal{N}(0, 1)$. Invoking the Hanson-Wright inequality (Thm. 6.2.1 in [139]), we conclude that

$$
\mathbb{P}\left(T \geq \delta \right) \leq \; 2 \exp \left(-c \left(\frac{\delta^2}{\left\| \text{diag}(B_\ell)_{\ell \neq 1} \right\|_{\text{F}}^2} \; \wedge \frac{\delta}{\left\| \text{diag}(B_\ell)_{\ell \neq 1} \right\|_{\text{OP}}} \right) \right).
$$

Setting δ as $\left(c_0 \sqrt{\log p} \sqrt{\sum_{\ell \neq 1} B_\ell^2} \right) \vee c_1 \left(\log p \times \max_{\ell \neq 1} |B_\ell| \right)$, we conclude that $\mathbb{P}(T \geq \delta) \leq 2p^{-3}$ and complete the proof. $\square$

Lemma 22. *Given a fixed vector* $\mathbf{B} \in \mathbb{R}^p$*,*

$$\left| \sum_{\ell \neq 1} B_\ell \left\langle \widetilde{\mathbf{A}}_1, \widetilde{\mathbf{A}}_\ell \right\rangle \right| \lesssim \sqrt{\frac{\log p}{d}} \sqrt{\sum_{\ell \neq 1} B_\ell^2},$$

holds with probability at least $1 - p^{-3} - e^{-0.8d}$*.*

Proof. Due to the independence between $\widetilde{\mathbf{A}}_1$ and $\widetilde{\mathbf{A}}_\ell$, where $\ell \neq 1$. We condition on $\widetilde{\mathbf{A}}_\ell$ and view $\sum_{\ell \neq 1} B_\ell \left\langle \widetilde{\mathbf{A}}_1, \widetilde{\mathbf{A}}_\ell \right\rangle$ as a Gaussian distributed RV $\mathcal{N}\left(0, d^{-1} \| \sum_{\ell \neq 1} B_\ell \widetilde{\mathbf{A}}_\ell \|_2^2\right)$. Then we obtain

$$\begin{aligned}
&\mathbb{P}\left(\left| \sum_{\ell \neq 1} B_\ell \left\langle \widetilde{\mathbf{A}}_1, \widetilde{\mathbf{A}}_\ell \right\rangle \right| \gtrsim \sqrt{\frac{\log p}{d}} \sqrt{\sum_{\ell \neq 1} B_\ell^2} \right) \\
= \; & \underbrace{\mathbb{P}\left(\left| \sum_{\ell \neq 1} B_\ell \left\langle \widetilde{\mathbf{A}}_1, \widetilde{\mathbf{A}}_\ell \right\rangle \right| \gtrsim \sqrt{\frac{\log p}{d}} \sqrt{\sum_{\ell \neq 1} B_\ell^2} \right) \times \Psi(\mathcal{E}_4(\mathbf{B}))}_{T_1} \\
+ \; & \underbrace{\mathbb{P}\left(\left| \sum_{\ell \neq 1} B_\ell \left\langle \widetilde{\mathbf{A}}_1, \widetilde{\mathbf{A}}_\ell \right\rangle \right| \gtrsim \sqrt{\frac{\log p}{d}} \sqrt{\sum_{\ell \neq 1} B_\ell^2} \right) \times \Psi(\overline{\mathcal{E}}_3(\mathbf{B}))}_{T_2}.
\end{aligned}$$

The proof is then completed by separately bounding T_1 and T_2. For term T_1, we have

$$T_1 \overset{①}{\leq} \mathbb{E}_{\widetilde{\mathbf{A}}_\ell} \exp\left(-\frac{c \log p (\sum_{\ell \neq 1} B_\ell^2)}{\| \sum_{\ell \neq 1} B_\ell \widetilde{\mathbf{A}}_1 \|_2^2} \right) \times \Psi(\mathcal{E}_4(\mathbf{B})) \overset{②}{\leq} \exp\left(-\frac{3 \log p (\sum_{\ell \neq 1} B_\ell^2)}{\sum_{\ell \neq 1} B_\ell^2} \right),$$

where ① is due to the tail bound for the Gaussian RV $\sum_{\ell \neq 1} B_\ell \left\langle \widetilde{\mathbf{A}}_1, \widetilde{\mathbf{A}}_\ell \right\rangle$ conditional on $\widetilde{\mathbf{A}}_\ell$, and ② is according to the definition of $\mathcal{E}_4(\mathbf{B})$. For term T_2, we have $T_2 \leq \Psi(\overline{\mathcal{E}}_3(\mathbf{B})) \leq e^{-0.8d}$. Summaring the above analysis finishes the proof.

□

Lemma 23. *Conditional on events $\mathcal{E}_1, \mathcal{E}_2$, we have*

$$\left|\sum_{\ell\neq 1,2} B_\ell \left\langle \widetilde{\mathbf{A}}_1, \widetilde{\mathbf{A}}_\ell \right\rangle \left\langle \widetilde{\mathbf{A}}_2, \widetilde{\mathbf{A}}_\ell \right\rangle \right| \lesssim \frac{\left|\sum_{\ell>2} B_\ell\right|}{d}\sqrt{\frac{\log p}{d}} + \frac{\sqrt{\log p}}{d}\left[\sqrt{\sum_{\ell>2} B_\ell^2} \vee \left(\sqrt{\log p}(\max_\ell |B_\ell|)\right)\right],$$

hold with probability at least $1-2p^{-3}$ for an arbitrary fixed vector $\mathbf{B}\in\mathbb{R}^p$.

Proof. First we rewrite the term $\sum_{\ell\neq 1,2} B_\ell \left\langle \widetilde{\mathbf{A}}_1, \widetilde{\mathbf{A}}_\ell \right\rangle \left\langle \widetilde{\mathbf{A}}_2, \widetilde{\mathbf{A}}_\ell \right\rangle$ as

$$\sum_{\ell\neq 1,2} B_\ell \left\langle \widetilde{\mathbf{A}}_1, \widetilde{\mathbf{A}}_\ell \right\rangle \left\langle \widetilde{\mathbf{A}}_2, \widetilde{\mathbf{A}}_\ell \right\rangle = \sum_{\ell\neq 1,2} \widetilde{\mathbf{A}}_\ell^\top \left(B_\ell \widetilde{\mathbf{A}}_1 \widetilde{\mathbf{A}}_2^\top\right) \widetilde{\mathbf{A}}_\ell.$$

Then we concatenate the vectors $\widetilde{\mathbf{A}}_\ell$, $\ell\neq 1,2$ to a vector of length $d(p-2)$ and denote it as $\mathrm{vec}\left(\widetilde{\mathbf{A}}\right)$. Hence the summarization can be rewritten as

$$\sum_{\ell\neq 1,2} \widetilde{\mathbf{A}}_\ell^\top \left(B_\ell \widetilde{\mathbf{A}}_1 \widetilde{\mathbf{A}}_2^\top\right) \widetilde{\mathbf{A}}_\ell = \mathrm{vec}\left(\widetilde{\mathbf{A}}\right)^\top \mathbf{\Lambda} \mathrm{vec}\left(\widetilde{\mathbf{A}}\right),$$

where $\mathbf{\Lambda}$ is a block-diagonal matrix whose ith block is $B_{i+2}\widetilde{\mathbf{A}}_1\widetilde{\mathbf{A}}_2^\top$, $1\le i\le p-2$. Due to the independence between $\widetilde{\mathbf{A}}_\ell$, $1\le \ell\le p$, we first condition on $\widetilde{\mathbf{A}}_1, \widetilde{\mathbf{A}}_2$ and perform the following decomposition

$$\left|\sum_{\ell\neq 1,2} B_\ell \left\langle \widetilde{\mathbf{A}}_1, \widetilde{\mathbf{A}}_\ell \right\rangle \left\langle \widetilde{\mathbf{A}}_2, \widetilde{\mathbf{A}}_\ell \right\rangle \right| \le \underbrace{d^{-1}\left|\widetilde{\mathbf{A}}_1^\top \widetilde{\mathbf{A}}_2\right| \left|\sum_{\ell\neq 1,2} B_\ell\right|}_{\vartheta_1} + \underbrace{d^{-1}\left|d\mathrm{vec}\left(\widetilde{\mathbf{A}}\right)^\top \mathbf{\Lambda} \mathrm{vec}\left(\widetilde{\mathbf{A}}\right) - \sum_{\ell\neq 1,2} B_\ell \widetilde{\mathbf{A}}_1^\top \widetilde{\mathbf{A}}_2\right|}_{\vartheta_2}.$$

The upper-bound for ϑ_1 is relatively easy, which reads as

$$\vartheta_1 \lesssim \left|\sum_{\ell>2} B_\ell\right| \times \sqrt{\frac{\log p}{d}}.$$

The following analysis focus on bound ϑ_2. Since ϑ_2 also reads as

$$\vartheta_2 = \left| d\text{vec}\left(\widetilde{\mathbf{A}}\right)^\top \mathbf{\Lambda} \text{vec}\left(\widetilde{\mathbf{A}}\right) - \mathbb{E}_{\widetilde{\mathbf{A}}_\ell, \ell>2}\left(d\text{vec}\left(\widetilde{\mathbf{A}}\right)^\top \mathbf{\Lambda} \text{vec}\left(\widetilde{\mathbf{A}}\right)\right)\right|,$$

we can invoke the Hanson-Wright inequality (Thm. 6.2.1 in [139]) and obtain

$$\mathbb{P}\left(\vartheta_2 \geq \delta\right) \leq 2\exp\left(-c\left(\frac{\delta^2}{\|\mathbf{\Lambda}\|_{\text{F}}^2} \wedge \frac{\delta}{\|\mathbf{\Lambda}\|_{\text{OP}}}\right)\right),$$

where $\widetilde{\mathbf{A}}_1, \widetilde{\mathbf{A}}_2$ are viewed as constants. We complete the proof by setting δ as

$$\delta \asymp \left(\sqrt{\log p}\|\mathbf{\Lambda}\|_{\text{F}}\right) \vee \left(\log p \|\mathbf{\Lambda}\|_{\text{OP}}\right),$$

which yields $\mathbb{P}(\vartheta_2 \geq \delta) \leq 2p^{-3}$. The specific values of $\|\mathbf{\Lambda}\|_{\text{F}}$ and $\|\mathbf{\Lambda}\|_{\text{OP}}$ are computed as

$$\begin{aligned}
\|\mathbf{\Lambda}\|_{\text{F}}^2 = \left(\sum_{\ell>2} B_\ell^2\right)\left\|\widetilde{\mathbf{A}}_1\widetilde{\mathbf{A}}_2^\top\right\|_{\text{F}}^2 &\overset{①}{=} \left(\sum_{\ell>2} B_\ell^2\right)\text{Tr}\left(\widetilde{\mathbf{A}}_2\widetilde{\mathbf{A}}_1^\top\widetilde{\mathbf{A}}_1\widetilde{\mathbf{A}}_2^\top\right) \\
&\overset{②}{=} \left\|\widetilde{\mathbf{A}}_1\right\|_2^2\left\|\widetilde{\mathbf{A}}_2\right\|_2^2\left(\sum_{\ell>2} B_\ell^2\right) \overset{③}{\lesssim} \sum_{\ell>2} B_\ell^2 \\
\|\mathbf{\Lambda}\|_{\text{OP}} = \max_\ell |B_\ell|\left\|\widetilde{\mathbf{A}}_1\widetilde{\mathbf{A}}_2^\top\right\|_{\text{OP}} &\overset{④}{=} \max_\ell |B_\ell| \times \left\|\widetilde{\mathbf{A}}_1\right\|_2\left\|\widetilde{\mathbf{A}}_2\right\|_2 \lesssim \max_\ell |B_\ell|,
\end{aligned}$$

where in ① we use $\|\mathbf{M}\|_{\text{F}}^2 = \text{Tr}(\mathbf{M}^\top\mathbf{M})$ for arbitrary matrix $\mathbf{M}$, in ② we use $\text{Tr}(\mathbf{M}_1\mathbf{M}_2) = \text{Tr}(\mathbf{M}_2\mathbf{M}_1)$, in ③ we condition on event $\mathcal{E}_1$, and in ④ we use $\left\|\mathbf{u}\mathbf{v}^\top\right\|_{\text{OP}} = \|\mathbf{u}\|_2\|\mathbf{v}\|_2$ for arbitrary vectors $\mathbf{u}, \mathbf{v}$.

□

Lemma 24. *We have*

$$\left| \sum_{\substack{\ell_1,\ell_2\neq 1,2\\ \ell_1\neq\ell_2}} B_{\ell_1,\ell_2} \left\langle \widetilde{\mathbf{A}}_1, \widetilde{\mathbf{A}}_{\ell_1} \right\rangle \left\langle \widetilde{\mathbf{A}}_2, \widetilde{\mathbf{A}}_{\ell_2} \right\rangle \right| \lesssim \frac{\log p}{d} \left(1 + c_0\sqrt{\frac{p}{d}}\right)^2 \sqrt{\sum_{\substack{i\neq 1,2\\ j\neq 1,2,i}} B_{ij}^2},$$

holds with probability exceeding $1 - 4p^{-3} - e^{-c_0 p}$ *for a fixed matrix* $\mathbf{B}$.

Proof. We begin the proof by first rewriting $\sum_{\substack{\ell_1,\ell_2\neq 1,2\\ \ell_1\neq\ell_2}} B_{\ell_1,\ell_2} \left\langle \widetilde{\mathbf{A}}_1, \widetilde{\mathbf{A}}_{\ell_1} \right\rangle \left\langle \widetilde{\mathbf{A}}_2, \widetilde{\mathbf{A}}_{\ell_2} \right\rangle$ as $\widetilde{\mathbf{A}}_1^\top \mathbf{\Lambda} \widetilde{\mathbf{A}}_2$, where $\mathbf{\Lambda}$ is defined as

$$\mathbf{\Lambda} \triangleq \sum_{\ell_1\neq 1,2} \sum_{\ell_2\neq 1,2,\ell_1} B_{\ell_1,\ell_2} \widetilde{\mathbf{A}}_{\ell_1} \widetilde{\mathbf{A}}_{\ell_2}^\top.$$

The whole proof procedure can be divided into the following stages.

Stage I. Due to the independence across $\widetilde{\mathbf{A}}_\ell$, we have

$$\begin{aligned} \mathbb{P}\left(\left|\widetilde{\mathbf{A}}_1^\top \mathbf{\Lambda} \widetilde{\mathbf{A}}_2\right| \geq \delta\right) \leq\ & \mathbb{P}\left(\left|\widetilde{\mathbf{A}}_1^\top \mathbf{\Lambda} \widetilde{\mathbf{A}}_2\right| \geq \delta,\ \left\|\mathbf{\Lambda}\widetilde{\mathbf{A}}_2\right\|_2 \leq \delta_1\right) + \mathbb{P}\left(\left\|\mathbf{\Lambda}\widetilde{\mathbf{A}}_2\right\|_2 \geq \delta_1\right) \\ \overset{①}{\leq}\ & 2\exp\left(-\frac{d\delta^2}{2\delta_1^2}\right) + \mathbb{P}\left(\left\|\mathbf{\Lambda}\widetilde{\mathbf{A}}_2\right\|_2 \geq \delta_1\right), \end{aligned} \tag{A.1.9}$$

where in ① we first condition on $\widetilde{\mathbf{A}}_\ell$, $(\ell > 2)$ and view $\widetilde{\mathbf{A}}_1^\top \mathbf{\Lambda} \widetilde{\mathbf{A}}_2$ as a Gaussian RV satisfying $\mathcal{N}\left(0, d^{-1}\|\mathbf{\Lambda}\widetilde{\mathbf{A}}_2\|_2^2\right)$.

Stage II. To bound the probability $\mathbb{P}\left(\left\|\mathbf{\Lambda}\widetilde{\mathbf{A}}_2\right\|_2 \geq \delta_1\right)$, we need to upper bound the Frobenius norm $\|\!|\mathbf{\Lambda}|\!\|_{\mathrm{F}}$. First we define two matrices, namely, $\widetilde{\widetilde{\mathbf{A}}}$ and $\widetilde{\mathbf{B}}$, for the conciseness of notation, which reads

$$\widetilde{\widetilde{\mathbf{A}}} \triangleq \left[\widetilde{\mathbf{A}}_3\ \cdots\ \widetilde{\mathbf{A}}_p\right], \quad (\widetilde{\mathbf{B}})_{i,j} \triangleq \begin{cases} B_{i+2,j+2}, & \text{if } i \neq j; \\ 0, & \text{otherwise.} \end{cases}$$

Easily we can verify $\mathbf{\Lambda}$ is equivalent to $\mathbf{\Lambda}$ as $\widetilde{\widetilde{\mathbf{A}}}\widetilde{\mathbf{B}}\widetilde{\widetilde{\mathbf{A}}}^\top$, which gives

$$\|\mathbf{\Lambda}\|_{\mathrm{F}} = \left\|\widetilde{\widetilde{\mathbf{A}}}\widetilde{\mathbf{B}}\widetilde{\mathbf{A}}^\top\right\|_{\mathrm{F}} \overset{②}{\leq} \left\|\widetilde{\widetilde{\mathbf{A}}}\right\|_{\mathrm{OP}}^2 \left\|\widetilde{\mathbf{B}}\right\|_{\mathrm{F}} \overset{③}{\leq} \left\|\widetilde{\mathbf{A}}\right\|_{\mathrm{OP}}^2 \left\|\widetilde{\mathbf{B}}\right\|_{\mathrm{F}},$$

where in ② we adopt the relation $\|\mathbf{M}_1\mathbf{M}_2\|_{\mathrm{F}} \leq \|\mathbf{M}_1\|_{\mathrm{OP}}\|\mathbf{M}_2\|_{\mathrm{F}}$ such that $\mathbf{M}_1, \mathbf{M}_2$ are arbitrary matrix, and in ③ we use the relation $\left\|\widetilde{\widetilde{\mathbf{A}}}\right\|_{\mathrm{OP}} \leq \left\|\widetilde{\mathbf{A}}\right\|_{\mathrm{OP}}$ in Corol. 2.4.2 [126] since $\widetilde{\widetilde{\mathbf{A}}}$ can be viewed as a sub-matrix of $\widetilde{\mathbf{A}}$.

Hence we conclude that

$$\begin{aligned}
&\mathbb{P}\left(\|\mathbf{\Lambda}\|_{\mathrm{F}} \geq \left(1 + c_0\sqrt{\frac{p}{d}}\right)^2 \left\|\widetilde{\mathbf{B}}\right\|_{\mathrm{F}}\right) \\
=\ &\mathbb{P}\left(\|\mathbf{\Lambda}\|_{\mathrm{F}} \gtrsim \frac{p}{d}\left\|\widetilde{\mathbf{B}}\right\|_{\mathrm{F}},\ \left\|\widetilde{\mathbf{A}}\right\|_{\mathrm{OP}} \leq \sqrt{\frac{c_0 p}{d}}\right) + \mathbb{P}\left(\|\mathbf{\Lambda}\|_{\mathrm{F}} \gtrsim \frac{p}{d}\left\|\widetilde{\mathbf{B}}\right\|_{\mathrm{F}},\ \left\|\widetilde{\mathbf{A}}\right\|_{\mathrm{OP}} > \sqrt{\frac{c_0 p}{d}}\right) \\
\leq\ &\underbrace{\mathbb{P}\left(\left\|\widetilde{\mathbf{A}}\right\|_{\mathrm{OP}}^2 \gtrsim \frac{p}{d}, \left\|\widetilde{\mathbf{A}}\right\|_{\mathrm{OP}} \leq \sqrt{\frac{c_0 p}{d}}\right)}_{0} + \mathbb{P}\left(\left\|\widetilde{\mathbf{A}}\right\|_{\mathrm{OP}} \geq \sqrt{\frac{c_0 p}{d}}\right) \overset{④}{\leq} e^{-c_0 p},
\end{aligned}$$

where ④ is due to Thm. 6.1 in [10].

Stage III. We bound $\mathbb{P}\left(\left\|\mathbf{\Lambda}\widetilde{\mathbf{A}}_2\right\|_2 \geq \delta_1\right)$ by splitting it as

$$\begin{aligned}
\mathbb{P}\left(\left\|\mathbf{\Lambda}\widetilde{\mathbf{A}}_2\right\|_2 \geq \delta_1\right) = \ &\underbrace{\mathbb{P}\left(\left\|\mathbf{\Lambda}\widetilde{\mathbf{A}}_2\right\|_2 \geq \delta_1,\ \|\mathbf{\Lambda}\|_{\mathrm{F}} \geq \left(1 + c_0\sqrt{\frac{p}{d}}\right)^2 \left\|\widetilde{\mathbf{B}}\right\|_{\mathrm{F}}\right)}_{\leq\ \mathbb{P}\left(|\mathbf{\Lambda}|_{\mathrm{F}} \geq \left(1+c_0\sqrt{\frac{p}{d}}\right)^2 \|\widetilde{\mathbf{B}}\|_{\mathrm{F}}\right)} \\
&+ \mathbb{P}\left(\left\|\mathbf{\Lambda}\widetilde{\mathbf{A}}_2\right\|_2 \geq \delta_1,\ \|\mathbf{\Lambda}\|_{\mathrm{F}} < \left(1 + c_0\sqrt{\frac{p}{d}}\right)^2 \left\|\widetilde{\mathbf{B}}\right\|_{\mathrm{F}}\right). \quad \text{(A.1.10)}
\end{aligned}$$

Notice that the first term is bounded in Stage II, we focus on bounding the second term in

this stage, which proceeds as

$$
\begin{aligned}
& \mathbb{P}\left(\left\|\boldsymbol{\Lambda}\widetilde{\mathbf{A}}_2\right\|_2 \geq \delta_1,\ \|\boldsymbol{\Lambda}\|_{\mathrm{F}} < \left(1+c_0\sqrt{\frac{p}{d}}\right)^2 \left\|\widetilde{\mathbf{B}}\right\|_{\mathrm{F}}\right) \\
\overset{⑤}{\leq}\ & \mathbb{E}\mathbb{1}\left(\left|d\left\|\boldsymbol{\Lambda}\widetilde{\mathbf{A}}_2\right\|_2^2 - \|\boldsymbol{\Lambda}\|_{\mathrm{F}}^2\right| \geq \delta_2,\ \|\boldsymbol{\Lambda}\|_{\mathrm{F}} < \left(1+c_0\sqrt{\frac{p}{d}}\right)^2 \left\|\widetilde{\mathbf{B}}\right\|_{\mathrm{F}}\right) \\
\overset{⑥}{\leq}\ & 2\exp\left(-c_0\left(\frac{\delta_2}{\left\|\boldsymbol{\Lambda}^\top\boldsymbol{\Lambda}\right\|_{\mathrm{OP}}} \wedge \frac{\delta_2^2}{\left\|\boldsymbol{\Lambda}^\top\boldsymbol{\Lambda}\right\|_{\mathrm{F}}^2}\right)\right) \times \mathbb{1}\left(\|\boldsymbol{\Lambda}\|_{\mathrm{F}} < \left(1+c_0\sqrt{\frac{p}{d}}\right)^2 \left\|\widetilde{\mathbf{B}}\right\|_{\mathrm{F}}\right) \\
\leq\ & 2\exp\left(-c_0\left(\frac{\delta_2}{\left\|\boldsymbol{\Lambda}^\top\boldsymbol{\Lambda}\right\|_{\mathrm{F}}} \wedge \frac{\delta_2^2}{\left\|\boldsymbol{\Lambda}^\top\boldsymbol{\Lambda}\right\|_{\mathrm{F}}^2}\right)\right) \times \mathbb{1}\left(\|\boldsymbol{\Lambda}\|_{\mathrm{F}} < \left(1+c_0\sqrt{\frac{p}{d}}\right)^2 \left\|\widetilde{\mathbf{B}}\right\|_{\mathrm{F}}\right) \\
\overset{⑦}{\leq}\ & 2p^{-3}, \qquad \text{(A.1.11)}
\end{aligned}
$$

where in ⑤ we require $d\delta_1^2 \geq \|\boldsymbol{\Lambda}\|_{\mathrm{F}}^2 + \delta_2$, ⑥ is due to the Hanson-Wright inequality (cf. Thm. 6.2.1 in [139]), and in ⑦ we set δ_2 as $(1+c_0\sqrt{p/d})^4 \log p \left\|\widetilde{\mathbf{B}}\right\|_{\mathrm{F}}^2$.

Combining (Equation A.1.9), (Equation A.1.10), and (Equation A.1.11), we set δ_1, δ as $c\sqrt{\log p/d}(1+c_0\sqrt{p/d})^2\left\|\widetilde{\mathbf{B}}\right\|_{\mathrm{F}}$ and $c_3\delta \asymp \sqrt{\log p/d}\delta_1$, respectively, which yields

$$
\mathbb{P}\left(\left|\widetilde{\mathbf{A}}_1^\top\boldsymbol{\Lambda}\widetilde{\mathbf{A}}_2\right| \gtrsim \frac{\log p}{d}\left(1+c_0\sqrt{\frac{p}{d}}\right)^2\left\|\widetilde{\mathbf{B}}\right\|_{\mathrm{F}}\right) \leq 4p^{-3} + e^{-c_0 p},
$$

and completes the proof. □

Lemma 25. *Conditional on the event $\mathcal{E}_1$, we have*

$$
\begin{aligned}
& \mathbb{P}\left[n^{-1}\left|\widetilde{\mathbf{A}}_i^\top\left(\sum_{\ell=1}^n \mathbf{W}^{(i)}\mathbf{W}^{(i)\top}\right)\widetilde{\mathbf{A}}_j\right| \geq c_0\sigma^2\left(1+c_1\sqrt{\frac{\log p}{d}}\right)\sqrt{\frac{\log p}{d}}\left(1+c_2\left(\sqrt{\frac{d}{n}}\vee\frac{d}{n}\right)\right)\right] \\
\leq\ & p^{-4} + c_3 e^{-c_4 d}
\end{aligned}
$$

with fixed i, j.

Proof. First we define the matrix $\widehat{\boldsymbol{\Xi}}_n$ as $\frac{1}{n}\sum_{\ell=1}^n \mathbf{W}^{(i)}\mathbf{W}^{(i)\top}$ for the conciseness of notation.

Then we upper-bound $\widetilde{\mathbf{A}}_i\widehat{\mathbf{\Xi}}_n\widetilde{\mathbf{A}}_j$, $i \neq j$ as

$$\begin{aligned}
&\mathbb{P}\left(\left|\widetilde{\mathbf{A}}_i^\top\widehat{\mathbf{\Xi}}_n\widetilde{\mathbf{A}}_j\right| \geq \delta\right) \overset{①}{\leq} \mathbb{P}\left(\|\widehat{\mathbf{\Xi}}_n\widetilde{\mathbf{A}}_j\|_2 \geq \delta_1\right) + \exp\left(-\frac{d\delta^2}{2\delta_1^2}\right) \\
\overset{②}{\leq}\ &\mathbb{P}\left(\left\|\widehat{\mathbf{\Xi}}_n\right\|_{\text{OP}}\left\|\widetilde{\mathbf{A}}_j\right\|_2 \geq \delta_1\right) + p^{-4} \overset{③}{\leq} \mathbb{P}\left(\left\|\widehat{\mathbf{\Xi}}_n\right\|_{\text{OP}} \geq \delta_2\right) + p^{-4} \\
\overset{④}{\leq}\ &\mathbb{P}\left(\left\|\widehat{\mathbf{\Xi}}_n - \sigma^2\mathbf{I}\right\|_{\text{OP}} \geq c_2\sigma^2\left(\frac{d}{n} \vee \sqrt{\frac{d}{n}}\right)\right) + p^{-4} \overset{⑤}{\leq} p^{-4} + c_0e^{-c_1d},
\end{aligned}$$

where in ① we exploit the independence between $\widetilde{\mathbf{A}}_i$ and $\widetilde{\mathbf{A}}_j$ when $i \neq j$ and treat $\widetilde{\mathbf{A}}_i^\top\widehat{\mathbf{\Xi}}_n\widetilde{\mathbf{A}}_j$ as a Gaussian RV with mean zero and variance $d^{-1}\|\widehat{\mathbf{\Xi}}_n\widetilde{\mathbf{A}}_j\|_2^2$, in ② we use the fact $\delta = 2\delta_1\sqrt{2\log p/d}$, and in ③ we condition on event $\mathcal{E}_1$ and set $\delta_1 \geq \delta_2\left(1 + c_0\sqrt{\log p/d}\right)$, ④ is because $\delta_2 = \sigma^2\left(1 + c_2\left(d/n \vee \sqrt{d/n}\right)\right)$, and in ⑤ we use Thm. 6.5 in [10]. The proof is then completed by setting δ as

$$\delta = c_0\sigma^2\left(1 + c_1\sqrt{\frac{\log p}{d}}\right)\sqrt{\frac{\log p}{d}}\left(1 + c_2\left(\sqrt{\frac{d}{n}} \vee \frac{d}{n}\right)\right).$$

□

A.2 Insight Behind the Design of the Covariance Matrix Estimator

We now explain the rational behind the covariance matrix estimators of $\mathbf{X}$ that we use in the graphical structure estimation via the parametric method. For this purpose, we exploit the statistical properties of $\widetilde{\mathbf{A}}$.

We approximate data samples, $\widehat{\mathbf{X}}^{(i)}$'s, as $\widehat{\mathbf{X}}^{(i)} = \widetilde{\mathbf{A}}^\top\widetilde{\mathbf{A}}\mathbf{X}^{(i)} = \widetilde{\mathbf{A}}^\top\mathbf{Y}^{(i)}$, $1 \leq i \leq n$. Due to the assumption on sensing matrix $\widetilde{\mathbf{A}}$, we have $\mathbb{E}_{\widetilde{\mathbf{A}}}\widehat{\mathbf{X}}^{(i)} = \mathbf{X}^{(i)}$. Hence, we can view the samples $\{\widehat{\mathbf{X}}^{(i)}\}_{i=1}^n$ as a "perturbed" version of the true data points $\left\{\mathbf{X}^{(i)}\right\}_{i=1}^n$. Hence, we propose to estimate the covariance matrix of $\mathbf{X}$ from $\{\widehat{\mathbf{X}}^{(i)}\}_{i=1}^n$. Following the above approach, a naive covariance estimator is given as

$$\widehat{\mathbf{\Sigma}}_{n,1} = \frac{1}{n}\sum_{i=1}^n \widehat{\mathbf{X}}^{(i)}\widehat{\mathbf{X}}^{(i)\top} = \widetilde{\mathbf{A}}^\top\left(\frac{1}{n}\sum_{i=1}^n \mathbf{Y}^{(i)}\mathbf{Y}^{(i)\top}\right)\widetilde{\mathbf{A}}.$$

However, through numerical experiments, we observed that this estimator performs poorly. To improve the performance of $\widehat{\mathbf{\Sigma}}_{n,1}$, we first analyze its properties thoroughly and then refine the estimator.

A.2.1 Theoretical Properties

First, we evaluate the mean and variance of the naive covariance estimator $\widehat{\mathbf{\Sigma}}_{n,1}$.

Lemma 26. *The mean of the naive covariance estimator is given by*

$$\mathbb{E}_{\widetilde{\mathbf{A}},\mathbf{X}}[\widehat{\mathbf{\Sigma}}_{n,1}] = \frac{d+1}{d}\mathbf{\Sigma}^{\natural} + \frac{p}{d}\mathbf{I} + \sigma^2\mathbf{I}.$$

Proof. Due to the independence between $\mathbf{X}$ and $\widetilde{\mathbf{A}}$, we first condition on $\widetilde{\mathbf{A}}$ and take expectation w.r.t $\mathbf{X}, \mathbf{W}$, which gives

$$\mathbb{E}_{\mathbf{X},\mathbf{W}}\widehat{\mathbf{\Sigma}}_{n,1} = \ \widetilde{\mathbf{A}}^\top\widetilde{\mathbf{A}}\mathbf{\Sigma}^{\natural}\widetilde{\mathbf{A}}^\top\widetilde{\mathbf{A}} + \sigma^2\widetilde{\mathbf{A}}^\top\widetilde{\mathbf{A}}.$$

Then we conclude that

$$\begin{aligned}
&\mathbb{E}_{\widetilde{\mathbf{A}}}\left(\widetilde{\mathbf{A}}^\top\widetilde{\mathbf{A}}\mathbf{\Sigma}^{\natural}\widetilde{\mathbf{A}}^\top\widetilde{\mathbf{A}}\right)_{ij} = \mathbb{E}_{\widetilde{\mathbf{A}}}\sum_{\ell_1,\ell_2}\mathbf{\Sigma}^{\natural}_{\ell_1,\ell_2}\ \left\langle\widetilde{\mathbf{A}}_{\ell_1},\widetilde{\mathbf{A}}_i\right\rangle\left\langle\widetilde{\mathbf{A}}_{\ell_2},\widetilde{\mathbf{A}}_j\right\rangle + \sigma^2\mathbb{1}(i=j)\\
=\ &\mathbb{E}_{\widetilde{\mathbf{A}}}\sum_{\ell_1,\ell_2}\mathbf{\Sigma}^{\natural}_{\ell_1,\ell_2}\ \left(\sum_{\ell_3}\widetilde{\mathbf{A}}_{\ell_3,\ell_1}\widetilde{\mathbf{A}}_{\ell_3,i}\right)\cdot\ \left(\sum_{\ell_4}\widetilde{\mathbf{A}}_{\ell_4,\ell_2}\widetilde{\mathbf{A}}_{\ell_4,j}\right) + \sigma^2\mathbb{1}(i=j)\\
=\ &\sum_{\ell_1,\ell_2,\ell_3,\ell_4}\mathbf{\Sigma}^{\natural}_{\ell_1,\ell_2}\,\mathbb{E}_{\widetilde{\mathbf{A}}}\left(\widetilde{\mathbf{A}}_{\ell_3,\ell_1}\widetilde{\mathbf{A}}_{\ell_3,i}\widetilde{\mathbf{A}}_{\ell_4,\ell_2}\widetilde{\mathbf{A}}_{\ell_4,j}\right) + \sigma^2\mathbf{I}\\
\overset{①}{=}\ &d^{-2}\Bigg[\sum_{\ell_1,\ell_2,\ell_3,\ell_4}\mathbf{\Sigma}^{\natural}_{\ell_1,\ell_2}\Big(\mathbb{1}\left(\ell_1=i\right)\mathbb{1}(\ell_2=j) + \ \mathbb{1}\left(\ell_3=\ell_4\right)\mathbb{1}(\ell_1=\ell_2)\mathbb{1}(i=j)\\
&\qquad\qquad + \mathbb{1}(\ell_3=\ell_4)\mathbb{1}(\ell_1=j)\ \mathbb{1}(\ell_2=i)\Big)\Bigg] + \sigma^2\mathbb{1}(i=j)\\
=\ &d^{-2}\left[\sum_{\ell_3,\ell_4}\mathbf{\Sigma}^{\natural}_{i,j} + \mathbb{1}(i=j)\left(\sum_{\ell_1}\sum_{\ell_2}\mathbf{\Sigma}^{\natural}_{\ell_1,\ell_1}\right) + \ \mathbf{\Sigma}^{\natural}_{j,i}\sum_{\ell_3,\ell_4}\mathbb{1}(\ell_3=\ell_4)\right] + \sigma^2\mathbb{1}(i=j)\\
=\ &d^{-2}\left[d^2\mathbf{\Sigma}^{\natural}_{i,j} + \mathbb{1}(i=j)d\sum_{\ell}\mathbf{\Sigma}^{\natural}_{\ell,\ell} + d\mathbf{\Sigma}^{\natural}_{i,j}\right] + \sigma^2\mathbb{1}(i=j)\\
=\ &\left(1+d^{-1}\right)\mathbf{\Sigma}^{\natural}_{i,j} + d^{-1}\left(\sum_{\ell}\mathbf{\Sigma}^{\natural}_{\ell,\ell}\right)\mathbb{1}(i=j) + \sigma^2\mathbb{1}(i=j),
\end{aligned}$$

which completes the proof with the fact $\mathbf{\Sigma}^{\natural}_{\ell,\ell} = 1$. In ①, we use the Wick's theorem, which is listed as Theorem 18 for the sake of self-containing. □

Then we study the variance $\mathrm{Var}_{\widetilde{\mathbf{A}}}\widehat{\mathbf{\Sigma}}_{n,1}$, which is listed as the following. Due to the complex formula of the variance, we only consider the noiseless case, namely, $\sigma^2 = 0$.

Lemma 27. *Consider the noiseless case where $\sigma^2 = 0$, we have* $\mathrm{Var}_{\widetilde{\mathbf{A}}}(\widehat{\mathbf{\Sigma}}_{n,1})_{i,j} = \Omega(d^{-1}) + \Omega(d^{-1})\mathbb{1}(i=j) + \Omega(d^{-2})$.

The detailed proof is given in the appendix. We use results of Lemma 26 to improve our naive covariance estimator in two perspectives: **bias correction** and **variance reduction**.

Proof. With the relation $\mathrm{Var}_{\widetilde{\mathbf{A}}}\widehat{\mathbf{\Sigma}}_{n,1} = \mathbb{E}_{\widetilde{\mathbf{A}}}(\widehat{\mathbf{\Sigma}}_{n,1})^2_{i,j} - \left(\mathbb{E}\widehat{\mathbf{\Sigma}}_{n,1}\right)^2_{i,j}$, we complete the proof by invoking Lemma 26 and Lemma 28. The following context focuses on proving Lemma 28. □

Lemma 28. *We have*

$$
\begin{aligned}
&\mathbb{E}_{\widetilde{\mathbf{A}}}(\widehat{\mathbf{\Sigma}}_{n,1})^2_{i,j} = (\mathbf{\Sigma}^{\text{param}}_n)^2_{i,j} + d^{-1}\left[\|(\mathbf{\Sigma}^{\text{param}}_n)_i\|_2^2 + \|(\mathbf{\Sigma}^{\text{param}}_n)_j\|_2^2 + 4(\mathbf{\Sigma}^{\text{param}}_n)^2_{i,j} + 2(\mathbf{\Sigma}^{\text{param}}_n)_{i,i}(\mathbf{\Sigma}^{\text{param}}_n)_{j,j}\right] \\
&+ d^{-2}\Bigg[2\left((\mathbf{\Sigma}^{\text{param}}_n)_{i,i} + (\mathbf{\Sigma}^{\text{param}}_n)_{j,j}\right)\mathrm{Tr}(\mathbf{\Sigma}^{\text{param}}_n) + 4(\mathbf{\Sigma}^{\text{param}}_n)_{i,i}(\mathbf{\Sigma}^{\text{param}}_n)_{j,j} + 2\|(\mathbf{\Sigma}^{\text{param}}_n)_j\|_2^2 \\
&+ 2\|(\mathbf{\Sigma}^{\text{param}}_n)_i\|_2^2 + \|\mathbf{\Sigma}^{\text{param}}_n\|_{\text{F}}^2 + 7(\mathbf{\Sigma}^{\text{param}}_n)^2_{i,j}\Bigg] \\
&+ d^{-3}\Bigg[3\|(\mathbf{\Sigma}^{\text{param}}_n)_i\|_2^2 + 3\|(\mathbf{\Sigma}^{\text{param}}_n)_j\|_2^2 + 2\left((\mathbf{\Sigma}^{\text{param}}_n)_{i,i} + (\mathbf{\Sigma}^{\text{param}}_n)_{j,j}\right)\mathrm{Tr}(\mathbf{\Sigma}^{\text{param}}_n) \\
&+ \ \mathrm{Tr}^2(\mathbf{\Sigma}^{\text{param}}_n) + 2(\mathbf{\Sigma}^{\text{param}}_n)_{i,i}(\mathbf{\Sigma}^{\text{param}}_n)_{j,j} + 4(\mathbf{\Sigma}^{\text{param}}_n)^2_{i,j}\Bigg] \\
&+ d^{-1}\mathbb{1}(i=j)\left[\langle(\mathbf{\Sigma}^{\text{param}}_n)_i, (\mathbf{\Sigma}^{\text{param}}_n)_j\rangle + 2(\mathbf{\Sigma}^{\text{param}}_n)_{i,j}\,\mathrm{Tr}(\mathbf{\Sigma}^{\text{param}}_n)\right] \\
&+ d^{-2}\mathbb{1}(i=j)\left[11\,\langle(\mathbf{\Sigma}^{\text{param}}_n)_i, (\mathbf{\Sigma}^{\text{param}}_n)_j\rangle + \mathrm{Tr}^2(\mathbf{\Sigma}^{\text{param}}_n) + 6(\mathbf{\Sigma}^{\text{param}}_n)_{i,j}\,\mathrm{Tr}(\mathbf{\Sigma}^{\text{param}}_n)\right] \\
&+ d^{-3}\mathbb{1}(i=j)\left[12\,\langle(\mathbf{\Sigma}^{\text{param}}_n)_i, (\mathbf{\Sigma}^{\text{param}}_n)_j\rangle + 8(\mathbf{\Sigma}^{\text{param}}_n)_{i,j}\,\mathrm{Tr}(\mathbf{\Sigma}^{\text{param}}_n) + \mathrm{Tr}^2(\mathbf{\Sigma}^{\text{param}}_n) + 2\|\mathbf{\Sigma}^{\text{param}}_n\|_{\text{F}}^2\right].
\end{aligned}
$$

Proof. The proof procedure is fundamentally the same as the steps in computing $\mathbb{E}_{\mathbf{X}}\widehat{\mathbf{\Sigma}}^{\text{param}}_n$ but is more involved (requires computing over 100 terms).

We begin the proof with the following expansion

$$\mathbb{E}\left[\left(\widetilde{\mathbf{A}}^\top\widetilde{\mathbf{A}}(\boldsymbol{\Sigma}_n^{\text{param}})\widetilde{\mathbf{A}}^\top\widetilde{\mathbf{A}}\right)_{ij}\right]^2$$

$$= \sum_{\ell_1,\ell_2,\ell_3,\ell_4,\ell_5,\ell_6,\ell_7,\ell_8} (\boldsymbol{\Sigma}_n^{\text{param}})_{\ell_1,\ell_2}(\boldsymbol{\Sigma}_n^{\text{param}})_{\ell_5,\ell_6}\,\mathbb{E}\left(\widetilde{\mathbf{A}}_{\ell_3,\ell_1}\widetilde{\mathbf{A}}_{\ell_3,i}\,\widetilde{\mathbf{A}}_{\ell_4,\ell_2}\widetilde{\mathbf{A}}_{\ell_4,j}\,\widetilde{\mathbf{A}}_{\ell_7,\ell_5}\widetilde{\mathbf{A}}_{\ell_7,i}\,\widetilde{\mathbf{A}}_{\ell_8,\ell_6}\widetilde{\mathbf{A}}_{\ell_8,j}\right).$$

Then we expand the term $\mathbb{E}\left(\widetilde{\mathbf{A}}_{\ell_3,\ell_1}\widetilde{\mathbf{A}}_{\ell_3,i}\,\widetilde{\mathbf{A}}_{\ell_4,\ell_2}\widetilde{\mathbf{A}}_{\ell_4,j}\,\widetilde{\mathbf{A}}_{\ell_7,\ell_5}\widetilde{\mathbf{A}}_{\ell_7,i}\,\widetilde{\mathbf{A}}_{\ell_8,\ell_6}\widetilde{\mathbf{A}}_{\ell_8,j}\right)$ via the Wick's theorem, which is also listed as Theorem 18 for the sake of self-containing. Additionally, we need to divide d^4 for the following result.

□

A.2.2 Estimator Refinement

Bias Correction. First we note that the naive estimator is biased $\mathbb{E}_{\widetilde{\mathbf{A}},\mathbf{X}}\widehat{\boldsymbol{\Sigma}}_{n,1} \neq \boldsymbol{\Sigma}^\natural$. Adopting ideas similar to the moment estimator, we correct the bias of the estimator via

$$\widehat{\boldsymbol{\Sigma}}_{n,2} \triangleq \frac{d}{d+1}\widetilde{\mathbf{A}}^\top\left(\frac{1}{n}\sum_{i=1}^n \mathbf{Y}^{(i)}\mathbf{Y}^{(i)\top}\right)\widetilde{\mathbf{A}} - \frac{p+d\sigma^2}{d+1}\mathbf{I}.$$

It can be easily verified that $\mathbb{E}_{\widetilde{\mathbf{A}},\mathbf{X}}[\widehat{\boldsymbol{\Sigma}}_{n,2}] = \boldsymbol{\Sigma}^\natural$.

Variance Reduction. To further improve the performance of the covariance estimator, we perform variance reduction. From Lemma 27, we observe that the diagonal entries $(\widehat{\boldsymbol{\Sigma}}_{n,2})_{i,i}$ have a higher variance than non-diagonal entries. On the other hand, there is no need for estimating $\text{diag}(\boldsymbol{\Sigma}^\natural)$ since by the assumptions, we know that the diagonal elements of the covariance matrix are 1. Therefore, we suggest refining the estimator $\widehat{\boldsymbol{\Sigma}}_{n,2}$ by fixing its diagonal entries to 1, i.e., the resulting refined covariance estimator is given as

$$\widehat{\boldsymbol{\Sigma}}_n^{\text{param}} = \mathbf{I} + \frac{d}{d+1}\left[\widetilde{\mathbf{A}}^\top\left(\frac{1}{n}\sum_{i=1}^n \mathbf{Y}^{(i)}\mathbf{Y}^{(i)\top}\right)\widetilde{\mathbf{A}}\right]_{\text{off}}, \tag{A.2.1}$$

where $(\cdot)_{\text{off}}$ denotes the operation of picking non-diagonal entries. It can be easily verified that the estimator $\widehat{\mathbf{\Sigma}}_n^{\text{param}}$ in (Equation A.2.1) is unbiased.

A.3 Proof for the Graphical Model Estimator

A.3.1 Proof of M-gLasso

The analysis is based on **primal-dual method**, which is adapted from [3]. First we write the optimality condition for (Equation 2.2.2) as

$$\widehat{\mathbf{\Sigma}}_n^{\text{param}} - \left(\widehat{\mathbf{\Theta}}_G^{\text{param}}\right)^{-1} + \lambda_G^{\text{param}}\mathbf{G} = \mathbf{0}, \tag{A.3.1}$$

where $\mathbf{G}$ is the sub-gradient [120] of $\left\|\left\|\widehat{\mathbf{\Theta}}_G^{\text{param}}\right\|\right\|_{1,\text{off}}$ and is defined as

$$G_{ij} \triangleq \begin{cases} \text{sgn}(\widehat{\mathbf{\Theta}}_G^{\text{param}})_{i,j}, & \text{if } (\widehat{\mathbf{\Theta}}_G^{\text{param}})_{i,j} \neq 0; \\ \in [-1,1], & \text{otherwise.} \end{cases}$$

for $i \neq j$. However, because of the complexity of (Equation A.3.1), directly bounding the deviation $\|\widehat{\mathbf{\Theta}}_G^{\text{param}} - \mathbf{\Theta}^\natural\|_\infty$ can be difficult. Instead, we construct a pair $\left(\widetilde{\mathbf{\Theta}}_G^{\text{param}}, \widetilde{\mathbf{G}}\right)$ which satisfies: (i) $\widetilde{\mathbf{G}}$ is the sub-differential of $\left\|\left\|\widetilde{\mathbf{\Theta}}_G^{\text{param}}\right\|\right\|_{1,\text{off}}$; and (ii) the pair $(\widetilde{\mathbf{\Theta}}_G^{\text{param}}, \widetilde{\mathbf{G}})$ satisfies the condition in (Equation A.3.1). Then we show it coincides with the solution of (5).

The basic rational is as follows. First we verify that $\widehat{\mathbf{\Theta}}_G^{\text{param}}$ is the unique solution of (Equation A.3.1). Since our constructed pairs $(\widetilde{\mathbf{\Theta}}_G^{\text{param}}, \widetilde{\mathbf{G}})$ satisfies the condition in (Equation A.3.1), which corresponds to the solution in (5) exclusively, we can hence show the constructed pair $(\widetilde{\mathbf{\Theta}}_G^{\text{param}}, \widetilde{\mathbf{G}})$ is the identical solution of (5), namely, $(\widehat{\mathbf{\Theta}}_G^{\text{param}}, \mathbf{G})$. Afterwards we can upper bound $\|\widehat{\mathbf{\Theta}}_G^{\text{param}} - \mathbf{\Theta}^\natural\|_\infty$ by investigating $\|\widetilde{\mathbf{\Theta}}_G^{\text{param}} - \mathbf{\Theta}^\natural\|_\infty$, which is more amenable for the analysis as following.

Stage I: construct $\widetilde{\mathbf{\Theta}}_G^{\text{param}}$. We construct the primal-dual witness solution $\left(\widetilde{\mathbf{\Theta}}_G^{\text{param}}, \widetilde{\mathbf{G}}\right)$ assuming the support set S is given as a prior. This step can further be divided into three stages, as illustrated in the main context. First we construct the matrix $\widetilde{\mathbf{\Theta}}_G^{\text{param}}$. For the

entries (i,j) restricted to the set S, we set them as

$$(\widetilde{\mathbf{\Theta}}_G^{\text{param}})_S = \text{argmin}_{\substack{\mathbf{\Theta}\succ\mathbf{0} \\ \mathbf{\Theta}=\mathbf{\Theta}^\top, \mathbf{\Theta}_{S^c}=\mathbf{0}}} - \log\det\mathbf{\Theta} + \left\langle \widehat{\mathbf{\Sigma}}_n^{\text{param}}, \mathbf{\Theta} \right\rangle + \lambda_G^{\text{param}} |\!|\!| \mathbf{\Theta} |\!|\!|_{1,\text{off}}.$$

For the rest of entries $(\widetilde{\mathbf{\Theta}}_G^{\text{param}})_{S^c}$, we set them to be zero values. Then we construct the sub-differential $\widetilde{\mathbf{G}}$ corresponding to the matrix $\widetilde{\mathbf{\Theta}}_G^{\text{param}}$. For the entry $(i,j) \in S$, we set $\widetilde{G}_{i,j} = \text{sign}(\widetilde{\mathbf{\Theta}}_G^{\text{param}})_{i,j}$. For the entry (i,j) that is outside of the support set S, we set $\widetilde{G}_{i,j}$ as

$$\widetilde{G}_{i,j} = (\lambda_G^{\text{param}})^{-1} \left[\left(\widetilde{\mathbf{\Theta}}_G^{\text{param}} \right)^{-1}_{i,j} - (\widehat{\mathbf{\Sigma}}_n^{\text{param}})_{i,j} \right].$$

The goal of this step is to ensure that $\left(\widetilde{\mathbf{\Theta}}_G^{\text{param}}, \widetilde{\mathbf{G}} \right)$ satisfies (Equation A.3.1). As illustrated in the main context, we have the pair $\left(\widetilde{\mathbf{\Theta}}_G^{\text{param}}, \widetilde{\mathbf{G}} \right)$ coincides with the solution of (Equation A.3.1) once $\left| \widetilde{G}_{i,j} \right| < 1$ for the entry $(i,j) \in S^c$. The following step focuses on showing $\left| \widetilde{G}_{i,j} \right| < 1$.

Stage II: construct $\widetilde{\mathbf{G}}$. For the entry $(i,j) \in S$, we set $\widetilde{G}_{i,j} = \text{sign}(\widetilde{\mathbf{\Theta}}_G^{\text{param}})_{i,j}$. For the entry (i,j) that is outside of the support set S, we set $\widetilde{G}_{i,j}$ as

$$\widetilde{G}_{i,j} = (\lambda_G^{\text{param}})^{-1} \left[\left(\widetilde{\mathbf{\Theta}}_G^{\text{param}} \right)^{-1}_{i,j} - (\widehat{\mathbf{\Sigma}}_n^{\text{param}})_{i,j} \right].$$

The goal of this step is to ensure that $\left(\widetilde{\mathbf{\Theta}}_G^{\text{param}}, \widetilde{\mathbf{G}} \right)$ satisfies (Equation A.3.1).

Stage III: verify $\widetilde{\mathbf{G}}$ to be the sub-differential of $\left| \left| \left| \widetilde{\mathbf{\Theta}}_G^{\text{param}} \right| \right| \right|_{1,\text{off}}$. In the following analysis, we verify that $|\widetilde{G}_{i,j}| < 1$, which yields the upper-bound on $\|\widetilde{\mathbf{\Theta}}_G^{\text{param}} - \mathbf{\Theta}^\natural\|_\infty$ as a byproduct. We first need the necessary lemmas from [3].

Lemma 29 (Lemma 6 in [3]). *Suppose that* $r \triangleq 2\kappa_{\mathbf{\Gamma}} \left(\left\| \widehat{\mathbf{\Sigma}}_n^{\text{param}} - \mathbf{\Sigma}^\natural \right\|_\infty + \lambda_G^{\text{param}} \right) \leq \frac{1 \wedge \left(\kappa_{\mathbf{\Sigma}}^2 \kappa_{\mathbf{\Gamma}} \right)^{-1}}{3\kappa_{\mathbf{\Sigma}} \text{deg}}$, *then* $\left\| \widetilde{\mathbf{\Theta}}_G^{\text{param}} - \mathbf{\Theta}^\natural \right\|_\infty \leq r$.

Lemma 30 (Lemma 5 in [3]). *Provided that we have* $\left\| \widetilde{\mathbf{\Theta}}_G^{\text{param}} - \mathbf{\Theta}^\natural \right\|_\infty \leq (3\kappa_{\mathbf{\Sigma}} \text{deg})^{-1}$,

then

$$\left\|\left(\widetilde{\mathbf{\Theta}}_G^{\text{param}}\right)^{-1} - \mathbf{\Theta}^{\natural-1} + \mathbf{\Theta}^{\natural-1}\left(\widetilde{\mathbf{\Theta}}_G^{\text{param}} - \mathbf{\Theta}^{\natural}\right)\mathbf{\Theta}^{\natural-1}\right\|_\infty \leq \frac{3}{2}\text{deg}\cdot\ \kappa_{\mathbf{\Sigma}}^3\left\|\widetilde{\mathbf{\Theta}}_G^{\text{param}} - \mathbf{\Theta}^{\natural}\right\|_\infty^2.$$

Lemma 31 (Lemma 4 in [3])**.** *If we have*

$$\left\|\widehat{\mathbf{\Sigma}}_n^{\text{param}} - \mathbf{\Sigma}^{\natural}\right\|_\infty \vee \left\|\left(\widetilde{\mathbf{\Theta}}_G^{\text{param}}\right)^{-1} - \mathbf{\Theta}^{\natural-1} + \mathbf{\Theta}^{\natural-1}\left(\widetilde{\mathbf{\Theta}}_G^{\text{param}} - \mathbf{\Theta}^{\natural}\right)\mathbf{\Theta}^{\natural-1}\right\|_\infty \leq \theta\lambda_G^{\text{param}}/8,$$

we conclude that $|\widetilde{G}_{i,j}| < 1$.

Now, setting $\lambda_G^{\text{param}} = 8\tau_\infty/\theta$, first we verify the conditions in Lemma 29. We have

$$r \overset{①}{\leq} 2\left(1 + 8\theta^{-1}\right)\kappa_{\mathbf{\Gamma}}\tau_\infty \overset{②}{\leq} \left(3\kappa_{\mathbf{\Sigma}}\text{deg}\right)^{-1}\left(1 \wedge \left(\kappa_{\mathbf{\Sigma}}^2\kappa_{\mathbf{\Gamma}}\right)^{-1}\right),$$

where in ① we use $\left\|\widehat{\mathbf{\Sigma}}_n^{\text{param}} - \mathbf{\Sigma}^{\natural}\right\|_\infty \leq \tau_\infty$ from Lemma 16, and in ② we use the assumptions of τ_∞ in Theorem 1. Then we conclude that

$$\left\|\widetilde{\mathbf{\Theta}}_G^{\text{param}} - \mathbf{\Theta}^{\natural}\right\|_\infty \leq 2\kappa_{\mathbf{\Gamma}}\ \left(\left\|\widehat{\mathbf{\Theta}}_n - \mathbf{\Theta}^{\natural}\right\|_\infty + \frac{8\tau_\infty}{\theta}\right) \leq \left(3\kappa_{\mathbf{\Sigma}}\text{deg}\right)^{-1}.$$

Invoking Lemma 30, we have

$$\left\|\left(\widetilde{\mathbf{\Theta}}_G^{\text{param}}\right)^{-1} - \mathbf{\Theta}^{\natural-1} + \mathbf{\Theta}^{\natural-1}\left(\widetilde{\mathbf{\Theta}}_G^{\text{param}} - \mathbf{\Theta}^{\natural}\right)\mathbf{\Theta}^{\natural-1}\right\|_\infty \leq \frac{3}{2}\text{deg}\times\ \kappa_{\mathbf{\Sigma}}^3\tau_\infty^2 \overset{③}{\leq} \tau_\infty,$$

where ③ is due to the requirement of τ_∞ in Theorem 1. In the end, we verify the condition in Lemma 31,

$$\theta\lambda_G^{\text{param}}/8 = \tau_\infty \geq \left\|\widehat{\mathbf{\Sigma}}_n^{\text{param}} - \mathbf{\Sigma}^{\natural}\right\|_\infty \vee \left\|\left(\widetilde{\mathbf{\Theta}}_G^{\text{param}}\right)^{-1} - \mathbf{\Theta}^{\natural-1} + \mathbf{\Theta}^{\natural-1}\left(\widetilde{\mathbf{\Theta}}_G^{\text{param}} - \mathbf{\Theta}^{\natural}\right)\mathbf{\Theta}^{\natural-1}\right\|_\infty.$$

which concludes that $\widetilde{\mathbf{\Theta}}_G^{\text{param}}$ is identical to the solution $\widehat{\mathbf{\Theta}}_G^{\text{param}}$.

Step IV: bound the error. For the entries $(i,j) \in S^c$ outside the support set S, we have $(\widehat{\mathbf{\Theta}}_G^{\text{param}})_{i,j}$ to be zero due to the construction method of $\widetilde{\mathbf{\Theta}}_G^{\text{param}}$. For the entries $(i,j) \in S$

inside the support set, we upper-bound the element-wise deviation $\left\|\widehat{\boldsymbol{\Theta}}_G^{\text{param}} - \boldsymbol{\Theta}^\natural\right\|_\infty$ as

$$\left\|\widehat{\boldsymbol{\Theta}}_G^{\text{param}} - \boldsymbol{\Theta}^\natural\right\|_\infty = \left\|\widetilde{\boldsymbol{\Theta}}_G^{\text{param}} - \boldsymbol{\Theta}^\natural\right\|_\infty \overset{①}{\leq} 2\kappa_{\boldsymbol{\Gamma}}(1+8\theta^{-1})\tau_\infty, \tag{A.3.2}$$

where ① is due to Lemma 29 and has been verified in Step II. Then we prove $\text{sign}(\widehat{\boldsymbol{\Theta}}_G^{\text{param}})$ reaches the ground truth once $\min_{(i,j)\in S^c}\left|\boldsymbol{\Theta}_{i,j}^\natural\right| \geq 2\kappa_{\boldsymbol{\Gamma}}(1+8\theta^{-1})\tau_\infty$. W.l.o.g. we assume $\boldsymbol{\Theta}_{i,j}^\natural > 0$ for $(i,j)\in S$. Then we have

$$(\widehat{\boldsymbol{\Theta}}_G^{\text{param}})_{i,j} \geq \left|\boldsymbol{\Theta}_{i,j}^\natural\right| - \left|\widehat{\boldsymbol{\Theta}}_G^{\text{param}} - \boldsymbol{\Theta}^\natural\right| \geq \left|\boldsymbol{\Theta}_{i,j}^\natural\right| - \left\|\widehat{\boldsymbol{\Theta}}_G^{\text{param}} - \boldsymbol{\Theta}^\natural\right\|_\infty \overset{②}{>} 0,$$

and complete the proof, where ② is due to the assumption on $\min_{(i,j)\in S^c}\left|\boldsymbol{\Theta}_{i,j}^\natural\right|$ and (Equation A.3.2).

A.3.2 Proof of M-CLIME

This proof largely follows the outline given in the main context and fills the technical details.

Stage I: We verify that $\boldsymbol{\Theta}^\natural$ lies within the region $\left\|\widehat{\boldsymbol{\Sigma}}_n^{\text{param}}\boldsymbol{\Theta}^\natural - \mathbf{I}\right\|_\infty \leq \lambda_C^{\text{param}}$ when setting $\lambda_C^{\text{param}} = M\tau_\infty$, which proceed as

$$\left\|\widehat{\boldsymbol{\Sigma}}_n^{\text{param}}\boldsymbol{\Theta}^\natural - \mathbf{I}\right\|_\infty = \left\|\left(\widehat{\boldsymbol{\Sigma}}_n^{\text{param}} - \boldsymbol{\Sigma}^\natural\right)\boldsymbol{\Theta}^\natural\right\|_\infty \leq \left\|\widehat{\boldsymbol{\Sigma}}_n^{\text{param}} - \boldsymbol{\Sigma}^\natural\right\|_\infty \left|\!\left|\!\left|\boldsymbol{\Theta}^{\natural\top}\right|\!\right|\!\right|_{1,1} \leq M\tau_\infty.$$

Stage II: We bound the element-wise ℓ_∞ norm on $\widehat{\boldsymbol{\Theta}}_C^{\text{param}} - \boldsymbol{\Theta}^\natural$, which reads

$$\begin{aligned}
&\left\|\widehat{\boldsymbol{\Theta}}_C^{\text{param}} - \boldsymbol{\Theta}^\natural\right\|_\infty = \left\|\boldsymbol{\Theta}^\natural\boldsymbol{\Sigma}^\natural\left(\widehat{\boldsymbol{\Theta}}_C^{\text{param}} - \boldsymbol{\Theta}^\natural\right)\right\|_\infty \\
\overset{①}{\leq}\ & M\left(\left\|\widehat{\boldsymbol{\Sigma}}_n^{\text{param}}\widehat{\boldsymbol{\Theta}}_C^{\text{param}} - \mathbf{I}\right\|_\infty + \left\|\widehat{\boldsymbol{\Sigma}}_n^{\text{param}}\boldsymbol{\Theta}^\natural - \mathbf{I}\right\|_\infty + \left|\!\left|\!\left|\widehat{\boldsymbol{\Theta}}_C^{\text{param}} - \boldsymbol{\Theta}^\natural\right|\!\right|\!\right|_{1,1}\left\|\boldsymbol{\Sigma}^\natural - \widehat{\boldsymbol{\Sigma}}_n^{\text{param}}\right\|_\infty\right) \\
\overset{②}{\leq}\ & M\left[2\lambda_C^{\text{param}} + \left(\left|\!\left|\!\left|\widehat{\boldsymbol{\Theta}}_C^{\text{param}}\right|\!\right|\!\right|_{1,1} + \left|\!\left|\!\left|\widehat{\boldsymbol{\Theta}}^\natural\right|\!\right|\!\right|_{1,1}\right)\left\|\boldsymbol{\Sigma}^\natural - \widehat{\boldsymbol{\Sigma}}_n^{\text{param}}\right\|_\infty\right],
\end{aligned} \tag{A.3.3}$$

where in ① we use the assumption that $\left|\!\left|\!\left|\boldsymbol{\Theta}^\natural\right|\!\right|\!\right|_{1,1} \leq M$, and in ② we use the constraints in (Equation 2.2.3) such that $\left\|\widehat{\boldsymbol{\Sigma}}_n^{\text{param}}\widehat{\boldsymbol{\Theta}}_C^{\text{param}} - \mathbf{I}\right\|_\infty \leq \lambda_C^{\text{param}}$.

Then we prove $\left\|\left\|\widehat{\boldsymbol{\Theta}}_C^{\text{param}}\right\|\right\|_{1,1} \leq \left\|\left\|\boldsymbol{\Theta}^\natural\right\|\right\|_{1,1}$. Notice that (Equation 2.2.3) is equivalent to solving the following series optimization functions

$$(\widetilde{\boldsymbol{\Theta}}_C^{\text{param}})_i = \text{argmin}_{\boldsymbol{\theta}} \|\boldsymbol{\theta}\|_1, \text{ s.t. } \left\|\widehat{\boldsymbol{\Sigma}}_n^{\text{param}}\boldsymbol{\theta} - \mathbf{e}_i\right\|_\infty \leq \lambda_C^{\text{param}}, \tag{A.3.4}$$

where $\mathbf{e}_i$ denotes the ith canonical basis with 1 on its ith entry and zero elsewhere. Hence we obtain

$$\left\|\left(\widehat{\boldsymbol{\Theta}}_C^{\text{param}}\right)_i\right\|_1 \overset{③}{\leq} \left\|\left(\widetilde{\boldsymbol{\Theta}}_C^{\text{param}}\right)_i\right\|_1 \overset{④}{\leq} \left\|\boldsymbol{\Theta}_i^\natural\right\|_1,$$

where ③ is due to the construction of $\widehat{\boldsymbol{\Theta}}_C^{\text{param}}$, and ④ is because $\widetilde{\boldsymbol{\Theta}}_C^{\text{param}}$ is the minimal in (Equation A.3.4). This suggests

$$\left\|\left\|\widehat{\boldsymbol{\Theta}}_C^{\text{param}}\right\|\right\|_{1,1} = \max_i \left\|\left(\widehat{\boldsymbol{\Theta}}_C^{\text{param}}\right)_i\right\|_1 \leq \max_i \left\|\boldsymbol{\Theta}_i^\natural\right\|_1 = \left\|\left\|\boldsymbol{\Theta}^\natural\right\|\right\|_{1,1}. \tag{A.3.5}$$

Combining (Equation A.3.3) and (Equation A.3.5) then yields the inequality

$$\left\|\widehat{\boldsymbol{\Theta}}_C^{\text{param}} - \boldsymbol{\Theta}^\natural\right\|_\infty \leq 2M\left(\lambda_C^{\text{param}} + \left\|\left\|\boldsymbol{\Theta}^\natural\right\|\right\|_{1,1}\left\|\boldsymbol{\Sigma}^\natural - \widehat{\boldsymbol{\Sigma}}_n^{\text{param}}\right\|_\infty\right) \leq 4M\lambda_C^{\text{param}}.$$

Stage III: We prove (Equation 2.5.1) given the conditions in Theorem 2. First we show that $(\widehat{\boldsymbol{\Theta}}_C^{\text{param}})_{i,j} = 0$ if $\boldsymbol{\Theta}_{i,j}^\natural = 0$. This is because

$$\left|(\widehat{\boldsymbol{\Theta}}_C^{\text{param}})_{i,j}\right| = \left|(\widehat{\boldsymbol{\Theta}}_C^{\text{param}})_{i,j} - \boldsymbol{\Theta}_{i,j}^\natural\right| \leq \left\|\widehat{\boldsymbol{\Theta}}_C^{\text{param}} - \boldsymbol{\Theta}^\natural\right\|_\infty \leq 4M^2\tau_\infty.$$

Due to the definition of hard-thresholding estimator $\mathcal{T}(\boldsymbol{\Theta}; 4M^2\tau_\infty)$, this entry will shrink to zero. Then we show that $\text{sign}((\widehat{\boldsymbol{\Theta}}_C^{\text{param}})_{i,j}) = \text{sign}(\boldsymbol{\Theta}_{i,j}^\natural)$ for $(i,j) \in S$. We assume that $(\widehat{\boldsymbol{\Theta}}_C^{\text{param}})_{i,j} > 0$ w.l.o.g. Then we have

$$\left|(\widehat{\boldsymbol{\Theta}}_C^{\text{param}})_{i,j}\right| \geq \left|\boldsymbol{\Theta}_{i,j}^\natural\right| - \left\|\widehat{\boldsymbol{\Theta}}_C^{\text{param}} - \boldsymbol{\Theta}^\natural\right\|_\infty \overset{⑤}{\geq} 4M\tau_\infty^2,$$

where ⑤ is due to the assumption in Theorem 2. Hence, we conclude that the sign is preserved by $\mathcal{T}(\boldsymbol{\Theta}; 4M^2\tau_\infty)$.

APPENDIX B

APPENDIX OF NONPARAMETRIC LEARNING OF GRAPHICAL MODELS

B.1 Proof of Theorem 3

B.1.1 Notations

For the conciseness of notation, we drop the subscript i in the marginal CDFs $F_i(\cdot)$, $\widehat{F}_i(\cdot)$, and entry $\widehat{X}_i^{(s)}$, and denote them as $F(\cdot)$, $\widehat{F}(\cdot)$, and $\widehat{X}^{(s)}$, respectively. We define the approximate characteristics function $\widehat{\phi}_{\widehat{w}}(t)$ as

$$\widehat{\phi}_{\widehat{w}}(t) \triangleq \exp\left(-\frac{\sigma^2 t^2}{2(d-p)}\right).$$

Additionally, we construct the function $\widetilde{F}(\cdot)$ as

$$\widetilde{F}(x) = \frac{1}{2} - \frac{1}{\pi}\int_0^\infty \frac{1}{t}\Im\left[\frac{\phi_{\widehat{w}}(-t)\widehat{\phi}_{\widehat{X}}(t)}{|\phi_{\widehat{w}}(t)|^2 \vee \gamma t^a} e^{-\mathbb{j}tx}\right] dt,$$

where the characteristic function $\phi_{\widehat{w}}(\cdot)$ denotes the ground-truth characteristics function of the noise $\widehat{w}$, and the function $\widehat{\phi}_{\widehat{X}}$ is defined as $n^{-1}\sum_{s=1}^n e^{-\mathbb{j}t\widehat{X}^{(s)}}$.

Let the term $\Delta_x^{(s)}$ be

$$\begin{aligned}\Delta_x^{(s)} =& \frac{1}{\pi}\int_0^\infty \frac{1}{t}\Im\left(\frac{\widehat{\phi}_{\widehat{w}}(-t)}{\left|\widehat{\phi}_{\widehat{w}}(t)\right|^2 \vee \gamma t^a}\exp\left(\mathbb{j}t\widehat{X}^{(s)} - \mathbb{j}tx\right)\right) dt \\ & - \mathbb{E}\left[\frac{1}{\pi}\int_0^\infty \frac{1}{t}\Im\left[\frac{\phi_{\widehat{X}}(t)}{\phi_{\widehat{w}}(t)} e^{-\mathbb{j}tx}\right] dt\right]. \end{aligned} \tag{B.1.1}$$

Our goal is to obtain the uniform convergence rate of the CDF estimator $\left\|\widehat{F} - F\right\|_\infty$, which is written as

$$\left\|\widehat{F}-F\right\|_{\infty}=\sup_{x\in[0,1]}\left|\widehat{F}(x)-F(x)\right|=\sup_{x\in[0,1]}\frac{1}{n}\left|\sum_{s=1}^{n}\Delta_x^{(s)}\right|\triangleq\Delta_x.$$

Before proceed, we define the event $\mathcal{E}_w$ as

$$\mathcal{E}_w\triangleq\left\{\left|\mathbb{E}(\widehat{w}_i)^2-\frac{\sigma^2}{d-p}\right|\leq\frac{\sigma^2}{5(d-p)},\ \ \forall\,1\leq i\leq p\right\},\tag{B.1.2}$$

where $\widehat{w}_i$ denotes the ith entry of the noise $\widehat{\mathbf{W}}$.

The parameter γ is set as $c_0\log(np)\left(\frac{\sigma^2}{d-p}\right)^{a/4}$ and the number $a>1$ is some fixed positive constant.

B.1.2 Main Proof

Proof. We decompose the probability $\sup_x\Delta_x\geq\mathbb{E}\sup_x\Delta_x+t$ as

$$\mathbb{P}\left(\left|\sup_x\Delta_x-\mathbb{E}\sup_x\Delta_x\right|\geq t\right)\leq\mathbb{E}\mathbb{1}(\overline{\mathcal{E}}_w)+\mathbb{E}\mathbb{1}\left[\left(\left|\sup_x\Delta_x-\mathbb{E}\sup_x\Delta_x\right|\geq t\right)\bigcap\mathcal{E}_w\right].$$

The first term $\mathbb{E}\mathbb{1}(\overline{\mathcal{E}}_w)$ is investigated in Lemma 32; while the second term is bounded with the Talagrand inequality (cf. Thm. 2.6 in [127]), which is stated as

$$\mathbb{E}\mathbb{1}\left[\left(\left|\sup_x\Delta_x-\mathbb{E}\sup_x\Delta_x\right|\geq t\right)\bigcap\mathcal{E}_w\right]\lesssim\mathbb{E}\left[\exp\left(-\frac{nt}{KC_U}\log\left(1+\frac{ntC_U}{V}\right)\right)\mathbb{1}(\mathcal{E}_w)\right],$$

where C_U is the uniform bound for $\Delta_x^{(s)}$, i.e., $|\Delta_x^{(s)}|\leq C_U$ for all x and s, and the variance V satisfies

$$V\geq n\sup_{x\in\mathbb{R}}\mathbb{E}\left|\Delta_x\right|^2+16C_U\cdot\left(\mathbb{E}\sup_x\left|\Delta_x\right|\right).$$

Setting t as $V\log n/n$, we conclude

$$\sup_x\Delta_x\leq\mathbb{E}\sup_x\Delta_x+\frac{cV\log n}{n}$$

holds with probability exceeding $1 - O(n^{-c})$. The following context focuses on computing the values of C_U, $\mathbb{E}\sup_x \Delta_x$, and $\sup_x \mathbb{E}\left|\Delta_x\right|^2$ conditional on event $\mathcal{E}_w$ in (Equation B.1.2).

Step I. We show there exists some positive constant C_U such that $|\Delta_x^{(s)}| \leq C_U$ for all x and s, $1 \leq s \leq n$ (cf. Lemma 34);

Step II. We prove that $\mathbb{E}\sup_x \Delta_x \leq \mathbb{E}\Delta_x + c_0/\sqrt{n}$, where c_0 is some positive constant. With the symmetrization inequalities (cf. Lemma 11.4 in [140]), we obtain

$$\mathbb{E}\sup_x \left(\Delta_x - \mathbb{E}\Delta_x\right) \leq \mathbb{E}\sup_x \frac{2}{n}\sum_{s=1}^{n} \varepsilon_s \Delta_x^{(s)}, \tag{B.1.3}$$

where $\{\varepsilon_s\}$ are the Rademacher RVs, i.e., $\mathbb{P}(\varepsilon_s = \pm 1) = 1/2$, $1 \leq s \leq n$. With regarding the empirical process $n^{-1}\left(\sum_s \varepsilon_s \Delta_x^{(s)}\right)$, we have

$$\begin{aligned}
\mathbb{E}e^{\lambda n^{-1}\left(\sum_s \varepsilon_s \left(\Delta_{x_1}^{(s)} - \Delta_{x_2}^{(s)}\right)\right)} &\overset{①}{=} \prod_{s=1}^{n} \mathbb{E}\exp\left[\frac{\lambda\varepsilon_s}{n}\left(\Delta_{x_1}^{(s)} - \Delta_{x_2}^{(s)}\right)\right] \\
&\overset{②}{\leq} \prod_{s=1}^{n} \mathbb{E}\exp\left[\frac{\lambda^2}{2n^2}\left(\Delta_{x_1}^{(s)} - \Delta_{x_2}^{(s)}\right)^2\right],
\end{aligned}$$

where in ① we exploit the independence across the samples, in ② we use the fact that ε_s is a Rademacher RV and the Hoeffding's lemma [140] (Lemma 2.2).

Invoking the Dudley's entropy integral (cf. Corol 13.2 in [140]), which is also listed as Theorem 17 for the sake of self-containing, we conclude

$$\begin{aligned}
\mathbb{E}\sup_{x,\varepsilon_s} \frac{1}{n}\sum_{s=1}^{n} \varepsilon_s \Delta_x^{(s)} &\lesssim \frac{1}{\sqrt{n}} \int_0^{2c_0} \sqrt{\mathcal{H}([0,1],\delta)}d\delta \\
&\overset{③}{\lesssim} \frac{1}{\sqrt{n}} \int_0^{2c_0} \left(1 + \sqrt{\log\frac{c_0}{t}}\right) d\delta \asymp \frac{1}{\sqrt{n}},
\end{aligned} \tag{B.1.4}$$

where $\mathcal{H}([0,1],\delta)$ denotes the δ-entropy number [140], in ③ we upper-bound the δ-entropy number $\mathcal{H}([0,1],\delta)$ as $c_0 + c_1 \log(b/\delta)$ (cf. Example 5.24 in [10]). The proof is then

completed by combining (Equation B.1.3) and (Equation B.1.4).

Step III. We set the variance V as

$$\begin{aligned} V = & \ n \sup_{x \in \mathbb{R}} \mathbb{E} \left| \Delta_x \right|^2 + \frac{c_0}{\sqrt{n}} + c_1 \sqrt{\mathbb{E}\Delta_x^2} \overset{④}{\geq} n \sup_{x \in \mathbb{R}} \mathbb{E} \left| \Delta_x \right|^2 + \frac{c_0}{\sqrt{n}} + c_1 \mathbb{E}\Delta_x \\ \overset{⑤}{\geq} & \ n \sup_{x \in \mathbb{R}} \mathbb{E} \left| \Delta_x \right|^2 + c_0 \mathbb{E} \sup_x \Delta_x, \end{aligned}$$

where in ④ we use the fact $\mathbb{E}\Delta_x \leq \sqrt{\mathbb{E}\Delta_x^2}$, and in ⑤ we use the results in Step II such that $\mathbb{E} \sup_x \Delta_x \leq \mathbb{E}\Delta_x + c_0/\sqrt{n}$. Invoking Lemma 32 and Lemma 35 will complete the proof.

□

B.1.3 Supporting Lemmas

Lemma 32. *The event $\mathcal{E}_w$ in* (Equation B.1.2) *holds with probability exceeding $1 - 2pe^{-c_0 p}$, where c_0 is some fixed positive constants.*

Proof. Perform SVD for $\mathbf{A}$ as $\mathbf{A} = \mathbf{U}\mathbf{S}\mathbf{V}^\top$, we can rewrite the product $\left(\mathbf{A}^\top \mathbf{A}\right)^{-1} \mathbf{A}^\top$ as

$$\left(\mathbf{A}^\top \mathbf{A}\right)^{-1} \mathbf{A}^\top = \mathbf{V}\mathbf{S}^{-2}\mathbf{V}^\top \mathbf{V}\mathbf{S}^\top \mathbf{U}^\top = \mathbf{V}\mathbf{S}^{-1}\mathbf{U}^\top.$$

Then the ith entry of $\widehat{\mathbf{W}}$ can be written as $\mathbf{a}_i^\top \mathbf{U}^\top \mathbf{W}$, where $\mathbf{a}_i$ as

$$\mathbf{a}_i = \left[\lambda_1^{-1} V_{i1} \ \ldots \ \lambda_p^{-1} V_{ip}\right],$$

and λ_i is the ith singular value of $\mathbf{S}$, and V_{ij} is the (i,j)th entry of the matrix $\mathbf{V}$. Since each entry A_{ij} is iid standard normal RV, i.e., $A_{ij} \sim \mathcal{N}(0,1)$, we conclude that its eigenvalues $\{\lambda_i\}_{1 \leq i \leq p}$ are independent from its eigenvectors $\mathbf{V}$, which is uniformly distributed on a Haar measure [151]. Hence we can rewrite $\mathbf{a}_i$ as a product as $\mathbf{S}^{-1}\mathbf{g}/\|\mathbf{g}_i\|_2$, where $\mathbf{g}_i$ is a Gaussian distributed RV with zero mean and unit variance, namely, $\mathbf{g}_i \sim \mathcal{N}(0, \mathbf{I}_{p \times p})$.

First, we define the event $\mathcal{E}_g$ as

$$\mathcal{E}_g \triangleq \left\{\exists\, 1 \leq i \leq p, \;\; \text{s.t.} \;\; \left|\|\mathbf{g}_i\|_2^2 - p\right| \geq p/4\right\}.$$

Then we bound $\mathbb{E}\mathbb{1}(\overline{\mathcal{E}}_w)$ as

$$\mathbb{E}\mathbb{1}\left(\overline{\mathcal{E}}_w\right) \leq \mathbb{E}\mathbb{1}\left(\overline{\mathcal{E}}_g\right) + \mathbb{E}\mathbb{1}\left(\overline{\mathcal{E}}_w \bigcap \mathcal{E}_g\right),$$

where $\overline{(\cdot)}$ denotes the complement of the event. Due to the fact that $\mathbf{g}$ is a Gaussian RV such that $\mathbf{g} \sim \mathcal{N}(0, \mathbf{I})$, we invoke Lemma 52 and bound the first term as $\mathbb{E}\mathbb{1}(\mathcal{E}_g) \leq 2pe^{-c_0 p}$. While for the second term, we first compute the expectation $\mathbb{E}\left\|\mathbf{S}^{-1}\mathbf{g}_i\mathbf{U}^\top\mathbf{W}\right\|_2^2$ as

$$\mathbb{E}\left\|\mathbf{S}^{-1}\mathbf{g}_i\mathbf{U}^\top\mathbf{W}\right\|_2^2 = \sigma^2\mathbb{E}\left\|\mathbf{S}^{-1}\mathbf{g}_i\right\|_2^2 = \sigma^2\left\|\mathbf{S}^{-1}\right\|_{\mathrm{F}}^2.$$

Invoking the Marcenko-Pastur law in [151] (cf. Thm. 2.35, which is also listed as Lemma Theorem 16 for the self-containing of paper), we have

$$\begin{aligned}\left\|\mathbf{S}^{-1}\right\|_{\mathrm{F}}^2 = &\sum_{i=1}^{p}\lambda_i^{-2} \to \frac{p}{d}\int_{L(\tau)}^{U(\tau)} t^{-1}\left[\left(1-\tau^{-1}\right)_+\mathbb{1}(t) + \frac{\sqrt{[t-L(\tau)][U(\tau)-t]}}{2\pi\tau t}\right]dt \\ = &\;\frac{p}{d}\times\frac{1}{1-\tau} = \frac{p}{d-p},\end{aligned}$$

where τ is defined as p/d, function $L(\cdot)$ is defined as $\left(1-\sqrt{\cdot}\right)^2$, and function $U(\cdot)$ is defined as $\left(1+\sqrt{\cdot}\right)^2$. Hence we have $\mathbb{E}\left\|\mathbf{S}^{-1}\mathbf{g}\mathbf{U}^\top\mathbf{w}\right\|_2^2 = \mathbb{E}\|\mathbf{S}^{-1}\|_{\mathrm{F}}^2\sigma^2 = p\sigma^2/(d-p)$ and will show $\mathbb{E}\mathbb{1}\left(\overline{\mathcal{E}}_w \bigcap \mathcal{E}_g\right)$ to be zero. This is because

$$\mathbb{E}\left[\frac{\left\|\mathbf{S}^{-1}\mathbf{g}_i\mathbf{U}^\top\mathbf{W}\right\|_2^2}{\|\mathbf{g}_i\|_2^2}\mathbb{1}(\mathcal{E}_g)\right] \overset{①}{\geq} \frac{4}{3p}\mathbb{E}\left\|\mathbf{S}^{-1}\mathbf{g}_i\mathbf{U}^\top\mathbf{W}\right\|_2^2 = \frac{4\sigma^2}{3(d-p)},$$

where ① is due to the definition of $\mathcal{E}_g$. Similarly we can show

$$\mathbb{E}\left[\frac{\left\|\mathbf{S}^{-1}\mathbf{g}_i\mathbf{U}^\top\mathbf{W}\right\|_2^2}{\|\mathbf{g}_i\|_2^2}\mathbb{1}(\mathcal{E}_g)\right] \leq \frac{4}{5p}\mathbb{E}\left\|\mathbf{S}^{-1}\mathbf{g}_i\mathbf{U}^\top\mathbf{W}\right\|_2^2 = \frac{4\sigma^2}{5(d-p)},$$

which suggests that $\mathcal{E}_w$ will always hold, and complete the proof. □

Lemma 33. *Conditional on the event $\mathcal{E}_w$ in* (Equation B.1.2)*, we have*

$$\left|\widehat{\phi}_{\widehat{w}}(t) - \phi_{\widehat{w}}(t)\right| \lesssim \frac{\log^2(np)\sigma^2t^2}{d-p}e^{-\frac{\sigma^2t^2}{2(d-p)}},$$

where $\widehat{\phi}_{\widehat{w}}(t)$ and $\phi_{\widehat{w}}(t)$ denotes the estimated characteristic function and the ground-truth characteristic function of $\widehat{w}_i$, respectively.

Proof. Notice that the characteristic function of the Gaussian $\mathcal{N}(0, \text{Var})$ is written as

$$\phi_{\text{Var}}(t) = \exp\left(-\frac{(\text{Var})t^2}{2}\right).$$

Then we conclude that

$$\begin{aligned}
\left|\widehat{\phi}_{\widehat{w}}(t) - \phi_{\widehat{w}}(t)\right| = & \left|\exp\left(-\frac{\sigma^2t^2}{2(d-p)}\right) - \exp\left(-\frac{\widehat{\sigma}^2t^2}{2}\right)\right| \\
\overset{①}{\leq} & \frac{|\sigma^2/(d-p) - \widehat{\sigma}^2|\,t^2}{2} \cdot \left(\exp\left(-\frac{\widehat{\sigma}^2t^2}{2}\right) + \exp\left(-\frac{\sigma^2t^2}{2(d-p)}\right)\right) \\
\overset{②}{\lesssim} & \frac{\log^2(np)\sigma^2t^2}{d-p}e^{-\frac{\sigma^2t^2}{2(d-p)}},
\end{aligned}$$

where $\widehat{\sigma}^2$ is defined as the ground-truth variance of the noise $\widehat{w}$, ① is because of the relation $|e^{-z_1} - e^{-z_2}| \leq |z_1 - z_2|\,|e^{-z_1} + e^{-z_2}|/2$ for arbitrary z_1 and z_2, ② is because of event $\mathcal{E}_w$. □

Lemma 34. *Setting $\gamma \asymp \log(np)\left(\frac{\sigma^2}{d-p}\right)^{a/4}$, we conclude $|\Delta_x^{(s)}| \lesssim 1$ for all s, $1 \leq s \leq n$, where $\Delta_x^{(s)}$ is defined in* (Equation B.1.1).

Proof. We verify that $\Delta_x^{(s)}$ to be bounded by some constant, which is written as

$$\Delta_x^{(s)} \leq \left| \frac{1}{\pi} \int_0^\infty \frac{1}{t} \Im \left(\frac{\widehat{\phi}_{\widehat{w}}(-t)}{\left|\widehat{\phi}_{\widehat{w}}(t)\right|^2 \vee \gamma t^a} \exp\left(\jmath t \left(\widehat{X}^{(s)} - x \right) \right) \right) dt \right| + \underbrace{F(x)}_{\leq 1}. \tag{B.1.5}$$

Defining the term $t_\perp$ as $(2\gamma)^{-1/a}$, we split the whole region $(0, \infty)$ as three disjoint subregions $\mathcal{R}_1 = (0, t_\perp)$ and $\mathcal{R}_2 = (t_\perp, \infty)$. Then we perform the decomposition as

$$\begin{aligned}
&\int_0^\infty \frac{1}{t} \Im \left(\frac{\widehat{\phi}_{\widehat{w}}(-t)}{\left|\widehat{\phi}_{\widehat{w}}(t)\right|^2 \vee \gamma t^a} \exp\left(\jmath t \widehat{X}^{(s)} - \jmath t x \right) \right) dt \\
= &\underbrace{\int_{\mathcal{R}_1} \frac{1}{t} \Im \left(\frac{\widehat{\phi}_{\widehat{w}}(-t)}{\left|\widehat{\phi}_{\widehat{w}}(t)\right|^2 \vee \gamma t^a} \exp\left(\jmath t \widehat{X}^{(s)} - \jmath t x \right) \right) dt}_{T_1} \\
+ &\underbrace{\int_{\mathcal{R}_2} \frac{1}{t} \Im \left(\frac{\widehat{\phi}_{\widehat{w}}(-t)}{\left|\widehat{\phi}_{\widehat{w}}(t)\right|^2 \vee \gamma t^a} \exp\left(\jmath t \widehat{X}^{(s)} - \jmath t x \right) \right) dt}_{T_2},
\end{aligned} \tag{B.1.6}$$

Then we separately bound the terms T_1 and T_2.

Step I. We can bound term T_1 as

$$\begin{aligned}
T_1 = &\int_{\mathcal{R}_1} \frac{1}{t} \Im \left(\widehat{\phi}_{\widehat{w}}(-t) \Im \left[\left(\exp\left(\jmath t \widehat{X}^{(s)} - \jmath t x \right) \right) \left[1 + \sum_{k=1}^\infty \left(1 - \left(\left|\widehat{\phi}_{\widehat{w}}(t)\right|^2 \vee \gamma t^a \right) \right)^k \right] \right] \right) dt \\
\overset{①}{\leq} &\int_{\mathcal{R}_1} \frac{\sin\left(t \left(\widehat{X}^{(s)} - x \right) \right)}{t} dt + \int_{\mathcal{R}_1} \frac{1}{t} \sum_{k=1}^\infty \left(\frac{\sigma^2 t^2}{d-p} \right)^k dt \\
\overset{②}{\lesssim} &1 + \sum_{k=1}^\infty \frac{1}{2k} \left(\frac{\sigma^2 t_\perp^2}{d-p} \right)^k \overset{③}{\lesssim} 1,
\end{aligned} \tag{B.1.7}$$

where in ① we use the fact $\left|\phi_{\widehat{w}}(t)\right|^2 \vee \delta t^a \geq 1 - \frac{c_1 \sigma^2 t^2}{d-p}$ for $t \in \mathcal{R}_1$, in ② we use the fact $\sup_{\tau > 0} \left| \int_0^\tau \sin(u)/u du \right| \leq 3$, and ③ is because $\sigma^2 t_\perp^2 \asymp \sqrt{d-p} (\log(np))^{-\frac{2}{a}} \leq \frac{d-p}{2}$ and hence $\sum_{k=1}^\infty \frac{1}{2k} \left(\frac{\sigma^2 t_\perp^2}{d-p} \right)^k \leq \sum_{k=1}^\infty \left(\frac{\sigma^2 t_\perp^2}{d-p} \right)^k \lesssim 1$.

Step II. For term T_3, we have

$$T_2 \leq \int_{\mathcal{R}_2} \frac{\widehat{\phi}_{\widehat{w}}(-t)}{t\sqrt{\left|\widehat{\phi}_{\widehat{w}}(-t)\right|^2 \vee \delta t^a}} dt \overset{④}{\leq} \int_{\mathcal{R}_2} \frac{1}{\sqrt{\gamma} t^{1+\frac{a}{2}}} dt = \frac{1}{a\sqrt{\gamma} t_\perp^{a/2}} = \frac{1}{\sqrt{2}a} \asymp 1, \quad \text{(B.1.8)}$$

where ④ is because $\widehat{\phi}_{\widehat{w}}(\cdot) \leq 1$, and complete the proof by summaring (Equation B.1.5), (Equation B.1.6) and (Equation B.1.8).

□

Lemma 35. *Under the setting of Theorem 3, we have*

$$\mathbb{E}\left(\Delta_x\right)^2 \lesssim \frac{\log^{2/a}(np)\sigma}{\sqrt{d-p}} + \frac{(\log(np))^2}{(d-p)^{\frac{a}{4}}} + \left(\frac{\sigma^2}{d-p}\right)^{\frac{2\alpha+1}{4}} + \frac{1}{n},$$

when setting $\gamma \asymp \log(np)\left(\frac{\sigma^2}{d-p}\right)^{a/4}$

Proof. The proof largely follows [41]. However, extra measurements are required to estimate the characteristic function $\widehat{\phi}_{\widehat{w}}(\cdot)$ in [41], which leads to a simple form of the error $|\widehat{\phi}_{\widehat{w}}(t) - \phi_{\widehat{w}}(t)|$ only depending on the number of extra measurements. In contrast, our setting does not need these additional measurements and the error $|\widehat{\phi}_{\widehat{w}}(t) - \phi_{\widehat{w}}(t)|$ varies with t.

With the decomposition

$$\mathbb{E}\left|\widehat{F}(x) - F(x)\right|^2 \leq 2\mathbb{E}\left|\widehat{F}(x) - \widetilde{F}(x)\right|^2 + 2\mathbb{E}\left|\widetilde{F}(x) - F(x)\right|^2,$$

we complete the proof by invoking Lemma 36 and Lemma 37.

□

Lemma 36. *Under the setting of Theorem 3, we can upper-bound the deviation* $\mathbb{E}\left|\widehat{F}(x) - \widetilde{F}(x)\right|$ *as*

$$\mathbb{E}\left|\widehat{F}(x)-\widetilde{F}(x)\right|^2 \lesssim \frac{\log^{2/a}(np)\sigma}{\sqrt{d-p}},$$

when setting $\gamma \asymp \log(np)\left(\frac{\sigma^2}{d-p}\right)^{a/4}$.

Proof. First we expand the term $\widehat{F}(x)-\widetilde{F}(x)$ as

$$\begin{aligned}\widehat{F}(x)-\widetilde{F}(x) =& \frac{1}{\pi}\int_0^\infty \frac{1}{t}\Im\left[\left(\frac{\widehat{\phi}_{\widehat{w}}(-t)}{\left|\widehat{\phi}_{\widehat{w}}(t)\right|^2\vee\gamma t^a}-\frac{\phi_{\widehat{w}}(-t)}{\left|\phi_{\widehat{w}}(t)\right|^2\vee\gamma t^a}\right)\widehat{\phi}_{\widehat{X}}(t)e^{-\mathbb{j}tx}\right]dt\\ \overset{①}{=}& \frac{1}{n\pi}\int_0^\infty \frac{D(t)}{t}\sum_{s=1}^n \sin\left(t\left(\widehat{X}^{(s)}-x\right)\right)dt\end{aligned}$$

where in ① we define $D(t)$ as

$$D(t)\triangleq \frac{\widehat{\phi}_{\widehat{w}}(-t)}{|\widehat{\phi}_{\widehat{w}}(t)|^2\vee\gamma t^a}-\frac{\phi_{\widehat{w}}(-t)}{\left|\phi_{\widehat{w}}(t)\right|^2\vee\gamma t^a}.$$

According to [41], it satisfies the relation

$$|D(t)|\le \frac{2\varepsilon_E(t)}{\sqrt{|\widehat{\phi}_{\widehat{w}}(t)|^2\vee\gamma t^a}\cdot\sqrt{\left|\phi_{\widehat{w}}(t)\right|^2\vee\gamma t^a}}+\frac{\varepsilon_E(t)}{\left|\phi_{\widehat{w}}(t)\right|^2\vee\gamma t^a}, \tag{B.1.9}$$

where $\varepsilon(t)$ is defined as $\left|\widehat{\phi}_{\widehat{w}}(t)-\phi_{\widehat{w}}(t)\right|$, which is upper bounded by Lemma 33.

Define the terms I_1 and I_2 as

$$\begin{aligned}I_1 \triangleq& \mathbb{E}\left(\frac{1}{n\pi}\int_0^{t_\perp}\left|\frac{D(t)}{t}\sum_{s=1}^n\sin\left(t\left(\widehat{X}^{(s)}-x\right)\right)\right|dt\right)^2,\\ I_2 \triangleq& \mathbb{E}\left(\frac{1}{n\pi}\int_{t_\perp}^{\infty}\left|\frac{D(t)}{t}\sum_{s=1}^n\sin\left(t\left(\widehat{X}^{(s)}-x\right)\right)\right|dt\right)^2,\end{aligned}$$

respectively, where $t_\perp$ is defined as $((d-p)/\sigma^2)^{1/4}\log^{1/a}(np)$. We upper-bound the term

$\mathbb{E}\left|\widehat{F}(x)-\widetilde{F}(x)\right|^2$ as

$$\mathbb{E}\left|\widehat{F}(x)-\widetilde{F}(x)\right|^2 \leq 2I_1+2I_2. \tag{B.1.10}$$

Stage I. We bound the term I_1 as

$$I_1 \overset{②}{\leq} \left(\frac{1}{\pi}\int_0^{t_\perp}\left[\left|\frac{D(t)}{t}\right|\times n^{-1}\left(\sum_{s=1}^{n}\left|t\left(\widehat{X}^{(s)}-x\right)\right|\right)\right]dt\right)^2 \overset{③}{\lesssim} \left(\int_0^{t_\perp}|D(t)|\,dt\right)^2,$$

where in ② we use the fact $\sin(\cdot)\leq|\cdot|$, in ③ we use the fact $|\widehat{X}^{(s)}-x|\leq 1$ for all $s, 1\leq s\leq n$.

Notice in the region $\mathcal{R}_1$, we can lower bound the function $\phi_{\widehat{w}}(\cdot)\geq c_1$ as

$$|\phi_{\widehat{w}}(t)| \overset{④}{\geq} |\phi_{\widehat{w}}(t_\perp)| = O\left[\exp\left(-\frac{c_0\sigma^2}{d-p}\cdot\frac{\sqrt{d-p}}{\sigma}\right)\right]=O(1),$$

where in ④ we use the fact such that $|\phi(\cdot)_{\widehat{w}}|$ is non-increasing. Then we invoke (Equation B.1.9) and bound $D(t)$ as $|D(t)|\lesssim\varepsilon_E(t)$, since $|\phi_{\widehat{w}}(t)|^2\vee\gamma t^a\geq|\phi_{\widehat{w}}(t)|^2\gtrsim 1$. Hence term I_1 is upper-bounded as

$$\begin{aligned} I_1 &\leq \left[\int_0^{t_\perp}\frac{\sigma^2\log^2(np)t^2}{d-p}e^{-\frac{\sigma^2t^2}{2(d-p)}}dt\right]^2 \overset{⑤}{\leq} \log^4(np)\left(\int_0^{\log^{1/a}(np)(\frac{\sigma^2}{d-p})^{1/4}}\xi^2e^{-\xi^2/2}d\xi\right)^2, \\ &\leq \frac{\sigma^2\log^{4+\frac{2}{a}}(np)}{d-p}\left(\int_0^{\infty}e^{-\xi^2/2}d\xi\right)^2 \asymp \frac{\sigma^2\log^{4+\frac{2}{a}}(np)}{d-p}, \end{aligned} \tag{B.1.11}$$

where in ⑤ we use the substitution $\xi=\sigma t/\sqrt{d-p}$.

Stage II. We define the function $\Lambda(t)$ as

$$\Lambda(t)=\frac{1}{n}\sum_{s=1}^{n}\sin\left[t\left(\widehat{X}^{(s)}-x\right)\right]-\Im\left(\phi_{\widehat{X}}(t)e^{-\mathbb{j}tx}\right),$$

and bound the term I_2 as

$$I_2 = \mathbb{E}\left|\int_{t_\perp}^{\infty} \frac{D(t)}{t}\left[\Lambda(t) + \Im\left(\phi_{\widehat{X}}(t)e^{-\mathbb{j}tx}\right)\right]\right|^2 \lesssim I_{2,1} + I_{2,2},$$

where $I_{2,1}$ and $I_{2,2}$ are defined as

$$I_{2,1} \triangleq \mathbb{E}\left|\int_{t_\perp}^{\infty} \frac{D(t)}{t}\Im\left(\phi_{\widehat{X}}(t)e^{-\mathbb{j}tx}\right)\right|^2,$$
$$I_{2,2} \triangleq \mathbb{E}\left|\int_{t_\perp}^{\infty} \frac{D(t)\Lambda(t)}{t}\right|^2.$$

Notice that within region $\mathcal{R}_2$, we can upper-bound $|D(t)|$ as $|D(t)| \lesssim \frac{\varepsilon_E(t)}{\gamma t^a}$ and hence

$$\begin{aligned}
I_{2,1} \leq & \left|\int_{t_\perp}^{\infty} \frac{\left|\phi_{\widehat{X}}(t)\right|\sqrt{\mathbb{E}|D(t)|^2}}{t}dt\right|^2 \overset{⑥}{\leq} \left|\int_{t_\perp}^{\infty} \frac{\sqrt{\mathbb{E}|D(t)|^2}}{t}dt\right|^2 \overset{⑦}{\leq} \left(\int_{t_\perp}^{\infty} \frac{\varepsilon_E(t)}{\gamma t^{1+a}}dt\right)^2 \\
= & \frac{\log^4(np)\sigma^4}{(d-p)^2\gamma^2}\left(\int_{t_\perp}^{\infty} \exp\left(-\frac{\sigma^2 t^2}{2(d-p)}\right) t^{1-a}dt\right)^2 \\
= & \frac{\log^4(np)\sigma^{2a}}{(d-p)^a\gamma^2}\left(\int_{\log^{1/a}(np)(\frac{\sigma^2}{d-p})^{1/4}}^{\infty} \xi^{1-a}e^{-\xi^2/2}d\xi\right)^2 \\
\overset{⑧}{\leq} & \frac{\log^4(np)\sigma^{2a}}{(d-p)^a\gamma^2}\log^{\frac{2}{a}-2}(np)\left(\frac{\sigma^2}{d-p}\right)^{\frac{1-a}{2}}\left(\int_0^{\infty} e^{-\xi^2/2}d\xi\right)^2 \\
\asymp & \frac{\log^{2/a}(np)\sigma}{\sqrt{d-p}},
\end{aligned}$$

where in ⑥ we use the fact $|\phi_{\widehat{X}}(\cdot)| \leq 1$, in ⑦ we use the bound $|D(t)| \leq \varepsilon_E/(\gamma t^a)$, and in ⑧ we use the assumption $a > 1$.

Afterwards, we bound term $I_{2,2}$ as

$$\begin{aligned}
I_{2,2} \leq & \ 2\mathbb{E}\left|\int_{t_\perp}^{\infty}\int_{t_\perp}^{\infty} \frac{D(u)D(v)\Lambda(u)\Lambda(v)}{uv}dudv\right| \\
\leq & \ 2\int_{t_\perp}^{\infty}\int_{t_\perp}^{\infty} \frac{\sqrt{\mathbb{E}|D(u)|^2}\sqrt{\mathbb{E}|D(v)|^2}\cdot\mathbb{E}\left(\Lambda(u)\Lambda(v)\right)}{uv}dudv.
\end{aligned}$$

According to Lemma 5.1 in [41], we can bound the term $\mathbb{E}\left(\Lambda(u)\Lambda(v)\right)$ as

$$
\begin{aligned}
&\mathbb{E}\left(\Lambda(u)\Lambda(v)\right) \\
=\ &\frac{1}{2n}\left[\Re\left[e^{\mathbb{j}(v-u)t}\phi_{\widehat{X}}(u-v)\right]-\Re\left[e^{-\mathbb{j}(u+v)x}\phi_{\widehat{X}}(u+v)\right]-2\Im\left[e^{-\mathbb{j}ux}\phi_{\widehat{X}}(u)\right]\cdot\Im\left[e^{-\mathbb{j}vx}\phi_{\widehat{X}}(s)\right]\right] \\
\leq\ &\frac{1}{2n}\left[\left|\phi_{\widehat{X}}(u+v)\right|+\left|\phi_{\widehat{X}}(u-v)\right|+2\left|\phi_{\widehat{X}}(u)\right|\left|\phi_{\widehat{X}}(v)\right|\right]\overset{⑨}{\leq}\frac{2}{n},
\end{aligned}
$$

where in ⑨ we use the fact $|\phi_{\widehat{X}}(\cdot)|\leq 1$.

Following the same strategy as above, we can upper-bound $|D(t)|$ as $|D(t)|\lesssim\frac{\varepsilon_E(t)}{\gamma t^a}$ and hence

$$
\sqrt{\mathbb{E}|D(u)|^2}\sqrt{\mathbb{E}|D(v)|^2}\leq\frac{\varepsilon_E(u)\varepsilon_E(v)}{\gamma^2u^av^a}.
$$

Combing the above then yields the bound

$$
I_{2,2}\lesssim\frac{1}{n\gamma^2}\int_{t_\perp}^{\infty}\int_{t_\perp}^{\infty}\frac{\varepsilon_E(u)\varepsilon_E(v)}{u^{1+a}v^{1+a}}dudv=\frac{\log^{4/a}(np)\sigma^{2+a}}{n(d-p)}.
$$

To sum up, we have

$$
I_2=I_{2,1}+I_{2,2}\lesssim\ \frac{\log^{2/a}(np)\sigma^{1+\frac{a}{2}}}{\sqrt{d-p}}+\ \frac{\log^{4/a}(np)\sigma^2}{n(d-p)}\asymp\frac{\log^{2/a}(np)\sigma}{\sqrt{d-p}},
$$

and complete the proof by combining it with (Equation B.1.10) and (Equation B.1.11).

□

Lemma 37. *Under the setting of Theorem 3, we can upper-bound the deviation* $\left|\widetilde{F}(x)-F(x)\right|$ *as*

$$
\mathbb{E}\left|\widetilde{F}(x)-F(x)\right|^2\lesssim\ \frac{(\log(np))^2}{(d-p)^{\frac{a}{4}}}+\left(\frac{\sigma^2}{d-p}\right)^{\frac{2\alpha+1}{4}}+\frac{1}{n},
$$

when setting $\gamma\asymp\log(np)\left(\frac{\sigma^2}{d-p}\right)^{a/4}$.

Proof. We decompose the deviation $\mathbb{E}|\widetilde{F}(x) - F(x)|^2$ as the the bias and variance, which are defined respectively as

$$\begin{aligned}\text{Bias} &\triangleq \left|\mathbb{E}\widetilde{F}(x) - F(x)\right|^2, \\ \text{Variance} &\triangleq \mathbb{E}\left|\widetilde{F}(x) - \mathbb{E}\widetilde{F}(x)\right|^2.\end{aligned}$$

The following context separately bound the bias and variance.

Bounding bias. We rewrite the difference $\mathbb{E}\widetilde{F}(x) - F(x)$ as

$$\mathbb{E}\widetilde{F}(x) - F(x) = \frac{1}{\pi}\int_0^\infty \frac{1}{t}\Im\left[\left(\frac{|\phi_{\widehat{w}}(t)|^2\,\phi_X(t)}{|\phi_{\widehat{w}}(t)|^2 \vee \gamma t^a} - \phi_X(t)\right)e^{-\mathbb{j}tx}\right]dt,$$

which yields

$$\begin{aligned}\text{Bias} &\leq \frac{1}{\pi^2}\left[\int_0^\infty \frac{|\phi_X(t)|}{t}\Im\left[\left(\frac{|\phi_{\widehat{w}}(t)|^2}{|\phi_{\widehat{w}}(t)|^2 \vee \gamma t^a} - 1\right)e^{-\mathbb{j}tx}\right]dt\right]^2 \\ &\leq \frac{1}{\pi^2}\left[\int_0^\infty \frac{|\phi_X(t)|}{t}\left|1 - \frac{|\phi_{\widehat{w}}(t)|^2}{|\phi_{\widehat{w}}(t)|^2 \vee \gamma t^a}\right|dt\right]^2 \\ &\lesssim \left[\int_0^{t_\square} \frac{|\phi_X(t)|}{t}\left|1 - \frac{|\phi_{\widehat{w}}(t)|^2}{|\phi_{\widehat{w}}(t)|^2 \vee \gamma t^a}\right|dt + \int_{t_\square}^\infty \frac{|\phi_X(t)|}{t}\left|1 - \frac{|\phi_{\widehat{w}}(t)|^2}{|\phi_{\widehat{w}}(t)|^2 \vee \gamma t^a}\right|dt\right]^2 \\ &\leq J_1^2 + J_2^2,\end{aligned}$$

where $t_\square$ is defined as $c_0\left(\frac{d-p}{\sigma^2}\right)^{1/8}$, and terms J_1 and J_2 are defined as

$$\begin{aligned}J_1 &\triangleq \int_0^{t_\square} \frac{|\phi_X(t)|}{t}\left|1 - \frac{|\phi_{\widehat{w}}(t)|^2}{|\phi_{\widehat{w}}(t)|^2 \vee \gamma t^a}\right|dt, \\ J_2 &\triangleq \int_{t_\square}^\infty \frac{|\phi_X(t)|}{t}\left|1 - \frac{|\phi_{\widehat{w}}(t)|^2}{|\phi_{\widehat{w}}(t)|^2 \vee \gamma t^a}\right|dt,\end{aligned}$$

respectively. For the term J_1, we have

$$1-\frac{|\phi_{\widehat{w}}(t)|^2}{|\phi_{\widehat{w}}(t)|^2\vee\gamma t^a}\leq\frac{\left(|\phi_{\widehat{w}}(t)|^2\vee\gamma t^a\right)-|\phi_{\widehat{w}}(t)|^2}{|\phi_{\widehat{w}}(t)|^2\vee\gamma t^a}\overset{①}{\leq}\frac{\gamma t^a}{|\phi_{\widehat{w}}(t)|^2\vee\gamma t^a}\overset{②}{\leq}\frac{\gamma t^a}{c_R},$$

where in ① we use the relation $|\phi_{\widehat{w}}(t)|^2\vee\gamma t^a-|\phi_{\widehat{w}}(t)|^2\leq\gamma t^a$; in ② we use the fact $|\phi_{\widehat{w}}(t)|^2\vee\gamma t^a\geq c_R$ in the regime $[0,t_\square)$, which can be easily verified. Then we obtain

$$J_1\leq\int_0^{t_\square}\frac{|\phi_X(t)|}{t}\frac{\gamma t^a}{c_R}dt=\frac{\gamma}{c_R}\int_0^{t_\square}t^{a-1}dt=\frac{\gamma}{c_R}\frac{t_\square^a}{a}\asymp\frac{\sigma^{\frac{a}{4}}\log(np)}{(d-p)^{\frac{a}{8}}a}. \tag{B.1.12}$$

Afterwards, we bound term J_2 as

$$J_2\leq\int_{t_\square}^{\infty}\frac{|\phi_X(t)|}{t}dt\overset{③}{\lesssim}t_\square^{-(2\alpha+1)/16}\asymp\left(\frac{\sigma^2}{d-p}\right)^{\frac{2\alpha+1}{8}}, \tag{B.1.13}$$

where in ③ we use the Lemma 6 from [41] since $\phi_X(\cdot)$ satisfies the Assumption 2. Combining (Equation B.1.12) and (Equation B.1.13) then yields

$$\text{Bias}\lesssim\frac{(\log(np))^2}{(d-p)^{\frac{a}{4}}}+\left(\frac{\sigma^2}{d-p}\right)^{\frac{2\alpha+1}{4}}. \tag{B.1.14}$$

Bounding variance. We bound the Var$\widetilde{F}(x)$ as

$$\begin{aligned}
&\text{Var}\widetilde{F}(x)\\
=\;&\text{Var}\left[\frac{1}{\pi}\int_0^{\infty}\frac{1}{t}\Im\left(\frac{\phi_{\widehat{w}}(-t)}{|\phi_{\widehat{w}}(t)|^2\vee\gamma t^a}\widehat{\phi}_{\widehat{X}}(t)e^{-\mathbb{j}tx}\right)dt\right]\\
\overset{④}{\leq}\;&\frac{1}{n\pi^2}\mathbb{E}\left[\int_0^{\infty}\frac{1}{t}\Im\left(\frac{\phi_{\widehat{w}}(-t)}{|\phi_{\widehat{w}}(t)|^2\vee\gamma t^a}e^{\mathbb{j}t(\widehat{X}-x)}\right)dt\right]^2\leq\frac{2}{n\pi^2}\left(K_1+K_2\right),
\end{aligned}$$

where in ④ we use the bound Var $(\cdot)\leq\mathbb{E}(\cdot)^2$, and the terms K_1 and K_2 are defined as

$$\begin{aligned}
K_1&\triangleq\mathbb{E}\left[\int_0^{t_\perp}\frac{1}{t}\Im\left(\frac{\phi_{\widehat{w}}(-t)}{|\phi_{\widehat{w}}(t)|^2\vee\gamma t^a}e^{\mathbb{j}t(\widehat{X}-x)}\right)dt\right]^2,\\
K_2&\triangleq\mathbb{E}\left[\int_{t_\perp}^{\infty}\frac{1}{t}\Im\left(\frac{\phi_{\widehat{w}}(-t)}{|\phi_{\widehat{w}}(t)|^2\vee\gamma t^a}e^{\mathbb{j}t(\widehat{X}-x)}\right)dt\right]^2,
\end{aligned}$$

and $t_\perp$ is defined as $(2\gamma)^{-1/a}$. First, we bound K_1 as

$$\begin{aligned}
K_1 =& \ \mathbb{E}\left|\int_0^{t_\perp} \frac{1}{t}\Im\left(\phi_{\widehat{w}}(-t)e^{\mathbb{j}t(\widehat{X}-x)}\left(1+\sum_{k=1}^{\infty}\left(1-\left(|\phi_{\widehat{w}}(t)|^2\vee\gamma t^a\right)\right)^k\right)\right)dt\right|^2 \\
\lesssim& \ \mathbb{E}\left|\int_0^{t_\perp} \frac{1}{t}\Im\left(\phi_{\widehat{w}}(-t)e^{\mathbb{j}t(\widehat{X}-x)}\right)dt\right|^2 + \mathbb{E}\left|\int_0^{t_\perp}\frac{1}{t}\sum_{k=1}^{\infty}\left(1-\left(|\phi_{\widehat{w}}(t)|^2\vee\gamma t^a\right)\right)^k dt\right|^2 \\
\overset{⑤}{\leq}& \ \mathbb{E}\sup_{\tau>0}\left|\int_0^{\tau}\frac{\sin t}{t}dt\right|^2 + \ \mathbb{E}\left|\int_0^{t_\perp}\frac{1}{t}\sum_{k=1}^{\infty}\left(1-|\phi_{\widehat{w}}(t)|^2\right)^k dt\right|^2 \\
\leq& \ 3+\mathbb{E}\left[\int_0^{t_\perp}\frac{1}{t}\sum_{k=1}^{\infty}\left(\frac{\sigma^2t^2}{d-p}\right)^k\right]^2 \overset{⑥}{\lesssim} 1,
\end{aligned} \tag{B.1.15}$$

where in ⑤ we use the fact $|\phi_{\widehat{w}}(t)|^2\vee\delta t^a \geq 1-\frac{c_1\sigma^2t^2}{d-p}$ for $t\in(0,t_\perp)$, and in ⑥ we use $\sigma^2t_\perp^2 \asymp \sqrt{d-p}(\log(np))^{-\frac{2}{a}} \leq \frac{d-p}{2}$.

Then we expand the term K_2 as a product of two terms reading as

$$\begin{aligned}
K_2 =& \ \mathbb{E}\left[\int_{t_\perp}^{\infty}\int_{t_\perp}^{\infty}\frac{1}{uv}\Im\left(\frac{\phi_{\widehat{w}}(-u)\phi_{\widehat{w}}(-v)e^{\mathbb{j}(u+v)(\widehat{X}-x)}}{\left[|\phi_{\widehat{w}}(u)|^2\vee\gamma u^a\right]\left[|\phi_{\widehat{w}}(v)|^2\vee\gamma v^a\right]}\right)dudv\right] \\
\leq& \ \mathbb{E}\left[\int_{t_\perp}^{\infty}\int_{t_\perp}^{\infty}\frac{\phi_{\widehat{w}}(-u)\phi_{\widehat{w}}(-v)}{uv}\cdot\frac{1}{|\phi_{\widehat{w}}(u)|^2\vee\gamma u^a}\cdot\frac{1}{|\phi_{\widehat{w}}(v)|^2\vee\gamma v^a}dudv\right] \\
\leq& \ \frac{1}{\gamma^2}\mathbb{E}\left[\int_{t_\perp}^{\infty}\frac{1}{t^{a+1}}dt\right]^2 = \ \frac{1}{a^2\gamma^2t_\perp^{2a}} \asymp 1.
\end{aligned} \tag{B.1.16}$$

Combining (Equation B.1.15) and (Equation B.1.16) generates

$$\mathrm{Var}\widetilde{F}(x) \lesssim n^{-1}. \tag{B.1.17}$$

And the proof is completed by combining (Equation B.1.14) and (Equation B.1.17).

□

B.2 Proof of Theorem 4

B.2.1 Notations

We assume that the correct estimation of $m_i = 0$ and $v_i = 1$ w.l.o.g. Let

$$h_i(x) = \Phi^{-1}\left(F_i(x)\right);$$
$$g_i(x) = h_i^{-1}(x),$$

where $(\cdot)^{-1}$ denotes the inverse of the function. For the conciseness of the notation, we define $\widehat{\varphi}_i^{(s)}$, $\widetilde{\varphi}_i^{(s)}$, and $\varphi_i^{(s)}$ as

$$\widehat{\varphi}_i^{(s)} = \widehat{h}_i(\widehat{X}_i^{(s)});$$
$$\widetilde{\varphi}_i^{(s)} = \widehat{h}_i(X_i^{(s)});$$
$$\varphi_i^{(s)} = h_i(X_i^{(s)}).$$

The (i,j)th entries of the corresponding covariance matrices $\widehat{\mathbf{\Sigma}}_n^{\text{non-param}}$, $\widetilde{\mathbf{\Sigma}}_n^{\text{non-param}}$, and $\mathbf{\Sigma}_n^{\text{non-param}}$ are written as

$$\left(\widehat{\mathbf{\Sigma}}_n^{\text{non-param}}\right)_{i,j} = \frac{1}{n}\sum_{s=1}^{n}\widehat{\varphi}_i^{(s)}\widehat{\varphi}_j^{(s)} - \widehat{\mu}_i\widehat{\mu}_j;$$
$$\left(\widetilde{\mathbf{\Sigma}}_n^{\text{non-param}}\right)_{i,j} = \frac{1}{n}\sum_{s=1}^{n}\widetilde{\varphi}_i^{(s)}\widetilde{\varphi}_j^{(s)} - \widetilde{\mu}_i\widetilde{\mu}_j;$$
$$\left(\mathbf{\Sigma}_n^{\text{non-param}}\right)_{i,j} = \frac{1}{n}\sum_{s=1}^{n}\varphi_i^{(s)}\varphi_j^{(s)} - \mu_i\mu_j.$$

Moreover, we define two regions $\mathcal{R}_E$ and $\mathcal{R}_M$ as

$$\begin{aligned}\mathcal{R}_E \triangleq &\left[-c_U\sqrt{\log(n\vee(d-p))}, -c_L\sqrt{\log n\vee\log(d-p)}\right)\\ &\bigcup\left(c_L\sqrt{\log(n\vee(d-p))}, c_U\sqrt{\log n\vee\log(d-p)}\right];\\ \mathcal{R}_M \triangleq &\left[-c_L\sqrt{\log(n\vee(d-p))}, c_L\sqrt{\log(n\vee(d-p))}\right].\end{aligned} \tag{B.2.1}$$

B.2.2 Main Proof

Proof. We bound the deviation between $\mathbf{\Sigma}_n^{\text{non-param}}$ and $\widehat{\mathbf{\Sigma}}_n^{\text{non-param}}$ as

$$\left\|\mathbf{\Sigma}_n^{\text{non-param}} - \widehat{\mathbf{\Sigma}}_n^{\text{non-param}}\right\|_\infty \leq \underbrace{\left\|\mathbf{\Sigma}_n^{\text{non-param}} - \widetilde{\mathbf{\Sigma}}_n^{\text{non-param}}\right\|_\infty}_{\triangleq T_1} + \underbrace{\left\|\widetilde{\mathbf{\Sigma}}_n^{\text{non-param}} - \widehat{\mathbf{\Sigma}}_n^{\text{non-param}}\right\|_\infty}_{\triangleq T_2}.$$

Step I. For the first term T_1, we invoke the triangle inequality and have

$$\left\|\mathbf{\Sigma}_n^{\text{non-param}} - \widetilde{\mathbf{\Sigma}}_n^{\text{non-param}}\right\|_\infty \leq \max_{i,j} \frac{1}{n}\left|\sum_{s=1}^n \widetilde{\varphi}_i^{(s)}\widetilde{\varphi}_j^{(s)} - \varphi_i^{(s)}\varphi_j^{(s)}\right| + \|\mu_i\mu_j - \widetilde{\mu}_i\widetilde{\mu}_j\|_\infty.$$

Following a similar strategy that is used in [25], we focus on the first term as the second term is of higher order.

We bound the value of $\max_{i,j} n^{-1}\left|\sum_{s=1}^n \widetilde{\varphi}_i^{(s)}\widetilde{\varphi}_j^{(s)} - \varphi_i^{(s)}\varphi_j^{(s)}\right|$ as

$$\begin{aligned}
&\mathbb{P}\left(\max_{i,j} n^{-1}\left|\sum_{s=1}^n \widetilde{\varphi}_i^{(s)}\widetilde{\varphi}_j^{(s)} - \varphi_i^{(s)}\varphi_j^{(s)}\right| \geq \vartheta\right) \\
\leq\ & p^2\mathbb{E}\left[\left(n^{-1}\left|\sum_{s=1}^n \widetilde{\varphi}_i^{(s)}\widetilde{\varphi}_j^{(s)} - \varphi_i^{(s)}\varphi_j^{(s)}\right| \geq \vartheta\right)\mathbb{1}\left(\varphi_i^{(s)} \in \mathcal{R}_E \bigcup \mathcal{R}_M, \forall\, 1 \leq s \leq n, 1 \leq i \leq p\right)\right] \\
&+ np\mathbb{E}\mathbb{1}\left(\varphi_i^{(s)} \notin \mathcal{R}_E \bigcap \mathcal{R}_M,\ \exists\, 1 \leq s \leq n, 1 \leq i \leq p\right).
\end{aligned}$$

Following a classical procedure as in [140], we can show the second probability $\mathbb{E}\mathbb{1}\left(\varphi_i^{(s)} \notin \mathcal{R}_E \bigcap \mathcal{R}_M\right)$ is no greater than $e^{-c_0(n\wedge(d-p))}$. For the conciseness of notation, we define the deviation $\delta_{i,j}^{(s)}$ as

$$\delta_{i,j}^{(s)} = \widetilde{\varphi}_i^{(s)}\widetilde{\varphi}_j^{(s)} - \varphi_i^{(s)}\varphi_j^{(s)}.$$

Then the summary $n^{-1}\left(\sum_{s=1}^n \widetilde{\varphi}_i^{(s)}\widetilde{\varphi}_j^{(s)} - \varphi_i^{(s)}\varphi_j^{(s)}\right)\mathbb{1}\left(\varphi_i^{(s)} \in \mathcal{R}_E \bigcup \mathcal{R}_M, \forall\, 1 \leq s \leq n, 1 \leq i \leq p\right)$

can be decomposed as

$$\frac{1}{n}\sum_{s=1}^{n}\delta_{i,j}^{(s)} = \underbrace{\frac{1}{n}\sum_{s=1}^{n}\delta_{i,j}^{(s)}\mathbb{1}[\mathcal{C}_1^{(s)}(i,j)]}_{\triangleq T_{1,1}} + \underbrace{\frac{1}{n}\sum_{s=1}^{n}\delta_{i,j}^{(s)}\mathbb{1}[\mathcal{C}_2^{(s)}(i,j)]}_{\triangleq T_{1,2}} + \underbrace{\frac{2}{n}\sum_{s=1}^{n}\delta_{i,j}^{(s)}\mathbb{1}[\mathcal{C}_3^{(s)}(i,j)]}_{\triangleq T_{1,3}},$$

where the events $\mathcal{C}_1^{(s)}(i,j)$, $\mathcal{C}_2^{(s)}(i,j)$, and $\mathcal{C}_3^{(s)}(i,j)$ are defined as

$$\begin{aligned}
\mathcal{C}_1^{(s)}(i,j) &\triangleq \left\{\varphi_i^{(s)} \in \mathcal{R}_E, \varphi_j^{(s)} \in \mathcal{R}_E\right\};\\
\mathcal{C}_2^{(s)}(i,j) &\triangleq \left\{\varphi_i^{(s)} \in \mathcal{R}_M, \varphi_j^{(s)} \in \mathcal{R}_M\right\};\\
\mathcal{C}_3^{(s)}(i,j) &\triangleq \left\{\varphi_i^{(s)} \in \mathcal{R}_E, \varphi_j^{(s)} \in \mathcal{R}_M\right\},
\end{aligned}$$

respectively, where the definitions of $\mathcal{R}_E$ and $\mathcal{R}_M$ can be found in (Equation B.2.1).

In the following, we will separately bound the three terms and show $n^{-1}\left|\sum_{s=1}^{n}\delta_{i,j}^{(s)}\right| \lesssim \vartheta \triangleq \vartheta_1 \vee \vartheta_2$, where the quantities ϑ_1 and ϑ_2 are defined in (Equation B.2.2) and (Equation B.2.4), respectively. The analysis of the first term $T_{1,1}$ and second term $T_{1,2}$ is deferred to Lemma 38 and Lemma 39, respectively; while that of the third term $T_{1,3}$ is omitted due to their similarities of Lemma 38 and Lemma 39.

Step II. The second term T_2 is upper-bounded in Lemma 40. The analysis is in the same spirit as the above procedure but requires some modifications. □

Lemma 38. *We have*

$$\frac{1}{n}\left|\sum_{s=1}^{n}\delta_{i,j}^{(s)}\mathbb{1}[\mathcal{C}_1^{(s)}(i,j)]\right| \leq 2c_0\left[n^{-c_1} \vee (d-p)^{-c_1}\right](\log n \vee \log(d-p))^{\frac{3}{2}} \triangleq \vartheta_1, \quad \text{(B.2.2)}$$

with probability exceeding $1 - c_2 n^{-c_3} \wedge (d-p)^{-c_4} - c_5 n^{-c_6}$*, where the parameters* c_i *are some fixed constant,* $0 \leq i \leq 6$*.*

Proof. Invoking the union bound, we obtain

$$
\begin{aligned}
&\mathbb{P}\left(\frac{1}{n}\left|\sum_{s=1}^{n}\delta_{i,j}^{(s)}\mathbb{1}[\mathcal{C}_1^{(s)}(i,j)]\right| \gtrsim 2c_0\left[n^{-c_1}\vee(d-p)^{-c_1}\right](\log n\vee\log(d-p))^{\frac{3}{2}}\right)\\
\overset{①}{\leq}\ &\underbrace{\mathbb{E}\mathbb{1}\left(\max_s\left|\delta_{i,j}^{(s)}\right|\gtrsim(\log n\vee\log(d-p))\right)\mathbb{1}[\mathcal{C}_1^{(s)}(i,j)]}_{P_1}+\underbrace{\mathbb{P}\left(\frac{1}{n}\sum_{s=1}^{n}\mathbb{1}[\mathcal{C}_1^{(s)}(i,j)]\geq\vartheta\right)}_{P_2},
\end{aligned}
$$

where ϑ is defined as

$$
\vartheta = 2c_0\left[n^{-c_1}\vee(d-p)^{-c_1}\right]\sqrt{\log n\vee\log(d-p)}, \tag{B.2.3}
$$

and in ① we use the union bound.

With the relation

$$
\left|\delta_{i,j}^{(s)}\right|\leq\left|\left(\widetilde{\varphi}_i^{(s)}-\varphi_i^{(s)}\right)\left(\widetilde{\varphi}_j^{(s)}-\varphi_j^{(s)}\right)\right|+\left|\varphi_i^{(s)}\left(\widetilde{\varphi}_j^{(s)}-\varphi_j^{(s)}\right)\right|+\left|\varphi_j^{(s)}\left(\widetilde{\varphi}_i^{(s)}-\varphi_i^{(s)}\right)\right|,
$$

we can upper bound the probability P_1 as

$$
\begin{aligned}
P_1\leq\ &np\mathbb{E}\mathbb{1}\left(\varphi_i^{(s)}\leq c_U\sqrt{\log p\vee\log(d-p)}\mathbb{1}[\mathcal{C}_1^{(s)}(i,j)],\ \widetilde{\varphi}_i^{(s)}\lesssim c_U\sqrt{\log n\vee\log(d-p)}\right)\\
\overset{②}{\lesssim}\ &n^{-c}\wedge(d-p)^{-c},
\end{aligned}
$$

where ② is due to Lemma 41.

While for probability P_2, we have

$$
\begin{aligned}
&\mathbb{P}\left(\sum_{s=1}^{n}\mathbb{1}[\mathcal{C}_1^{(s)}(i,j)]\geq n\vartheta\right)\leq\mathbb{P}\left(\frac{1}{n}\sum_{s=1}^{n}\mathbb{1}[\varphi_i^{(s)}\in\mathcal{R}_E]\geq\vartheta\right)\\
=\ &\mathbb{P}\left(\frac{1}{n}\sum_{s=1}^{n}\left[\mathbb{1}[\varphi_i^{(s)}\in\mathcal{R}_E]-\mathbb{E}\mathbb{1}\left(\varphi_i^{(s)}\in\mathcal{R}_E\right)\right]\geq\ \vartheta-\frac{1}{n}\left[\sum_{s=1}^{n}\mathbb{E}\mathbb{1}\left(\varphi_i^{(s)}\in\mathcal{R}_E\right)\right]\right)\\
\overset{③}{\leq}\ &\exp\left(-\frac{n}{2}\left[\vartheta-\mathbb{P}\left(\varphi_i^{(s)}\in\mathcal{R}_E\right)\right]^2\right),
\end{aligned}
$$

where in ③ we use the Hoeffding's inequality (cf. Thm. 2.8 in [140]). Notice that the

probability $\mathbb{P}\left(\varphi_i^{(s)} \in \mathcal{R}_E\right)$ can be bounded as

$$\begin{aligned}
&\mathbb{P}\left(\varphi_i^{(s)} \in \mathcal{R}_E\right) \\
=\ & \frac{2}{\sqrt{2\pi}} \int_{c_L\sqrt{\log n \vee \log(d-p)}}^{c_U\sqrt{\log n \vee \log(d-p)}} e^{-t^2/2} dt \lesssim \sqrt{\frac{2}{\pi}} e^{-\frac{c_L}{2}(\log n \vee \log(d-p))} \sqrt{\log n \vee \log(d-p)} \\
\leq\ & c_0 \left[n^{-c_1} \vee (d-p)^{-c_1}\right] \sqrt{\log n \vee \log(d-p)},
\end{aligned}$$

where $0 < c_1 < 1/2$ is some fixed positive constant. Recalling the value of ϑ in (Equation B.2.3), we have

$$\mathbb{P}\left(\sum_{s=1}^{n} \mathbb{1}[\mathcal{C}_1^{(s)}(i,j)] \geq n\vartheta\right) \leq \exp\left(-c_0 n^{1-2c_1} \log n\right) \ll n^{-c},$$

and complete the proof.

□

Lemma 39. *We have*

$$\frac{1}{n}\left|\sum_{s=1}^{n} \delta_{i,j}^{(s)} \mathbb{1}\left(C_2^{(s)}(i,j)\right)\right| \lesssim \frac{\sqrt{\log n}}{n^{1/4}} \vee \frac{\sqrt{\log(d-p)}}{(d-p)^{\beta/4}} \triangleq \vartheta_2, \tag{B.2.4}$$

with probability exceeding the probability $1 - p^2 \exp\left(-\frac{c_0\sqrt{n}}{\log^2 n} - \frac{c_1 n \log^4(np)}{\log(d-p)(d-p)^{\beta/2}}\right) - p^2 n^{-c_3} - 2p^3 e^{-c_4 p} - 4n^{-c_5} p^{-c_6}$*, where* β *is defined as* $\frac{1}{2} \wedge \frac{a}{4} \wedge \frac{2\alpha+1}{4}$.

Proof. For each term $\delta_{i,j}^{(s)}$, we can decompose it as

$$\delta_{i,j}^{(s)} = \left(\widetilde{\varphi}_i^{(s)} - \varphi_i^{(s)}\right)\left(\widetilde{\varphi}_j^{(s)} - \varphi_j^{(s)}\right) + \varphi_i^{(s)}\left(\widetilde{\varphi}_j^{(s)} - \varphi_j^{(s)}\right) + \varphi_j^{(s)}\left(\widetilde{\varphi}_i^{(s)} - \varphi_i^{(s)}\right).$$

Then we can decompose the summary as

$$\begin{aligned}\frac{1}{n}\left|\sum_{s=1}^{n}\delta_{i,j}^{(s)}\mathbb{1}\left(C_2^{(s)}(i,j)\right)\right| \leq\ & \frac{1}{n}\sum_{s=1}^{n}\left|\left(\widehat{\varphi}_i^{(s)}-\widetilde{\varphi}_i^{(s)}\right)\left(\widehat{\varphi}_j^{(s)}-\widetilde{\varphi}_j^{(s)}\right)\mathbb{1}\left(C_2^{(s)}(i,j)\right)\right| \\ & + \frac{1}{n}\sum_{s=1}^{n}\left|\widetilde{\varphi}_i^{(s)}\left(\widehat{\varphi}_j^{(s)}-\widetilde{\varphi}_j^{(s)}\right)\mathbb{1}\left(C_2^{(s)}(i,j)\right)\right| \\ & + \frac{1}{n}\sum_{s=1}^{n}\left|\widetilde{\varphi}_j^{(s)}\left(\widehat{\varphi}_i^{(s)}-\widetilde{\varphi}_i^{(s)}\right)\mathbb{1}\left(C_2^{(s)}(i,j)\right)\right|.\end{aligned}$$

Our next goal is to investigate the behavior of $\sup_i\left|\widetilde{\varphi}_i^{(s)}-\widehat{\varphi}_i^{(s)}\right|\mathbb{1}\left[C_2^{(s)}(i,j)\right]$. Define the an event $\mathcal{E}_F(\cdot)$ as

$$\mathcal{E}_F(i)=\left\{\delta_{n,d,p}\leq\widehat{F}_i\leq 1-\delta_{n,d,p}\right\},\ \ 1\leq i\leq n.$$

We have

$$\begin{aligned}&\mathbb{P}\left(\frac{1}{n}\left|\sum_{s=1}^{n}\delta_{i,j}^{(s)}\mathbb{1}\left(C_2^{(s)}(i,j)\right)\right|\geq\vartheta_2\right)\leq\mathbb{P}\left(\sup_i\left|\widetilde{\varphi}_i^{(s)}-\widehat{\varphi}_i^{(s)}\right|\mathbb{1}\left[C_2^{(s)}(i,j)\right]\geq\vartheta_2\right)\\ \leq\ & p^2\underbrace{\mathbb{E}\mathbb{1}\left(\mathbb{1}\left(C_2^{(s)}(i,j)\right)\overline{\mathcal{E}}_F(i)\right)}_{T_1}+p^2\underbrace{\mathbb{E}\mathbb{1}\left(\left(\left|\widetilde{\varphi}_i^{(s)}-\widehat{\varphi}_i^{(s)}\right|\mathbb{1}\left(C_2^{(s)}(i,j)\right)\geq\vartheta_2\right)\bigcup\mathcal{E}_F(i)\right)}_{T_2}.\end{aligned}$$

Easily we can verify that $\delta_{n,d,p}$ satisfy the relation

$$2\delta_{n,d,p}\leq 1-\Phi\left(c_L\sqrt{\log n\vee\log(d-p)}\right)-\sqrt{\varepsilon_x},$$

where ε_x is defined in (Equation 3.5.2). Invoking Lemma 42, we can bound term T_1 as

$$\begin{aligned}T_1\leq\ & 2\exp\left(-2n\left(1-\delta_{n,d,p}-\Phi\left(c_L\sqrt{\log n\vee\log(d-p)}\right)-\sqrt{\varepsilon_x}\right)^2\right)\leq 2\exp(-2n\delta_{n,d,p}^2)\\ \lesssim\ & 2\exp\left(-\frac{c_0\sqrt{n}}{\log^2 n}-\frac{c_1 n\log^4(np)}{\log(d-p)(d-p)^{\beta/2}}\right).\end{aligned}$$

Conditional on event $\mathcal{E}_F(i)$, we study the term T_1 by investigating the difference $\widetilde{\varphi}_i^{(s)}-\widehat{\varphi}_i^{(s)}$. We assume $\widehat{F}_i^{\text{tr}}(X_i^{(s)})\geq F_i(X_i^{(s)})$ w.l.o.g. According to the mean value theorem, we have

$$\widetilde{\varphi}_i^{(s)} - \varphi_i^{(s)} = \Phi^{-1}\left(\widehat{F}_i^{\text{tr}}(X_i^{(s)})\right) - \Phi^{-1}\left(F_i(X_i^{(s)})\right) = \left(\Phi^{-1}\right)'(\xi)\left|\widehat{F}_i^{\text{tr}}(X_i^{(s)}) - F_i(X_i^{(s)})\right|,$$

where ξ is some point such that $F_i(X_i^{(s)}) \le \xi \le \widehat{F}_i^{\text{tr}}(X_i^{(s)})$. Due to the fact that $X_i^{(s)} \in \mathcal{R}_M$ and conditional on event $\mathcal{E}_F(i)$, we conclude $\delta_n \le \xi \le 1 - \delta_n$ and hence

$$\begin{aligned}\left|\left(\Phi^{-1}(\xi)\right)'\right| \le & \left|\left(\Phi^{-1}(1-\delta_{n,d,p})\right)'\right| \vee \left|\left(\Phi^{-1}(\delta_{n,d,p})\right)'\right| = \left|\left(\Phi^{-1}(1-\delta_{n,d,p})\right)'\right| \\ = & \frac{1}{\phi\left(\Phi^{-1}(1-\delta_{n,d,p})\right)} \le \exp\left[\frac{1}{2}\left(\Phi^{-1}(1-\delta_{n,d,p})\right)^2\right] \overset{①}{\le} \frac{1}{\delta_{n,d,p}},\end{aligned}$$

where ① is due to Lemma 53 and the fact that $\delta_{n,d,p} \to 0$. Set ϑ_2 such that

$$\vartheta_2 \delta_{n,d,p} \ge (\log n)\varepsilon_x + \frac{c_0}{\sqrt{n}} + c_1\sqrt{\varepsilon_x},$$

where ε_x is defined in (Equation 3.5.2). We invoke Theorem 3 and conclude

$$T_1 \le \mathbb{P}\left(\left|\widehat{F}_i^{\text{tr}}(X_i^{(s)}) - F_i(X_i^{(s)})\right| \ge \delta_{n,d,p}\vartheta_2\right) \le n^{-c_3} + 2pe^{-c_4 p} + 4n^{-c_5}p^{-c_6}.$$

Recalling the definition of $\delta_{n,d,p}$ in (Equation 3.6.2), we conclude ϑ_2 to be approximately

$$\vartheta_2 \asymp \frac{\sqrt{\log n}}{n^{1/4}} \vee \frac{\sqrt{\log(d-p)}}{(d-p)^{\beta/4}},$$

where β is defined as $\frac{1}{2} \wedge \frac{a}{4} \wedge \frac{2\alpha+1}{4}$. □

Lemma 40. *Under the Assumption 3, we have*

$$\left\|\widehat{\mathbf{\Sigma}}_n^{\text{non-param}} - \widetilde{\mathbf{\Sigma}}_n^{\text{non-param}}\right\|_\infty \tag{B.2.5}$$

$$\lesssim \underbrace{\sqrt{\log n \vee \log(d-p)}\left(\frac{\sqrt{\log n}}{n^{1/4}} \vee \frac{\sqrt{\log(d-p)}}{(d-p)^{\beta/4}}\right) + \frac{L\sigma\left(\log n \vee \log(d-p)\right)}{c_0 \log^2(np)(d-p)^{1/4}}}_{\triangleq \vartheta_3}, \tag{B.2.6}$$

with probability exceeding $1 - e^{-c_0(n\wedge(d-p))} - e^{-c_1 n}$.

Proof. The proof conditions on the event

$$\left|\widetilde{\varphi}_i^{(s)}\right| \lesssim c_U \sqrt{\log n \vee \log(d-p)},$$

holds for all s and i with probability exceeding $1 - e^{-c_0(n\wedge(d-p))}$.

Following the same argument as in Theorem 4, our analysis focus on the error $n^{-1}\sum_{s=1}^n \left(\widehat{\varphi}_i^{(s)}\widehat{\varphi}_j^{(s)} - \varphi_i^{(s)}\varphi_j^{(s)}\right)$. Adopting the decomposition such that

$$\widehat{\varphi}_i^{(s)}\widehat{\varphi}_j^{(s)} - \widetilde{\varphi}_i^{(s)}\widetilde{\varphi}_j^{(s)} = \widetilde{\varphi}_i^{(s)}\left(\widehat{\varphi}_j^{(s)} - \widetilde{\varphi}_j^{(s)}\right) + \widetilde{\varphi}_j^{(s)}\left(\widehat{\varphi}_i^{(s)} - \widetilde{\varphi}_i^{(s)}\right) + \left(\widehat{\varphi}_i^{(s)} - \widetilde{\varphi}_i^{(s)}\right)\left(\widehat{\varphi}_j^{(s)} - \widetilde{\varphi}_j^{(s)}\right),$$

we have

$$\frac{1}{n}\sum_{s=1}^n \left(\widehat{\varphi}_i^{(s)}\widehat{\varphi}_j^{(s)} - \varphi_i^{(s)}\varphi_j^{(s)}\right) = \underbrace{\frac{1}{n}\sum_{s=1}^n \widetilde{\varphi}_i^{(s)}\left(\widehat{\varphi}_j^{(s)} - \widetilde{\varphi}_j^{(s)}\right)}_{T_1} + \underbrace{\frac{1}{n}\sum_{s=1}^n \widetilde{\varphi}_j^{(s)}\left(\widehat{\varphi}_i^{(s)} - \widetilde{\varphi}_i^{(s)}\right)}_{T_2}$$
$$+ \underbrace{\frac{1}{n}\sum_{s=1}^n \left(\widehat{\varphi}_i^{(s)} - \widetilde{\varphi}_i^{(s)}\right)\left(\widehat{\varphi}_j^{(s)} - \widetilde{\varphi}_j^{(s)}\right)}_{T_3}.$$

We only need to analyze the behavior of the terms T_1 and T_2, since the term T_3 is of higher order. Conditional on the event discussed in Theorem 3, we have

$$
\begin{aligned}
&\left|\widehat{\varphi}_i^{(s)} - \widetilde{\varphi}_i^{(s)}\right| \\
=\ &\left|\left(\Phi^{-1}(\xi)\right)'\right| \left|\widehat{F}^{\text{tr}}(\widehat{X}_i^{(s)}) - \widehat{F}^{\text{tr}}(X_i^{(s)})\right| \leq \frac{1}{\delta_{n,d,p}} \left|\widehat{F}^{\text{tr}}(\widehat{X}_i^{(s)}) - \widehat{F}^{\text{tr}}(X_i^{(s)})\right| \\
\leq\ &\frac{1}{\delta_{n,d,p}} \left[\left|\widehat{F}^{\text{tr}}(\widehat{X}_i^{(s)}) - F(\widehat{X}_i^{(s)})\right| + \left|F(\widehat{X}_i^{(s)}) - F(X_i^{(s)})\right| + \left|F(X_i^{(s)}) - \widehat{F}^{\text{tr}}(X_i^{(s)})\right|\right] \\
\overset{①}{\leq}\ &\frac{2}{\delta_{n,d,p}} \left[(\log n)\varepsilon_x + \frac{c_0}{\sqrt{n}} + c_1\sqrt{\varepsilon_x}\right] + \frac{L\left|\widehat{w}_i^{(s)}\right|}{\delta_{n,d,p}},
\end{aligned}
$$

where ① is because of the Lipschitz property in Assumption 3. Then we obtain

$$
\begin{aligned}
T_1 \lesssim\ &\underbrace{\frac{2\sqrt{\log n \vee \log(d-p)}}{\delta_{n,d,p}} \left[(\log n)\varepsilon_x + \frac{c_0}{\sqrt{n}} + c_1\sqrt{\varepsilon_x}\right]}_{T_{1,1}} \\
&+ \underbrace{\frac{L\sqrt{\log n \vee \log(d-p)}}{n\delta_{n,d,p}} \sum_{s=1}^{n} |\widehat{w}_i^{(s)}|}_{T_{1,2}} \\
\overset{②}{\lesssim}\ &2\sqrt{\log n \vee \log(d-p)} \left(\frac{\sqrt{\log n}}{n^{1/4}} \vee \frac{\sqrt{\log(d-p)}}{(d-p)^{\beta/4}}\right) \\
&+ \frac{L\sqrt{\log n \vee \log(d-p)}}{\delta_{n,d,p}} \sqrt{\frac{\sum_{s=1}^{n} |\widehat{w}_i^{(s)}|^2}{n}},
\end{aligned}
$$

where in ② we plug in the definition of ε_x in (Equation 3.5.2), that is,

$$
T_{1,1} \asymp 2\sqrt{\log n \vee \log(d-p)} \left(\frac{\sqrt{\log n}}{n^{1/4}} \vee \frac{\sqrt{\log(d-p)}}{(d-p)^{\beta/4}}\right).
$$

Since the $\widehat{w}_i^{(s)}$ is approximately Gaussian distribution with mean zero and $\sigma^2/(d-p)$ variance, we have $(d-p)/\sigma^2 \sum_{s=1}^{n} |\widehat{w}_i^{(s)}|^2$ be ξ^2-RV with freedom n, which means $\sum_{s=1}^{n} |\widehat{w}_i^{(s)}|^2 \leq 2n\sigma^2/(d-p)$ holds with probability at least $1 - e^{-cn}$. To sum up, we obtain

$$
\begin{aligned}
T_1 &\lesssim \sqrt{\log n \vee \log(d-p)} \left(\frac{\sqrt{\log n}}{n^{1/4}} \vee \frac{\sqrt{\log(d-p)}}{(d-p)^{\beta/4}} \right) + \frac{L\sigma\sqrt{\log n \vee \log(d-p)}}{\delta_{n,d,p}\sqrt{d-p}} \\
&\lesssim \sqrt{\log n \vee \log(d-p)} \left(\frac{\sqrt{\log n}}{n^{1/4}} \vee \frac{\sqrt{\log(d-p)}}{(d-p)^{\beta/4}} \right) + \frac{L\sigma\left(\log n \vee \log(d-p)\right)}{c_0 \log^2(np)(d-p)^{1/4}},
\end{aligned}
$$

and complete the proof. □

B.2.3 Supporting Lemmas

Lemma 41. *For all possible i ($1 \le i \le n$), we conclude*

$$
\sup_{t \in \mathcal{R}_E} \left| \Phi^{-1}\left(\widehat{F}_i^{\text{tr}}(t)\right) - \Phi^{-1}\left(F_i(t)\right) \right| \le 2c_U \sqrt{\log n \vee \log(d-p)},
$$

where $\mathcal{R}_E$ is defined in (Equation B.2.1).

Proof. We conclude that

$$
\left| \Phi^{-1}\left(\widehat{F}_i^{\text{tr}}(t)\right) - \Phi^{-1}\left(F_i(t)\right) \right| \le \left| \Phi^{-1}\left(F_i(t)\right) \right| + \left| \Phi^{-1}\left(\widehat{F}_i^{\text{tr}}(t)\right) \right|.
$$

For the first term, we have

$$
\left| \Phi^{-1}\left(F_i(t)\right) \right| \le c_U \sqrt{\log n \vee \log(d-p)},
$$

according to the definitions of $\mathcal{R}_E$. Meanwhile for the second term $\left| \Phi^{-1}\left(\widehat{F}_i^{\text{tr}}(t)\right) \right|$, we have

$$
\Phi^{-1}\left(\widehat{F}_i^{\text{tr}}(t)\right) \overset{①}{\le} \Phi^{-1}\left(1-\delta_{n,d,p}\right) \overset{②}{\le} \sqrt{2\log\frac{1}{1-\delta_{n,d,p}}} \overset{③}{\le} c_U \sqrt{\log n \vee \log(d-p)},
$$

where in ① we exploit the fact $\widehat{F}_i^{\text{tr}}(t) \le 1 - \delta_{n,d,p}$, in ② we invoke Lemma 11 in [25] (cf. Lemma 53), and in ③ we use the fact that $\delta_{n,d,p} \ge \frac{1}{n} \vee \frac{1}{d-p}$.

□

Lemma 42. *Provided that* $\delta_{n,d,p} \leq 1 - \Phi\left(c_L\sqrt{\log n \vee \log(d-p)}\right) - \sqrt{\varepsilon_x}$*, we can bound the probability*

$$\begin{aligned}
&\mathbb{P}\left(\widehat{F}_i(g_i(c_L\sqrt{\log n \vee \log(d-p)})) \geq 1 - \delta_{n,d,p}\right) \\
\leq\ & \exp\left(-2n\left(1 - \delta_{n,d,p} - \Phi\left(c_L\sqrt{\log n \vee \log(d-p)}\right) - \sqrt{\varepsilon_x}\right)^2\right); \\
&\mathbb{P}\left(\widehat{F}_i(g_i(-c_L\sqrt{\log n \vee \log(d-p)})) \leq \delta_{n,d,p}\right) \\
\leq\ & \exp\left(-2n\left(1 - \delta_{n,d,p} - \Phi\left(c_L\sqrt{\log n \vee \log(d-p)}\right) - \sqrt{\varepsilon_x}\right)^2\right),
\end{aligned}$$

where ε_x *is defined in* (Equation 3.5.2).

Proof. We have

$$\begin{aligned}
&\mathbb{P}\left(\widehat{F}_i(g_i(c_L\sqrt{\log n \vee \log(d-p)})) \geq 1 - \delta_{n,d,p}\right) \\
=\ & \mathbb{P}\Bigg[\widehat{F}_i(g_i(c_L\sqrt{\log n \vee \log(d-p)})) - \mathbb{E}\widehat{F}_i(g_i(c_L\sqrt{\log n \vee \log(d-p)})) \\
&\qquad \geq 1 - \delta_{n,d,p} - \mathbb{E}\widehat{F}_i(g_i(c_L\sqrt{\log n \vee \log(d-p)}))\Bigg] \\
\leq\ & \exp\left[-2n\left(1 - \delta_{n,d,p} - \mathbb{E}\widehat{F}_i(g_i(c_L\sqrt{\log n \vee \log(d-p)}))\right)^2\right].
\end{aligned}$$

The term is bounded as

$$\begin{aligned}
&1 - \delta_{n,d,p} - \mathbb{E}\widehat{F}_i\left(g_i(c_L\sqrt{\log n \vee \log(d-p)})\right) \\
\geq\ & \left|1 - \delta_{n,d,p} - F_i\left(g_i(c_L\sqrt{\log n \vee \log(d-p)})\right)\right| \\
-\ & \left|F_i\left(g_i(c_L\sqrt{\log n \vee \log(d-p)})\right) - \mathbb{E}\widehat{F}_i(g_i(c_L\sqrt{\log n \vee \log(d-p)}))\right| \\
=\ & \left|1 - \delta_{n,d,p} - \Phi\left(c_L\sqrt{\log n \vee \log(d-p)}\right)\right| - \sqrt{\varepsilon_x}.
\end{aligned}$$

Similarly, we can prove

$$\begin{aligned}
&\mathbb{P}\left(\widehat{F}_i(g_i(-c_L\sqrt{\log n \vee \log(d-p)})) \leq \delta_{n,d,p}\right) \\
\leq\ & \exp\left(-2n\left(1 - \delta_{n,d,p} - \Phi\left(c_L\sqrt{\log n \vee \log(d-p)}\right) - \sqrt{\varepsilon_x}\right)^2\right).
\end{aligned}$$

APPENDIX C

APPENDIX OF DESIGN OF COMPRESSIVE SENSING SYSTEMS USING DENSITY EVOLUTION

C.1 Proof of Theorem 6

Proof. We begin the proof by restating the DE equation w.r.t. $E^{(t+1)}$ and $V^{(t+1)}$ as

$$E^{(t+1)} = \underbrace{\mathbb{E}_{\text{prior}(s),z\sim\mathcal{N}(0,1)}\left[\mathsf{prox}\left(s + a_1 z\sqrt{E^{(t)}}; \beta a_2 V^{(t)}\right) - s\right]^2}_{\triangleq \Psi_E\left(E^{(t)};V^{(t)}\right)};$$

$$V^{(t+1)} = \underbrace{\mathbb{E}_{\text{prior}(s),z\sim\mathcal{N}(0,1)}\left[\beta a_2 V^{(t)} \mathsf{prox}'\left(s + a_1 z\sqrt{E^{(t)}}; \beta a_2 V^{(t)}\right)\right]}_{\triangleq \Psi_V\left(E^{(t)};V^{(t)}\right)}.$$

The derivation of the necessary conditions for $\lim_{t\to\infty}\left(E^{(t)}, V^{(t)}\right) = (0,0)$ consists of two parts:

- **Part I**. We verify that $(0,0)$ is a fixed-point of the DE equation;
- **Part II**. We consider the necessary condition such that DE equation converges within the proximity of the origin points, i.e., $E^{(t)}$ and $V^{(t)}$ are close to zero.

Since Part I can be easily verified, we put our major focus on Part II. Define the difference across iterations as $\delta_E^{(t)} = E^{(t+1)} - E^{(t)}$ and $\delta_V^{(t)} = V^{(t+1)} - V^{(t)}$, we would like to show $\lim_{t\to\infty}\left(\delta_E^{(t)}, \delta_V^{(t)}\right) = (0,0)$. With Taylor expansion, we obtain

$$\begin{aligned}
\delta_E^{(t+1)} =& \ \Psi_E\left(E^{(t+1)}, V^{(t+1)}\right) - \Psi_E\left(E^{(t)}, V^{(t)}\right) \\
=& \ \left(\frac{\partial \Psi_E(E,V)}{\partial E}\Big|_{E=E^{(t)},V=V^{(t)}}\right)\cdot\delta_E^{(t)} + \left(\frac{\partial \Psi_E(E,V)}{\partial V}\Big|_{E=E^{(t)},V=V^{(t)}}\right)\cdot\delta_V^{(t)} \\
&+ O\left(\left(\delta_E^{(t)}\right)^2\right) + O\left(\left(\delta_V^{(t)}\right)^2\right). \qquad \text{(C.1.1)}
\end{aligned}$$

Consider the region where $\delta_E^{(t)}$ and $\delta_V^{(t)}$ are sufficiently small, we require $\delta_E^{(t)}$ and $\delta_V^{(t)}$ to converge to zero. Notice the quadratic terms in (Equation C.1.1) can be safely omitted in this region. Denote the gradients $\left(\frac{\partial \Psi_E(E,V)}{\partial E}\right)^{(t)}\Big|_{E=E^{(t)},V=V^{(t)}}$, $\frac{\partial \Psi_E(E,V)}{\partial V}\Big|_{E=E^{(t)},V=V^{(t)}}$, $\frac{\partial \Psi_V(E,V)}{\partial E}\Big|_{E=E^{(t)},V=V^{(t)}}$, and $\frac{\partial \Psi_V(E,V)}{\partial V}\Big|_{E=E^{(t)},V=V^{(t)}}$ as $\left(\frac{\partial \Psi_E(E,V)}{\partial E}\right)^{(t)}$, $\left(\frac{\partial \Psi_E(E,V)}{\partial V}\right)^{(t)}$, $\left(\frac{\partial \Psi_V(E,V)}{\partial E}\right)^{(t)}$, and $\left(\frac{\partial \Psi_V(E,V)}{\partial V}\right)^{(t)}$, respectively. We obtain the linear equation

$$\begin{bmatrix}\delta_E^{(t+1)}\\ \delta_V^{(t+1)}\end{bmatrix} = \underbrace{\begin{bmatrix}\left(\frac{\partial \Psi_E(E,V)}{\partial E}\right)^{(t)} & \left(\frac{\partial \Psi_E(E,V)}{\partial V}\right)^{(t)}\\ \left(\frac{\partial \Psi_V(E,V)}{\partial E}\right)^{(t)} & \left(\frac{\partial \Psi_V(E,V)}{\partial V}\right)^{(t)}\end{bmatrix}}_{\triangleq \mathbf{L}^{(t)}} \begin{bmatrix}\delta_E^{(t)}\\ \delta_V^{(t)}\end{bmatrix},$$

and would require the lower bound of the operator norm of the matrix $\mathbf{L}^{(t)}$ to be less than 1, i.e., $\inf_t \left\|\mathbf{L}^{(t)}\right\|_{\text{OP}} \leq 1$, since otherwise the values of $\delta_E^{(t)}$ and $\delta_V^{(t)}$ will keep increasing. Exploiting the fact $\frac{\partial \Psi_V(E,V)}{\partial E} = 0$, we conclude

$$\left\|\mathbf{L}^{(t)}\right\|_{\text{OP}} = \max\left[\left(\frac{\partial \Psi_E\left(E,V\right)}{\partial E}\right)^{(t)}, \left(\frac{\partial \Psi_V\left(E,V\right)}{\partial V}\right)^{(t)}\right].$$

The proof is then concluded by computing the lower bounds of the gradients $\frac{\partial \Psi_E(E,V)}{\partial E}$ and $\frac{\partial \Psi_V(E,V)}{\partial V}$ as

$$
\begin{aligned}
& \frac{\partial \Psi_E\left(E,V\right)}{\partial E}\Big|_{E=E^{(t)},V=V^{(t)}} \\
= \; & a_1^2 \cdot \mathbb{E}_{\text{prior}(s)}\left[\Phi\left(-\frac{s+a_2V^{(t)}}{a_1\sqrt{E^{(t)}}}\right)+\Phi\left(\frac{s-a_2V^{(t)}}{a_1\sqrt{E^{(t)}}}\right)\right] \\
\overset{①}{=} \; & \frac{a_1^2k}{n}\left[\Phi\left(-\frac{c_0+a_2V^{(t)}}{a_2\sqrt{E^{(t)}}}\right)+\Phi\left(\frac{c_0-a_2V^{(t)}}{a_1\sqrt{E^{(t)}}}\right)\right]+2a_1^2\left(1-\frac{k}{n}\right)\Phi\left(-\frac{a_2V^{(t)}}{a_1E^{(t)}}\right) \\
\overset{②}{\to} \; & \frac{ka_1^2}{n}+2a_1^2\left(1-\frac{k}{n}\right)\Phi\left(-\frac{a_2V^{(t)}}{\sqrt{a_1E^{(t)}}}\right) \overset{③}{\geq} \frac{ka_1^2}{n}; \\
& \frac{\partial \Psi_V\left(E,V\right)}{\partial V}\Big|_{E=E^{(t)},V=V^{(t)}} \\
= \; & \beta a_2 \cdot \mathbb{E}_{\text{prior}(s)}\left[\Phi\left(-\frac{s+a_2V^{(t)}}{a_1\sqrt{E^{(t)}}}\right)+\Phi\left(\frac{s-a_2V^{(t)}}{a_1\sqrt{E^{(t)}}}\right)\right] \\
\overset{④}{=} \; & \frac{\beta a_2k}{n}\left[\Phi\left(-\frac{c_0+a_2V^{(t)}}{a_2\sqrt{E^{(t)}}}\right)+\Phi\left(\frac{c_0-a_2V^{(t)}}{a_1\sqrt{E^{(t)}}}\right)\right]+2\beta a_2\left(1-\frac{k}{n}\right)\Phi\left(-\frac{a_2V^{(t)}}{a_1E^{(t)}}\right) \\
\overset{⑤}{\to} \; & \frac{k\beta a_2}{n}+2\beta a_2\left(1-\frac{k}{n}\right)\Phi\left(-\frac{a_2V^{(t)}}{\sqrt{a_1E^{(t)}}}\right) \overset{⑥}{\geq} \frac{k\beta a_2}{n},
\end{aligned}
\tag{C.1.2}
$$

where $\Phi(\cdot)=(2\pi)^{-1/2}\int_{-\infty}^{(\cdot)}e^{-z^2/2}dz$ is the CDF of the standard normal RV z, namely, $z\sim\mathcal{N}(0,1)$. In ① and ④ we use the prior distribution $\text{prior}(s)=k/n\cdot\mathbb{1}(c_0)+(1-k/n)\mathbb{1}(0)$. Further, in ② and ⑤ we use the fact

$$
\lim_{E^{(t)}\to 0}\Phi\left(-\frac{c_0+a_2V^{(t)}}{\sqrt{a_1E^{(t)}}}\right)+\Phi\left(\frac{c_0-a_2V^{(t)}}{\sqrt{a_1E^{(t)}}}\right)=1,
$$

since $c_0\neq 0$. Finally, in ③ and ⑥ we omit the non-negative terms $\Phi(\cdot)$. □

C.2 Example of regular sensing with a Gaussian prior

In addition to the Laplacian prior studied in subsection 4.3.3, we also investigate the Gaussian prior. Assuming the ground-truth $\mathbf{x}^\natural$ to be Gaussian distributed with zero mean and unit variance, we would like to recover the signal $\mathbf{x}^\natural$ with the regularizer $f(\mathbf{x})=\|\mathbf{x}\|_2^2$. In

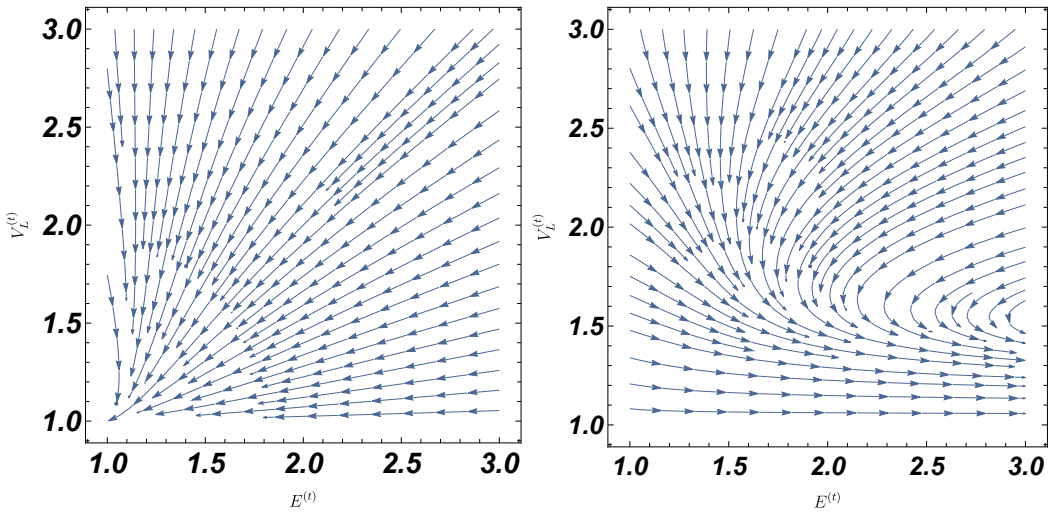

Figure C.1. Illustration of DE in (Equation C.2.1) when setting prior$(s) = \mathbb{1}(s = 1)$. **Left panel**: $\sum_{i,j} \rho_i \lambda_j \sqrt{i/j} < 1$. **Right panel**: $\sum_{i,j} \rho_i \lambda_j \sqrt{i/j} > 1$. Notice that the left panel has a fix-point $(0, 0)$ while the right panel is with non-zero fix-point.

this case, the DE equation reduces to

$$E^{(t+1)} = \frac{a_1^2 E^{(t)} + a_2^2 (V^{(t)})^2}{\left(1 + a_2 V^{(t)}\right)^2}; \tag{C.2.1}$$

$$V^{(t+1)} = \frac{a_2 V^{(t)}}{1 + a_2 V^{(t)}}, \tag{C.2.2}$$

where a_1, a_2 are defined the same as above. Then we have the following theorem.

Theorem 15. *Provided that $\sum_{i,j} \rho_i \lambda_j \sqrt{i/j} < 1$, the average error $E^{(t)}$ and the variance $V^{(t)}$ decrease exponentially after some iteration index T, that is, $E^{(t)} \le e^{-c_0(t-T)} E^{(T)}$ and $V^{(t)} \le e^{-c_1(t-T)} V^{(T)}$ whenever $t \ge T$, where $c_0, c_1 > 0$ are some fixed constants.*

An illustration of the DE in (Equation C.2.1) is shown in Figure C.1.

Proof. We begin the proof by restating that the functions $\mathbb{E}_z h_{\text{mean}}(\cdot;\cdot)$ and $\mathbb{E}_z h_{\text{var}}\,(\text{mean; var})$ are written as

$$\mathbb{E}_z h_{\text{mean}}\left(s + a_1 z\sqrt{E^{(t)}}; a_2 V^{(t)}\right) = \frac{a_1^2 E^{(t)} + a_2^2 \left(V^{(t)}\right)^2 s^2}{\left(1 + a_2 V^{(t)}\right)^2};$$

$$\mathbb{E}_z h_{\text{var}}\left(s + a_1 z\sqrt{E^{(t)}}; a_2 V^{(t)}\right) = \frac{a_2 V^{(t)}}{1 + a_2 V^{(t)}},$$

which can be easily verified. Then we prove that $V^{(t)}$ decreases exponentially since $a_2 > 0$ and hence for an arbitrary time index T_1 the relation

$$V^{(t)} \leq \left(\frac{a_2}{1+a_2}\right)^{t-T_1} V^{(T_1)} = e^{-c_1(t-T_1)} V^{(T_1)}$$

holds for $t \geq T_1$, where c_1 is defined as $\log(1 + a_2^{-1}) > 0$.

Afterwards, we study the behavior of $E^{(t)}$. Denote V_S as $\mathbb{E}_{\text{prior}(s)}(s^2)$, we have

$$\begin{aligned} E^{(t+1)} \leq\ & a_1^2 E^{(t)} + \frac{a_2 V_S V^{(t)}}{2} \\ \overset{①}{\leq}\ & a_1^2 E^{(t)} + \frac{a_2 V_S}{2}\left(\frac{a_2}{1+a_2}\right)^t V^{(0)}, \end{aligned} \tag{C.2.3}$$

where in ① we use the relation $V^{(t)} \leq (a_2/(1+a_2))^t V^{(0)}$. Define a new sequence $\widetilde{E}^{(t)} = E^{(t)}/a_1^{2t}$, we can transform (Equation C.2.3) to

$$\begin{aligned} \widetilde{E}^{(t+1)} =\ & \frac{E^{(t+1)}}{a_1^{2(t+1)}} \leq \frac{E^{(t)}}{a_1^{2t}} + \frac{a_2 V_S V^{(0)}}{2a_1^2}\left(\frac{a_2}{(1+a_2)a_1^2}\right)^t \\ =\ & \widetilde{E}^{(t)} + \frac{a_2 V_S V^{(0)}}{2a_1^2}\left(\frac{a_2}{(1+a_2)a_1^2}\right)^t, \end{aligned}$$

after rearranging the terms. Due to the time-invariance, we also have the relation

$$\widetilde{E}^{(t)} \leq \widetilde{E}^{(t-1)} + \frac{a_2 V_S V^{(0)}}{2a_1^2}\left(\frac{a_2}{(1+a_2)a_1^2}\right)^{t-1}.$$

Iterating over all such inequalities, we obtain the equation

$$\widetilde{E}^{(t+1)} \leq \widetilde{E}^{(1)} + \frac{a_2 V_S V^{(0)}}{2a_1^2} \frac{\frac{a_2}{(1+a_2)a_1^2}\left(1 - \left(\frac{a_2}{(1+a_2)a_1^2}\right)^t\right)}{1 - \left(\frac{a_2}{(1+a_2)a_1^2}\right)},$$

which leads to

$$E^{(t+1)} \leq a_1^{2t} E^{(1)} + \underbrace{\frac{a_2 V_S V^{(0)}}{2a_1^2} \cdot \frac{a_2}{1+a_2} \frac{a_1^{2t} - \left(\frac{a_2}{1+a_2}\right)^t}{1 - \frac{a_2}{(1+a_2)a_1^2}}}_{I}. \tag{C.2.4}$$

Since $a_1 < 1$ and $a_2/(1+a_2) < 1$, we have the second term I in (Equation C.2.4) to be negligible as t goes to infinity. Hence we can choose a sufficiently large T such that for $t \geq T$, we have $E^{(t+1)}$ is approximately equal to $a_1^{2t} E^{(1)}$ and conclude the exponential decay of $E^{(t)}$. □

C.3 Discussion of the DE for both regular and irregular designs

First we explain the physical meaning of the quantities $E^{(t)}$ and $V^{(t)}$, which track the average error and the average variance at the tth iteration, respectively. Since the physical meaning of $V^{(t)}$ can be easily obtained, we focus on the explanation of $E^{(t)}$. For the convenience of the analysis, we rewrite the MAP estimator as

$$\widehat{\mathbf{x}} = \text{argmax}_{\mathbf{x}} \exp\left(-\frac{\gamma \|\mathbf{y} - \mathbf{A}\mathbf{x}\|_2^2}{2\sigma^2}\right) \cdot \exp\left(-\gamma f(\mathbf{x})\right),$$

where $\gamma > 0$ is a redundant positive constant. Then we restate the message-passing algorithm, which is used to solve the MAP estimator, as

$$\widehat{m}_{a\to i}^{(t+1)}(x_i) \cong \int \prod_{j \in \partial a \backslash i} m_{j\to a}^{(t)}(x_i) \times e^{-\frac{\gamma\left(y_a - \sum_{j=1}^n A_{aj} x_j\right)^2}{2\sigma^2}} dx_j$$

$$m_{i\to a}^{(t+1)}(x_i) \cong e^{-\gamma f(x_i)} \prod_{b \in \partial i \backslash a} \widehat{m}_{b\to i}^{(t+1)}(x_i).$$

The MAP estimator of $\widehat{x}_i$ is hence written as

$$\widehat{x}_i = \text{argmax}_{x_i} \mathbb{P}\left(x_i|\mathbf{y}\right) \approx \text{argmax}_{x_i} e^{-\gamma f(x_i)} \prod_{a \in \partial i} \widehat{m}_{a\to i}^{(t)}(x_i).$$

Notice that $\widehat{x}_i$ can be rewritten as the mean w.r.t. the probability measure $e^{-\gamma f(x_i)} \prod_{a\in\partial i} \widehat{m}_{a\to i}^{(t)}$, namely,

$$\widehat{x}_i \approx \int_{x_i} x_i e^{-\gamma f(x_i)} \prod_{a \in \partial i} \widehat{m}_{a\to i}^{(t)}(x_i) dx_i,$$

by letting $\gamma \to \infty$. Since the mean $\mu_{i\to a}$ is computed as

$$\mu_{i\to a} = \int_{x_i} x_i e^{-\gamma f(x_i)} \prod_{b \in \partial i \backslash a} \widehat{m}_{b\to i}^{(t)}(x_i) dx_i,$$

which is close to $\widehat{x}_i$, we obtain the approximation $m^{-1}\sum_{a=1}^{m}(\mu_{i\to a} - x_i^\natural)^2$ as $(\widehat{x}_i - x_i^\natural)^2$. We then conclude

$$E^{(t)} = \frac{1}{mn}\sum_{i=1}^{n}\sum_{a=1}^{m}\left(\mu_{i\to a} - x_i^\natural\right)^2 \approx \frac{1}{n}\sum_{i=1}^{n}\left(\widehat{x}_i - x_i^\natural\right)^2,$$

which is approximately the average of error at the tth iteration. Having discussed the physical meaning of the quantities $E^{(t)}$ and $V^{(t)}$, we turn to the derivation of the DE equation.

C.3.1 Supporting Lemmas

We begin the derivation with the following lemma, which is stated as

Lemma 43. *Consider the message flow $\widehat{m}_{a\to i}^{(t+1)}$ from the check node a to the variable node i and approximate it as a Gaussian RV with mean $\widehat{\mu}_{a\to i}^{(t+1)}$ and variance $\widehat{v}_{a\to i}^{(t+1)}$, i.e., $\widehat{m}_{a\to i}^{(t+1)} \sim \mathcal{N}\left(\widehat{\mu}_{a\to i}^{(t+1)}, \widehat{v}_{a\to i}^{(t+1)}\right)$. Then, we can obtain the following update equation at the $(t+1)$th iteration*

$$\widehat{\mu}_{a\to i}^{(t+1)} = x_i + A\sum_{j\in\partial a\setminus i} A_{ai}A_{aj}\left(x_j - \mu_{j\to a}^{(t)}\right) + AA_{ai}w_a;$$
$$\widehat{v}_{a\to i}^{(t+1)} = A\sigma^2 + |\partial a|V^{(t)},$$

where $|\partial a|$ denotes the degree of the check node a.

Proof. Consider the message flow $\widehat{m}_{a\to i}^{(t+1)}$ from check-node to variable node at the $(t+1)$th iteration

$$\widehat{m}_{a\to i}^{(t+1)} = \frac{1}{Z_{a\to i}^{t}}\int \prod_{j\in\partial a\setminus i} m_{j\to a}^{(t)}(x_j) \times \exp\left(-\frac{\gamma\left(y_a - \sum_{j=1} A_{aj}x_j\right)^2}{2\sigma^2}\right) dx_j. \quad \text{(C.3.1)}$$

Approximate the message flow $m_{j\to a}^{(t+1)}$ as a Gaussian RV with mean $\mu_{j\to a}^{(t+1)}$ and variance $v_{j\to a}^{(t+1)}$. Plugging into (Equation C.3.1) yields

$$\widehat{m}_{a\to i}^{(t+1)} = \frac{1}{Z_{a\to i}^{t}}\int \prod_{j\in\partial a\setminus i} \exp\left[-\frac{\gamma\left(x_j - \mu_{j\to a}^{(t)}\right)^2}{2v_{j\to a}^{(t+1)}}\right] \times \exp\left[-\frac{\gamma\left(y_a - \sum_{j=1} A_{aj}x_j\right)^2}{2\sigma^2}\right] dx_j. \quad \text{(C.3.2)}$$

The direct calculation of the above integral involves the cross terms such as $A_{aj_1}A_{aj_2}x_{j_1}x_{j_2}$ ($j_1 \neq j_2$), which can be cumbersome. To handle this issue, we adopt the trick in [152, 55], whose basic idea is to introduce a redundant variable ω and exploit the relation

$$e^{-\frac{t^2}{2\sigma^2}} = \frac{1}{\sqrt{2\pi\sigma^2}}\int e^{-\frac{\omega^2}{2\sigma^2}+\frac{it\omega}{\sigma^2}} d\omega,$$

where t is an arbitrary number. As such, we can transform (Equation C.3.2) to

$$\widehat{m}_{a\to i}^{(t+1)} \cong \int d\omega \prod_{j\in\partial a\setminus i} dx_j \cdot \exp\left[-\frac{\gamma\left(x_j-\mu_{j\to a}^{(t)}\right)^2}{2v_{j\to a}^{(t+1)}}\right] \cdot \exp\left[-\frac{i\omega\gamma\left(y_a-\sum_{j=1}A_{aj}x_j\right)}{\sigma^2}\right]\cdot\exp\left[-\frac{\gamma\omega^2}{2\sigma^2}\right],$$

which diminishes the cross term $x_{j_1}x_{j_2}$ ($j_1\neq j_2$). Rearranging the terms for each x_j, we can iteratively perform the integral such that

$$\begin{aligned}
&\int dx_j\cdot\exp\left(-\frac{\gamma\left(x_j-\mu_{j\to a}^{(t)}\right)^2}{2v_{j\to a}^{(t)}}+\frac{i\omega\gamma A_{aj}x_j}{\sigma^2}\right)\\
=&\sqrt{\frac{2\pi v_{j\to a}^{(t)}}{\gamma}}\cdot\exp\left[-\frac{\gamma(\widehat{\mu}_{j\to a}^{(t)})^2}{2\widehat{v}_{j\to a}^{(t)}}+\frac{v_{j\to a}^{(t)}\left(\frac{\gamma\mu_{j\to a}^{(t)}}{v_{j\to a}^{(t)}}+\frac{i\gamma\omega A_{aj}}{\sigma^2}\right)^2}{2\gamma}\right]\\
=&\sqrt{\frac{2\pi v_{j\to a}^{(t)}}{\gamma}}\cdot\exp\left(-\frac{\gamma\omega^2A_{aj}^2v_{j\to a}^{(t)}}{2\sigma^4}+\frac{i\gamma\omega A_{aj}\mu_{j\to a}^{(t)}}{\sigma^2}\right).
\end{aligned}$$

With some algebraic manipulations, we can compute its mean $\widehat{\mu}_{a\to i}^{(t+1)}$ and its variance $\widehat{v}_{a\to i}^{(t+1)}$ as

$$\begin{aligned}
\widehat{\mu}_{a\to i}^{(t+1)}&=\frac{A_{ai}\left(y_a-\sum_{j\in\partial a\setminus i}A_{aj}\mu_{j\to a}^{(t)}\right)}{A_{ai}^2};\\
\widehat{v}_{a\to i}^{(t+1)}&=\frac{\sigma^2+\sum_{j\in\partial a\setminus i}A_{aj}^2v_{j\to a}^{(t)}}{A_{ai}^2}.
\end{aligned}$$

The following analysis focuses on how to approximate these two values. We begin by the discussion w.r.t. the variance $\widehat{v}_{a\to i}^{(t+1)}$. Note we have

$$\widehat{v}_{a\to i}^{(t+1)}\overset{①}{\approx} A\sigma^2+\sum_{j\in\partial a\setminus i}v_{j\to a}^{(t)},$$

where in ① we use $A_{ai}^2\approx\mathbb{E}\left(A_{ai}^2|A_{ai}\neq 0\right)=A^{-1}$ for $i\in\partial a$. As for the sum $\sum_{j\in\partial a\setminus i}v_{j\to a}^{(t)}$,

we can view it to be randomly sampled from the set of variances $\left\{v_{j\to a}^{(t)}\right\}$ and approximate it as

$$\sum_{j\in\partial a\backslash i} v_{j\to a}^{(t)} \approx \left(|\partial a|-1\right) V^{(t)} \approx |\partial a| V^{(t)}.$$

Notice that the variance is closely related with the check node degree $|\partial a|$. Having obtained the variance $\widehat{v}_{a\to i}^{(t+1)}$, we turn to the mean $\widehat{\mu}_{a\to i}^{(t+1)}$, which is computed as

$$\begin{aligned}
\widehat{\mu}_{a\to i}^{(t+1)} &= \frac{A_{ai}\left(y_a - \sum_{j\in\partial a\backslash i} A_{aj}\mu_{j\to a}^{(t)}\right)}{A_{ai}^2} \\
&\overset{②}{\approx} AA_{ai}\left(A_{ai}x_i + \sum_{j\in\partial a\backslash i} A_{aj}\left(x_j - \mu_{j\to a}^{(t)}\right) + w_a\right) \\
&\overset{③}{\approx} x_i + A\sum_{j\in\partial a\backslash i} A_{ai}A_{aj}\left(x_j - \mu_{j\to a}^{(t)}\right) + AA_{ai}w_a,
\end{aligned}$$

where in ② and ③ we use the approximation $A_{ai}^2 \approx A^{-1}$ for $i \in \partial a$.

□

C.3.2 Derivation of DE

We study the message flow $m_{i\to a}^{(t+1)}$ from the variable node i to the check node a

$$m_{i\to a}^{(t+1)} \cong e^{-\gamma f(x_i)} \prod_{b\in\partial i\backslash a} e^{-\frac{\gamma\left(x_i-\widehat{\mu}_{b\to i}^{(t+1)}\right)^2}{2\widehat{v}_{b\to i}^{(t+1)}}}.$$

To begin with, we study the product $\prod_{b\in\partial i\backslash a}\exp\left(-\frac{\gamma\left(x_i-\widehat{\mu}_{b\to i}^{(t+1)}\right)^2}{2\widehat{v}_{b\to i}^{(t)}}\right)$. Its variance $\widetilde{v}_{i\to a}^{(t+1)}$ is approximately computed as

$$\frac{\gamma}{\widetilde{v}_{i\to a}^{(t+1)}} \approx \sum_{b\in\partial i\backslash a}\frac{\gamma}{\widehat{v}_{b\to i}^{(t+1)}},$$

which yields

$$\widetilde{v}_{i\to a}^{(t+1)} = \left(\frac{|\partial i|-1}{A\sigma^2+|\partial a|V^{(t)}}\right)^{-1} \approx \frac{A\sigma^2+|\partial a|V^{(t)}}{|\partial i|}.$$

Further, the mean $\widetilde{\mu}_{i\to a}^{(t+1)}$ is calculated as

$$\begin{aligned}
\widetilde{\mu}_{i\to a}^{(t+1)} &= \left(\sum_{b\in\partial i\backslash a}\frac{\widehat{\mu}_{b\to i}^{(t+1)}}{\widehat{v}_{b\to i}^{(t+1)}}\right) / \left(\sum_{b\in\partial i\backslash a}\frac{1}{\widehat{v}_{b\to i}^{(t+1)}}\right)^{-1} \\
&\overset{①}{=} \frac{A\sigma^2+|\partial a|V^{(t)}}{|\partial i|} \\
&\times \left(\sum_{b\in\partial i\backslash a}\frac{x_i + A\sum_{j\in\partial b\backslash i}A_{bi}A_{bj}\left(x_j - \mu_{j\to b}^{(t)}\right) + AA_{bi}w_b}{A\sigma^2+|\partial a|V^{(t)}}\right) \\
&\approx x_i + \frac{A}{|\partial i|}\left[\sum_{j\in\partial b\backslash i}A_{bi}A_{bj}\left(x_j - \mu_{j\to b}^{(t)}\right) + \sum_{b\in\partial i\backslash a}A_{bi}w_b\right],
\end{aligned}$$

where in ① we invoke Lemma 43. We then approximate the term $\sum_{j\in\partial b\backslash i}A_{bi}A_{bj}\left(x_j - \mu_{j\to b}^{(t)}\right)$ + $\sum_{b\in\partial i\backslash a}A_{bi}w_b$ as a Gaussian RV with its mean being calculated as

$$\mathbb{E}\left[\sum_{b\in\partial i\backslash a}\sum_{j\in\partial b\backslash i}A_{bi}A_{bj}\left(x_j - \mu_{j\to b}^{(t)}\right) + \sum_{b\in\partial i\backslash a}A_{bi}w_b\right] = 0,$$

and its variance as

$$\begin{aligned}
&\mathbb{E}\left[\sum_{b\in\partial i\backslash a}\sum_{j\in\partial b\backslash i}A_{bi}A_{bj}\left(x_j - \mu_{j\to b}^{(t)}\right) + \sum_{b\in\partial i\backslash a}A_{bi}w_b\right]^2 \\
&= \mathbb{E}\left[\sum_{b\in\partial i\backslash a}\sum_{j\in\partial b\backslash i}A_{bi}A_{bj}\left(x_j - \mu_{j\to b}^{(t)}\right)\right]^2 + \mathbb{E}\left[\sum_{b\in\partial i\backslash a}A_{bi}w_b\right]^2 \\
&\approx A^{-2}|\partial i|\sum_{j\in\partial a\backslash i}\left(x_j - \mu_{j\to b}^{(t)}\right)^2 + A^{-1}\sigma^2|\partial i| \\
&\overset{②}{\approx} |\partial i|\left(A^{-2}|\partial a|E^{(t)} + A^{-1}\sigma^2\right).
\end{aligned}$$

In ② we assume the term $\left(x_j - \mu_{j\to b}^{(t)}\right)^2$ is randomly sampled among all possible pairs (i,a). Hence for the fixed degree $|\partial i|$ and $|\partial a|$, we can approximate the mean $\widetilde{\mu}_{i\to a}^{(t+1)}$ as a Gaussian RV with mean $x_i + z\sqrt{\left(A\sigma^2 + |\partial a|E^{(t)}\right)/|\partial i|}$ and variance $\left(A\sigma^2 + |\partial a|V^{(t)}\right)/|\partial i|$, namely,

$$x \sim \mathcal{N}\left(x_i + z\sqrt{\frac{A\sigma^2 + |\partial a|E^{(t)}}{|\partial i|}}, \frac{A\sigma^2 + |\partial a|V^{(t)}}{|\partial i|}\right),$$

where z is a standard normal RV. Recalling that distribution of the degrees of the variable node i and check node a satisfies $\mathbb{P}(|\partial i| = \alpha) = \lambda_\alpha$ and $\mathbb{P}\left(|\partial a| = \beta\right) = \rho_\beta$, we can approximate the distribution of the product $\prod_{b\in\partial i\setminus a} \exp\left(-\gamma\left(x_i - \widehat{\mu}_{b\to i}^{(t)}\right)^2/(2\widehat{v}_{b\to i}^{(t)})\right)$ as the mixture Gaussian $\sum_{i,j}\rho_i\lambda_j\mathcal{N}\left(z\sqrt{\frac{iE^{(t)}+A\sigma^2}{j}}, \frac{A\sigma^2+iV^{(t)}}{j}\right)$ [1] and further approximate it as a single Gaussian RV with mean $x_i + \sum_{i,j}\rho_i\lambda_j z\sqrt{\frac{iE^{(t)}+A\sigma^2}{j}}$ and variance $\sum_{i,j}\rho_i\lambda_j\frac{A\sigma^2+iV^{(t)}}{j}$. Invoking the definitions of $h_{\text{mean}}(\cdot;\cdot)$ and $h_{\text{var}}(\cdot;\cdot)$ as in (Equation 4.3.6), we then approximate the mean $\mu_{i\to a}^{(t+1)}$ and the variance $v_{i\to a}^{(t+1)}$ as

$$\mu_{i\to a}^{(t+1)} \approx h_{\text{mean}}\left(x_i + z\sum_{i,j}\rho_i\lambda_j\sqrt{\frac{iE^{(t)}+A\sigma^2}{j}}; \sum_{i,j}\rho_i\lambda_j\frac{A\sigma^2+iV^{(t)}}{j}\right);$$
$$v_{i\to a}^{(t+1)} \approx h_{\text{var}}\left(x_i + z\sum_{i,j}\rho_i\lambda_j\sqrt{\frac{iE^{(t)}+A\sigma^2}{j}}; \sum_{i,j}\rho_i\lambda_j\frac{A\sigma^2+iV^{(t)}}{j}\right).$$

Then, the DE w.r.t. the average error $E^{(t+1)}$ is derived as

$$E^{(t+1)} = \frac{1}{mn}\sum_{a=1}^{m}\sum_{i=1}^{n}\left(\mu_{i\to a}^{(t+1)} - x_i^\natural\right)^2$$
$$\approx \mathbb{E}_{\text{prior}(s)}\mathbb{E}_z\left[h_{\text{mean}}\left(x_i^\natural + z\sum_{i,j}\rho_i\lambda_j\sqrt{\frac{iE^{(t)}+A\sigma^2}{j}}; \sum_{i,j}\rho_i\lambda_j\frac{A\sigma^2+iV^{(t)}}{j}\right) - x_i^\natural\right]^2.$$

[1] One hidden assumption is that there is no-local loops in the graphical model we constructed, which is widely used in the previous work [43].

Following a similar method, we obtain the DE w.r.t. the average variance $V^{(t+1)}$ as stated in (Equation 4.3.4). This completes the proof.

C.3.3 Derivation of DE for Irregular Design

Different from the regular design, we separately track the average error and average variance w.r.t. the high-priority part and low-priority part. Then we define four quantities, namely, $E_L^{(t)}$, $E_H^{(t)}$, $V_L^{(t)}$, and $V_H^{(t)}$, which are written as

$$
\begin{aligned}
E_L^{(t)} &= \frac{1}{mn_L} \sum_{a=1}^{m} \sum_{i \in L} \left(\mu_{i \to a}^{(t)} - x_i^{\natural} \right)^2; \\
E_H^{(t)} &= \frac{1}{mn_H} \sum_{a=1}^{m} \sum_{i \in H} \left(\mu_{i \to a}^{(t)} - x_i^{\natural} \right)^2; \\
V_L^{(t)} &= \frac{1}{mn_L} \sum_{a=1}^{m} \sum_{i \in L} v_{i \to a}^{(t)}; \\
V_H^{(t)} &= \frac{1}{mn_H} \sum_{a=1}^{m} \sum_{i \in H} v_{i \to a}^{(t)},
\end{aligned}
$$

where n_H and n_L denote the length of the high-priority part $\mathbf{x}_H^{\natural}$ and low-priority part $\mathbf{x}_L^{\natural}$, respectively. Following the same procedure as above then yields the proof of (Equation 4.4.1). The derivation details are omitted for the clarify of presentation.

C.4 Discussion of subsection 4.4.3

We start the discussion by outlining the DE equation w.r.t. $E_H^{(t)}$, $E_L^{(t)}$, $V_H^{(t)}$, and $V_L^{(t)}$

$$
\begin{aligned}
E_H^{(t+1)} &= \mathbb{E}_{\text{prior}(s)}\mathbb{E}_{z\sim\mathcal{N}(0,1)}\left[\mathsf{prox}\left(s+z\cdot b_{H,1}^{(t)};\beta_H b_{H,2}^{(t)}\right)-s\right]^2 \\
&\triangleq \Psi_{E,H}\left(E_H^{(t)},E_L^{(t)},V_H^{(t)},V_L^{(t)}\right); \\
E_L^{(t+1)} &= \mathbb{E}_{\text{prior}(s)}\mathbb{E}_{z\sim\mathcal{N}(0,1)}\left[\mathsf{prox}\left(s+z\cdot b_{L,1}^{(t)};\beta_L b_{L,2}^{(t)}\right)-s\right]^2 \\
&\triangleq \Psi_{E,L}\left(E_H^{(t)},E_L^{(t)},V_H^{(t)},V_L^{(t)}\right); \\
V_H^{(t+1)} &= \mathbb{E}_{\text{prior}(s)}\mathbb{E}_{z\sim\mathcal{N}(0,1)}\left[\beta_H b_{H,2}\cdot\mathsf{prox}'\left(s+z\cdot b_{H,1}^{(t)};\beta_H b_{H,2}^{(t)}\right)\right] \\
&\triangleq \Psi_{V,H}\left(E_H^{(t)},E_L^{(t)},V_H^{(t)},V_L^{(t)}\right); \\
V_L^{(t+1)} &= \mathbb{E}_{\text{prior}(s)}\mathbb{E}_{z\sim\mathcal{N}(0,1)}\left[\beta_L b_{L,2}\cdot\mathsf{prox}'\left(s+z\cdot b_{L,1}^{(t)};\beta_L b_{L,2}^{(t)}\right)\right] \\
&\triangleq \Psi_{V,L}\left(E_H^{(t)},E_L^{(t)},V_H^{(t)},V_L^{(t)}\right),
\end{aligned}
$$

where notation $\mathsf{prox}(a;b)$ is the soft-thresholding estimator defined as $\text{sign}(a)\max(|a|-b,0)$, notation $\mathsf{prox}'(a;b)$ is the derivative w.r.t. the first argument, and the notations $b_{H,1}^{(t)}, b_{H,2}^{(t)}, b_{L,1}^{(t)}$, and $b_{L,2}^{(t)}$ are defined as

$$
\begin{aligned}
b_{H,1}^{(t)} &= \sum_{\ell,i,j}\lambda_{H,\ell}\rho_{H,i}\rho_j^L\sqrt{\frac{A\sigma^2+iE_H^{(t)}+jE_L^{(t)}}{\ell}}; \\
b_{H,2}^{(t)} &= \sum_{\ell,i,j}\lambda_{H,\ell}\rho_{H,i}\rho_j^L\frac{A\sigma^2+iV_H^{(t)}+jV_L^{(t)}}{\ell}; \\
b_{L,1}^{(t)} &= \sum_{\ell,i,j}\lambda_{\ell}^L\rho_{L,i}\rho_{H,j}\sqrt{\frac{A\sigma^2+iE_L^{(t)}+jE_H^{(t)}}{\ell}}; \\
b_{L,2}^{(t)} &= \sum_{\ell,i,j}\lambda_{\ell}^L\rho_{L,i}\rho_{H,j}\frac{A\sigma^2+iV_L^{(t)}+jV_H^{(t)}}{\ell}.
\end{aligned}
$$

Similar to the proof in section C.1, we define the differences across iterations as

$$\delta_{E,H}^{(t)} \triangleq E_H^{(t+1)} - E_H^{(t)};$$
$$\delta_{E,L}^{(t)} \triangleq E_L^{(t+1)} - E_L^{(t)};$$
$$\delta_{V,H}^{(t)} \triangleq V_H^{(t+1)} - V_H^{(t)};$$
$$\delta_{V,L}^{(t)} \triangleq V_H^{(t+1)} - V_H^{(t)}.$$

C.4.1 Discussion of (Equation 4.4.7)

This subsection follows the same logic as in section C.1. We first relax the Requirement 5 w.r.t. the average variance $V_H^{(t)}$ and $V_L^{(t)}$. Performing the Taylor-expansion, we obtain

$$\begin{aligned}
&\delta_{V,H}^{(t+1)} \\
=\ & \Psi_{V,H}\left(V_H^{(t+1)}, V_L^{(t+1)}, E_H^{(t+1)}, E_L^{(t+1)}\right) - \Psi_{V,H}\left(V_H^{(t)}, V_L^{(t)}, E_H^{(t)}, E_L^{(t)}\right) \\
=\ & \left(\frac{\partial \Psi_{V,H}(\cdot)}{\partial E_H}\Big|_{E_H=E_H^{(t)}, E_L=E_L^{(t)}, V_H=V_H^{(t)}, V_L=V_L^{(t)}}\right)\delta_{E,H}^{(t)} \\
+\ & \left(\frac{\partial \Psi_{V,H}(\cdot)}{\partial E_L}\Big|_{E_H=E_H^{(t)}, E_L=E_L^{(t)}, V_H=V_H^{(t)}, V_L=V_L^{(t)}}\right)\delta_{E,L}^{(t)} \\
+\ & \left(\frac{\partial \Psi_{V,H}(\cdot)}{\partial V_H}\Big|_{E_H=E_H^{(t)}, E_L=E_L^{(t)}, V_H=V_H^{(t)}, V_L=V_L^{(t)}}\right)\delta_{V,H}^{(t)} \\
+\ & \left(\frac{\partial \Psi_{V,H}(\cdot)}{\partial E_H}\Big|_{E_H=E_H^{(t)}, E_L=E_L^{(t)}, V_H=V_H^{(t)}, V_L=V_L^{(t)}}\right)\delta_{V,L}^{(t)} \\
&+ O\left(\left(\delta_{V,H}^{(t)}\right)^2\right) + O\left(\left(\delta_{V,L}^{(t)}\right)^2\right).
\end{aligned} \tag{C.4.1}$$

Following the same logic in section C.1, our derivation consists of two parts:

- **Part I**. We verify that $(0,0)$ is a fixed point of the DE equation w.r.t. $V_H^{(t)}$ and $V_L^{(t)}$;
- **Part II**. We show the DE equation w.r.t. $V_H^{(t)}$ and $V_L^{(t)}$ converges within the proximity of the origin points.

Our following derivation focuses on showing that DE converges, or equivalently, $\lim_{t\to\infty}\left(\delta_{V,H}^{(t)}, \delta_{V,L}^{(t)}\right) = (0,0)$, as the second part can be easily verified. We consider the region where $V_H^{(t)}, V_L^{(t)}, \delta_{V,H}^{(t)}$, and $\delta_{V,L}^{(t)}$ are sufficiently small and hence can safely omit

the quadratic terms in (Equation C.4.1). Exploiting the fact that $\partial\Psi_{V,H}/\partial E_H = 0$ and $\partial\Psi_{V,H}/\partial E_L = 0$, we obtain the linear relation

$$\begin{bmatrix} \delta_{V,H}^{(t+1)} \\ \delta_{V,L}^{(t+1)} \end{bmatrix} = \underbrace{\begin{bmatrix} \left(\frac{\partial\Psi_{V,H}(\cdot)}{\partial V_H}\right)^{(t)} & \left(\frac{\partial\Psi_{V,H}(\cdot)}{\partial V_L}\right)^{(t)} \\ \left(\frac{\partial\Psi_{V,L}(\cdot)}{\partial V_H}\right)^{(t)} & \left(\frac{\partial\Psi_{V,L}(\cdot)}{\partial V_L}\right)^{(t)} \end{bmatrix}}_{\mathbf{L}_V^{(t)}} \begin{bmatrix} \delta_{V,H}^{(t)} \\ \delta_{V,L}^{(t)} \end{bmatrix},$$

where the notation $\left(\frac{\partial\Psi_{V,H}(\cdot)}{\partial V_H}\right)^{(t)}$ is a abbreviation for the gradient

$$\left(\frac{\partial\Psi_{V,H}(\cdot)}{\partial V_H}\right)^{(t)} = \frac{\partial\Psi_{V,H}(\cdot)}{\partial V_H}\Big|_{E_H=E_H^{(t)},E_L=E_L^{(t)},V_H=V_H^{(t)},V_L=V_L^{(t)}}.$$

Similarly we define the notations $\left(\partial\Psi_{V,H}(\cdot)/\partial V_L\right)^{(t)}$, $\left(\partial\Psi_{V,L}(\cdot)/\partial V_H\right)^{(t)}$, and $\left(\partial\Psi_{V,L}(\cdot)/\partial V_L\right)^{(t)}$. Then we require $\inf_t \left\|\mathbf{L}_V^{(t)}\right\|_{\text{OP}} \leq 1$. Otherwise, the values of $\delta_{V,H}^{(t)}$ and $\delta_{V,L}^{(t)}$ will keep increasing and stay away from zero. We then lower bound the gradients $\left(\partial\Psi_{V,H}(\cdot)/\partial V_H\right)^{(t)}$ and $\left(\partial\Psi_{V,H}(\cdot)/\partial V_L\right)^{(t)}$ as

$$\begin{aligned}
&\left(\frac{\partial\Psi_{V,H}(\cdot)}{\partial V_H}\right)^{(t)} \overset{①}{=} \beta_H \left(\sum_\ell \frac{\lambda_{H,\ell}}{\ell}\right)\cdot\left(\sum_i i\rho_{H,i}\right)\cdot\left[2\left(1-\frac{k_H}{n_H}\right)\Phi\left(-\frac{\beta_H b_{H,2}^{(t)}}{b_{H,1}^{(t)}}\right)+\frac{k_H}{n_H}\right] \\
\overset{②}{\geq}\ & \frac{k_H\beta_H}{n_H}\left(\sum_\ell \frac{\lambda_{H,\ell}}{\ell}\right)\cdot\left(\sum_i i\rho_{H,i}\right); \\
&\left(\frac{\partial\Psi_{V,H}(\cdot)}{\partial V_L}\right)^{(t)} \overset{③}{=} \beta_H \left(\sum_\ell \frac{\lambda_{H,\ell}}{\ell}\right)\cdot\left(\sum_i i\rho_{L,i}\right)\cdot\left[2\left(1-\frac{k_H}{n_H}\right)\Phi\left(-\frac{\beta_H b_{H,2}^{(t)}}{b_{H,1}^{(t)}}\right)+\frac{k_H}{n_H}\right] \\
\overset{④}{\geq}\ & \frac{k_H\beta_H}{n_H}\left(\sum_\ell \frac{\lambda_{H,\ell}}{\ell}\right)\cdot\left(\sum_i i\rho_{L,i}\right),
\end{aligned}$$

where $\Phi(\cdot) = (2\pi)^{-1/2}\int_{-\infty}^{(\cdot)} e^{-z^2/2}dz$ is the CDF of the standard normal RV z, i.e., $z \sim \mathcal{N}(0,1)$. In ① and ③, we follow the same computation procedure as in (Equation C.1.2), and in ② and ④ we drop the non-negative terms $\Phi(\cdot)$. Following a similar procedure, we lower bound the gradients $\left(\partial\Psi_{V,L}(\cdot)/\partial V_H\right)^{(t)}$ and $\left(\partial\Psi_{V,L}(\cdot)/\partial V_L\right)^{(t)}$ as

$$\left(\frac{\partial \Psi_{V,L}(\cdot)}{\partial V_H}\right)^{(t)} \geq \frac{k_L \beta_L}{n_L}\left(\sum_{\ell}\frac{\lambda_{L,\ell}}{\ell}\right)\cdot\left(\sum_i i\rho_{H,i}\right);$$
$$\left(\frac{\partial \Psi_{V,L}(\cdot)}{\partial V_L}\right)^{(t)} \geq \frac{k_L \beta_L}{n_L}\left(\sum_{\ell}\frac{\lambda_{L,\ell}}{\ell}\right)\cdot\left(\sum_i i\rho_{L,i}\right),$$

and conclude the discussion.

C.4.2 Discussion of (Equation 4.4.8)

This subsection relaxes the requirement $\lim_{t\to\infty} E_H^{(t)} = 0$, which consists of two parts:

- **Part I.** we consider the necessary conditions such that DE equation w.r.t. $E_H^{(t)}$ converges;
- **Part II**. We verify that 0 is a fixed point of DE w.r.t. $E_H^{(t)}$ given that $\lim_{t\to\infty}\left(V_H^{(t)}, V_L^{(t)}\right) = (0,0)$.

Since the second part can be easily verified, we focus on the first part. We consider the region where $E_H^{(t)}$ and $\delta_{E,H}^{(t)}$ are all sufficiently small and require $\delta_{E,H}^{(t)}$ to converge to zero. Via the Taylor expansion, we obtain the following linear equation

$$\delta_{E,H}^{(t+1)} \approx \left(\frac{\Psi_{E,H}(\cdot)}{\partial E_H}\right)^{(t)}\delta_{E,H}^{(t)} + \left(\frac{\Psi_{E,H}(\cdot)}{\partial E_L}\right)^{(t)}\delta_{E,L}^{(t)}, \tag{C.4.2}$$

where $\left(\frac{\Psi_{E,H}(\cdot)}{\partial E_H}\right)^{(t)}$ denotes the gradient $\frac{\Psi_{E,H}(\cdot)}{\partial E_H}$ at the point $\left(E_H^{(t)}, E_L^{(t)}, V_H^{(t)}, V_L^{(t)}\right)$. Enforcing the variable $\delta_{E,H}^{(t)}$ to converge to zero, we require

$$\inf_t \left[\left(\frac{\Psi_{E,H}(\cdot)}{\partial E_H}\right)^{(t)}\right]^2 + \left[\left(\frac{\Psi_{E,H}(\cdot)}{\partial E_L}\right)^{(t)}\right]^2 \leq 1.$$

Then our goal becomes lower-bounding the gradients, which are written as

$$
\begin{aligned}
&\left(\frac{\Psi_{E,H}(\cdot)}{\partial E_H}\right)^{(t)} \\
&= b_{H,1}^{(t)} \left(\sum_{\ell} \frac{\lambda_{H,\ell}}{\sqrt{\ell}}\right) \left(\sum_{i,j} \frac{i\rho_{H,i}\rho_{L,j}}{\sqrt{iE_H^{(t)} + jE_L^{(t)}}}\right) \cdot \left[2\left(1 - \frac{k_H}{n_H}\right)\Phi\left(-\frac{\beta_H b_{H,2}^{(t)}}{b_{H,1}^{(t)}}\right) + \frac{k_H}{n_H}\right] \\
&\geq \frac{k_H b_{H,1}^{(t)}}{n_H} \left(\sum_{\ell} \frac{\lambda_{H,\ell}}{\sqrt{\ell}}\right) \left(\sum_{i,j} \frac{i\rho_{H,i}\rho_{L,j}}{\sqrt{iE_H^{(t)} + jE_L^{(t)}}}\right); \qquad \text{(C.4.3)} \\
&\left(\frac{\Psi_{E,H}(\cdot)}{\partial E_L}\right)^{(t)} \\
&= b_{H,1}^{(t)} \left(\sum_{\ell} \frac{\lambda_{H,\ell}}{\sqrt{\ell}}\right) \left(\sum_{i,j} \frac{j\rho_{H,i}\rho_{L,j}}{\sqrt{iE_H^{(t)} + jE_L^{(t)}}}\right) \cdot \left[2\left(1 - \frac{k_H}{n_H}\right)\Phi\left(-\frac{\beta_H b_{H,2}^{(t)}}{b_{H,1}^{(t)}}\right) + \frac{k_H}{n_H}\right] \\
&\geq \frac{k_H b_{H,1}^{(t)}}{n_H} \left(\sum_{\ell} \frac{\lambda_{H,\ell}}{\sqrt{\ell}}\right) \left(\sum_{i,j} \frac{j\rho_{H,i}\rho_{L,j}}{\sqrt{iE_H^{(t)} + jE_L^{(t)}}}\right). \qquad \text{(C.4.4)}
\end{aligned}
$$

Taking the limit $E_H^{(t)} \to 0$, we can conclude the relaxation by simplifying (Equation C.4.3) and (Equation C.4.4) as

$$
\begin{aligned}
\left(\frac{\Psi_{E,H}(\cdot)}{\partial E_H}\right)^{(t)} &\geq \frac{k_H}{n_H} \left(\sum_{\ell} \frac{\lambda_{H,\ell}}{\sqrt{\ell}}\right)^2 \left(\sum_{i} \sqrt{i}\rho_{H,i}\right)^2; \\
\left(\frac{\Psi_{E,H}(\cdot)}{\partial E_L}\right)^{(t)} &\geq \frac{k_H}{n_H} \left(\sum_{\ell} \frac{\lambda_{H,\ell}}{\sqrt{\ell}}\right)^2 \left(\sum_{i} \sqrt{i}\rho_{L,i}\right)^2.
\end{aligned}
$$

C.4.3 Discussion of (Equation 4.4.9)

The basic idea is to linearize the DE update equation with Taylor expansion and enforce the difference $\delta_{V,H}^{(t)}$ to decrease at a faster rate than $\delta_{V,L}^{(t)}$:

$$\left(\frac{\Psi_{E,H}(\cdot)}{\partial E_H}\right)^{(t)} \leq \left(\frac{\Psi_{E,L}(\cdot)}{\partial E_H}\right)^{(t)}; \tag{C.4.5}$$

$$\left(\frac{\Psi_{E,H}(\cdot)}{\partial E_L}\right)^{(t)} \leq \left(\frac{\Psi_{E,L}(\cdot)}{\partial E_L}\right)^{(t)}. \tag{C.4.6}$$

Following the same logic as (Equation C.4.3) and (Equation C.4.4), we can lower-bound the gradients $\left(\frac{\Psi_{E,L}(\cdot)}{\partial E_H}\right)^{(t)}$ and $\left(\frac{\Psi_{E,L}(\cdot)}{\partial E_L}\right)^{(t)}$ as

$$\left(\frac{\Psi_{E,L}(\cdot)}{\partial E_H}\right)^{(t)} \geq \frac{k_L}{n_L}\left(\sum_{\ell}\frac{\lambda_{L,\ell}}{\sqrt{\ell}}\right)^2\left(\sum_{i}\sqrt{i}\rho_{H,i}\right)^2;$$

$$\left(\frac{\Psi_{E,L}(\cdot)}{\partial E_L}\right)^{(t)} \geq \frac{k_L}{n_L}\left(\sum_{\ell}\frac{\lambda_{L,\ell}}{\sqrt{\ell}}\right)^2\left(\sum_{i}\sqrt{i}\rho_{L,i}\right)^2.$$

Combining with (Equation C.4.5) will then yield the Requirement 6.

APPENDIX D

APPENDIX OF RECOVERING NOISY-PSEUDO-SPARSE SIGNALS FROM LINEAR MEASUREMENTS VIA INFINITY NORM

D.1 Proof of Lemma 12

Proof. Assume that the recovered results $(\widehat{\mathbf{x}}', \widehat{\mathbf{e}}')$ with at least one entry violating the above condition. We would prove that we can always make the objective function smaller by making $\text{sign}(\widehat{x}_i) = \text{sign}(\widehat{e}_i)$. Without loss of generality, we can assume that $\mathbf{x}^\natural + \mathbf{e}^\natural$ and $\|\mathbf{e}^\natural\|_\infty$ are perfectly recovered. Assume that $\text{sign}(\widehat{x}_i) = -\text{sign}(\widehat{e}_i)$. Hence,

$$\begin{aligned} & x_i^\natural + e_i^\natural = \widehat{x}_i + \widehat{e}_i = \text{sign}(\widehat{x}_i)(|\widehat{x}_i| - |\widehat{e}_i|) \\ \Rightarrow & \big||\widehat{x}_i| - |\widehat{e}_i|\big| = |x_i^\natural + e_i^\natural| \\ \Rightarrow & |\widehat{x}_i| = |\widehat{e}_i| + |x_i^\natural + e_i^\natural| \text{ or } |\widehat{e}_i| = |\widehat{x}_i| + |x_i^\natural + e_i^\natural|. \end{aligned}$$

If $|\widehat{e}_i| = |\widehat{x}_i| + |x_i^\natural + e_i^\natural|$, then

$$|\widehat{e}_i| \geq |x_i^\natural| - |e_i^\natural| > \ 2\|\mathbf{e}\|_\infty - |e_i^\natural| \geq \|\mathbf{e}\|_\infty,$$

which is a contradiction. Hence, $|\widehat{x}_i| = |\widehat{e}_i| + |x_i^\natural + e_i^\natural|$. On the other hand, by defining $\widetilde{x}_i$ and $\widetilde{e}_i$ as

$$(\widetilde{x}_i, \widetilde{e}_i) = \ \text{sign}(x_i^\natural + e_i^\natural) \left(|x_i^\natural + e_i^\natural| - |e_i^\natural|, |e_i^\natural|\right), \tag{D.1.1}$$

it can be easily verified that they satisfy the constraints in (Equation 6.2.2). However,

$$\|\widetilde{\mathbf{e}}\|_\infty = \|\widehat{\mathbf{e}}\|_\infty \quad \|\widetilde{\mathbf{x}}\|_1 < \|\widehat{\mathbf{x}}\|_1.$$

In other words, (Equation 6.2.2) achieves a lower value at $(\widetilde{\mathbf{x}}, \ \widetilde{\mathbf{e}})$, which is a contradiction. This completes the proof of the lemma. □

D.2 Proof of Lemma 13

Proof. Assume that solution $(\widehat{\mathbf{x}},\ \widehat{\mathbf{e}})$ is not unique or not equal to $(\widetilde{\mathbf{x}}, \widetilde{\mathbf{e}})$. Consider $(\mathbf{a}, \mathbf{b}) = (\widehat{\mathbf{x}} - \widetilde{\mathbf{x}},\ \widehat{\mathbf{e}} - \widetilde{\mathbf{e}})$. According to Lemma 44, we have $\mathbf{a} + \mathbf{b} \neq \mathbf{0}$ in the following. Consider $\frac{(\mathbf{a},\ \mathbf{b})}{\|\mathbf{a}+\mathbf{b}\|_2} \in \mathbb{S}^{n-1}$ in the following:

- First, note that $\frac{(\mathbf{a},\ \mathbf{b})}{\|\mathbf{a}+\mathbf{b}\|_2} \in \text{null}(\mathbf{A})$, since

$$\mathbf{A}(\widetilde{\mathbf{x}} + \widetilde{\mathbf{e}}) = \ \mathbf{A}(\widehat{\mathbf{x}} + \widehat{\mathbf{e}}) \implies \frac{\mathbf{A}\,(\mathbf{a}+\mathbf{b})}{\|\mathbf{a}+\mathbf{b}\|_2} = 0,$$

  which indicates that $(\widehat{\mathbf{x}} - \widetilde{\mathbf{x}}, \widehat{\mathbf{e}} - \widetilde{\mathbf{e}}) \in \text{null}(\mathbf{A})$.

- Then, we can verify that $\frac{(\mathbf{a},\ \mathbf{b})}{\|\mathbf{a}+\mathbf{b}\|_2} \in \mathcal{T}^{\lambda}_{\mathbf{x},\mathbf{e}} \setminus \{\mathbf{0}, \mathbf{0}\}$. Further, we have

$$\left\| \widetilde{\mathbf{e}} + \frac{t\mathbf{b}}{\|\mathbf{a}+\mathbf{b}\|_2} \right\|_2^2 \leq \ \|\mathbf{e}^{\natural}\|_2^2 = \|\widetilde{\mathbf{e}}\|_2^2,$$

  which leads to $\left\langle \widetilde{\mathbf{e}}, \frac{\mathbf{b}}{\|\mathbf{a}+\mathbf{b}\|_2} \right\rangle \leq 0$. Combining the above together, we have $\frac{\mathbf{a}+\mathbf{b}}{\|\mathbf{a}+\mathbf{b}\|_2} \in \Omega_{\widetilde{\mathbf{x}},\widetilde{\mathbf{e}}}$.

Since $\frac{\mathbf{a}+\mathbf{b}}{\|\mathbf{a}+\mathbf{b}\|_2} \in \mathbb{S}^{n-1}$ belongs to both $\text{null}(\mathbf{A})$ and $\Omega_{\widetilde{\mathbf{x}},\widetilde{\mathbf{e}}}$, we encounter contradictions with (Equation 6.3.3) and thus have proved this lemma. □

Lemma 44. *If* $\|\mathbf{b} + \widetilde{\mathbf{e}}\|_2^2 \leq \|\widetilde{\mathbf{e}}\|_2^2$*, then*

$$\mathbf{a} + \mathbf{b} \neq \mathbf{0}, \quad \forall\, (\mathbf{a}, \mathbf{b}) \in \mathcal{T}^{\lambda}_{\widetilde{\mathbf{x}},\widetilde{\mathbf{e}}} \setminus \{\mathbf{0}, \mathbf{0}\}.$$

Proof. If $\mathbf{b} = \mathbf{0}$, then by definition $\mathbf{a} \neq \mathbf{0}$. Suppose that $\mathbf{b} \neq \mathbf{0}$ but $\mathbf{a} + \mathbf{b} = \mathbf{0}$. By the definition of sub-differential [153], we have

$$\|\widetilde{\mathbf{x}} + t\mathbf{a}\|_1 + \lambda\|\widetilde{\mathbf{e}} + t\mathbf{b}\|_\infty \geq \|\widetilde{\mathbf{x}}\|_1 + \ \langle \partial\|\widetilde{\mathbf{x}}\|_1, t\mathbf{a}\rangle \ + \ \lambda\|\widetilde{\mathbf{e}}\|_\infty + \lambda \ \langle \partial\|\widetilde{\mathbf{e}}\|_\infty, t\mathbf{b}\rangle\,. \quad \text{(D.2.1)}$$

Combining (Equation D.2.1) and $(\mathbf{a}, \mathbf{b}) \in \ \mathcal{T}^{\lambda}_{\widetilde{\mathbf{x}},\widetilde{\mathbf{e}}}$, we obtain

$$\langle \partial \|\widetilde{\mathbf{x}}\|_1, \mathbf{a} \rangle + \lambda \ \langle \partial \|\widetilde{\mathbf{e}}\|_\infty, \mathbf{b} \rangle \leq 0.$$

Since magnitudes of the elements of $\widetilde{\mathbf{e}}$ are the uniformly distributed, we have [107]

$$\partial \|\widetilde{\mathbf{e}}\|_\infty = \ \{\mathbf{w} : \ w_i \widetilde{e}_i \geq 0, \ \|\mathbf{w}\|_1 = 1\}.$$

For example, we have $\text{sign}(\mathbf{e})/\|\mathbf{e}\|_1 \in \partial \|\widetilde{\mathbf{e}}\|_\infty$. For $\partial \|\mathbf{x}\|_1$, we have

$$(\partial \|\widetilde{\mathbf{x}}\|_1)_i = \text{sign}(\widetilde{x}_i), \ i \in T,$$
$$\left| \ (\partial \|\widetilde{\mathbf{x}}\|_1)_i \ \right| \leq 1, \ \ i \in T^c.$$

Here we set the ith entry in $\partial \|\widetilde{\mathbf{x}}\|_1$ as $\text{sign}(\widetilde{e}_i), \ i \in T^c$. Since we have $\text{sign}(\widetilde{x}_i) = \text{sign}(\widetilde{e}_i)$ for $i \in T$ as shown in Property 1, we have $\partial \|\widetilde{\mathbf{x}}\|_1 = \text{sign}(\widetilde{\mathbf{e}})$. If $\mathbf{a} + \mathbf{b} = \mathbf{0}$, we have

$$\left(1 - \frac{\lambda}{n}\right) \ \langle \text{sign}(\widetilde{\mathbf{e}}), \mathbf{b} \rangle \geq 0 \ \overset{①}{\Longrightarrow} \ \langle \widetilde{\mathbf{e}}, \mathbf{b} \rangle \geq 0, \tag{D.2.2}$$

where ① is because of $k < \lambda < n - k$, and $\widetilde{\mathbf{e}} = \text{sign}(\widetilde{\mathbf{e}}) \|\widetilde{\mathbf{e}}\|_\infty$ shown in Property 1. Note that $\widetilde{\mathbf{e}} + \mathbf{b}$ should satisfy

$$\|\widetilde{\mathbf{e}} + \mathbf{b}\|_2^2 \leq \|\mathbf{e}^\natural\|_2^2 = \ \|\widetilde{\mathbf{e}}\|_2^2,$$

which leads to $\langle \widetilde{\mathbf{e}}, \mathbf{b} \rangle \leq \ -\frac{\|\mathbf{b}\|_2^2}{2} \overset{②}{<} 0$, where ② is due to the fact that $\mathbf{b} \neq \mathbf{0}$. Since this inequality is contradictory to (Equation D.2.2), we have $\mathbf{a} + \mathbf{b} \neq \mathbf{0}$. □

D.3 Proof of Theorem 9

Proof. To prove the theorem, it suffices to show that

$$\omega(\Omega \bigcap \mathbb{S}^{n-1}) \leq \ \sqrt{n} - (1 - 2^{-n}) \sqrt{\frac{\log n}{2}} - \frac{2^{\frac{1}{2}-n}}{\sqrt{\pi}}.$$

First, we define $\Theta_{\widetilde{\mathbf{e}}}$, $\mathcal{S}_1$, and $\mathcal{S}_2$ as

$$\begin{aligned}\Theta_{\widetilde{\mathbf{e}}} &= \{\boldsymbol{\theta}:\ \theta_i\widetilde{e}_i \geq 0,\ \boldsymbol{\theta}\neq \mathbf{0}\};\\ \mathcal{S}_1 &= \Omega\bigcap\mathbb{B}^n,\quad \mathcal{S}_2 = \Theta_{\widetilde{\mathbf{e}}}\bigcap\mathbb{B}^n,\end{aligned} \tag{D.3.1}$$

where $\mathbb{B}^n$ denotes an n-dimensional ball. Easily we can verify that $\mathcal{S}_1$, $\mathcal{S}_2$, and $\mathcal{S}_1\cup\mathcal{S}_2$ are all convex. Further, according to Lemma 45, we have $\mathcal{S}_1\bigcap\mathcal{S}_2{=}\emptyset$. Since $\Omega(\mathcal{S}_1\cup\mathcal{S}_2)\ \leq \omega(\mathbb{B}^n)=\sqrt{n}$, using [107] we have

$$\begin{aligned}\omega(\Omega\bigcap\mathbb{S}^{n-1})+\omega(\mathcal{S}_2) &\overset{①}{\leq}\ \omega(\mathcal{S}_1)+\omega(\mathcal{S}_2){=}\omega(\mathcal{S}_1\cup\mathcal{S}_2)\ +\omega(\mathcal{S}_1\bigcap\mathcal{S}_2)\\ &=\ \omega(\mathcal{S}_1\cup\mathcal{S}_2)\ \leq\omega(\mathbb{B}^n)=\sqrt{n},\end{aligned}$$

where ① is because $\Omega\bigcap\mathbb{S}^{n-1}\subset\mathcal{S}_1$. Combining with Lemma 46, we have

$$\omega(\Omega\bigcap\mathbb{S}^{n-1})\leq\sqrt{n}-(1-2^{-n})\sqrt{\frac{\log n}{2}}-\frac{2^{\frac{1}{2}-n}}{\sqrt{\pi}}.$$

The proof is completed by plugging $\omega(\mathcal{S}_1)$ into

$$m\geq\omega^2(\Omega\bigcap\mathbb{S}^{n-1})+1.$$

□

Lemma 45. *For* Ω *defined in* (Equation 6.3.2) *and* Θ *defined in* (Equation D.3.1)*, we have* $\Omega\ \bigcap\ \Theta=\emptyset$*, which means that* $\boldsymbol{\theta}\in\Theta$ *cannot be decomposed as* $\mathbf{a}+\mathbf{b}$ *such that* $(\mathbf{a},\ \mathbf{b})\in\mathcal{T}^{\lambda}_{\widetilde{\boldsymbol{x}},\widetilde{\boldsymbol{e}}},\ \langle\mathbf{b},\widetilde{\mathbf{e}}\rangle\leq 0$.

Proof. Assume the above argument is untrue. Then we can write $(\mathbf{a},\mathbf{b})=\ (\boldsymbol{\theta}+\mathbf{c},\mathbf{b})\in\mathcal{T}^{\lambda}_{\widetilde{\boldsymbol{x}},\widetilde{\boldsymbol{e}}}$ and have

$$\mathbf{a}+\mathbf{b}=\boldsymbol{\theta}+\mathbf{c}+\mathbf{b}=\boldsymbol{\theta}\implies\mathbf{c}+\mathbf{b}=\mathbf{0}. \tag{D.3.2}$$

Note that $\theta_i\widetilde{e}_i\geq 0$ and $\text{sign}(\widetilde{x}_i)=\text{sign}(\widetilde{e}_i)$ in Property 1. Then, we can verify that

$$\|\widetilde{\mathbf{x}}+\boldsymbol{\theta}\|_1>\|\widetilde{\mathbf{x}}\|_1,\quad \text{sign}(\widetilde{x}_i+\theta_i)=\text{sign}(\widetilde{x}_i),\ i\in T. \tag{D.3.3}$$

According to the definition of $(\boldsymbol{\theta}+\mathbf{c},\ \mathbf{b})\in\ \mathcal{T}^{\lambda}_{\widetilde{\boldsymbol{x}},\widetilde{\boldsymbol{e}}}$, we have

$$\|\widetilde{\mathbf{x}}+\boldsymbol{\theta}+\mathbf{c}\|_1+\lambda\|\widetilde{\mathbf{e}}+\mathbf{b}\|_\infty \leq \|\widetilde{\mathbf{x}}\|_1+\lambda\|\widetilde{\mathbf{e}}\|_\infty \overset{①}{<} \|\widetilde{\mathbf{x}}+\boldsymbol{\theta}\|_1+\lambda\|\widetilde{\mathbf{e}}\|_\infty, \tag{D.3.4}$$

where inequality ① in (Equation D.3.4) is because of (Equation D.3.3). Then we can conclude that $(\mathbf{c},\mathbf{b}) \in \mathcal{T}^{\lambda}_{\widetilde{\boldsymbol{x}}+\boldsymbol{\theta},\widetilde{\boldsymbol{e}}}$. Further, we can verify that $(\mathbf{c},\mathbf{b}) \neq (\mathbf{0},\ \mathbf{0})$ since otherwise we have $\|\widetilde{\mathbf{x}}+\boldsymbol{\theta}\|_1+\lambda\|\widetilde{\mathbf{e}}\|_\infty \leq \|\widetilde{\mathbf{x}}\|_1+\lambda\|\widetilde{\mathbf{e}}\|_\infty$, which is contradictory to (Equation D.3.3).

Similar to the proof in Lemma 44, we can prove $\mathbf{c}+\mathbf{b} \neq 0$, which is omitted for the conciseness of the presentation and is contradictory to (Equation D.3.2). Hence, we have $\Omega \bigcap \Theta = \emptyset$. □

Lemma 46. *For* Θ *defined in* (Equation D.3.1)*, we have*

$$\omega(\Theta \bigcap \mathbb{B}^n) \geq\ (1-2^{-n})\sqrt{\frac{\log n}{2}}+\frac{2^{\frac{1}{2}-n}}{\sqrt{\pi}}.$$

Proof. First, we define a unitary matrix $\mathbf{U}$ as

$$\mathbf{U}=\{\text{diag}(u_i)\}_{i=1}^n,\ \ u_i=\text{sign}(e_i).$$

Based on the rotation invariant property of Gaussian RVs, [139] we have $\omega(\mathbf{U}\Omega)=\omega(\Omega)$, where $\mathbf{U}\Omega$ is written as $\mathbf{U}\Omega=\{\boldsymbol{\theta}:\ \theta_i\geq 0,\ \boldsymbol{\theta}\neq\mathbf{0}\}$. For a specific Gaussian RV $\mathbf{g}$, define an event E as $\{\exists\, i,\ \text{s.t. } g_i\geq 0\}$ whose probability is $1-2^{-n}$. Then we have

$$\begin{aligned}
\mathbb{E}_{\mathbf{g}} \sup_{u\in\Omega\bigcap\mathbb{B}^n} \langle \mathbf{g},\mathbf{U}\rangle &= \mathbb{E}\mathbb{E}_{\mathbf{g}|E} \sup_{u\in\Omega\bigcap\mathbb{B}^n} \langle \mathbf{g},\mathbf{U}\rangle \\
&= \mathbb{P}(E)\mathbb{E}\max_{\substack{1\leq i\leq n\\ \exists g_i\geq 0}} g_i+\ \mathbb{P}(E^c)\mathbb{E}\max_{\substack{1\leq i\leq n\\ \forall g_i<0}} g_i \\
&\geq \mathbb{P}(E)\mathbb{E}\max_i g_i+\mathbb{P}(E^c)\mathbb{E}(g_i\,|g_i<0) \\
&\geq (1-2^{-n})\sqrt{\frac{\log n}{2}}+\frac{2^{\frac{1}{2}-n}}{\sqrt{\pi}},
\end{aligned}$$

where $\mathbb{P}(E)$ and $\mathbb{P}(E^c)$ denote the probability of event E and its complement E^c, respectively. □

APPENDIX E

APPENDIX OF SPARSE SIGNAL RECONSTRUCTION WITH A MULTIPLE CONVEX SETS DOMAIN

E.1 Proof of Theorem 10

Proof. Note that for any-vector non-zero $\boldsymbol{h} \in \text{null}(\mathbf{A}) \bigcap \mathcal{T} \bigcap \left(\bigcup_{i,j} \widetilde{\mathcal{C}}_{i,j} \right)$, we can always rescale to make it unit-norm. Hence we can rewrite the event $\mathcal{E}$ as

$$\mathcal{E} = \left\{ \text{null}(\mathbf{A}) \bigcap \mathbb{S}_2^{n-1} \bigcap \mathcal{T} \bigcap \left(\bigcup_{i,j} \widetilde{\mathcal{C}}_{i,j} \right) = \emptyset \right\}.$$

For the conciseness of notation, we define $\widetilde{\mathcal{C}}$ to be $\widetilde{\mathcal{C}} = \bigcup_{i,j} \widetilde{\mathcal{C}}_{i,j}$. Then we upper-bound $1 - \mathbb{P}(\mathcal{E})$ as

$$\begin{aligned} 1 - \mathbb{P}(\mathcal{E}) = & \ \mathbb{P}\left(\text{null}(\mathbf{A}) \bigcap \mathbb{S}_2^{n-1} \bigcap \mathcal{T} \bigcap \widetilde{\mathcal{C}} \neq \emptyset \right) \\ \overset{①}{\leq} & \underbrace{\mathbb{P}\left(\text{null}(\mathbf{A}) \bigcap \mathbb{S}_2^{n-1} \bigcap \mathcal{T} \neq \emptyset \right)}_{\mathcal{P}_1} \wedge \underbrace{\mathbb{P}\left(\text{null}(\mathbf{A}) \bigcap \mathbb{S}_2^{n-1} \bigcap \widetilde{\mathcal{C}} \neq \emptyset \right)}_{\mathcal{P}_2}, \end{aligned}$$

where ① is because

$$\begin{aligned} \left\{ \text{null}(\mathbf{A}) \bigcap \mathbb{S}_2^{n-1} \bigcap \mathcal{T} \bigcap \widetilde{\mathcal{C}} \neq \emptyset \right\} & \subseteq \left\{ \text{null}(\mathbf{A}) \bigcap \mathbb{S}_2^{n-1} \bigcap \mathcal{T} \neq \emptyset \right\}, \\ \left\{ \text{null}(\mathbf{A}) \bigcap \mathbb{S}_2^{n-1} \bigcap \mathcal{T} \bigcap \widetilde{\mathcal{C}} \neq \emptyset \right\} & \subseteq \left\{ \text{null}(\mathbf{A}) \bigcap \mathbb{S}_2^{n-1} \bigcap \widetilde{\mathcal{C}} \neq \emptyset \right\} \end{aligned}$$

With Lemma 47 and Lemma 48, we can separately bound $\mathcal{P}_1$ and $\mathcal{P}_2$ and finish the proof.

□

Lemma 47. *We have* $\mathcal{P}_1 \leq 1 \wedge \exp\left(-\frac{(a_m - \omega(\mathcal{T}))^2}{2} \right)$, *if* $a_m \geq \omega(\mathcal{T})$.

Proof. Note that we have

$$\underbrace{\mathbb{P}\left(\text{null}(\mathbf{A})\bigcap\mathbb{S}_2^{n-1}\bigcap\mathcal{T}\neq\emptyset\right)}_{\mathcal{P}_1}+\underbrace{\mathbb{P}\left(\text{null}(\mathbf{A})\bigcap\mathbb{S}_2^{n-1}\bigcap\mathcal{T}=\emptyset\right)}_{\mathcal{P}_1^c}=1.$$

Then we lower-bound $\mathcal{P}_1^c$ as

$$\mathcal{P}_1^c=\mathbb{P}\left(\min_{\mathbf{u}\in\mathbb{S}_2^{n-1}\bigcap\mathcal{T}}\|\mathbf{A}\mathbf{u}\|_2>0\right)\overset{①}{\geq}1-\exp\left(-\frac{\left(a_m-\omega\left(\mathcal{T}\right)\right)^2}{2}\right),$$

provided $a_m\geq\omega(\mathcal{T})$, where ① is because of Corollary 3.3 in [107], and $\omega(\cdot)$ denotes the Gaussian width. □

Lemma 48. *If $\omega(\widetilde{\mathcal{C}}_{ij})\leq 1-2\epsilon a_M$, we have*

$$\mathcal{P}_2\leq 1\wedge\frac{3}{2}\exp\left(-\frac{\epsilon^2a_M^2}{2}\right)+\sum_{i\leq j}\exp\left(-\frac{\left((1-2\epsilon)a_M-\omega(\widetilde{\mathcal{C}}_{ij})\right)^2}{2}\right),$$

Proof. Note that we have

$$\underbrace{\mathbb{P}\left(\text{null}(\mathbf{A})\bigcap S_2^{n-1}\bigcap\widetilde{\mathcal{C}}\neq\emptyset\right)}_{\mathcal{P}_2}+\underbrace{\mathbb{P}\left(\text{null}(\mathbf{A})\bigcap S_2^{n-1}\bigcap\widetilde{\mathcal{C}}=\emptyset\right)}_{\mathcal{P}_2^c}=1.$$

Here we upper-bound $\mathcal{P}_2$ via lower-bounding $\mathcal{P}_2^c$. First we define $\mathcal{P}_2^c(d)$ as

$$\mathcal{P}_2^c(d)\triangleq\mathbb{P}\left(\min_{\mathbf{u}\in\bigcup\mathcal{S}_{i,j},\,\mathbf{v}\in\text{null}(\mathbf{A})}\|\mathbf{u}-\mathbf{v}\|_2\geq d\right).$$

Then we have $\mathcal{P}_2^c=\lim_{d\to 0}\mathcal{P}_2^c(d)$. The following proof trick is fundamentally the same as that are used in Thm. 4.1 in [108] but in a clear format by only keeping the necessary parts for this scenario. We only present it for the self-containing of the thesis and do not claim any novelties.

We first define $\mathcal{S}_{i,j} = \mathbb{S}_2^{n-1} \bigcap \widetilde{\mathcal{C}}_{i,j}$ and two quantities Q_1 and Q_2 as

$$
\begin{aligned}
Q_1 &\triangleq \mathbb{P}\left(\min_{\mathbf{u}\in\bigcup \mathcal{S}_{i,j}} \|\mathbf{A}\mathbf{u}\|_2 \geq d(1+\epsilon_1)\mathbb{E}\|\mathbf{A}\|_2\right), \\
Q_2 &\triangleq \mathbb{P}\left(\bigcap_{i_1\leq j_1}\bigcap_{\mathbf{u}\in\mathcal{S}_{i_1,j_1}}\left(\left(\sum_{i_2=1}^{M} g_{i_2}^2\right)^{1/2} + \sum_{j_2} u_{j_2}h_{j_2} \geq\ d(1+\epsilon_1)\mathbb{E}\|\mathbf{A}\|_2 + \epsilon_2 a_M\right)\right),
\end{aligned}
$$

where $a_M = \mathbb{E}\|\mathbf{g}\|_2,\ \mathbf{g}\in\mathcal{N}(\mathbf{0},\ \mathbf{I}_{M\times M})$, and g_j, h_i are iid standard normal random variables $\mathcal{N}(0,1)$. The following proof is divided into 3 parts.

Step I. We prove that $\mathcal{P}_2^c(d) + e^{-\epsilon_1^2 a_M^2/2} \geq Q_1$, which is done by

$$
\begin{aligned}
Q_1 &= \mathbb{P}\left(\min_{\mathbf{u}\in\bigcup \mathcal{S}_{i,j}} \|\mathbf{A}\mathbf{u}\|_2 \geq\ d(1+\epsilon_1)\mathbb{E}\|\mathbf{A}\|_2\right) \\
&= \mathbb{P}\left(\min_{\mathbf{u}\in\bigcup \mathcal{S}_{i,j},\ \mathbf{v}\in\text{null}(\mathbf{A})} \|\mathbf{A}(\mathbf{u}-\mathbf{v})\|_2 \geq d(1+\epsilon_1)\mathbb{E}\|\mathbf{A}\|_2\right) \\
&\overset{①}{\leq} \mathbb{P}\left(\min_{\mathbf{u}\in\bigcup \mathcal{S}_{i,j},\ \mathbf{v}\in\text{null}(\mathbf{A})} \|\mathbf{A}\|_2\|\mathbf{u}-\mathbf{v}\|_2 \geq d(1+\epsilon_1)\mathbb{E}\|\mathbf{A}\|_2\right) \\
&\overset{②}{\leq} \mathbb{P}\left(\|\mathbf{A}\|_2 \geq (1+\epsilon_1)\mathbb{E}\|\mathbf{A}\|_2\right) + \underbrace{\mathbb{P}\left(\min_{\mathbf{u}\in\bigcup \mathcal{S}_{i,j},\ \mathbf{v}\in\text{null}(\mathbf{A})} \|\mathbf{u}-\mathbf{v}\|_2 \geq d\right)}_{\leq\ \mathcal{P}_2^c(d)} \\
&\overset{③}{\leq} \exp\left(-\frac{\epsilon_1^2(\mathbb{E}\|\mathbf{A}\|_2)^2}{2}\right) + \mathcal{P}_2^c(d) \\
&\overset{④}{\leq} \exp\left(-\frac{\epsilon_1^2 a_M^2}{2}\right) + \mathcal{P}_2^c(d),
\end{aligned}
$$

where in ① we use $\|\mathbf{A}\|_2\|\mathbf{u}-\mathbf{v}\|_2 \geq \|\mathbf{A}(\mathbf{u}-\mathbf{v})\|_2$, in ② we use the union bound for

$$
\begin{aligned}
&\left\{\min_{\mathbf{u}\in\bigcup \mathcal{S}_{i,j},\ \mathbf{v}\in\text{null}(\mathbf{A})} \|\mathbf{A}\|_2\|\mathbf{u}-\mathbf{v}\|_2 \geq d(1+\epsilon_1)\mathbb{E}\|\mathbf{A}\|_2\right\} \\
\subseteq\ &\{\|\mathbf{A}\|_2 \geq (1+\epsilon_1)\mathbb{E}\|\mathbf{A}\|_2\}\bigcup\left\{\min_{\mathbf{u}\in\bigcup \mathcal{S}_{i,j},\ \mathbf{v}\in\text{null}(\mathbf{A})} \|\mathbf{u}-\mathbf{v}\|_2 \geq d\right\},
\end{aligned}
$$

in ③ we use the Gaussian concentration inequality Lipschitz functions (Theorem 5.6 in [140]) for $\|\mathbf{A}\|_2$, and in ④ we use $\|\mathbf{A}\|_2 \geq \|\mathbf{A}\mathbf{e}_1\|_2 = \|\sum_{i=1}^{M} A_{i,1}\|_2$, where $\mathbf{e}_1$ denotes the canonical basis.

Step II. We prove that $Q_1 + \frac{1}{2}e^{-\epsilon_2^2 a_M^2/2} \geq Q_2$, which is done by

$$
\begin{aligned}
& Q_1 + \frac{1}{2}e^{-\epsilon^2 a_M^2/2} \overset{⑤}{\geq} Q_1 + \mathbb{P}\{g \geq \epsilon_2 a_M\} \\
\overset{⑥}{\geq} & \ \mathbb{P}\left(\min_{\mathbf{u}\in\bigcup \mathcal{S}_{i_1,j_1}} \|\mathbf{A}\mathbf{u}\|_2 + g\|\mathbf{u}\|_2 \geq \ d(1+\epsilon)\mathbb{E}\|\mathbf{A}\|_2 + \ \epsilon_2 a_M \|\mathbf{u}\|_2 \right) \\
= & \ \mathbb{P}\left(\bigcap_{i_1\leq j_1} \bigcap_{\mathbf{u}\in\mathcal{S}_{i_1,j_1}} \|\mathbf{A}\mathbf{u}\|_2 + g\|\mathbf{u}\|_2 \geq \ d(1+\epsilon)\mathbb{E}\|\mathbf{A}\|_2 + \ \epsilon_2 a_M \|\mathbf{u}\|_2 \right) \\
\overset{⑦}{\geq} & \underbrace{\mathbb{P}\left(\bigcap_{i_1\leq j_1} \bigcap_{u\in\mathcal{S}_{i_1,j_1}} \left(\sum_{i_2=1}^{M} g_{i_2}^2\right)^{\frac{1}{2}} + \sum_{j_2=1}^{N} u_{j_2}h_{j_2} \geq \ d(1+\epsilon_1)\mathbb{E}\|\mathbf{A}\|_2 + \ \epsilon_2 a_M \right)}_{Q_2},
\end{aligned}
$$

where in ⑤ $\mathbf{g}$ is a RV satisfying standard normal distribution, in ⑥ we use the union bound, and ⑦ comes from Lemma 3.1 in [108] and $\|\mathbf{u}\|_2 = 1$.

Step III. We lower bound Q_2 as

$$
\begin{aligned}
& 1 - Q_2 = \mathbb{P}\left(\bigcup_{i_1\leq j_1} \bigcup_{u\in\mathcal{S}_{i_1,j_1}} \left[\left(\sum_{i_2=1}^{M} g_{i_2}^2\right)^{\frac{1}{2}} + \sum_{j_2=1}^{N} u_{j_2}h_{j_2} \leq \ d(1+\epsilon_1)\mathbb{E}\|\mathbf{A}\|_2 + \epsilon_2 a_M \right] \right) \\
\leq & \ \mathbb{P}\left(\left(\sum_{i_2=1}^{M} g_{i_2}^2\right)^{\frac{1}{2}} - \ a_M \leq -\epsilon_2 a_M \right) \\
& + \mathbb{P}\left(\bigcup_{i_1\leq j_1} \bigcup_{u\in\mathcal{S}_{i_1,j_1}} \sum_{j_2=1}^{N} u_{j_2}h_{j_2} \leq \ d(1+\epsilon_1)\mathbb{E}\|\mathbf{A}\|_2 - (1-2\epsilon_2)a_M \right) \\
\overset{⑧}{\leq} & \ \exp\left(-\frac{\epsilon_2^2 a_M^2}{2}\right) + \mathbb{P}\left(\bigcup_{i_1\leq j_1} \bigcup_{u\in\mathcal{S}_{i_1,j_1}} \sum_{j_2=1}^{N} u_{j_2}h_{j_2} \leq \ d(1+\epsilon_1)\mathbb{E}\|\mathbf{A}\|_2 - (1-2\epsilon_2)a_M \right) \\
\overset{⑨}{\leq} & \ \exp\left(-\frac{\epsilon_2^2 a_M^2}{2}\right) + \sum_{i_1\leq j_1} \mathbb{P}\left(\bigcup_{u\in\mathcal{S}_{i_1,j_1}} \sum_{j_2=1}^{N} u_{j_2}h_{j_2} \leq \ d(1+\epsilon_1)\mathbb{E}\|\mathbf{A}\|_2 - (1-2\epsilon_2)a_M \right) \\
\overset{Ⓐ}{\leq} & \ \exp\left(-\frac{\epsilon_2^2 a_M^2}{2}\right) + \sum_{i_1\leq j_1} \mathbb{P}\left(\max_{u\in\mathcal{S}_{i_1,j_1}} \sum_{j_2=1}^{N} u_{j_2}h_{j_2}' \geq \ (1-2\epsilon_2)a_M - d(1+\epsilon_1)\mathbb{E}\|\mathbf{A}\|_2 \right) \\
\overset{Ⓑ}{\leq} & \ \exp\left(-\frac{\epsilon_2^2 a_M^2}{2}\right) + \sum_{i_1\leq j_1} \exp\left(-\frac{\left((1-2\epsilon_2)a_M - d(1+\epsilon_1)\mathbb{E}\|\mathbf{A}\|_2 - \omega(\widetilde{\mathcal{C}}_{ij})\right)^2}{2} \right),
\end{aligned}
$$

where in ⑧ we use $\mathbb{E}\sqrt{\sum_{i_2=1}^{M} g_{i_2}^2} = a_M$ and Gaussian concentration inequality in [140], in ⑨ we use union-bound, in Ⓐ we define $h^{'} = -h$ and flip the sign by the symmetry of Gaussian variables, and in Ⓑ we use the definition of $\omega(\widetilde{\mathcal{C}}_{ij})$. Assuming $(1-2\epsilon_2)a_M \geq d(1+\epsilon_1)\mathbb{E}\|\mathbf{A}\|_2 + \omega(\widetilde{\mathcal{C}}_{ij})$, we finish the proof via the Gaussian concentration inequality in [140].

Combining the above together and set $d(1+\epsilon_1) \to 0$ while $\epsilon_1 \to \infty$, we conclude that

$$\mathcal{P}_2^c \geq 1 - \frac{3}{2}\exp\left(-\frac{\epsilon^2 a_M^2}{2}\right) - \sum_{i\leq j}\exp\left(-\frac{\left((1-2\epsilon)a_M - \omega(\widetilde{\mathcal{C}}_{ij})\right)^2}{2}\right),$$

provided $(1-2\epsilon)a_M \geq \omega(\widetilde{\mathcal{C}}_{ij})$, and finish the proof.

□

E.2 Proof of Theorem 11

Proof. Define $\mathbf{p}^*$ and $\mathbf{x}^*$ as

$$\mathbf{p}^* = \text{argmin}_{\mathbf{p}} \sum_t \mathcal{L}\left(\mathbf{p}, \mathbf{x}^{(t)}\right), \quad \mathbf{x}^* = \text{argmin}_{\mathbf{x}} \sum_t \mathcal{L}\left(\mathbf{p}^{(t)}, \mathbf{x}\right). \tag{E.2.1}$$

respectively First we define $\mathcal{T}_1^t$ and $\mathcal{T}_2^t$ as

$$\mathcal{T}_1^t = \mathcal{L}(\mathbf{p}^{(t)}, \mathbf{x}^{(t)}) - \mathcal{L}(\mathbf{p}^*, \mathbf{x}^{(t)});$$
$$\mathcal{T}_2^t = \mathcal{L}(\mathbf{p}^{(t)}, \mathbf{x}^{(t)}) - \mathcal{L}(\mathbf{p}^{(t)}, \mathbf{x}^*),$$

respectively. Then our goal becomes bounding $|\sum_t \mathcal{T}_1^t| + |\sum_t \mathcal{T}_2^t|$. With Lemma 49 and Lemma 50, we have finished the proof. □

Lemma 49. *Define $\mathcal{T}_1^t = \mathcal{L}(\mathbf{p}^{(t)}, \mathbf{x}^{(t)}) - \mathcal{L}(\mathbf{p}^*, \mathbf{x}^{(t)})$, where $\mathbf{p}^*$ is defined in (Equation E.2.1), then we have*

$$0 < \sum_t \mathcal{T}_1^t \leq R_f \sqrt{T \log L},$$

when $\eta_p^{(t)} = R_f \sqrt{2 \log L / T}$.

Proof. Based on the definition of $\mathbf{p}^*$, we note that $\sum_t \mathcal{T}_1^t$ is non-negative and prove the lower-bound. Then we prove its upper-bound.

Since the function is linear, optimal $\mathbf{p}^*$ must be at the edge of Δ_L and we denote the non-zero entry as i^*. Hence, we could study it via the *multiplicative weight algorithm* analysis [117]. First we rewrite the update (Equation 7.4.2). Define $\mathbf{w}^{(0)} = \mathbf{1} \in \mathbb{R}^L$ and update $\mathbf{w}^{(t+1)}$ as

$$w_i^{(t+1)} = w_i^{(t)} \exp\left(-\eta_p^{(t)} f_i(\mathbf{x}^{(t)})\right), \; p_i^{(t+1)} = \frac{w_i^{(t+1)}}{\sum_i w_i^{(t+1)}}.$$

where $(\cdot)_i$ denotes the ith element, and $\mathbf{p}^{(t+1)}$ can be regarded as the normalized version of $\mathbf{w}^{(t+1)}$.

First we define Ψ_t $\Psi_t = \sum_{i=1}^L w_i^{(t)}$. Then we have $\Psi_0 = L$ while

$$\Psi_T \geq w_{i^*}^{(T)} = \exp\left(-\sum_{t=1}^T \eta_p^{(t)} f_{i^*}(\mathbf{x}^{(t)})\right) = \exp\left(-\eta_p \sum_{t=1}^T f_{i^*}(\mathbf{x}^{(t)})\right),$$

where $\eta_p^{(t)} = \eta_p = \sqrt{2 \log L / T}$. Then we study the division Ψ_{t+1}/Ψ_t as

$$\begin{aligned}\Psi_{t+1} = \sum_i w_i^{(t+1)} = \sum_i w_i^t \exp\left(-\eta_p \boldsymbol{f}_i(\mathbf{x}^{(t)})\right) &\overset{①}{\leq} \sum_i w_i^t \left(1 - \eta_p \boldsymbol{f}_i(\mathbf{x}^{(t)}) + \frac{\eta_p^2 f_i^2(\mathbf{x}^{(t)})}{2}\right) \\ = \Psi_t \left(1 - \eta_p \left\langle \mathbf{p}^{(t)}, \boldsymbol{f}(\mathbf{x}^{(t)}) \right\rangle + \frac{\eta_p^2 R_f^2}{2}\right) &\overset{②}{\leq} \Psi_t \exp\left(-\eta_p \left\langle \mathbf{p}^{(t)}, \boldsymbol{f}(\mathbf{x}^{(t)}) \right\rangle + \frac{\eta_p^2 R_f^2}{2}\right)\end{aligned}$$

where in ① we use $e^{-x} \leq 1 + x + x^2/2$ for $x \geq 0$, and in ② we use $e^x \geq 1 + x$ for all $x \in \mathbb{R}$. Using the above relation iteratively, we conclude that

$$\frac{\Psi_T}{\Psi_0} \leq \exp\left(-\eta_p \sum_t \left\langle \mathbf{p}^{(t)}, \boldsymbol{f}(\mathbf{x}^{(t)}) \right\rangle + \frac{\eta_p^2 T R_f^2}{2}\right),$$

which gives us

$$\log \Psi_T \leq \log L - \eta_p \sum_t \left\langle \mathbf{p}^{(t)}, \boldsymbol{f}(\mathbf{x}^{(t)}) \right\rangle + \frac{T\eta_p^2 R_f^2}{2}.$$

With relation $\log \Psi_T \geq \log w_{i^*}^{(T)}$, we obtain

$$\begin{aligned}\eta_p \sum_t \left(\left\langle \mathbf{p}^{(t)}, \boldsymbol{f}(\mathbf{x}^{(t)}) \right\rangle - \left\langle \mathbf{e}_{i^*}, \boldsymbol{f}(\mathbf{x}^{(t)}) \right\rangle\right) &= \eta_p \sum_t \left(\left\langle \mathbf{p}^{(t)}, \boldsymbol{f}(\mathbf{x}^{(t)}) \right\rangle - \left\langle \mathbf{p}^{*}, \boldsymbol{f}(\mathbf{x}^{(t)}) \right\rangle\right) \\ &\leq \log L + \frac{T\eta_p^2 R_f^2}{2},\end{aligned}$$

where $\mathbf{e}_{i^*}$ denotes the canonical basis, namely, has 1 in its i^*th entry and all others to be zero.

□

Lemma 50. *Define $\mathcal{T}_2^t = \mathcal{L}(\mathbf{p}^{(t)}, \mathbf{x}^{(t)}) - \mathcal{L}(\mathbf{p}^{(t)}, \mathbf{x}^*)$, where $\mathbf{x}^*$ is defined in (Equation E.2.1), and set $\eta_x^{(t)} = \eta_x \leq L_h^{-1}$, then we have*

$$0 \leq \sum_t \mathcal{T}_2^t \leq \frac{1}{2\eta_x}\|\mathbf{x}^{(0)} - \mathbf{x}^*\|_2^2.$$

Proof. From the definition of $\mathbf{x}^*$, we can prove the non-negativeness of $\sum_t \mathcal{T}_2^t$. Here we focus on upper-bounding $\sum_t \mathcal{T}_2^t$ by separately analyzing each term $\mathcal{T}_2^t$. For the conciseness of notation, we drop the time index t. Define $h(\mathbf{x})$ as

$$h(\mathbf{x}) = \sum_i p_i h_i(\mathbf{x}) + \frac{\lambda_1\|\mathbf{y} - \boldsymbol{A}\boldsymbol{x}\|_2^2}{2} + \frac{\lambda_2\|\mathbf{x}\|_2^2}{2}.$$

First, we rewrite the update equation as

$$\mathbf{x}^{(t+1)} = \mathbf{x}^{(t)} - \underbrace{\left(\mathbf{x}^{(t)} - \mathsf{prox}_{\eta_x\|\cdot\|_1}\left[\mathbf{x}^{(t)} - \eta_w \nabla h(\mathbf{x}^{(t)})\right]\right)}_{\eta_x H(\mathbf{x}^{(t)})},$$

which means that

$$H(\mathbf{x}^{(t)}) = \frac{\mathbf{x}^{(t)} - \mathsf{prox}_{\eta_x\|\cdot\|_1}\left(\mathbf{x}^{(t)} - \eta_w \nabla h(\mathbf{x}^{(t)})\right)}{\eta_x},$$

where $\mathsf{prox}_{\eta_x\|\cdot\|_1}(\mathbf{x})$ is defined as [112]

$$\mathsf{prox}_{\eta_x\|\cdot\|_1}(\mathbf{x}) = \text{argmin}_{\mathbf{z}} \ \eta_x\|\mathbf{z}\|_1 + \frac{1}{2}\|\mathbf{x}-\mathbf{z}\|_2^2.$$

Here we need one important property of $H(\mathbf{x}^{(t)})$, that is widely in the analysis of proximal gradient descent (direct results of Theorem 6.39 in [112]) and states

$$H(\mathbf{x}^{(t)}) \in \nabla h(\mathbf{x}^{(t)}) + \partial\|\mathbf{x}^{(t+1)}\|_1.$$

Here we consider the update relation $f(\mathbf{x}^{(t+1)}) - f(z)$ as

$$\begin{aligned}
\mathcal{T}_2^{t+1} = \sum_i p_i^{(t)}\left[f_i(\mathbf{x}^{(t+1)}) - f_i(\mathbf{x}^*)\right] =& \ \|\mathbf{x}^{(t+1)}\|_1 + h(\mathbf{x}^{(t+1)}) - \|\mathbf{x}^*\|_1 - h(\mathbf{x}^*) \\
\overset{①}{\leq}& \ \left\langle \partial\|\mathbf{x}^{(t+1)}\|_1,\, \mathbf{x}^{(t+1)} - \mathbf{x}^*\right\rangle + \ h(\mathbf{x}^{(t)}) + \left\langle \nabla h(\mathbf{x}^{(t)}),\, \mathbf{x}^{(t+1)} - \mathbf{x}^{(t)}\right\rangle + \frac{L_h}{2}\|\mathbf{x}^{(t+1)} - \mathbf{x}^{(t)}\|_2^2 - h(\mathbf{x}^*) \\
\overset{②}{\leq}& \ \left\langle \partial\|\mathbf{x}^{(t+1)}\|_1,\, \mathbf{x}^{(t+1)} - \mathbf{x}^*\right\rangle + \ \left\langle \nabla h(\mathbf{x}^{(t)}),\, \mathbf{x}^{(t)} - \mathbf{x}^* + \mathbf{x}^{(t+1)} - \mathbf{x}^{(t)}\right\rangle + \frac{L_h}{2}\|\mathbf{x}^{(t+1)} - \mathbf{x}^{(t)}\|_2^2 \\
=& \ \left\langle \partial\|\mathbf{x}^{(t+1)}\|_1 + \nabla h(\mathbf{x}^{(t)}),\, \mathbf{x}^{(t+1)} - \mathbf{x}^*\right\rangle + \frac{L_h}{2}\|\mathbf{x}^{(t+1)} - \mathbf{x}^{(t)}\|_2^2 \\
\overset{③}{\leq}& \ \left\langle H(\mathbf{x}^{(t)}),\, \mathbf{x}^{(t+1)} - \mathbf{x}^*\right\rangle + \frac{L_h}{2}\|\mathbf{x}^{(t+1)} - \mathbf{x}^{(t)}\|_2^2 \\
\overset{④}{=}& \ \frac{1}{\eta_x}\left\langle \mathbf{x}^{(t)} - \mathbf{x}^{(t+1)}, \mathbf{x}^{(t+1)} - \mathbf{x}^*\right\rangle + \frac{L_h}{2}\|\mathbf{x}^{(t+1)} - \mathbf{x}^{(t)}\|_2^2 \\
\overset{⑤}{\leq}& \ \frac{1}{\eta_x}\left\langle \mathbf{x}^{(t)} - \mathbf{x}^{(t+1)}, \mathbf{x}^{(t+1)} - \mathbf{x}^*\right\rangle + \frac{1}{2\eta_x}\|\mathbf{x}^{(t+1)} - \mathbf{x}^{(t)}\|_2^2 \\
=& \ \frac{1}{\eta_x}\left\langle \mathbf{x}^{(t)} - \mathbf{x}^{(t+1)}, \mathbf{x}^{(t+1)} - \mathbf{x}^*\right\rangle + \frac{1}{2\eta_x}\|\mathbf{x}^{(t+1)} - \mathbf{x}^*\|_2^2 \ + \frac{1}{2\eta_x}\|\mathbf{x}^{(t)} - \mathbf{x}^*\|_2^2 \\
+& \ \frac{1}{\eta_x}\left\langle \mathbf{x}^{(t+1)} - \mathbf{x}^*,\, \mathbf{x}^* - \mathbf{x}^{(t)}\right\rangle \\
=& \ \frac{1}{2\eta_x}\|\mathbf{x}^{(t)} - \mathbf{x}^*\|_2^2 + \frac{1}{2\eta_x}\|\mathbf{x}^{(t+1)} - \mathbf{x}^*\|_2^2 + \ \frac{1}{\eta_x}\left\langle \mathbf{x}^{(t+1)} - \mathbf{x}^*,\, \mathbf{x}^* - \mathbf{x}^{(t)} + \mathbf{x}^{(t)} - \mathbf{x}^{(t+1)}\right\rangle \\
=& \ \frac{1}{2\eta_x}\|\mathbf{x}^{(t)} - \mathbf{x}^*\|_2^2 - \ \frac{1}{2\eta_x}\|\mathbf{x}^{(t+1)} - \mathbf{x}^*\|_2^2,
\end{aligned}$$

where in ① we use $\|\mathbf{x}^*\|_1 \geq \|\mathbf{x}^{(t+1)}\|_1 + \left\langle \partial\|\mathbf{x}^{(t+1)}\|_1, \mathbf{x}^* - \mathbf{x}^{(t+1)}\right\rangle$ based on the definition

of sub-gradients, and $h(\mathbf{x}^{t+1}) \leq h(\mathbf{x}^{(t)}) + \left\langle \nabla h(\mathbf{x}^{(t)}),\, \mathbf{x}^{(t+1)} \right\rangle + L_h \|\mathbf{x}^{(t+1)} - \mathbf{x}^{(t)}\|_2^2/2$ from the L_h smoothness of $h(\cdot)$, in ② we use $h(\mathbf{x}^*) \geq h(\mathbf{x}^{(t)}) + \left\langle \nabla h(\mathbf{x}^{(t)}), \mathbf{x}^* - \mathbf{x}^{(t)} \right\rangle$ since $h(\cdot)$ is convex, in ③ we use $H(\mathbf{x}^{(t)}) \in \nabla h(\mathbf{x}^{(t)}) + \partial \|\mathbf{x}^{(t+1)}\|_1$, and in ④ we use $\mathbf{x}^{(t+1)} = \mathbf{x}^{(t)} - \eta_x H(\mathbf{x}^{(t)})$, and in ⑤ we use $\eta_x \leq L^{-1}$.

Hence, we finishes the proof by

$$\begin{aligned}
&\sum_t \mathcal{T}_2^t \leq \sum_t \left[\frac{1}{2\eta_x} \|\mathbf{x}^{(t-1)} - \mathbf{x}^*\|_2^2 - \frac{1}{2\eta_x} \|\mathbf{x}^{(t)} - \mathbf{x}^*\|_2^2 \right] \\
&= \frac{1}{2\eta_x} \|\mathbf{x}^{(0)} - \mathbf{x}^*\|_2^2 - \frac{1}{2\eta_x} \|\mathbf{x}^{(T)} - \mathbf{x}^*\|_2^2 \leq \frac{1}{2\eta_x} \|\mathbf{x}^{(0)} - \mathbf{x}^*\|_2^2 \overset{(i)}{\leq} \frac{4R^2}{2\eta_x},
\end{aligned}$$

where in (i) we use $\|\mathbf{x}^{(0)} - \mathbf{x}^*\|_2 \leq \|\mathbf{x}^*\|_2 + \|\mathbf{x}^{(0)}\| \leq 2R$. □

E.3 Proof of Theorem 12

Proof. First we define $h(\mathbf{x}) = \sum_i p_i h_i(\mathbf{x}) + \lambda_1 \|\mathbf{y} - \boldsymbol{A}\boldsymbol{x}\|_2^2/2 + \lambda_2 \|\mathbf{x}\|_2^2/2$. Then we consider the term $\mathcal{L}(\mathbf{p}^{(t)}, \mathbf{x}^{(t+1)}) - \mathcal{L}(\mathbf{p}^{(t)}, \mathbf{x}^{(t)})$ and have

$$\begin{aligned}
&\mathcal{L}(\mathbf{p}^{(t)}, \mathbf{x}^{(t+1)}) - \mathcal{L}(\mathbf{p}^{(t)}, \mathbf{x}^{(t)}) = \|\mathbf{x}^{(t+1)}\|_1 - \|\mathbf{x}^{(t)}\|_1 + \sum_i p_i^{(t)} \left(h_i(\mathbf{x}^{(t+1)}) - h_i(\mathbf{x}^{(t)}) \right) \\
&\overset{①}{\leq} \left\langle \partial \|\mathbf{x}^{(t+1)}\|_1, \mathbf{x}^{(t+1)} - \mathbf{x}^{(t)} \right\rangle + \sum_i p_i^{(t)} \left[\left\langle \nabla h_i(\mathbf{x}^{(t)}),\, \mathbf{x}^{(t+1)} - \mathbf{x}^{(t)} \right\rangle + \frac{L_h}{2} \|\mathbf{x}^{(t+1)} - \mathbf{x}^{(t)}\|_2^2 \right] \\
&\overset{②}{=} \left\langle \underbrace{\partial \|\mathbf{x}^{(t+1)}\|_1 + \sum_i p_i^{(t)} \nabla h_i(\mathbf{x}^{(t)})}_{H(\mathbf{x}^{(t)})},\; \mathbf{x}^{(t+1)} - \mathbf{x}^{(t)} \right\rangle + \frac{L_h}{2} \|\mathbf{x}^{(t+1)} - \mathbf{x}^{(t)}\|_2^2 \\
&\overset{③}{=} \left\langle \frac{\mathbf{x}^{(t)} - \mathbf{x}^{(t+1)}}{\eta_w^{(t)}},\, \mathbf{x}^{(t+1)} - \mathbf{x}^{(t)} \right\rangle + \frac{L_h}{2} \|\mathbf{x}^{(t+1)} - \mathbf{x}^{(t)}\|_2^2 \\
&= \frac{1}{2} \left(L_h - \frac{2}{\eta_w^{(t)}} \right) \|\mathbf{x}^{(t+1)} - \mathbf{x}^{(t)}\|_2^2 \overset{④}{\leq} -\frac{L_h}{2} \|\mathbf{x}^{(t+1)} - \mathbf{x}^{(t)}\|_2^2,
\end{aligned}$$

where in ① we have $\|\mathbf{x}^{(t)}\|_1 \geq \|\mathbf{x}^{(t+1)}\|_1 + \left\langle \partial \|\mathbf{x}^{(t+1)}\|_1,\, \mathbf{x}^{(t)} - \mathbf{x}^{(t+1)} \right\rangle$ from the definition of sub-gradient [112], and $h_i(\mathbf{x}^{(t+1)}) \leq h_i(\mathbf{x}^{(t)}) + \left\langle \nabla h_i(\mathbf{x}^{(t)}), \mathbf{x}^{(t+1)} - \mathbf{x}^{(t)} \right\rangle + \frac{L_h}{2} \|\mathbf{x}^{(t+1)} - \mathbf{x}^{(t)}\|_2^2$, in ② we use the property $\partial \|\mathbf{x}^{(t+1)}\|_1 + \sum_i p_i^{(t)} \nabla h_i(\mathbf{x}^{(t)}) \in H(\mathbf{x}^{(t)})$, in ③ we use $\mathbf{x}^{(t+1)} = \mathbf{x}^{(t)} - \eta_w^{(t)} H(\mathbf{x}^{(t)})$, and in ④ we use $\eta_w^{(t)} \leq L^{-1}$.

Adopting similar tricks as [154], we could upper-bound $\|\mathbf{x}^{(t+1)} - \mathbf{x}^{(t)}\|_2^2$ as

$$\begin{aligned}
&\|\mathbf{x}^{(t+1)} - \mathbf{x}^{(t)}\|_2^2 \leq \frac{2}{L_h} \left[\mathcal{L}(\mathbf{p}^{(t)}, \mathbf{x}^{(t)}) - \mathcal{L}(\mathbf{p}^{(t)}, \mathbf{x}^{(t+1)})\right] \\
= \ & \frac{2}{L_h} \left[\underbrace{\mathcal{L}(\mathbf{p}^{(t)}, \mathbf{x}^{(t)}) - \mathcal{L}(\mathbf{p}^{(t+1)}, \mathbf{x}^{(t+1)})}_{\mathcal{T}_1^t} + \underbrace{\mathcal{L}(\mathbf{p}^{(t+1)}, \mathbf{x}^{(t+1)}) - \mathcal{L}(\mathbf{p}^{(t)}, \mathbf{x}^{(t+1)})}_{\mathcal{T}_2^t} \right].
\end{aligned}$$

Then we separately discuss bound $\mathcal{T}_1^t$ and $\mathcal{T}_2^t$. Since most terms of $\sum_t \mathcal{T}_1^t$ will be cancelled after summarization, we focus the analysis on bounding $\mathcal{T}_2^t$, which is

$$\mathcal{T}_2^t = \left\langle \mathbf{p}^{(t+1)} - \mathbf{p}^{(t)}, \boldsymbol{f}(\mathbf{x}^{(t+1)}) \right\rangle \ \leq \ \|\mathbf{p}^{(t+1)} - \mathbf{p}^{(t)}\|_1 \underbrace{\|\boldsymbol{f}(\mathbf{x}^{(t+1)})\|_\infty}_{\leq R_f},$$

where $\boldsymbol{f}(\mathbf{x}^{(t+1)})$ denotes the vector whose ith element is $f_i(\mathbf{x}^{(t+1)})$. Notice that we have

$$\begin{aligned}
\|\mathbf{p}^{(t+1)} - \mathbf{p}^{(t)}\|_1^2 \ &\overset{⑤}{\leq} \ 2D_{KL}\left(\mathbf{p}^{(t+1)} || \mathbf{p}^{(t)}\right) \ \overset{⑥}{\leq} \ 2\eta_p^{(t)} \left\langle \mathbf{p}^{(t)} - \mathbf{p}^{(t+1)}, \ \boldsymbol{f}(\mathbf{x}^{(t)}) \right\rangle \\
&\leq \ 2\eta_p^{(t)} \ \|\mathbf{p}^{(t+1)} - \mathbf{p}^{(t)}\|_1 \|\boldsymbol{f}(\mathbf{x}^{(t)})\|_\infty \leq 2\eta_p^{(t)} R_f \|\mathbf{p}^{(t+1)} - \mathbf{p}^{(t)}\|_1,
\end{aligned}$$

which gives us $\|\mathbf{p}^{(t+1)} - \mathbf{p}^{(t)}\|_1 \ \leq \ 2\eta_p^{(t)} R_f$, where ⑤ is because of *Pinsker's inequality* (Thm. 4.19 in [140]) and ⑥ is because of Lemma 51. To conclude, we have upper-bound $\mathcal{T}_2^t$ as $\mathcal{T}_2^t \leq 2\eta_p^{(t)} R_f^2$. Then we finish the proof as

$$\begin{aligned}
\sum_t \|\mathbf{x}^{(t+1)} - \mathbf{x}^{(t)}\|_2^2 \leq \ & \frac{2\mathcal{L}(\mathbf{p}^{(0)}, \mathbf{x}^{(0)}) - 2\mathcal{L}(\mathbf{p}^{(T+1)}, \mathbf{x}^{(T+1)})}{L_h} + \frac{4R_f^2 \sum_t \eta_p^{(t)}}{L_h} \\
&\overset{⑦}{\leq} \ \frac{2\mathcal{L}(\mathbf{p}^{(0)}, \mathbf{x}^{(0)})}{L_h} + \frac{4R_f^2 \sum_t \eta_p^{(t)}}{L_h},
\end{aligned}$$

where ⑦ is because $\mathcal{L}(\mathbf{p}^{(T+1)}, \mathbf{x}^{(T+1)}) \geq 0$. □

Lemma 51. *With Algorithm 5, we have*

$$D_{KL}\left(\mathbf{p}^{(t+1)} || \mathbf{p}^{(t)}\right) \leq \ \eta_p^{(t)} \left\langle \mathbf{p}^{(t)} - \mathbf{p}^{(t+1)}, \ \boldsymbol{f}(\mathbf{x}^{(t)}) \right\rangle,$$

where $\boldsymbol{f}(\mathbf{x}^{(t)})$ denotes the vector whose ith element is $f_i(\mathbf{x}^{(t)})$.

Proof. Here we have

$$
\begin{aligned}
& D_{KL}(\mathbf{p}^{(t+1)}||\mathbf{p}^{(t)}) = \sum_i p_i^{(t+1)} \log\left(\frac{p_i^{(t+1)}}{p_i^{(t)}}\right) \\
= & \sum_i p_i^{(t+1)} \log \frac{e^{-\eta_p^{(t)} f_i(x_t)}}{Z_t} = -\log(Z_t) - \eta_p^{(t)} \sum_i p_i^{(t+1)} f_i(\mathbf{x}^{(t)}) \\
= & -\log(Z_t) - \eta_p^{(t)} \left\langle \mathbf{p}^{(t)}, \boldsymbol{f}(\mathbf{x}^{(t)}) \right\rangle - \eta_p^{(t)} \left\langle \mathbf{p}^{(t+1)} - \mathbf{p}^{(t)}, \boldsymbol{f}(\mathbf{x}^{(t)}) \right\rangle,
\end{aligned}
$$

where $Z_t \triangleq \sum_i p_i^{(t)} e^{-\eta_p f_i(\mathbf{x}^{(t)})}$. Then we have

$$
\begin{aligned}
& \eta_p^{(t)} \left\langle \mathbf{p}^{(t)} - \mathbf{p}^{(t+1)}, \boldsymbol{f}(\mathbf{x}^{(t)}) \right\rangle \\
= & D_{KL}(\mathbf{p}^{(t+1)}||\mathbf{p}^{(t)}) + \log\left(\sum_i p_i^{(t)} e^{-\eta_p^{(t)} f_i(\mathbf{x}^{(t)})}\right) + \eta_p^{(t)} \left\langle \mathbf{p}^{(t)}, f(\mathbf{x}_t) \right\rangle \\
\overset{①}{\geq} & D_{KL}(\mathbf{p}^{(t+1)}||\mathbf{p}^{(t)}) + \log\left[\prod_i e^{-\eta_p^{(t)} p_i^t f_i(\mathbf{x}^{(t)})}\right] + \eta_p^{(t)} \left\langle \mathbf{p}^{(t)}, \boldsymbol{f}(\mathbf{x}^{(t)}) \right\rangle \\
= & D_{KL}(\mathbf{p}^{(t+1)}||\mathbf{p}^{(t)}) + \underbrace{\sum_i \log\left(e^{-\eta_p^{(t)} p_i^{(t)} f_i(\mathbf{x}^{(t)})}\right) + \eta_p^{(t)} \left\langle \mathbf{p}^{(t)}, f(\mathbf{x}_t) \right\rangle}_{0} \\
= & D_{KL}(\mathbf{p}^{(t+1)}||\mathbf{p}^{(t)}),
\end{aligned}
$$

where in ① we use $\sum_i p_i x_i \geq \prod_i x_i^{p_i}$ such that $\sum_i p_i = 1, p_i \geq 0$. □

E.4 Proof of Theorem 13

Proof. Define $\mathbf{p}^*$ and $\mathbf{x}^*$ as

$$
\mathbf{p}^* = \text{argmin}_{\mathbf{p}} \sum_t \mathcal{LR}\left(\mathbf{p}, \mathbf{x}^{(t)}\right), \quad \mathbf{x}^* = \text{argmin}_{\mathbf{x}} \sum_t \mathcal{LR}\left(\mathbf{p}^{(t)}, \mathbf{x}\right). \tag{E.4.1}
$$

respectively First we define $\mathcal{T}_1^t$ and $\mathcal{T}_2^t$ as

$$
\begin{aligned}
\mathcal{T}_1^t &= \mathcal{LR}(\mathbf{p}^{(t)}, \mathbf{x}^{(t)}) - \mathcal{LR}(\mathbf{p}^*, \mathbf{x}^{(t)}); \\
\mathcal{T}_2^t &= \mathcal{LR}(\mathbf{p}^{(t)}, \mathbf{x}^{(t)}) - \mathcal{LR}(\mathbf{p}^{(t)}, \mathbf{x}^*),
\end{aligned}
$$

respectively. Then our goal becomes bounding $|\sum_t \mathcal{T}_1^t| + |\sum_t \mathcal{T}_2^t|$, For term $|\sum_t \mathcal{T}_2^t|$, the analysis stays the same as Lemma 50. Here we focus on bounding $\sum_t \mathcal{T}_1^t$, which proceeds as

$$\begin{aligned}
\sum_t \mathcal{T}_1^t =& \sum_t \left(\mathcal{LR}(\mathbf{p}^{(t)}, \mathbf{x}^{(t)}) - \mathcal{LR}(\mathbf{p}, \mathbf{x}^{(t)})\right) \\
=& \sum_t \left\{ -\left\langle \underbrace{\nabla_t \mathcal{LR}(\mathbf{p}^{(t)}, \mathbf{x}^{(t)})}_{\mathbf{g}^{(t)}},\ \mathbf{p} - \mathbf{p}^{(t)} \right\rangle - \frac{\lambda_3}{2}\|\mathbf{p}^{(t)} - \mathbf{p}\|_2^2 \right\} \\
=& \sum_t \left\{ \left\langle \mathbf{g}^{(t)}, \mathbf{p}^{(t)} - \mathbf{p} \right\rangle - \frac{\lambda_3}{2}\|\mathbf{p}^{(t)} - \mathbf{p}\|_2^2 \right\}
\end{aligned}$$

Then we consider the distance $\|\mathbf{p}^{(t+1)} - \mathbf{p}\|_2^2$ which is

$$\begin{aligned}
\|\mathbf{p}^{(t+1)} - \mathbf{p}\|_2^2 =& \left\|\mathbb{P}_\Delta(\mathbf{p}^{(t)} - \eta_p^t \mathbf{g}^{(t)}) - \mathbf{p}\right\|_2^2 \overset{①}{\leq} \left\|\mathbf{p}^{(t)} - \eta_p^{(t)}\mathbf{g}^{(t)} - \mathbf{p}\right\|_2^2 \\
=& \left\|\mathbf{p}^{(t)} - \mathbf{p}\right\|_2^2 + (\eta_p^{(t)})^2 \left\|\mathbf{g}^{(t)}\right\|_2^2 - 2\eta_p^{(t)} \left\langle \mathbf{g}^{(t)},\ \mathbf{p}^{(t)} - \mathbf{p} \right\rangle,
\end{aligned}$$

where in ① we use the contraction property for projection, which gives us

$$\left\langle \mathbf{g}^{(t)}, \mathbf{p}^{(t)} - \mathbf{p} \right\rangle \leq \frac{\eta_p^{(t)}\|\mathbf{g}^{(t)}\|_2^2}{2} + \frac{\|\mathbf{p}^{(t)} - \mathbf{p}\|_2^2 - \|\mathbf{p}^{(t+1)} - \mathbf{p}\|_2^2}{2\eta_p^{(t)}}$$

By setting $\eta_p^{(t)} = (\lambda t)^{-1}$, we have

$$\begin{aligned}
&\sum_t \mathcal{T}_1^t \leq \frac{R_g^2 \log T}{2\lambda_3} + \frac{\lambda_3}{2}\sum_t t(\|\mathbf{p}^{(t)} - \mathbf{p}\|_2^2 - \|\mathbf{p}^{(t+1)} - \mathbf{p}\|_2^2) - \frac{\lambda_3}{2}\sum_t \|\mathbf{p}^{(t)} - \mathbf{p}\|_2^2 \\
=& \frac{R_g^2 \log T}{2\lambda_3} + \frac{\lambda_3}{2}\sum_t \|\mathbf{p}^{(t)} - \mathbf{p}\|_2^2 - \frac{\lambda_3(T+1)}{2}\|\mathbf{p}^{(T+1)} - \mathbf{p}\|_2^2 - \frac{\lambda_3}{2}\sum_t \|\mathbf{p}^{(t)} - \mathbf{p}\|_2^2 \\
=& \frac{R_g^2 \log T}{2\lambda_3} - \frac{\lambda_3(T+1)}{2}\|\mathbf{p}^{(T+1)} - \mathbf{p}\|_2^2 \leq \frac{R_g^2 \log T}{2\lambda_3}.
\end{aligned}$$

Hence, we have

$$\frac{\sum_t \mathcal{T}_1^t + \mathcal{T}_2^t}{T} \leq \frac{R_g^2 \log T}{2\lambda_3 T} + \frac{R^2}{2\eta_x T},$$

which completes the proof.

□

E.5 Proof of Theorem 14

Proof. Following the same procedure in section E.3, we can bound

$$\|\mathbf{x}^{(t+1)}-\mathbf{x}^{(t)}\|_2^2 \le \frac{2}{L_h}\left[\mathcal{LR}(\mathbf{p}^{(t)},\mathbf{x}^{(t)})-\mathcal{LR}(\mathbf{p}^{(t)},\mathbf{x}^{(t+1)})\right]$$

$$= \frac{2}{L_h}\left[\underbrace{\mathcal{LR}(\mathbf{p}^{(t)},\mathbf{x}^{(t)})-\mathcal{LR}(\mathbf{p}^{(t+1)},\mathbf{x}^{(t+1)})}_{\mathcal{T}_1^t}+\underbrace{\mathcal{LR}(\mathbf{p}^{(t+1)},\mathbf{x}^{(t+1)})-\mathcal{LR}(\mathbf{p}^{(t)},\mathbf{x}^{(t+1)})}_{\mathcal{T}_2^t}\right].$$

Since $\mathcal{T}_1^t$ will cancel themselves after summarization, we focus on bounding $\mathcal{T}_2^t$. Then we have

$$\mathcal{LR}(\mathbf{p}^{(t)},\mathbf{x}^{(t+1)}) = \mathcal{LR}(\mathbf{p}^{(t+1)},\mathbf{x}^{(t+1)}) + \left\langle \nabla_{\mathbf{p}}\mathcal{LR}(\mathbf{p}^{(t+1)},\mathbf{x}^{(t+1)}),\ \mathbf{p}^{(t)}-\mathbf{p}^{(t+1)}\right\rangle$$

$$+ \frac{\lambda_3}{2}\|\mathbf{p}^{(t+1)}-\mathbf{p}^{(t)}\|_2^2$$

$$\overset{①}{=} \mathcal{LR}(\mathbf{p}^{(t+1)},\mathbf{x}^{(t+1)}) + \left\langle \boldsymbol{f}(\mathbf{x}^{(t+1)})+\lambda_3(\mathbf{p}^{(t+1)}-q),\ \mathbf{p}^{(t)}-\mathbf{p}^{(t+1)}\right\rangle + \frac{\lambda_3}{2}\|\mathbf{p}^{(t+1)}-\mathbf{p}^{(t)}\|_2^2,$$

where in ① we have $\nabla_{\mathbf{p}}\,\mathcal{LR}(\mathbf{p}^{(t+1)},\mathbf{x}^{(t+1)}) = \boldsymbol{f}(\mathbf{x}^{(t+1)})+\lambda_3\left(\mathbf{p}^{(t+1)}-\boldsymbol{q}\right)$. Then we have

$$\mathcal{LR}(\mathbf{p}^{(t+1)},\mathbf{x}^{(t+1)})-\mathcal{LR}(\mathbf{p}^{(t)},\mathbf{x}^{(t+1)}) = \left\langle \mathbf{g}^{(t+1)},\ \mathbf{p}^{(t)}-\mathbf{p}^{(t+1)}\right\rangle + \frac{\lambda_3}{2}\|\mathbf{p}^{(t+1)}-\mathbf{p}^{(t)}\|_2^2$$

$$\le \|\mathbf{g}^{(t+1)}\|_2\left\|\mathbf{p}^{(t+1)}-\mathbf{p}^{(t)}\right\|_2 + \frac{\lambda_3}{2}\left\|\mathbf{p}^{(t+1)}-\mathbf{p}^{(t)}\right\|_2^2$$

$$\le \|\mathbf{g}^{(t+1)}\|_2\|\eta_p^{(t)}\mathbf{g}^{(t)}\|_2 + \frac{\lambda_3\left(\eta_p^{(t)}\right)^2}{2}\|\mathbf{g}^{(t)}\|_2^2 \le R_g^2\left(\eta_p^{(t)}+\frac{\lambda_3\left(\eta_p^{(t)}\right)^2}{2}\right).$$

Hence, we conclude that

$$\sum_t \|\mathbf{x}^{(t+1)}-\mathbf{x}^{(t)}\|_2^2 \le \frac{2\mathcal{LR}(\mathbf{p}^{(0)},\mathbf{x}^{(0)})}{L_h} + \frac{2R_g^2}{L_h}\sum_t\left(\eta_p^{(t)}+\frac{\lambda_3\left(\eta_p^{(t)}\right)^2}{2}\right),$$

where $\|\mathbf{g}^{(t)}\|_2 \le R_g$.

□

APPENDIX F
USEFUL FACTS ABOUT PROBABILITY INEQUALITIES, EMPIRICAL PROCESS, AND RANDOM MATRICES

For the self-containing of this thesis, we list some useful facts about probability inequalities, empirical process, and random matrices.

Lemma 52 ([10] (Example 2.11, P29)). *For a χ^2-RV Z with ℓ degrees of freedom, we have*

$$\mathbb{P}\left(|Z-\ell| \geq t\right) \leq 2\exp\left(-\left(\frac{t^2}{8\ell} \wedge \frac{t}{8}\right)\right), \ \ \forall\, t \geq 0.$$

Theorem 16 (Theorem 2.35 in [151]). *For a $d \times p$ matrix $\mathbf{A}$ whose entries are independent zero-mean real RVs with variance d^{-1} and fourth moment of order $O(d^{-2})$, we have the empirical distribution of the eigenvalues of $\mathbf{A}^\top\mathbf{A}$ converge to the distribution with density*

$$f_\tau(x) = \left[0 \vee \left(1-\tau^{-1}\right)\right]\mathbb{1}(x) + \frac{\sqrt{\left[\left((1+\sqrt{\tau})^2 - x\right) \vee 0\right] \times \left[\left(x-(1-\sqrt{\tau})^2\right) \vee 0\right]}}{2\pi\tau x},$$

as d and p approaches to infinity with $p/d \to \tau$.

Theorem 17 (Corol. 13.2 in [140]). *Consider a totally bounded pseudo-metric space $(\mathcal{T}, \text{dist}(\cdot,\cdot))$. Provided a collection of RVs $\{Z_u\}_{u\in\mathcal{T}}$ satisfying*

$$\mathbb{E}e^{\lambda(Z_u - Z_v)} \leq \frac{\nu\lambda^2 \text{dist}^2(u,v)}{2}, \ \ \forall\, \lambda \geq 0,$$

we have

$$\mathbb{E}\sup_u\left(Z_u - Z_{u_0}\right) \leq 12\sqrt{\nu}\int_0^{\text{diam}(T)/2}\sqrt{\mathcal{H}\left(\delta,\mathcal{T}\right)}d\delta,$$

where $\mathcal{H}(t, \mathcal{T})$ denotes the δ-covering entropy with pseudo-metric $\text{dist}(\cdot,\cdot)$*, and* $\text{diam}(\cdot) \triangleq \sup \text{dist}(u, u_0)$ *is the diameter of the set $\mathcal{T}$.*

Lemma 53 (Lemma 11 in [25])**.** *Denote the distribution function and density function of the standard normal RV as $\Phi(\cdot)$ and $\phi(\cdot)$, respectively. We have*

$$\left(\Phi^{-1}\right)'(\eta) = \frac{1}{\phi\left(\Phi^{-1}(\eta)\right)}.$$

Furthermore, we have

$$\Phi^{-1}(\eta) \leq \sqrt{2\log\frac{1}{1-\eta}},$$

for $\eta \geq 0.99$.

Theorem 18 (Wick's theorem, Thm. 1.28 (P11) in [155])**.** *Considering the centered jointly normal variables $\xi_1, \xi_2, \cdots, \xi_n$, we conclude*

$$\mathbb{E}\left(\xi_1\xi_2\cdots\xi_n\right) = \sum_{\substack{\text{all possible disjoint} \\ \text{pairs } (i_k, j_k) \text{ of } [n]}} \prod_k \mathbb{E}\left(\xi_{i_k}\xi_{j_k}\right).$$

Notice that the variables $\{\xi_i\}_{1\leq i\leq n}$ are not necessarily different nor independent. To illustrate this theorem, we consider two special cases. First we let $\xi_1 = \xi_2 = \xi_3 = \xi_4 = \xi \sim \mathcal{N}(0,1)$, then we have

$$\mathbb{E}\xi^4 = \mathbb{E}\left(\xi_1\xi_2\xi_3\xi_4\right) = \mathbb{E}(\xi_1\xi_2)\mathbb{E}(\xi_3\xi_4) + \mathbb{E}(\xi_1\xi_3)\mathbb{E}(\xi_2\xi_4) + \mathbb{E}(\xi_1\xi_4)\mathbb{E}(\xi_2\xi_3) = 3.$$

Second we consider the case where n is odd. Since we cannot partition $\{1, 2, \cdots, n\}$ into disjoint pairs (ξ_{i_k}, ξ_{j_k}), we always have $\mathbb{E}(\xi_1\cdots\xi_n) = 0$.

REFERENCES

[1] D. Koller and N. Friedman, *Probabilistic graphical models: principles and techniques*. 2009.

[2] N. Friedman, "Inferring cellular networks using probabilistic graphical models," *Science*, vol. 303, no. 5659, pp. 799–805, 2004.

[3] P. Ravikumar, M. J. Wainwright, G. Raskutti, B. Yu, *et al.*, "High-dimensional covariance estimation by minimizing ℓ_1-penalized log-determinant divergence," *Electronic Journal of Statistics*, vol. 5, pp. 935–980, 2011.

[4] T. Cai, W. Liu, and X. Luo, "A constrained ℓ_1 minimization approach to sparse precision matrix estimation," *Journal of the American Statistical Association*, vol. 106, no. 494, pp. 594–607, 2011.

[5] R. Tibshirani, M. Wainwright, and T. Hastie, *Statistical learning with sparsity: the lasso and generalizations*. Chapman and Hall/CRC, 2015.

[6] V. Chandrasekaran, P. A. Parrilo, and A. S. Willsky, "Latent variable graphical model selection via convex optimization," in *2010 48th Annual Allerton Conference on Communication, Control, and Computing (Allerton)*, IEEE, 2010, pp. 1610–1613.

[7] S. S. Jeffrey, "Cancer biomarker profiling with microRNAs," *Nature biotechnology*, vol. 26, no. 4, pp. 400–401, 2008.

[8] K. Asakura, T. Kadota, J. Matsuzaki, Y. Yoshida, Y. Yamamoto, K. Nakagawa, S. Takizawa, Y. Aoki, E. Nakamura, J. Miura, *et al.*, "A mirna-based diagnostic model predicts resectable lung cancer in humans with high accuracy," *Communications biology*, vol. 3, no. 1, pp. 1–9, 2020.

[9] T. Hastie, R. Tibshirani, and M. Wainwright, *Statistical learning with sparsity: the lasso and generalizations*. Chapman and Hall/CRC, 2015.

[10] M. J. Wainwright, *High-Dimensional Statistics: A Non-Asymptotic Viewpoint*, ser. Cambridge Series in Statistical and Probabilistic Mathematics. Cambridge University Press, 2019.

[11] E. Yang, A. C. Lozano, and P. K. Ravikumar, "Closed-form estimators for high-dimensional generalized linear models," in *Advances in Neural Information Processing Systems*, 2015, pp. 586–594.

[12] R. Mazumder and T. Hastie, "The graphical lasso: New insights and alternatives," *Electronic journal of statistics*, vol. 6, p. 2125, 2012.

[13] B. M. Marlin and K. P. Murphy, "Sparse gaussian graphical models with unknown block structure," in *Proceedings of the 26th Annual International Conference on Machine Learning*, 2009, pp. 705–712.

[14] P. Xu, J. Ma, and Q. Gu, "Speeding up latent variable gaussian graphical model estimation via nonconvex optimization," in *Advances in Neural Information Processing Systems*, 2017, pp. 1933–1944.

[15] H. Wang, A. Banerjee, C.-J. Hsieh, P. K. Ravikumar, and I. S. Dhillon, "Large scale distributed sparse precision estimation," in *Advances in Neural Information Processing Systems*, 2013, pp. 584–592.

[16] T. Hastie, R. Mazumder, J. D. Lee, and R. Zadeh, "Matrix completion and low-rank svd via fast alternating least squares," *The Journal of Machine Learning Research*, vol. 16, no. 1, pp. 3367–3402, 2015.

[17] C.-J. Hsieh, I. S. Dhillon, P. K. Ravikumar, and M. A. Sustik, "Sparse inverse covariance matrix estimation using quadratic approximation," in *Advances in neural information processing systems*, 2011, pp. 2330–2338.

[18] M. J. Wainwright, J. D. Lafferty, and P. K. Ravikumar, "High-dimensional graphical model selection using ℓ_1-regularized logistic regression," in *Advances in neural information processing systems*, 2007, pp. 1465–1472.

[19] A. Jalali, P. Ravikumar, V. Vasuki, and S. Sanghavi, "On learning discrete graphical models using group-sparse regularization," in *Proceedings of the Fourteenth International Conference on Artificial Intelligence and Statistics*, 2011, pp. 378–387.

[20] P. Ravikumar, M. J. Wainwright, J. D. Lafferty, *et al.*, "High-dimensional ising model selection using ℓ_1-regularized logistic regression," *The Annals of Statistics*, vol. 38, no. 3, pp. 1287–1319, 2010.

[21] J. Lee and T. Hastie, "Structure learning of mixed graphical models," in *Artificial Intelligence and Statistics*, 2013, pp. 388–396.

[22] E. Yang, Y. Baker, P. Ravikumar, G. Allen, and Z. Liu, "Mixed graphical models via exponential families," in *Artificial Intelligence and Statistics*, 2014, pp. 1042–1050.

[23] I. Tur and R. Castelo, "Learning mixed graphical models from data with p larger than n," *arXiv preprint arXiv:1202.3765*, 2012.

[24] J. Fan, H. Liu, Y. Ning, and H. Zou, "High dimensional semiparametric latent graphical model for mixed data," *Journal of the Royal Statistical Society: Series B (Statistical Methodology)*, vol. 79, no. 2, pp. 405–421, 2017.

[25] H. Liu, J. Lafferty, and L. Wasserman, "The nonparanormal: Semiparametric estimation of high dimensional undirected graphs.," *Journal of Machine Learning Research*, vol. 10, no. 10, 2009.

[26] H. Liu, M. Xu, H. Gu, A. Gupta, J. Lafferty, and L. Wasserman, "Forest density estimation," *Journal of Machine Learning Research*, vol. 12, no. Mar, pp. 907–951, 2011.

[27] H. Liu, F. Han, M. Yuan, J. Lafferty, L. Wasserman, *et al.*, "High-dimensional semiparametric gaussian copula graphical models," *The Annals of Statistics*, vol. 40, no. 4, pp. 2293–2326, 2012.

[28] T. Zhao, K. Roeder, and H. Liu, "Positive semidefinite rank-based correlation matrix estimation with application to semiparametric graph estimation," *Journal of Computational and Graphical Statistics*, vol. 23, no. 4, pp. 895–922, 2014.

[29] P. Xu and Q. Gu, "Semiparametric differential graph models," in *Proceedings of the 30th International Conference on Neural Information Processing Systems*, 2016, pp. 1072–1080.

[30] L. Xue, H. Zou, *et al.*, "Regularized rank-based estimation of high-dimensional nonparanormal graphical models," *The Annals of Statistics*, vol. 40, no. 5, pp. 2541–2571, 2012.

[31] C.-H. Zhang, "Fourier methods for estimating mixing densities and distributions," *The Annals of Statistics*, pp. 806–831, 1990.

[32] J. Fan, "On the optimal rates of convergence for nonparametric deconvolution problems," *The Annals of Statistics*, pp. 1257–1272, 1991.

[33] E. Masry, "Multivariate probability density deconvolution for stationary random processes," *IEEE Transactions on Information Theory*, vol. 37, no. 4, pp. 1105–1115, 1991.

[34] P. Hall and A. Meister, "A ridge-parameter approach to deconvolution," *The Annals of Statistics*, vol. 35, no. 4, pp. 1535–1558, 2007.

[35] I. Dattner, A. Goldenshluger, and A. Juditsky, "On deconvolution of distribution functions," *The Annals of Statistics*, pp. 2477–2501, 2011.

[36] D. D. Trong and C. X. Phuong, "Deconvolution of a cumulative distribution function with some non-standard noise densities," *Vietnam Journal of Mathematics*, vol. 47, no. 2, pp. 327–353, 2019.

[37] É. Youndjé and M. T. Wells, "Optimal bandwidth selection for multivariate kernel deconvolution density estimation," *Test*, vol. 17, no. 1, pp. 138–162, 2008.

[38] M. Pensky and B. Vidakovic, "Adaptive wavelet estimator for nonparametric density deconvolution," *The Annals of Statistics*, vol. 27, no. 6, pp. 2033–2053, 1999.

[39] I. Dattner and B. Reiser, "Estimation of distribution functions in measurement error models," *Journal of Statistical Planning and Inference*, vol. 143, no. 3, pp. 479–493, 2013.

[40] J. Kappus and G. Mabon, "Adaptive density estimation in deconvolution problems with unknown error distribution," *Electronic journal of statistics*, vol. 8, no. 2, pp. 2879–2904, 2014.

[41] C. X. Phuong, "Deconvolution of cumulative distribution function with unknown noise distribution," *Acta Applicandae Mathematicae*, vol. 170, no. 1, pp. 483–514, 2020.

[42] R. Gallager, "Low-density parity-check codes," *IRE Transactions on information theory*, vol. 8, no. 1, pp. 21–28, 1962.

[43] M. Mezard, M. Mezard, and A. Montanari, *Information, physics, and computation*. Oxford University Press, 2009.

[44] J. Pearl, *Probabilistic reasoning in intelligent systems: networks of plausible inference*. Elsevier, 2014.

[45] C. Berrou and A. Glavieux, "Near optimum error correcting coding and decoding: Turbo-codes," *IEEE Transactions on communications*, vol. 44, no. 10, pp. 1261–1271, 1996.

[46] R. J. McEliece, D. J. C. MacKay, and J.-F. Cheng, "Turbo decoding as an instance of pearl's" belief propagation" algorithm," *IEEE Journal on selected areas in communications*, vol. 16, no. 2, pp. 140–152, 1998.

[47] T. J. Richardson and R. L. Urbanke, "The capacity of low-density parity-check codes under message-passing decoding," *IEEE Transactions on information theory*, vol. 47, no. 2, pp. 599–618, 2001.

[48] S. Sarvotham, D. Baron, and R. G. Baraniuk, "Compressed sensing reconstruction via belief propagation," *preprint*, vol. 14, 2006.

[49] F. Zhang and H. D. Pfister, "Verification decoding of high-rate ldpc codes with applications in compressed sensing," *IEEE Transactions on Information Theory*, vol. 58, no. 8, pp. 5042–5058, 2012.

[50] S. Kudekar and H. D. Pfister, "The effect of spatial coupling on compressive sensing," in *2010 48th Annual Allerton Conference on Communication, Control, and Computing (Allerton)*, IEEE, 2010, pp. 347–353.

[51] Y. Eftekhari, A. Heidarzadeh, A. H. Banihashemi, and I. Lambadaris, "Density evolution analysis of node-based verification-based algorithms in compressed sensing," *IEEE transactions on information theory*, vol. 58, no. 10, pp. 6616–6645, 2012.

[52] H. Zhang, M. Slawski, and P. Li, "Permutation recovery from multiple measurement vectors in unlabeled sensing," in *Proceedings of the IEEE International Symposium on Information Theory (ISIT)*, Paris, France, 2019, pp. 1857–1861.

[53] F. Krzakala, M. Mézard, F. Sausset, Y. Sun, and L. Zdeborová, "Statistical-physics-based reconstruction in compressed sensing," *Physical Review X*, vol. 2, no. 2, p. 021 005, 2012.

[54] H. Zhang, M. Slawski, and P. Li, "The benefits of diversity: Permutation recovery in unlabeled sensing from multiple measurement vectors," *arXiv preprint arXiv:1909.02496*, 2019.

[55] F. Krzakala, M. Mézard, F. Sausset, Y. Sun, and L. Zdeborová, "Probabilistic reconstruction in compressed sensing: Algorithms, phase diagrams, and threshold achieving matrices," *Journal of Statistical Mechanics: Theory and Experiment*, vol. 2012, no. 08, P08009, 2012.

[56] L. Zdeborová and F. Krzakala, "Statistical physics of inference: Thresholds and algorithms," *Advances in Physics*, vol. 65, no. 5, pp. 453–552, 2016.

[57] D. L. Donoho, A. Maleki, and A. Montanari, "Message-passing algorithms for compressed sensing," *Proceedings of the National Academy of Sciences*, vol. 106, no. 45, pp. 18 914–18 919, 2009.

[58] M. A. Maleki, *Approximate message passing algorithms for compressed sensing*. Stanford University, 2010.

[59] H. Zhang and P. Li, "Optimal estimator for unlabeled linear regression," in *Proceedings of the 37th International Conference on Machine Learning (ICML)*, Virtual Event, 2020, pp. 11 153–11 162.

[60] S. Li, T. Chi, J. S. Park, and H. Wang, "A multi-feed antenna for antenna-level power combining," in *2016 IEEE International Symposium on Antennas and Propagation (APSURSI)*, IEEE, 2016, pp. 1589–1590.

[61] S. Sarvotham, D. Baron, and R. G. Baraniuk, "Sudocodes fast measurement and reconstruction of sparse signals," in *2006 IEEE International Symposium on Information Theory*, IEEE, 2006, pp. 2804–2808.

[62] D. Baron, S. Sarvotham, and R. G. Baraniuk, "Bayesian compressive sensing via belief propagation," *IEEE Transactions on Signal Processing*, vol. 58, no. 1, pp. 269–280, 2009.

[63] V. Chandar, D. Shah, and G. W. Wornell, "A simple message-passing algorithm for compressed sensing," in *2010 IEEE International Symposium on Information Theory*, IEEE, 2010, pp. 1968–1972.

[64] A. G. Dimakis, R. Smarandache, and P. O. Vontobel, "Ldpc codes for compressed sensing," *IEEE Transactions on Information Theory*, vol. 58, no. 5, pp. 3093–3114, 2012.

[65] M. G. Luby and M. Mitzenmacher, "Verification-based decoding for packet-based low-density parity-check codes," *IEEE Transactions on Information Theory*, vol. 51, no. 1, pp. 120–127, 2005.

[66] A. Montanari, "Graphical models concepts in compressed sensing," *Compressed Sensing: Theory and Applications*, pp. 394–438, 2012.

[67] W. Xu and B. Hassibi, "Efficient compressive sensing with deterministic guarantees using expander graphs," in *2007 IEEE Information Theory Workshop*, IEEE, 2007, pp. 414–419.

[68] M. A. Khajehnejad, A. G. Dimakis, and B. Hassibi, "Nonnegative compressed sensing with minimal perturbed expanders," in *2009 IEEE 13th Digital Signal Processing Workshop and 5th IEEE Signal Processing Education Workshop*, IEEE, 2009, pp. 696–701.

[69] W. Xu and B. Hassibi, "Further results on performance analysis for compressive sensing using expander graphs," in *2007 Conference Record of the Forty-First Asilomar Conference on Signals, Systems and Computers*, IEEE, 2007, pp. 621–625.

[70] S. Jafarpour, W. Xu, B. Hassibi, and R. Calderbank, "Efficient and robust compressed sensing using optimized expander graphs," *IEEE Transactions on Information Theory*, vol. 55, no. 9, pp. 4299–4308, 2009.

[71] W. Lu, K. Kpalma, and J. Ronsin, "Sparse binary matrices of ldpc codes for compressed sensing," in *Data compression conference (DCC)*, 2012, 10–pages.

[72] J. Zhang, G. Han, and Y. Fang, "Deterministic construction of compressed sensing matrices from protograph ldpc codes," *IEEE Signal Processing Letters*, vol. 22, no. 11, pp. 1960–1964, 2015.

[73] H. Zhang, T. Wang, L. Song, and Z. Han, "Turning interference weakness into phy security enhancement for cognitive radio networks," in *2013 International Conference on Wireless Communications and Signal Processing*, IEEE, 2013, pp. 1–6.

[74] H. Zhang, A. Abdi, F. Fekri, and H. Esmaeilzadeh, "Error correction for approximate computing," in *2016 54th Annual Allerton Conference on Communication, Control, and Computing (Allerton)*, IEEE, 2016, pp. 948–953.

[75] H. Zhang, T. Wang, L. Song, and Z. Han, "Radio resource allocation for physical-layer security in d2d underlay communications," in *2014 IEEE International Conference on Communications (ICC)*, IEEE, 2014, pp. 2319–2324.

[76] H. Zhang, A. Abdi, and F. Fekri, "Recovery of sign vectors in quadratic compressed sensing.," in *IEEE Information Theory Workshop (ITW'17)*, Kaohsiung, Taiwan, Nov. 2017.

[77] H. Zhang, T. Wang, L. Song, and Z. Han, "Interference improves phy security for cognitive radio networks," *IEEE Transactions on Information Forensics and Security*, vol. 11, no. 3, pp. 609–620, 2015.

[78] H. Zhang, A.Abdi, and F. Fekri, "Analysis of sparse-integer measurement matrices in compressive sensing," in *2019 IEEE International Conference on Acoustics, Speech and Signal Processing (ICASSP)*, Brighton, United Kingdom, May 2019.

[79] H. Zhang, A. Abdi, and F. Fekri, "Compressive sensing with energy constraint.," in *IEEE Information Theory Workshop (ITW'17)*, Kaohsiung, Taiwan, Nov. 2017.

[80] S. Li, T. Chi, J.-S. Park, H. T. Nguyen, and H. Wang, "A 28-ghz flip-chip packaged chireix transmitter with on-antenna outphasing active load modulation," *IEEE Journal of Solid-State Circuits*, vol. 54, no. 5, pp. 1243–1253, 2019.

[81] S. Li, M.-Y. Huang, D. Jung, T.-Y. Huang, and H. Wang, "A 28ghz current-mode inverse-outphasing transmitter achieving 40%/31% pa efficiency at p sat/6db pbo and supporting 15gbit/s 64-qam for 5g communication," in *2020 IEEE International Solid-State Circuits Conference-(ISSCC)*, IEEE, 2020, pp. 366–368.

[82] H. Zhang, A. Abdi, and F. Fekri, "A general framework for the design of compressive sensing using density evolution," in *IEEE Information Theory Workshop (ITW'21)*.

[83] S. Foucart and H. Rauhut, *A mathematical introduction to compressive sensing*, 3, vol. 1.

[84] E. J. Candès, "Mathematics of sparsity (and a few other things)."

[85] D. L. Donoho, M. Elad, and V. N. Temlyakov, "Stable recovery of sparse overcomplete representations in the presence of noise," *IEEE Transactions on information theory*, vol. 52, no. 1, pp. 6–18, 2005.

[86] H. Zhang, A. Abdi, and F. Fekri, "Sparse recovery of sign vectors under uncertain sensing matrices.," in *IEEE Information Theory Workshop (ITW'18)*, Guangzhou, China Nov. 2018.

[87] M. A. Herman and T. Strohmer, "General deviants: An analysis of perturbations in compressed sensing," *IEEE Journal of Selected topics in signal processing*, vol. 4, no. 2, pp. 342–349, 2010.

[88] H. Zhu, G. Leus, and G. B. Giannakis, "Sparsity-cognizant total least-squares for perturbed compressive sampling," *IEEE Transactions on Signal Processing*, vol. 59, no. 5, pp. 2002–2016, 2011.

[89] Z. Yang, C. Zhang, and L. Xie, "Robustly stable signal recovery in compressed sensing with structured matrix perturbation," *IEEE Transactions on Signal Processing*, vol. 60, no. 9, pp. 4658–4671, 2012.

[90] H. Zhang and P. Li, "Sparse recovery with shuffled labels: Statistical limits and practical estimators," in *2021 IEEE International Symposium on Information Theory (ISIT)*, IEEE, 2021, pp. 1760–1765.

[91] S. Wang, Y. Li, and J. Wang, "Sparse bayesian learning for compressed sensing under measurement matrix uncertainty," in *Wireless Communications & Signal Processing (WCSP), 2013 International Conference on*, IEEE, 2013, pp. 1–5.

[92] S. Li, M.-Y. Huang, D. Jung, T.-Y. Huang, and H. Wang, "A mm-wave current-mode inverse outphasing transmitter front-end: A circuit duality of conventional voltage-mode outphasing," *IEEE Journal of Solid-State Circuits*, vol. 56, no. 6, pp. 1732–1744, 2020.

[93] S. Li, T. Chi, and H. Wang, "Multi-feed antenna and electronics co-design: An e-band antenna-lna front end with on-antenna noise-canceling and g_m-boosting," *IEEE Journal of Solid-State Circuits*, vol. 55, no. 12, pp. 3362–3375, 2020.

[94] S. Li, T.-Y. Huang, Y. Liu, H. Yoo, Y. Na, Y. Hur, and H. Wang, "A millimeter-wave lna in 45nm cmos soi with over 23db peak gain and sub-3db nf for different 5g operating bands and improved dynamic range," in *2021 IEEE Radio Frequency Integrated Circuits Symposium (RFIC)*, IEEE, 2021, pp. 31–34.

[95] S. Li, T. Chi, Y. Wang, and H. Wang, "A millimeter-wave dual-feed square loop antenna for 5g communications," *IEEE Transactions on Antennas and Propagation*, vol. 65, no. 12, pp. 6317–6328, 2017.

[96] K. Lounici *et al.*, "Sup-norm convergence rate and sign concentration property of lasso and dantzig estimators," *Electronic Journal of statistics*, vol. 2, pp. 90–102, 2008.

[97] M. Rosenbaum, A. B. Tsybakov, *et al.*, "Sparse recovery under matrix uncertainty," *The Annals of Statistics*, vol. 38, no. 5, pp. 2620–2651, 2010.

[98] L. Wroblewska, T. Kitada, K. Endo, V. Siciliano, B. Stillo, H. Saito, and R. Weiss, "Mammalian synthetic circuits with rna binding proteins for RNA-only delivery," *Nature biotechnology*, vol. 33, no. 8, pp. 839–841, 2015.

[99] H. Zhang, A. Abdi, and F. Fekri, "Recovering noisy-pseudo-sparse signals from linear measurements via ℓ_∞," in *2019 57th Annual Allerton Conference on Communication, Control, and Computing (Allerton)*, IEEE, 2019, pp. 1154–1159.

[100] G. Pope, A. Bracher, and C. Studer, "Probabilistic recovery guarantees for sparsely corrupted signals," *IEEE Transactions on Information Theory*, vol. 59, no. 5, pp. 3104–3116, 2013.

[101] X. Li, "Compressed sensing and matrix completion with constant proportion of corruptions," *Constructive Approximation*, vol. 37, no. 1, pp. 73–99, 2013.

[102] T. Wimalajeewa and P. K. Varshney, "Sparse signal detection with compressive measurements via partial support set estimation," *IEEE Transactions on Signal and Information Processing over Networks*, vol. 3, no. 1, pp. 46–60, 2017.

[103] M. A. Davenport, P. T. Boufounos, and R. Baraniuk, "Compressive domain interference cancellation," in *SPARS'09-Signal Processing with Adaptive Sparse Structured Representations*, 2009.

[104] E. Arias-Castro and Y. C. Eldar, "Noise folding in compressed sensing," *IEEE Signal Processing Letters*, vol. 18, no. 8, pp. 478–481, 2011.

[105] H. Zhang, A.Abdi, and F. Fekri, "Compressive sensing with a multiple convex sets domain," in *2019 IEEE International Symposium on Information Theory, (ISIT)*, Paris, France, 2019. Jul.

[106] D. Donoho and J. Tanner, "Counting faces of randomly projected polytopes when the projection radically lowers dimension," *Journal of the American Mathematical Society*, vol. 22, no. 1, pp. 1–53, 2009.

[107] V. Chandrasekaran, B. Recht, P. A. Parrilo, and A. S. Willsky, "The convex geometry of linear inverse problems," *Foundations of Computational mathematics*, vol. 12, no. 6, pp. 805–849, 2012.

[108] Y. Gordon, "On milman's inequality and random subspaces which escape through a mesh in $\mathbb{R}^n$," in *Geometric Aspects of Functional Analysis*, Springer, 1988, pp. 84–106.

[109] J. A. Tropp, "Convex recovery of a structured signal from independent random linear measurements," in *Sampling Theory, a Renaissance*, Springer, 2015, pp. 67–101.

[110] E. J. Candes, J. K. Romberg, and T. Tao, "Stable signal recovery from incomplete and inaccurate measurements," *Communications on Pure and Applied Mathematics: A Journal Issued by the Courant Institute of Mathematical Sciences*, vol. 59, no. 8, pp. 1207–1223, 2006.

[111] P. Schniter, S. Rangan, and A. K. Fletcher, "Vector approximate message passing for the generalized linear model," in *Signals, Systems and Computers, 2016 50th Asilomar Conference on*, IEEE, 2016, pp. 1525–1529.

[112] A. Beck, *First-Order Methods in Optimization*, ser. MOS-SIAM Series on Optimization. Society for Industrial and Applied Mathematics, 2017, ISBN: 9781611974997.

[113] A. Beck and M. Teboulle, "A fast iterative shrinkage-thresholding algorithm for linear inverse problems," *SIAM journal on imaging sciences*, vol. 2, no. 1, pp. 183–202, 2009.

[114] R. G. Baraniuk, V. Cevher, M. F. Duarte, and C. Hegde, "Model-based compressive sensing," *IEEE Transactions on Information Theory*, vol. 56, no. 4, pp. 1982–2001, 2010.

[115] M. F. Duarte and Y. C. Eldar, "Structured compressed sensing: From theory to applications," *IEEE Transactions on Signal Processing*, vol. 59, no. 9, pp. 4053–4085, 2011.

[116] J. Silva, M. Chen, Y. C. Eldar, G. Sapiro, and L. Carin, "Blind compressed sensing over a structured union of subspaces," *arXiv preprint arXiv:1103.2469*, 2011.

[117] S. Arora, E. Hazan, and S. Kale, "The multiplicative weights update method: A meta-algorithm and applications.," *Theory of Computing*, vol. 8, no. 1, pp. 121–164, 2012.

[118] S. Shalev-Shwartz *et al.*, "Online learning and online convex optimization," *Foundations and Trends in Machine Learning*, vol. 4, no. 2, pp. 107–194, 2012.

[119] R. A. Horn, R. A. Horn, and C. R. Johnson, *Matrix Analysis*. Cambridge University Press, 1990.

[120] R. T. Rockafellar, *Convex analysis*, 28. Princeton university press, 1970.

[121] A. Bhattacharya, A. M. Hamilton, M. A. Troester, and M. I. Love, "Decompress: Tissue compartment deconvolution of targeted mrna expression panels using compressed sensing," *bioRxiv*, 2020. eprint: https://www.biorxiv.org/content/early/2020/08/17/2020.08.14.250902.full.pdf.

[122] A. Yokoi, J. Matsuzaki, Y. Yamamoto, Y. Yoneoka, K. Takahashi, H. Shimizu, T. Uehara, M. Ishikawa, S.-i. Ikeda, T. Sonoda, *et al.*, "Integrated extracellular microrna profiling for ovarian cancer screening," *Nature communications*, vol. 9, no. 1, pp. 1–10, 2018.

[123] M. L. Slattery, J. S. Herrick, D. F. Pellatt, J. R. Stevens, L. E. Mullany, E. Wolff, M. D. Hoffman, W. S. Samowitz, and R. K. Wolff, "Microrna profiles in colorectal carcinomas, adenomas and normal colonic mucosa: Variations in mirna expression and disease progression," *Carcinogenesis*, vol. 37, no. 3, pp. 245–261, 2016.

[124] K. Sudo, K. Kato, J. Matsuzaki, N. Boku, S. Abe, Y. Saito, H. Daiko, S. Takizawa, Y. Aoki, H. Sakamoto, *et al.*, "Development and validation of an esophageal squamous cell carcinoma detection model by large-scale microrna profiling," *JAMA network open*, vol. 2, no. 5, e194573–e194573, 2019.

[125] T. Hastie, R. Tibshirani, and J. Friedman, *The elements of statistical learning: data mining, inference, and prediction*. Springer Science & Business Media, 2009.

[126] G. H. Golub and C. F. Van Loan, *Matrix computations*. JHU Press, 2012, vol. 3.

[127] V. Koltchinskii, *Oracle Inequalities in Empirical Risk Minimization and Sparse Recovery Problems: Ecole d'Eté de Probabilités de Saint-Flour XXXVIII-2008*. Springer Science & Business Media, 2011, vol. 2033.

[128] E. J. Candès, J. Romberg, and T. Tao, "Robust uncertainty principles: Exact signal reconstruction from highly incomplete frequency information," *IEEE Transactions on information theory*, vol. 52, no. 2, pp. 489–509, 2006.

[129] N. Meinshausen, P. Bühlmann, *et al.*, "High-dimensional graphs and variable selection with the lasso," *The annals of statistics*, vol. 34, no. 3, pp. 1436–1462, 2006.

[130] P. Zhao and B. Yu, "On model selection consistency of lasso," *Journal of Machine learning research*, vol. 7, no. Nov, pp. 2541–2563, 2006.

[131] T. Richardson and R. Urbanke, *Modern coding theory*. Cambridge university press, 2008.

[132] T. J. Richardson, M. A. Shokrollahi, and R. L. Urbanke, "Design of capacity-approaching irregular low-density parity-check codes," *IEEE transactions on information theory*, vol. 47, no. 2, pp. 619–637, 2001.

[133] S.-Y. Chung, "On the construction of some capacity-approaching coding schemes," Ph.D. dissertation, Massachusetts Institute of Technology, 2000.

[134] R. Tibshirani, "Regression shrinkage and selection via the lasso," *Journal of the Royal Statistical Society: Series B (Methodological)*, vol. 58, no. 1, pp. 267–288, 1996.

[135] S. Foucart, "Hard thresholding pursuit: An algorithm for compressive sensing," *SIAM Journal on Numerical Analysis*, vol. 49, no. 6, pp. 2543–2563, 2011.

[136] T. Hastie, R. Tibshirani, and J. Friedman, *The Elements of Statistical Learning*, ser. Springer Series in Statistics. New York, NY, USA: Springer New York Inc., 2001.

[137] Y. LeCun, L. Bottou, Y. Bengio, and P. Haffner, "Gradient-based learning applied to document recognition," *Proceedings of the IEEE*, vol. 86, no. 11, pp. 2278–2324, 1998.

[138] M. Rosenbaum and A. B. Tsybakov, "Improved matrix uncertainty selector," in *From Probability to Statistics and Back: High-Dimensional Models and Processes – A Festschrift in Honor of Jon A. Wellner*, Beachwood, Ohio, USA: Institute of Mathematical Statistics, 2013, pp. 276–290.

[139] R. Vershynin, *High dimensional probability*, 2016.

[140] S. Boucheron, G. Lugosi, and P. Massart, *Concentration Inequalities: A Nonasymptotic Theory of Independence*. Oxford University Press, 2013.

[141] E. J. Candès, "The restricted isometry property and its implications for compressed sensing," *Comptes Rendus Mathematique*, vol. 346, no. 9-10, pp. 589–592, May 2008.

[142] E. J. Candes and T. Tao, "Decoding by linear programming," *IEEE transactions on information theory*, vol. 51, no. 12, pp. 4203–4215, 2005.

[143] S. Li, T. Chi, D. Jung, T.-Y. Huang, M.-Y. Huang, and H. Wang, "4.2 an e-band high-linearity antenna-lna front-end with 4.8 db nf and 2.2 dbm iip3 exploiting multi-feed on-antenna noise-canceling and gm-boosting," in *2020 IEEE International Solid-State Circuits Conference-(ISSCC)*, IEEE, 2020, pp. 1–3.

[144] C. Studer, W. Yin, and R. G. Baraniuk, "Signal representations with minimum ℓ_∞-norm," in *Communication, Control, and Computing (Allerton), 2012 50th Annual Allerton Conference on*, IEEE, 2012, pp. 1270–1277.

[145] E. J. Candes, Y. C. Eldar, T. Strohmer, and V. Voroninski, "Phase retrieval via matrix completion," 2011.

[146] Y. Chen and E. Candes, "Solving random quadratic systems of equations is nearly as easy as solving linear systems," in *Advances in Neural Information Processing Systems*, 2015, pp. 739–747.

[147] K. Jaganathan, S. Oymak, and B. Hassibi, "Sparse phase retrieval: Convex algorithms and limitations," in *2013 IEEE International Symposium on Information Theory*, IEEE, 2013, pp. 1022–1026.

[148] W. Dai, H. V. Pham, and O. Milenkovic, "Quantized compressive sensing," *arXiv preprint arXiv:0901.0749*, 2009.

[149] S. Boyd, "Alternating direction method of multipliers."

[150] M. Talagrand, *Upper and lower bounds for stochastic processes: modern methods and classical problems*. Springer Science & Business Media, 2014, vol. 60.

[151] A. M. Tulino, S. Verdú, and S. Verdu, *Random matrix theory and wireless communications*. Now Publishers Inc, 2004.

[152] H. Nishimori, *Statistical physics of spin glasses and information processing: an introduction*, 111. Clarendon Press, 2001.

[153] R. T. Rockafellar, *Convex analysis*. Princeton university press, 2015.

[154] Q. Qian, S. Zhu, J. Tang, R. Jin, B. Sun, and H. Li, "Robust optimization over multiple domains," *arXiv preprint arXiv:1805.07588*, 2018.

[155] S. Janson *et al.*, *Gaussian hilbert spaces*. Cambridge university press, 1997, vol. 129.